

Factors Regulating Epithelial-Mesenchymal Transition and Metastasis of Gastric Cancer

By

SUVASMITA RATH

LIFE11201004016

**National Institute of Science Education and Research (NISER)
Bhubaneswar**

*A thesis submitted to the
Board of Studies in Life Sciences*

*In partial fulfillment of the requirements
for the Degree of*

DOCTOR OF PHILOSOPHY

of

HOMI BHABHA NATIONAL INSTITUTE



DECEMBER, 2016

Homi Bhabha National Institute

Recommendations of the Viva Voce Board

As members of the Viva Voce Board, we certify that we have read the dissertation prepared by Suvasmita Rath entitled "Factors Regulating Epithelial-Mesenchymal Transition (EMT) and Metastasis of Gastric Cancer" and recommend that it may be accepted as fulfilling the dissertation requirement for the Degree of Doctor of Philosophy.

Suman K Dhar
-----Date: 16/12/2016

Chairman

Prof. Suman K. Dhar, JNU

-----Date:

Convener:

Dr. Asima Bhattacharyya

Asima Bhattacharyya

-----Date: 16.12.16

External examiner:

Prof. Suman K. Dhar

Suman K Dhar

-----Date: 16/12/2016

External member (Doctoral Committee):

Prof. Jagneshwar Dandapat, Utkal Univ

Jagneshwar Dandapat

-----Date: 16.12.16

Member 1:

Dr. Chandan Goswami

Chandan Goswami

16/12/16

-----Date:

Member 2:

Dr. Subhasis Chattopadhyay

Subhasis Chattopadhyay

16/12/16

-----Date:

Member 3:

Dr. Harapriya Mohapatra

Harapriya Mohapatra

-----Date: 16.12.16

Final approval and acceptance of this dissertation is contingent upon the candidate's submission of the final copies of the dissertation to HBNI.

I hereby certify that I have read this dissertation prepared under my direction and recommend that it may be accepted as fulfilling the dissertation requirement.

Date: 16-12-2016

Place: NISER, Bhubaneswar

Asima Bhattacharyya
(Dr. Asima Bhattacharyya)
PhD Thesis Supervisor

STATEMENT BY AUTHOR

This dissertation has been submitted in partial fulfillment of requirements for an advanced degree at Homi Bhabha National Institute (HBNI) and is deposited in the Library to be made available to borrowers under rules of the HBNI.

Brief quotations from this dissertation are allowable without special permission, provided that accurate acknowledgment of source is made. Requests for permission for extended quotation from or reproduction of this manuscript in whole or in part may be granted by the Competent Authority of HBNI when in his or her judgment the proposed use of the material is in the interests of scholarship. In all other instances, however, permission must be obtained from the author.

Suvasmita Rath

DECLARATION

I, hereby declare that the investigation presented in the thesis has been carried out by me. The work is original and has not been submitted earlier as a whole or in part for a degree/diploma at this or any other Institution/University.

Suvasmita Rath

CERTIFICATE

This is to certify that the thesis entitled "**Factors Regulating Epithelial-Mesenchymal Transition and Metastasis of Gastric Cancer**", which is being submitted by **Ms. Suvasmita Rath** in partial fulfillment of the degree of **Doctor of Philosophy in Life Science** of **Homi Bhabha National Institute** is a record of her own research work carried by her. She has carried out her investigations for the last five years on the subject matter of the thesis under my supervision at **National Institute of Science Education and Research, Bhubaneswar**. To the best of our knowledge, the matter embodied in this thesis has not been submitted for the award of any other degree.

Signature of the Candidate

Suvasmita Rath
National Institute of Science
Education and Research (NISER)
Bhubaneswar, HBNI

Signature of the Supervisor

Dr Asima Bhattacharyya
Reader F
National Institute of Science
Education and Research (NISER)
Bhubaneswar, HBNI

List of Publications

- *1. Regulation of Noxa-mediated apoptosis in *Helicobacter pylori*-infected gastric epithelial cells. **S Rath**, L. Das, S.B. Kokate, B.M. Pratheek, S. Chattopadhyay, C. Goswami, R. Chattopadhyay, S.E. Crowe, A. Bhattacharyya. *FASEB J.* 2015 Mar; 29(3):796-806
- *2. Cobalt chloride-mediated protein kinase C α (PKC α) phosphorylation induces hypoxia-inducible factor 1 α (HIF1 α) in the nucleus of gastric cancer cell. #**S. Rath**, #A. Anand, N. Ghosh, L. Das, S. B. Kokate, P. Dixit, S. Majhi, N. Rout, S. P. Singh, A. Bhattacharyya. *Biochem Biophys Res Commun.* 2016 Feb 26; 471(1):205-12
- *3. Inhibition of histone/lysine acetyltransferase activity kills CoCl₂-treated and hypoxia-exposed gastric cancer cells and reduces their invasiveness. **S. Rath**, L. Das, S. B. Kokate, N. Ghosh, P. Dixit, N. Rout, S. P. Singh, S. Chattopadhyay, H. Ashktorab, D. T. Smoot, M. M. Swamy, T. K. Kundu, S. E. Crowe, A. Bhattacharyya. *International Journal of Biochemistry & Cell Biology* volume 82, January 2017, 28-40
4. ETS2 and Twist1 promote invasiveness of *Helicobacter pylori*-infected gastric cancer cells by inducing Siah2. L. Das, S. B. Kokate, **S. Rath**, N. Rout, S. P. Singh, S. E. Crowe, A. K. Mukhopadhyay, A. Bhattacharyya. *Biochemical Journal* 473 (11), 1629-1640 (2016)
5. Membrane-bound β -catenin degradation is enhanced by ETS2-mediated Siah1 induction in *Helicobacter pylori*-infected gastric cancer cells. L. Das, S. B. Kokate, **S. Rath**, P. Dixit, N. Rout, S.P. Singh, S. E. Crowe, A. Bhattacharyya. (*Communicated-2016*)

(* pertaining to this thesis; # shared 1st authors)

Suvasmita Rath

Conference Presentations

1. Regulation of Mitochondria-Mediated Apoptosis Induction in Hypoxic Gastric Epithelial Cancer Cells. **S. Rath**, S.B. Kokate, L. Das, T.K. Kundu, S.P. Singh, A. Bhattacharyya. *Cell Symposia: Multifaceted Mitochondria, P 1.088, 2015 – Chicago, IL, USA.*
2. Regulation of Apoptosis induction in hypoxic gastric epithelial cancer cells with metastatic property. **S. Rath**, L. Das, S.B. Kokate, T.K. Kundu, S.P. Singh, A. Bhattacharyya. *2nd international conference on frontiers in Biological Sciences (InCoFIBS-2015), NIT Rourkela, India.*
3. Selective killing of hypoxic gastric epithelial cancer cells showing metastatic properties. **S. Rath**, L. Das, S.B. Kokate, T.K. Kundu, S.P. Singh, A. Bhattacharyya. *2nd International meet on advanced studies on cell signaling network (CeSiN-2014, IL-20)IICB, Kolkata, India.*
4. Regulation of *Helicobacter pylori* mediated gastric cancer: a prospective on Siah2. L. Das, S.B. Kokate, **S. Rath**, S. P. Singh, A. Bhattacharyya. *2nd International meet on advanced studies on cell signaling network (CeSiN-2014, OP-7), IICB, Kolkata, India.*
5. Regulation and role of the E3 ubiquitin ligase SIAH1 in *Helicobacter pylori* mediated gastric cancer. L. Das, S. B. Kokate, **S. Rath**, S. P. Singh, A. Bhattacharyya. *2nd International meet on advanced studies on cell signaling network (CeSiN-2014, PP-1),IICB, Kolkata, India.*
6. *Helicobacter pylori* Protect Gastric Epithelial Cancer Cells from Apoptosis. **S. Rath**, L. Das, R. Chattopadhyaya, S.E. Crowe, A. Bhattacharyya. *81st Annual Meeting of the Society of Biological Chemists (SBC: 2012) and Symposium on Chemistry and Biology, Kolkata, India (IL 19.1(O): CB 04).*
7. Regulation of hypoxia-inducible factor 1 α in gastric cancer metastasis. **S. Rath**, L. Das, T.K. Kundu, A. Bhattacharyya. *81st Annual Meeting of the Society of Biological Chemists (SBC: 2012) and Symposium on Chemistry and Biology, Kolkata, India PP: CBC16.*

Dedicated to.....

My Family

Acknowledgment

I express my deepest gratitude to my supervisor Dr. Asima Bhattacharyya for her supervision, advice, guidance and encouragement throughout my research tenure. Her punctuality and dedication towards research encouraged me to work hard and to achieve my goal.

I wish to express my sincere thanks to the director Prof. V. Chandrashekar, NISER, for giving me an opportunity to work in this institute. I am very much thankful to my doctoral committee members Prof. Jagneshwar Dandapat, Dr. Subhasis Chattopadhyaya, Dr. Chandan Goswami, Dr. Harapriya Mohapatra and the PGCS convenor Dr. Tirumala K. Chowdary for their continuous advice and valuable suggestions during my work. I would like to thank Prof. Shivaram Prasad Singh of SCB Med College, Cuttack and Dr. Niranjana Rout, AHRCC, Cuttack for providing tissue samples used in this study. My special thanks also go to Prof. Tapas K Kundu for providing a crucial reagent, CTK7A for the study. I am very much thankful to Indian council of medical research (ICMR) for the fellowship.

I am thankful to my lab mates Mrs. Lopamudra Das, Mr. Shrikant B Kokate, Mr. Pragyesh Dixit, Mr. Nilabh Ghosh, Mr. Aditya Anand and Mr. Indrajit Poirah for their timely help. I enjoyed the company of all my friends (especially Mrs. Anantara Garai and Miss Sushmita Shukla) and seniors who have made my stay pleasant at NISER. I acknowledge the central instrumentation facilities, computer centre, library staff and timely help received from the academic, non-academic staff at NISER (Homi Bhabha National Institute (HBNI)).

I am very much thankful to all the faculty members and staff of SBS for their blessings and encouragement. I sincerely appreciate the help received from all the scientists who gifted plasmids constructs, antibodies and reagents used in this study.

I would like to express my unfailing gratitude to my husband Dr. Ashutosh Rath for his continuous moral and mental support for completion of my PhD work.

Finally, but not the least, I am very much thankful to my parents for their unconditional love, blessings and endless support without which it would have been difficult to achieve my goal. My gratitude goes to my father-in-law and mother-in-law and all other family members for their inspiration and assistance at every step. I am also thankful to my elder sister, brother-in-law and younger brother for their continuous encouragement and support.

Above all, thanks to the Almighty for every blessing, strength and wisdom to complete this work.

Suvasmita Rath

CONTENTS

	Page No.
SYNOPSIS	i-x
Abbreviations	xi-xv
List of figures	xvi-xvii
List of tables	xviii
<i>Chapter 1. INTRODUCTION</i>	1-17
Section A. Factors regulating gastric cancer epithelial to mesenchymal transition (EMT) and metastasis progression	
1.A.1. Overview of gastric cancer	2
1.A.2. Etiology	2
1.A.3. Overview of metastasis	3
1.A.4. EMT	4-5
1.A.5. EMT and metastasis progression in gastric epithelial cancer cells (GECs)	5-6
1.A.6. Hypoxia: as a regulator of EMT and metastasis	
(a) Physiological hypoxia	7-8
(b) Chemical hypoxia	8
1.A.7. <i>H. pylori</i> : an inducer of EMT and metastasis	
(a) An overview	8-9
(b) Epidemiology and transmission	9
(c) Pathogenesis	9-10
(d) Role of <i>H. pylori</i> in EMT progression	10-11
1.A.8. Hif1	11

(a) Domain structure of Hif1	11-12
(b) Hif1 α , p300 and their roles in cancer progression	12-13
Section B. Apoptosis as a negative-regulator of metastasis progression	
1.B.1. Apoptosis: An overview	14-15
1.B.2. Noxa-mediated apoptosis induction	15-16
1.B.3. ROS-mediated apoptosis induction	16
1.B.4. Apoptosis in metastatic cells	16-17
1.B.5. Apoptosis induction in metastatic cells	17
1.C. Objectives of the study	17
Chapter 2. MATERIALS and METHODS	18-43
2.1 MATERIALS	
2.1.1. Cell lines and reagents	19
2.1.2. Constructs and antibodies	19
2.1.3. Tissue samples	19
2.2. METHODOLOGY	
2.2.1. Maintenance of GECs	19-20
2.2.2. Freezing and revival of cell lines	20
2.2.3. Maintenance of <i>H. pylori</i> culture	20
2.2.4. Cloning, expression and mutagenesis	
Cloning and expression of human <i>noxa</i> gene	21
Primer designing	21
Polymerase chain reaction and cloning of human <i>noxa</i> gene	21
PCR	21-22
Agarose gel electrophoresis and gel extraction of the PCR product	22
PCR purification method	22

Restriction digestion of PCR purified product	23
DNA ligation	23
Transformation	23-24
Selection of positive clones	24
Miniprep plasmid isolation	24-25
Generation of S13A mutant of Noxa by site-directed mutagenesis	25-26
Maxiprep plasmid isolation	26-27
2.2.5. Transfection of cell lines	27-28
2.2.6. Infection of GECs with <i>H. pylori</i>	29
2.2.7. Exposure of cells to chemical hypoxia induced by CoCl ₂ .6H ₂ O, physiological hypoxia and a HAT inhibitor (CTK7A)	29
2.2.8. Whole cell lysate preparation	29
2.2.9. Mitochondrial and cytosolic lysate preparation	30
2.2.10. Nuclear and cytosolic lysate preparation	30-31
2.2.11. Sodium dodecyl sulfate polyacrylamide gel electrophoresis (SDS-PAGE)	31-34
2.2.12. Immunoblotting	34-36
2.2.13. Immunoprecipitation (IP) assays	36-37
2.2.14. Generation of stable cell lines	37-38
2.2.15. Confocal microscopy	38-39
2.2.16. Sectioning of gastric biopsy tissue samples	39
2.2.17. Immunofluorescence microscopy	39-40
2.2.18. Flow cytometry	40
2.2.19. Trypan blue dye-exclusion assay	40

2.2.20. Detection of reactive oxygen species (ROS)	40-41
2.2.21. Soft agar assay	41
2.2.22. Scratch assay or wound-healing assay	42
2.2.23. Transwell migration and invasion assay	42-43
2.2.24. Densitometric and statistical analysis	43

RESULTS **44-100**

Chapter 3: Apoptosis induction in hypoxic GECs expressing EMT markers and showing invasive properties

3.1. Hif1 α and metastatic markers are upregulated in CoCl ₂ -treated GECs	45-46
3.2. Hif1 α and EMT markers are upregulated in metastatic gastric cancer biopsy samples	46-47
3.3. Inhibition of HAT activity downregulates expression of Hif1 α in CoCl ₂ -treated GECs	47-48
3.4. HAT inhibition downregulates EMT markers expression in chemically-induced and physiological hypoxia	49-50
3.5. Metastatic property of GECs are suppressed in CoCl ₂ and HAT inhibitor-treated cells	51-54
3.6. Inhibition of HAT activity induces Noxa expression in CoCl ₂ -treated hypoxic GECs	54-57
3.7. HAT inhibition induces Noxa translocation to mitochondria and Cyt <i>c</i> release in CoCl ₂ -treated GECs	57-60
3.8. Induction of intrinsic apoptotic pathway in CoCl ₂ and CTK7A-treated GECs	60-63
3.9. Noxa upregulation is independent of Hif1 α expression in CTK7A and CoCl ₂ - treated hypoxic GECs	63-64

3.10. HAT inhibition induces H ₂ O ₂ generation in CoCl ₂ -treated GECs	64-66
3.11. H ₂ O ₂ induces p38 MAPK-mediated Noxa induction in CTK7A and CoCl ₂ -treated GECs	66-68
3.12. Discussion	69-70
Chapter 4: Role of <i>H. pylori</i> in inducing antiapoptotic pathways in GECs	71-90
4.1. <i>H. pylori</i> infection induces Noxa expression without downregulating Mcl1 in human GECs	72-73
4.2. <i>H. pylori</i> infection induces Noxa phosphorylation at S ¹³ residue in GECs	73-75
4.3. Cloning, expression and S13A mutation of <i>noxa</i> gene	75-76
4.4. JNK phosphorylation induces Noxa phosphorylation at S ¹³ residue in <i>H. pylori</i> -infected GECs	76-80
4.5. Inhibition of Noxa phosphorylation at S ¹³ induces Mcl1 degradation and mitochondria-mediated intrinsic apoptotic pathway in <i>H. pylori</i> -infected GECs	80-82
4.6. Phosphorylation deficient Noxa S ¹³ mutant induces mitochondrial fragmentation in <i>H. pylori</i> -infected GECs	83-85
4.7. Effect of Noxa dephosphorylation on apoptosis of <i>H. pylori</i> -infected GECs	85-87
4.8. Discussion	88-90
Chapter 5: Effect of HAT/KAT inhibition in <i>H. pylori</i>- infected metastatic GECs	91-100
5.1. HAT/KAT inhibition suppresses <i>H. pylori</i> -mediated	

expression of EMT markers in GECs	92-93
5.2. <i>H. pylori</i> -mediated enhancement in GEC invasion and migration are downregulated by HAT inhibition	94-95
5.3. Noxa expression is induced in HAT inhibitor-treated and <i>H. pylori</i> -infected GECs	95-97
5.4. Induction of the intrinsic apoptotic pathway in CTK7A-treated and <i>H. pylori</i> -infected GECs	97-99
5.5. Discussion	100
Chapter 6. SUMMARY AND CONCLUSION	101-104
BIBLIOGRAPHY	105-131
APPENDIX	132-136
PUBLICATIONS	



HOMI BHABHA NATIONAL INSTITUTE

PhD PROGRAMME

- | | |
|---|---|
| 1. Name of the Student | : Suvasmita Rath |
| 2. Name of the Constituent Institution | : National Institute of Science Education and Research (NISER) |
| 3. Enrolment No. | : LIFE11201004016 |
| 4. Title of the Thesis | : Factors Regulating Epithelial-Mesenchymal Transition and Metastasis of Gastric Cancer |
| 5. Board of studies | : Life Sciences |

SYNOPSIS

This thesis work reports the molecular events initiated by two major factors responsible for gastric carcinogenesis, hypoxia and *Helicobacter pylori* in promoting epithelial to mesenchymal transition and metastasis. As the spreading of malignant cells is restricted by apoptosis induction, this work identifies the interaction of programmed cell death with gastric cancer metastasis.

Gastric cancer is one of the prevalent cancers in the modern industrialized world. Many factors are involved in gastric cancer progression but nearly more than 80% of the cases have been attributed to *H. pylori* infection (1). Primary tumors migrate to the distant organs through metastasis attributing to the systemic nature and treatment failure prevalent in cancer (2-4). Metastasis proceeds through several steps which include local invasion, intravasation, survival in the circulation, extravasation and colonization (5). Epithelial to mesenchymal transition (EMT) is the first event that happens during metastasis in which epithelial cells possessing cancerous properties can shed their epithelial characteristics and get transformed into mesenchymal cells. EMT promotes the invasive and migratory properties of cancer cells and helps in the development of distant metastasis (6). Hypoxia inducible factor 1 α (Hif1 α) is a transcription factor which is induced in hypoxia also plays a major role in EMT and metastasis process (7, 8). p300 is a transcriptional cofactor for Hif1 α which has histone/lysine acetyl transferase (HAT/KAT) activity and plays a crucial role as a tumor suppressor as well as a proto-oncogene (9). Chemical hypoxia can be induced by cobalt chloride hexahydrate (CoCl₂.6H₂O) which has similar biochemical response as that of physiological hypoxia (10, 11). Apart from hypoxia, *H. pylori* is another major factor which induces EMT and metastasis in GECs (12, 13). *H. pylori* is a Gram-negative bacteria which colonizes in the human stomach leading to gastritis, gastric and duodenal ulcers, gastric carcinoma and mucosa-associated lymphoid tissue (MALT) lymphoma (14). *H. pylori* induce reactive oxygen species (ROS) generation which stabilizes Hif1 α in normoxic condition (15, 16). *H. pylori* infection also enhances the expression of the Bcl2 family antiapoptotic and tumorigenic protein, myeloid cell leukemia 1 (Mcl1), and a proapoptotic BH3-only tumor-suppressor protein Noxa. Both of these proteins contain hypoxia-response elements (HREs) in their promoters (17, 18). Maintenance of Mcl1 and Noxa balance is a very crucial parameter for cell survival and apoptosis. Killing of metastatic GECs is a hard to achieve

goal in terms of therapy since metastatic cells mostly resist apoptosis. This thesis work focuses to understand the role of hypoxia and *H. pylori* infection in regulation of gastric cancer EMT and metastasis. Inhibition of HAT activity as well as Hif1 α activity however, were achieved by treating hypoxic or *H. pylori*-infected cells with a HAT/KAT inhibitor.

This thesis has been organized in six chapters and contents of each chapter have been discussed as follows.

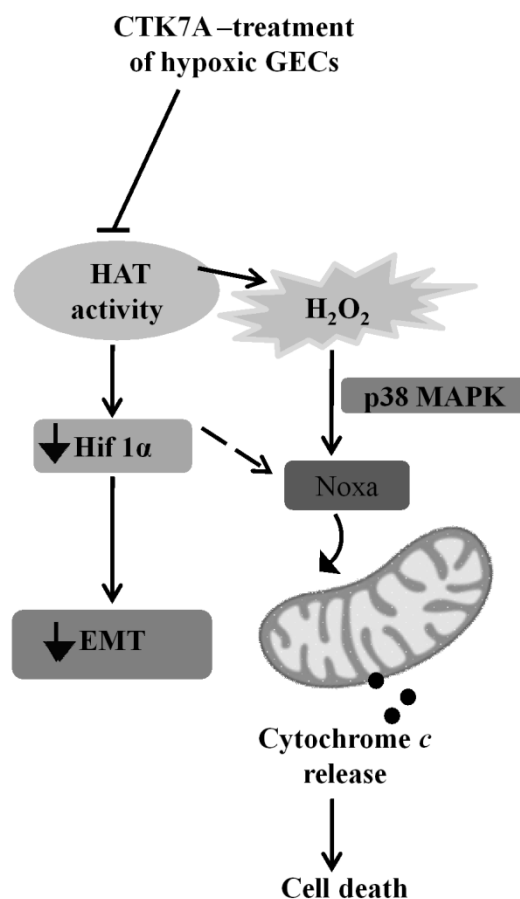
Chapter 1 (Introduction): This chapter provides an introduction to the thesis which includes a brief overview of gastric cancer, EMT and metastasis. It also focuses on two important factors that drive the EMT process which are hypoxia and *H. pylori* infection. Both of these factors induce Hif1 α for which p300 acts as a transcriptional cofactor. p300 has a histone acetyl transferase (HAT) activity which is crucial for cell signalling events. Hif1 α induces the expression of several EMT markers such as Twist1, N-cadherin, SNAIL etc. and actively participates in the metastasis process. This chapter also explains various pathways involved in selective apoptosis induction in metastatic cells.

Chapter 2 (Experimental methodologies): This chapter covers the details on the methodologies employed to accomplish the objectives of this thesis work. It includes the description of various cell lines, reagents, chemicals and tissue samples used for the work. CoCl₂.6H₂O has been used as a chemical inducer of hypoxia. BD GasPak EZ gas generating system has been used to generate physiological hypoxia (1% oxygen). CTK7A [(Sodium 4-(3, 5-bis (4-hydroxy-3-methoxystyryl)-1H-pyrazol-1-yl) benzoate], a curcumin-derived water soluble HAT/KAT and p300 auto-acetylation inhibitor (19) have been extensively used for this work. This chapter describes all cell culture techniques which include maintenance of various gastric epithelial cancer cell lines as well as maintenance of *H. pylori* culture.

This chapter also describes several molecular biology techniques including cloning of proapoptotic gene Noxa, introducing mutation in Noxa by site-directed mutagenesis and

characterization of Noxa S13A mutant by western blotting, immunoprecipitation assay, flow cytometry and confocal microscopy. *In vitro* binding assay has been described to show molecular interaction between proteins. Detailed methodology for stable cell line generation has also been explained. Invasion assay, migration assay, soft agar assay, wound-healing assay has been described which are done to study the metastatic properties of GECs under different experimental conditions. Experimental details that were used to study human gastric biopsy samples by immunofluorescence microscopy have been presented in this chapter.

Chapter 3 (Selective apoptosis induction in hypoxic GECs expressing EMT markers and metastasis property): Chapter 3 establishes the role of hypoxia in gastric carcinogenesis. In this work, BD GasPak EZ Gas Generating Pouch System was used to generate 1% oxygen that creates physiological hypoxia and $\text{CoCl}_2 \cdot 6\text{H}_2\text{O}$ was used as a chemical mimetic agent for hypoxia. Hypoxia induces expression of Hif1 α and other EMT markers such as Twist1, N-Cadherin etcetera. p300 which is one of the transcriptional coactivator of Hif1 α which has Histone acetyl transferase (HAT) activity. Inhibition of p300 HAT activity by CTK7A in hypoxic cells downregulated expression of Hif1 α and other EMT markers. HAT inhibition also upregulated Noxa expression in hypoxic GECs as well as hypoxic primary cells. As Hif1 α binds to the HRE region of Noxa (20) promoter, we expected decreased expression of Noxa with suppression of Hif1 α . Surprisingly, we did not observe any changes in Noxa expression in Hif1 α suppressed hypoxic cells after HAT inhibition. We also observed that HAT inhibition induced ROS generation and p38 activation which in turn activated Noxa expression and intrinsic cell death selectively in hypoxic cells. Thus, we reported for the first time HAT inhibition induced Noxa-mediated apoptosis in hypoxic GECs.

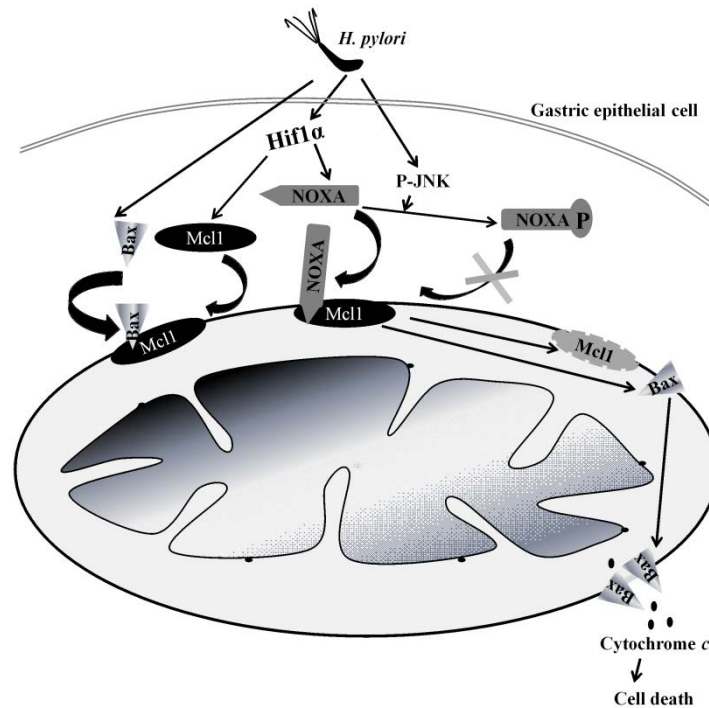


Scheme 1. Mechanism of CTK7A-mediated apoptosis induction in hypoxic GECs.

Inhibition of HAT activity downregulates Hif1 α expression and reduces expression of EMT markers leading to suppression of metastatic property of hypoxic GECs. Apoptotic killing of these hypoxic metastatic GECs is achieved by H₂O₂ generation and activation of p38 MAPK which subsequently increases Noxa expression in CTK7A treated GECs. Noxa is translocated to mitochondria and induces intrinsic apoptosis pathway. Curved arrow= mitochondrial translocation; solid-headed arrow= down-regulation; \Rightarrow dotted arrow= minor pathway, arrow-headed= activation; blunt end-headed= inhibition.

Chapter 4 (Role of *H. pylori* in cell survival mechanism in GECs): This chapter describes the role of *H. pylori* in gastric cancer. The BH3-only apoptotic protein Noxa binds with the anti-apoptotic protein Mcl1 and forms a complex that is targeted for proteasomal degradation. Thus, Noxa functions as a critical regulator of apoptosis in Mcl1-expressing cells (21). *H. pylori* infection also induces ROS generation and Hif1 α stabilization in normoxic condition

(16). Both Mcl1 and Noxa contain HREs in their promoters and hence interact with Hif1 α (17, 22). We have observed that Noxa phosphorylation at the 13th serine by c-Jun N-terminal kinase (JNK) inhibits mitochondrial translocation of Noxa and its interaction with Mcl1, thus protecting cells from intrinsic apoptosis pathway.



Scheme 2. Regulation of Noxa mediated apoptosis in *H. pylori*-infected GECs.

H. pylori-infection induces Hif1 α expression in GECs which enhances Noxa expression. *H. pylori* infection also induces mitochondrial translocation of Bax followed by its interaction with Mcl1. Non-phosphorylated form of Noxa has higher mitochondrial translocation potential which further displaces Bax from Mcl1 and induces Mcl1 degradation followed by Bax oligomerization and Cytochrome *c* release resulting in apoptosis. But Noxa phosphorylation at S¹³ residue by JNK is activated in *H. pylori*-infected GECs inhibits its mitochondrial translocation resulting in impairment of apoptosis. Curved arrow= translocation.

Chapter 5 (Effect of HAT inhibition on *H. pylori*-infected GECs expressing EMT markers): Chapter 5 explains the role of HAT inhibition on EMT regulation and apoptosis

induction in *H. pylori*-infected GECs. Previous findings explain the role of *H. pylori* in the progression of EMT in gastric cancer cells (13, 23, 24). We observed that upregulation of EMT markers such as N-cadherin and Twist1 in GECs upon *H. pylori* infection. Inhibition of HAT activity by CTK7A upregulated proapoptotic protein Noxa expression in *H. pylori*-infected GECs while downregulating expression of EMT markers. Whereas, uninfected GECs, that did not express metastatic markers, had significantly less apoptosis than infected GECs. Thus, we found that HAT inhibition selectively killed *H. pylori*-infected GECs which might provide a new insight in controlling GEC cancer.

Chapter 6 (Summary and Conclusion): Chapter 6 provides concluding remarks about our findings which demonstrate crucial role of hypoxia and *H. pylori* infection in regulating metastatic properties of GECs. Further, we show inhibition of HAT/KAT activity induces Noxa-mediated apoptosis selectively in *H. pylori*-infected and hypoxic gastric epithelial cancer cells.

REFERENCES

1. Nagini, S. (2012) Carcinoma of the stomach: A review of epidemiology, pathogenesis, molecular genetics and chemoprevention. *World journal of gastrointestinal oncology* **4**, 156-169
2. Leber, M. F., and Efferth, T. (2009) Molecular principles of cancer invasion and metastasis (review). *Int. J. Oncol.* **34**, 881-895
3. Chaffer, C. L., and Weinberg, R. A. (2011) A perspective on cancer cell metastasis. *Science* **331**, 1559-1564
4. Valastyan, S., and Weinberg, R. A. (2011) Tumor metastasis: molecular insights and evolving paradigms. *Cell* **147**, 275-292
5. Nguyen, D. X., Bos, P. D., and Massague, J. (2009) Metastasis: from dissemination to organ-specific colonization. *Nature reviews. Cancer* **9**, 274-284

6. Yang, J., and Weinberg, R. A. (2008) Epithelial-mesenchymal transition: at the crossroads of development and tumor metastasis. *Developmental cell* **14**, 818-829
7. Semenza, G. L. (2002) HIF-1 and tumor progression: pathophysiology and therapeutics. *Trends in molecular medicine* **8**, S62-67
8. Rankin, E. B., and Giaccia, A. J. (2008) The role of hypoxia-inducible factors in tumorigenesis. *Cell Death Differ.* **15**, 678-685
9. Goodman, R. H., and Smolik, S. (2000) CBP/p300 in cell growth, transformation, and development. *Genes Dev.* **14**, 1553-1577
10. Ji, Z., Yang, G., Shahzidi, S., Tkacz-Stachowska, K., Suo, Z., Nesland, J. M., and Peng, Q. (2006) Induction of hypoxia-inducible factor-1alpha overexpression by cobalt chloride enhances cellular resistance to photodynamic therapy. *Cancer Lett.* **244**, 182-189
11. Jeon, E. S., Shin, J. H., Hwang, S. J., Moon, G. J., Bang, O. Y., and Kim, H. H. (2014) Cobalt chloride induces neuronal differentiation of human mesenchymal stem cells through upregulation of microRNA-124a. *Biochem. Biophys. Res. Commun.* **444**, 581-587
12. Baud, J., Varon, C., Chabas, S., Chambonnier, L., Darfeuille, F., and Staedel, C. (2013) Helicobacter pylori initiates a mesenchymal transition through ZEB1 in gastric epithelial cells. *PloS one* **8**, e60315
13. Lee, D. G., Kim, H. S., Lee, Y. S., Kim, S., Cha, S. Y., Ota, I., Kim, N. H., Cha, Y. H., Yang, D. H., Lee, Y., Park, G. J., Yook, J. I., and Lee, Y. C. (2014) Helicobacter pylori CagA promotes Snail-mediated epithelial-mesenchymal transition by reducing GSK-3 activity. *Nature communications* **5**, 4423
14. Polk, D. B., and Peek, R. M., Jr. (2010) Helicobacter pylori: gastric cancer and beyond. *Nature reviews. Cancer* **10**, 403-414

15. Bhattacharyya, A., Chattopadhyay, R., Hall, E. H., Mebrahtu, S. T., Ernst, P. B., and Crowe, S. E. (2010) Mechanism of hypoxia-inducible factor 1 alpha-mediated Mcl1 regulation in Helicobacter pylori-infected human gastric epithelium. *American journal of physiology. Gastrointestinal and liver physiology* **299**, G1177-1186
16. Park, J. H., Kim, T. Y., Jong, H. S., Chun, Y. S., Park, J. W., Lee, C. T., Jung, H. C., Kim, N. K., and Bang, Y. J. (2003) Gastric epithelial reactive oxygen species prevent normoxic degradation of hypoxia-inducible factor-1alpha in gastric cancer cells. *Clin. Cancer Res.* **9**, 433-440
17. Piret, J. P., Minet, E., Cosse, J. P., Ninane, N., Debaq, C., Raes, M., and Michiels, C. (2005) Hypoxia-inducible factor-1-dependent overexpression of myeloid cell factor-1 protects hypoxic cells against tert-butyl hydroperoxide-induced apoptosis. *J. Biol. Chem.* **280**, 9336-9344
18. Wei, J., O'Brien, D., Vilgelm, A., Piazuelo, M. B., Correa, P., Washington, M. K., El-Rifai, W., Peek, R. M., and Zaika, A. (2008) Interaction of Helicobacter pylori with gastric epithelial cells is mediated by the p53 protein family. *Gastroenterology* **134**, 1412-1423
19. Arif, M., Vedamurthy, B. M., Choudhari, R., Ostwal, Y. B., Mantelingu, K., Kodaganur, G. S., and Kundu, T. K. (2010) Nitric oxide-mediated histone hyperacetylation in oral cancer: target for a water-soluble HAT inhibitor, CTK7A. *Chem. Biol.* **17**, 903-913
20. Rath, S., Das, L., Kokate, S. B., Pratheek, B. M., Chattopadhyay, S., Goswami, C., Chattopadhyay, R., Crowe, S. E., and Bhattacharyya, A. (2015) Regulation of Noxa-mediated apoptosis in Helicobacter pylori-infected gastric epithelial cells. *FASEB J.* **29**, 796-806

21. Alves, N. L., Derks, I. A., Berk, E., Spijker, R., van Lier, R. A., and Eldering, E. (2006) The Noxa/Mcl-1 axis regulates susceptibility to apoptosis under glucose limitation in dividing T cells. *Immunity* **24**, 703-716
22. Kim, J. Y., Ahn, H. J., Ryu, J. H., Suk, K., and Park, J. H. (2004) BH3-only protein Noxa is a mediator of hypoxic cell death induced by hypoxia-inducible factor 1alpha. *J. Exp. Med.* **199**, 113-124
23. Choi, Y. J., Kim, N., Chang, H., Lee, H. S., Park, S. M., Park, J. H., Shin, C. M., Kim, J. M., Kim, J. S., Lee, D. H., and Jung, H. C. (2015) Helicobacter pylori-induced epithelial-mesenchymal transition, a potential role of gastric cancer initiation and an emergence of stem cells. *Carcinogenesis* **36**, 553-563
24. Yin, Y., Grabowska, A. M., Clarke, P. A., Whelband, E., Robinson, K., Argent, R. H., Tobias, A., Kumari, R., Atherton, J. C., and Watson, S. A. (2010) Helicobacter pylori potentiates epithelial:mesenchymal transition in gastric cancer: links to soluble HB-EGF, gastrin and matrix metalloproteinase-7. *Gut* **59**, 1037-1045

ABBREVIATIONS

ADA2	Adenosine deaminase
APAF1	Apoptosis-activating factor 1
APS	Ammonium per sulfate
ARNT	Aryl hydrocarbon receptor nuclear translocator
ASPP2	Apoptosis stimulating protein 2
bHLB	Basic helix-loop-helix
Bcl-2	B-cell lymphoma 2
BH	Bcl-2 homology domains
BH3	Bcl-2 homology
BM	Basement membrane
BMDCs	Bone marrow derived cells
BSA	Bovine serum albumin
Cag	Cytotoxin-associated antigen
CDH1	Cadherin1
CH	Cysteine and histidine
ChIP	Chromatin immunoprecipitation
CKD	Chronic kidney disease
c-Myc	Myelocytomatosis oncogene
CoCl ₂	Cobalt chloride
COX	Cyclooxygenase
CREB	cAMP-response element binding protein
CT	Computed tomography

CTK7A	Sodium 4-(3,5-bis(4-hydroxy-3-methoxystyryl)1H pyrazol-1-yl) benzoate
Cyt <i>c</i>	Cytochrome <i>c</i>
DCFDA	2',7' –dichlorofluorescein diacetate
DMSO	Dimethyl sulfoxide
ECs	Endothelial cells
ECM	Extra cellular matrix
EDTA	Ethylene-diamine-tetra-acetic acid
EGTA	Ethyleneglycol-bis (b-aminoethylether)- N, N, N', N'-tetra-acetic acid
EMSA	Electrophoretic mobility shift assay
EMT	Epithelial to mesenchymal transition
ERK	Extracellular signal-regulated kinase
FBS	Fetal bovine serum
FGF2	Fibroblast growth factor 2
FOX	Forkhead box
GEC	Gastric epithelial cell
H	Hour
HAT	Histone acetyl transferase
HEPES	N-(2-hydroxyethyl) piperazine Na-2- ethanesulfonic Acid
Hif	Hypoxia-inducible factor
H ₂ O ₂	Hydrogen peroxide
<i>H. pylori</i>	<i>Helicobacter pylori</i>
HRE	Hypoxia-response element

HRP	Horseradish peroxidase
ID	Inhibitory domain
IHC	Immunohistochemistry
IGF-1	Insulin-like growth factor 1
ILK	Integrin-linked kinase
JNK	c-jun N-terminal kinase
KLF8	Krüppel-like factor 8
MALT	Mucosa-associated lymphoid tissue
MAP	Mitogen-activated protein
MAPK	Mitogen-activated protein kinase
Mcl1	Myeloid cell leukemia 1
MEK	MAPK/ERK kinase
MET	Mesenchymal to epithelial transition
miRNA	MicroRNA
MMPs	Matrix metalloprotease
MOI	Multiplicity of infection
Mut	Mutant
NFDM	Non-fat-dry milk
NF- κ B	Nuclear factor- κ B
NLS	Nuclear localization signal
O ₂	Oxygen
OD	Optical density
PAGE	Polyacrylamide gel electrophoresis
PAMP1	Phorbol-12-myristate-13-acetate-induced protein 1
PAI	Pathogenicity island

PAS	PER-ARNT-SIM
PBS	Phosphate-buffered saline
PCR	Polymerase chain reaction
PDGF-B	Platelet-derived growth factors B
PET	Positron-emission tomography
PFA	Paraformaldehyde
PI 3	Phosphoinositide 3
P-Noxa	Phosphorylated Noxa
PVDF	Polyvinylidene fluoride
RECK	Reversion-inducing-cysteine-rich protein with kazal motifs
Ref	Reference
RT	Room temperature
RTKs	Receptor tyrosine kinases
RUNX	Runt-related transcription factor3
ROS	Reactive oxygen species
SDS	Sodium dodecyl sulphate
shRNA	Short hairpin RNA
SIP1	Smad-interacting protein 1
siRNA	Short interfering RNA
SUMO	Small ubiquitin like modifier proteins
rRNA	Ribosomal RNA
TAD	Trans activation domain
TBS	Tris-buffered saline
TE	Tris-EDTA

TEM	Trans-endothelial migration
TEMED	N, N, N', N'-Tetramethylethylenediamine
TFSS	Type IV secretion system
TGF β	Transforming growth factor β
TID	Transcriptional Inhibitory domain
TSA	Trypticase soy agar
Vac A	Vacuolating cytotoxin A
VCAM1	Vascular cell adhesion molecule 1
VEGF	Vascular endothelial growth factor
WT	Wild type
ZEB1	Zinc finger E-box-binding homeobox 1
ZEB2	Zinc finger E-box-binding homeobox 2
ZNF-139	Zinc finger protein 139

LIST OF FIGURES

	Figure description	Page No.
Figure 1.1	Risk factors for gastric cancer	2
Figure 1.2	Mechanism of metastasis progression	4
Figure 1.3	EMT and MET markers	5
Figure 1.4	Domain structure of Hif1 protein	12
Figure 1.5	Domain structure of p300 protein	13
Figure 1.6	Apoptosis pathways	14
Figure 1.7	Apoptosis acts as a negative regulator of metastasis	17
Figure 3.1	Induced expression of Hif1 α and EMT markers in CoCl ₂ -treated GECs	46
Figure 3.2	Expression pattern of metastatic factors in metastatic cancer biopsy samples	47
Figure 3.3	Effect of HAT inhibition on Hif1 α expression in CoCl ₂ -treated GECs	48
Figure 3.4	Effect of HAT inhibition on EMT marker expression in chemically-induced and physiological hypoxia	50
Figure 3.5	HAT inhibition suppresses metastatic properties in CoCl ₂ -treated GECs	52-53
Figure 3.6	Noxa induction in CTK7A-treated and hypoxic GECs	55-57
Figure 3.7	CTK7A induced mitochondrial translocation of Noxa in CoCl ₂ -treated GECs	58-59
Figure 3.8	CTK7A induced Cyt <i>c</i> release in CoCl ₂ -treated GECs	60
Figure 3.9	Mitochondrial morphology of HAT inhibitor and CoCl ₂ -treated GECs	61
Figure 3.10	Intrinsic apoptotic cell death in CTK7A and CoCl ₂ -treated GECs	62
Figure 3.11	Noxa upregulation is independent of Hif1 α status in CTK7A and CoCl ₂ - treated hypoxic GECs	64
Figure 3.12	CTK7A-mediated ROS generation in CoCl ₂ -treated GECs leads to increase Noxa expression	65

Figure 3.13	H ₂ O ₂ induces p38 MAPK-mediated Noxa upregulation in CTK7A and CoCl ₂ -treated GECs	67
Figure 4.1	Concurrent expression of Noxa and McI1 in <i>H. pylori</i> -infected GECs	72
Figure 4.2	Noxa phosphorylation by <i>H. pylori</i> is independent of CagA status	74
Figure 4.3	Cloning, expression and mutation of <i>noxa</i>	76
Figure 4.4	Noxa phosphorylation at S ¹³ residue was induced by JNK1 and JNK2 in <i>H. pylori</i> -infected GECs	78-79
Figure 4.5	Effect of S13A Noxa mutant on intrinsic apoptotic pathway	81
Figure 4.6	Noxa S13A mutant transfection enhances mitochondrial fragmentation in <i>H. pylori</i> -infected GECs.	84
Figure 4.7	S13A-mutated Noxa enhances <i>H. pylori</i> -mediated apoptosis in AGS cells	86
Figure 5.1	Effect of HAT/KAT inhibition on <i>H. pylori</i> -induced EMT marker expression	93
Figure 5.2	Metastatic properties of <i>H. pylori</i> -infected GECs were downregulated by HAT inhibition	94
Figure 5.3	Status of Noxa in CTK7A treated and <i>H. pylori</i> -infected GECs	96
Figure 5.4	Activation of intrinsic apoptotic pathway in HAT inhibitor treated <i>H. pylori</i> -infected GECs	98
Figure 6.1	Pictorial depiction of selective apoptosis induction in hypoxic GECs expressing EMT markers and metastasis property	102
Figure 6.2	Regulation of Noxa mediated apoptosis in <i>H. pylori</i> -infected GECs	103

LIST OF TABLES

	Table description	Page no.
Table 1.	Components used for PCR amplification of <i>nox</i> a gene	21
Table 2.	Reaction conditions for PCR amplification of <i>nox</i> a gene	21
Table 3.	Components used for restriction digestion	23
Table 4.	Components used for ligation	23
Table 5.	Components of site-directed mutagenesis reaction	26
Table 6.	PCR reaction conditions of site directed mutagenesis reaction	26
Table 7.	Parameters for transient transfection	28
Table 8.	Buffers used in NE-PER isolation	31
Table 9.	Composition of resolving gels	32
Table 10.	Composition of stacking gels	33

INTRODUCTION

Chapter 1

Section A: Factors regulating gastric cancer epithelial to mesenchymal transition (EMT) and metastasis progression

1.A.1. Overview of gastric cancer

Gastric cancer is ranked as the fourth most common cancer and the second most common cause of cancer-related deaths. Globally, more than 700,000 people die every year from this disease (1). Rate of gastric cancer incidence is two to three fold more in males as compared to females. The highest incidences are observed in East Asia, East Europe, and South America, while the lowest rates are observed in North America and most part of Africa (2). In India, stomach cancer is the fifth leading cancer in males and the seventh in females (3). Progression of gastric adenocarcinoma is a multistep process which includes chronic gastritis, atrophy, intestinal metaplasia, dysplasia, and cancer (4).

1.A.2. Etiology

Many factors are involved in gastric cancer progression, but nearly more than 80% of the cases have been associated with *Helicobacter pylori* infection (5). According to the International Agency for Research in Cancer (IARC), *H. pylori* have been classified as a type I carcinogen for gastric cancer (6). Near about half of the world's population are found to be infected with *H. pylori* and 1-3% of them develop gastric cancer (7-9). In addition, diet, lifestyle, genetic, socioeconomic and other factors contribute to gastric carcinogenesis (10).

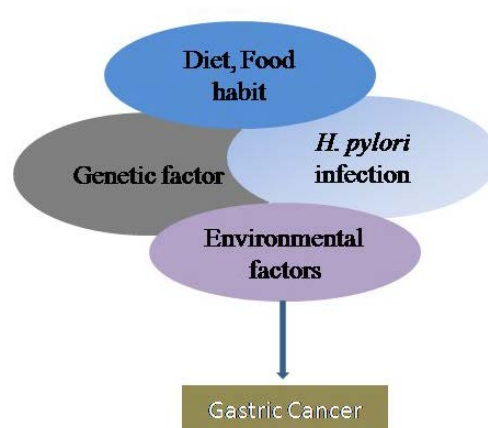


Figure 1.1. Risk factors for gastric cancer

1.A.3. Overview of metastasis

Metastasis is the phenomena in which cancer cells from the primary tumor mass leave the origin and migrate to lymphatics and distant organs (11, 12). Metastatic tumor cell shows resistance to therapeutic agents and enhances systemic nature which induces spreading of cancer (13). Metastasis proceeds through several steps which include local invasion, intravasation, survival of the invading cells in the circulation, extravasation and colonization in the new destination tissue (14). The metastatic cascade starts with local invasion which includes physical dislocation of cancer cells from the primary tumor site and invasion through the surrounding tissue. The second step is intravasation during which invasive tumor cells penetrate the lumina of the lymphatics or blood vessels. After successful intravasation, circulating tumor cells reside in the venous and arterial circulation for a brief time period. The next step is the extravasation in which the circulating cancer cells enter in the tissue parenchyma by rupturing the endothelial wall and the pericyte layer. The extravasation step begins with the attachment of cancer cells to endothelial cells (ECs) followed by the trans-endothelial migration (TEM). Extravasated cancer cells inhabit in the distant organs and form micro-metastases after being adapted within the new niche. The final step in the metastasis process is the metastatic colonization which includes the establishment and outgrowth of cancer cells at the distant site. These micro-metastases survive and proliferate in the distant organs and cause formation of new metastatic masses (13, 15). Various events in the metastasis progression are schematically summarized in Figure 1.2. The EMT acts as a driving force for metastasis progression which is discussed in subsequent sections.

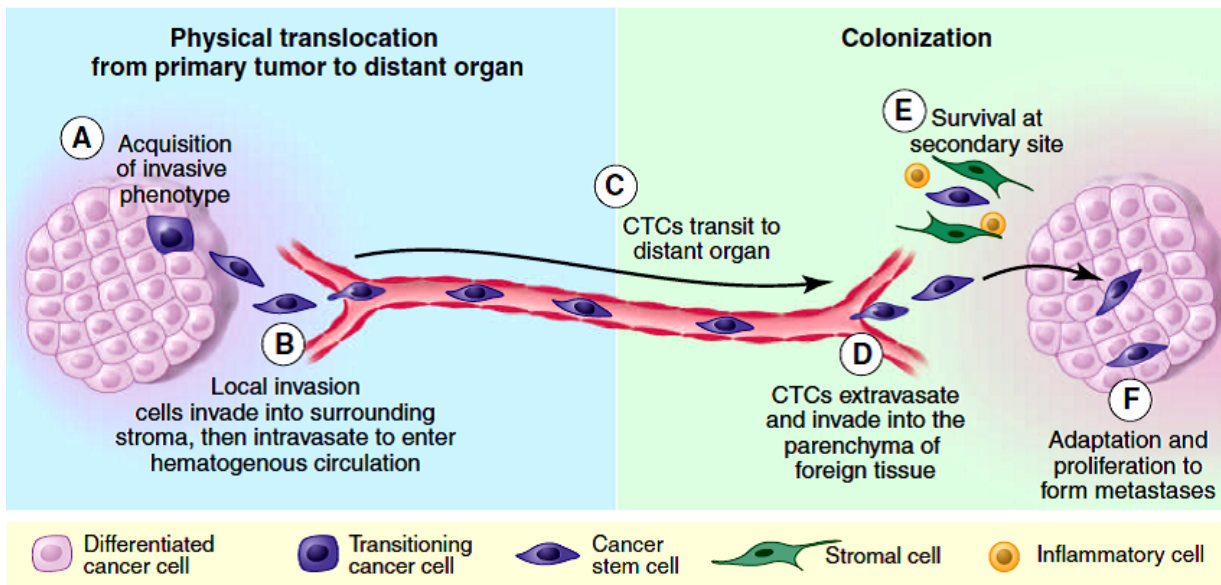


Figure 1. 2. Mechanism of metastasis progression (Courtesy: Ref 11).

1.A.4. EMT

EMT, apart from its extensive role in the embryogenesis and several developmental processes, plays a crucial role in metastasis progression. During EMT, epithelial cells possessing cancerous properties attend mesenchymal cell shape and acquire mesenchymal properties. EMT promotes invasiveness and motility of cancer cells and helps in the development of distant metastasis (16). Mesenchymal to epithelial transition (MET) is the reverse process of EMT in which cancer cells regain their epithelial nature and take part in establishing distant metastasis (17). Various factors involved in the EMT and MET processes are depicted in Figure 1.3.

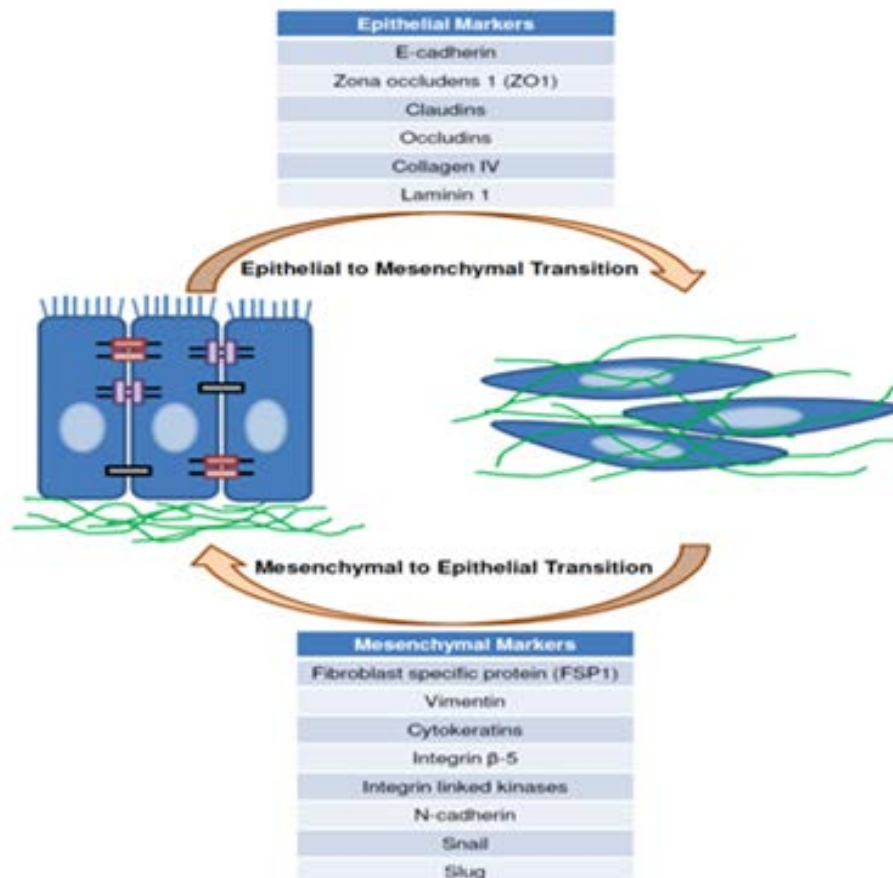


Figure 1.3. EMT and MET markers

1.A.5. EMT and metastasis progression in gastric epithelial cells (GECs)

Metastasis of gastric cancer is the most common cause of poor prognosis of the disease. Deregulation of different signaling pathways leads to metastasis. Some of these are discussed here. Epithelial property of gastric cancer cells are determined by sequential arrangement of adherence junction, tight junction and desmosomes. Formation of adherence junction depends on E-cadherin synthesis which is encoded by cadherin 1 (*CDH1*) gene. Due to aberrant EMT progression, E-cadherin synthesis switch gets shifted to N-cadherin formation which is a mesenchymal marker. This event finally leads to change in cell shape as well as motility and spreading of cancer (18, 19). Another important signaling pathway which regulates EMT is transforming growth factor- β (TGF- β)-mediated signaling. TGF- β is a cytokine that induces

metastatic property of cells by inducing its anchorage-independent growth (20). Apart from signaling pathways, several transcriptional factors are also involved in the metastasis regulation. Zinc finger protein 139 (ZNF-139) is one of the transcription factors which induces tumor metastasis and invasiveness of GECs (21). Another EMT-inducing transcription factor is forkhead box C2 (FOXC2) regulated by small ubiquitin-like modifier proteins (SUMO1)/Sentrin/(suppressor of mif two 3) SMT3-specific peptidase 3 (SEN3), a redox-sensitive SUMO2/3-specific protease. Many mesenchymal genes are expressed through the transcriptional activity of FOXC2 which is regulated by SEN3 through de-SUMOylation (22). Krüppel-like factor 8 (KLF8) is a transcriptional repressor which is expressed in gastric cancer tissues and induces EMT by activating Hypoxia inducible factor 1 (Hif1) in hypoxic cells (23). Calcium/calmodulin-dependent protein kinase II activates nuclear factor κ B (NF κ B) and protein kinase B or Akt which in turn induces matrix metalloproteinase-9 (MMP9) production and metastasis induction in gastric epithelial cancer cells (24).

Apart from transcription factors, miRNAs also play pivotal role in the regulation of gastric cancer metastasis. A few miRNAs induce EMT while others inhibit EMT process. For example, miR-25 promotes gastric cancer metastasis and invasiveness by targeting reversion-inducing-cysteine-rich protein with kazal motifs (RECK) (25) which acts as a metastatic suppressor. miR-27 promotes EMT and metastasis of GECs by upregulating EMT-associated genes ZEB1, ZEB2, Slug, and Vimentin. It also decreases E-cadherin levels (26). Another miR which is involved in negative regulation of EMT is miR-34a. This miR suppresses invasiveness and metastasis by downregulating MET (27).

Many of the above-mentioned factors regulating gastric cancer EMT are modulated by hypoxia as well as *H. pylori* infection, the role of which are being discussed in the following section.

1.A.6. Hypoxia as a regulator of EMT and metastasis

Oxygen (O₂) is very essential for the physiological functioning of aerobic organisms. Deprivation of normal O₂ level is known as hypoxia (28). Human tumor tissues are heterogeneous in nature in terms of O₂ distribution as compared to original normal tissues (29). Hypoxia occurs in tumor tissue that is >100–200 μm away from a functional blood supply (30, 31). Solid tumors are more resistant to chemotherapy as well as radiotherapy due to the alteration in the tumor microenvironment. The tumor microenvironment becomes deprived of O₂ which leads to the hypoxic or anoxic condition. Tumor cells protect themselves from the hypoxic environment by adapting to glycolysis or anaerobic respiration (32). These tumor masses invade to the nearby organs to get an adequate supply of O₂ which results in the metastasis of cancer cells (33). Several genes are controlled by hypoxia, which further alter non-specific stress responses, anaerobic metabolism, angiogenesis, tissue remodeling and cell-cell contacts (34). Enhanced angiogenesis are observed in hypoxic tumor cells which are mediated by vascular endothelial growth factor (VEGF) (35, 36). Hif1 is a major transcription factor expressed during hypoxia and it regulates several other downstream pathways leading to EMT and metastasis progression (37).

After the above discussion, it might seem contradictory that hypoxia can also induce apoptosis by mitochondria-mediated intrinsic cell death pathway (38) as well as mitochondria-independent pathway (39). Hypoxia-induced Hif1 can reportedly stabilize the proapoptotic protein p53 (40) which may induce apoptotic cell death. Hypoxia can be induced by lack of oxygen supply to the body or tissue (physiological hypoxia) or it can be induced by chemical treatment or exposure (chemical hypoxia).

(a) Physiological hypoxia

Deprivation of normal O₂ concentration (20%) in the body creates physiological hypoxia. 2-5% O₂ concentrations is considered to be hypoxic. Hypoxia enhances mesenchymal properties of

cells (41). Many diseases are contributed by hypoxic condition, a few of which include cerebral ischemia, myocardial ischemia and tumor angiogenesis (42). Hypoxia upregulates Hif1 in many diseases. For example, renal hypoxia induces chronic kidney disease (CKD) progression by inducing the α subunit of Hif1 (43).

(b) Chemical hypoxia

Cobalt chloride hexahydrate ($\text{CoCl}_2 \cdot 6\text{H}_2\text{O}$) is a chemical hypoxia-mimetic agent (44, 45). This chemical induces the same biochemical responses as that of physiological hypoxia (46, 47). CoCl_2 plays a crucial role in the progression of EMT and metastasis (48, 49) which increases invasiveness of GECs and enhances cancer aggressiveness (50, 51). It also induces stem cell-like characters in cancerous cells (52, 53). CoCl_2 is generally used as a hypoxia-mimetic agent as it induces Hif1 α expression in a similar manner as that of physiological hypoxia (54). Further, CoCl_2 -induced hypoxia also enhances expression of p300, a transcriptional coactivator for Hif1 (55). Another hypoxia-mimetic agent desferrioxamine is an iron chelator and also enhances Hif1 expression (46). One more important factor inducing Hif1 expression in GECs is *H. pylori* infection, which is discussed elaborately in subsequent sections.

1.A.7. *H. pylori*: an inducer of EMT and metastasis

(a) An overview

H. pylori are gram negative bacteria that infect half of the world's population. This pathogen colonizes in the human stomach and cause gastritis, gastric and duodenal ulcers, gastric carcinoma and mucosa-associated lymphoid tissue (MALT) lymphoma (56). *H. pylori* infection induces gastric carcinogenesis by enhancing either the cancer-promoting effects of the pathogen or host inflammatory responses to chronic infection. A key feature of *H. pylori* is its microaerophilic nature; with optimal growth at O_2 levels of 2-5% and an additional need of 5-10% CO_2 , high humidity and an optimum temperature of 37°C. The successful life-lasting colonization of *H. pylori* in the human stomach is achieved through a combination of virulence

factors such as urease enzyme, vacuolating cytotoxin A (Vac A), cytotoxin-associated antigen (Cag), type IV secretion system (TFSS) which prepare the pathogen for various challenges presented by the harsh environment of the human stomach (57).

(b) Epidemiology and transmission

H. pylori have a narrow host range and infection spreads from human to human or environment to human (58). Prevalence of *H. pylori* infection is more in developing countries as compared to the developed nations. In the developing countries, 70-90 % of the population before the age of 10 get infected. Out of which, 10–20 % individuals develop gastritis (59). *H. pylori* is mostly transmitted by the faecal–oral route (60). Contaminated water is a major source of *H. pylori* (61) infection. Zoonotic mode of *H. pylori* transmission has been reported mainly via the milk and faeces of cow (62).

(c) Pathogenesis

H. pylori reside in the antral gastric epithelium of the infected individual (63). This pathogen survives within the acidic mucus layer of the host by its acid tolerance capacity. It produces abundant amount of urease in the gastric lumen which hydrolyses urea into carbon dioxide and ammonia (8). *H. pylori* have flagella which make it mobile and allow to swim in the gastric lumen and to enter the mucus layer. *H. pylori* then binds to the epithelial cell by multiple bacterial surface components like Bab A (64). After contacting the gastric epithelium, *cag* pathogenicity island (PAI) determines its virulence (65). The *cag* PAI is of 40 kb length and contains 27 genes, a majority of which encodes for TFSS. TFSS induces translocation of effector molecule CagA into the host epithelium which is further phosphorylated at its C-terminal tyrosine residues that leads to the activation of receptor tyrosine kinase activation (RTKs) (66). Dephosphorylation of CagA is also involved in several signaling events. This phosphorylation and dephosphorylation loop of CagA is crucial for *H. pylori* pathogenesis which includes disruption of the cytoskeleton, interference with adhesion between adjacent

cells and modulation of pro-inflammatory as well as anti-inflammatory responses (67). *H. pylori* are classified as *cag* (+) or type I strains or *cag* (-) or type II strains based on the presence and absence of the *cag* region. *cag* (+) strains are more virulent and carcinogenic as compared to the *cag* (-) strains (68). *Cag A* is part of the *cag* PAI and is considered as one of the major virulent and carcinogenic antigens. *Vac A* is one of the major vacuolating factors secreted by *H. pylori* that enhances peptic ulcer. *H. pylori* antigens cross the epithelial layer to activate macrophages to release several pro-inflammatory cytokines such as interleukin-8 (IL-8), IL-6, IL-1, and possibly IL-12 (8). IL-12 and *H. pylori* antigens polarize the CD4⁺ T helper cells into a prominent Th1 phenotype. There is release of pro-inflammatory cytokines such as TNF- α and IFN γ at the site of infection which contributes in causing gastritis (69).

(d) Role of *H. pylori* in EMT progression

Involvement of *H. pylori* in EMT and metastasis progression is being studied relatively recently and not completely understood yet. Some of the studies are being discussed here. *H. pylori* CagA protein alters the association between apoptosis-stimulating protein of p53-2 (ASPP2) and p53 to stimulate the proteasomal degradation of p53, which inactivates the gastric tumor-suppressor runt-related transcription factor 3 (RUNX3) and enhances tumor necrosis factor receptor-associated factor 6 (TRAF6)-mediated Lys 63-linked ubiquitination of transforming growth factor β (TGF β)-activated kinase 1 (TAK1) (70-72). *H. pylori* also induces NF- κ B which further upregulates IL-8 secretion in GECs which is a crucial factor responsible for *H. pylori*-induced chronic inflammation and gastric carcinogenesis (73). The role of bone-marrow (BM)-derived cells (BMDCs) in *H. pylori*-induced gastric carcinogenesis has recently been demonstrated which shows that *H. pylori* recruit BM stem cells to the gastric mucosa which develops into gastric glands with the potential to evolve toward metaplasia and dysplasia (74). *Cag A* (+) *H. pylori* strains also induce p53 mutation that contributes in gastric carcinogenesis (75). One of the recent findings states the role of ETS2 and Twist1, promoting invasiveness of

H. pylori-infected gastric cancer cells by inducing seven in absentia homolog 2 (Siah2) protein (76). Involvement of *H. pylori* in epigenetic modifications and inflammation-induced malignancies during gastric carcinogenesis has been recently reported (77).

Role of *H. pylori* in the EMT process is currently being extensively studied. *H. pylori* infection induces invasiveness as well as stem cell-like properties in cancer cells which further enhance EMT (78). Several mesenchymal markers like ZEB1, twist1, N cadherin, vimentin, snail and slug are upregulated upon *cagA* (+) *H. pylori* infection (79-82). *H. pylori* CagA induces expression of carcinogenic miRNAs that drive metaplasia progression in GECs (83). Also, *H. pylori* stimulate some miRNAs that suppress EMT while some others induce EMT (84). The prometastatic transcription factor Hif1 is expressed in GECs after *H. pylori* infection (85, 86). The role of Hif1 in metastasis is detailed in the next section.

1.A.8. Hif1

Hif1 is a transcription factor that regulates expression of several genes involved in cancer progression. It is a member of Hif family proteins and is upregulated by hypoxia. Other members of Hif families are Hif2 and Hif3 (87, 88) . Hif1 is a heterodimer that consists of an oxygen-dependent α subunit and a constitutively-expressed β subunit. *H. pylori*-induced reactive oxygen species (ROS) can stabilize Hif1 α in normoxic condition (89), thus further contributing to metastasis progression.

(a) Domain structure of Hif1

Hif1 α is a basic helix-loop-helix (bHLH) protein and consists of 826 aminoacid polypeptide. The amino-terminal half of each subunit contains a basic helix-loop-helix (bHLH) and a PER-ARNT-SIM homology (PAS) domain. Hif1 α has amino and carboxy terminal nuclear localization signals (NLS-N and NLS-C, respectively) which help the protein to act as a transcription factor. The other domains include the proline-serine-threonine-rich protein stabilization domain (PSTD), amino and carboxy-terminal transactivation domains (TAD-N

and TAD-C, respectively), and the transcriptional inhibitory domain (ID). Transactivation domain of Hif1 α is very critical for its biological function as it interacts with its transcriptional coactivators CBP and p300 towards its C-terminal (90). The other subunit, Hif1 β , is expressed as a 774 or 789-amino-acid polypeptide (due to alternative splicing of an exon encoding 15 amino acids). The Hif1 β subunit, which is identical to the aryl hydrocarbon receptor nuclear translocator (ARNT), is a constitutively expressed nuclear protein. Hif1 α and Hif2 α have similar domain architecture and are regulated in a similar manner. Hif3 α is less closely related to Hif1 α and its regulation is less understood (91).

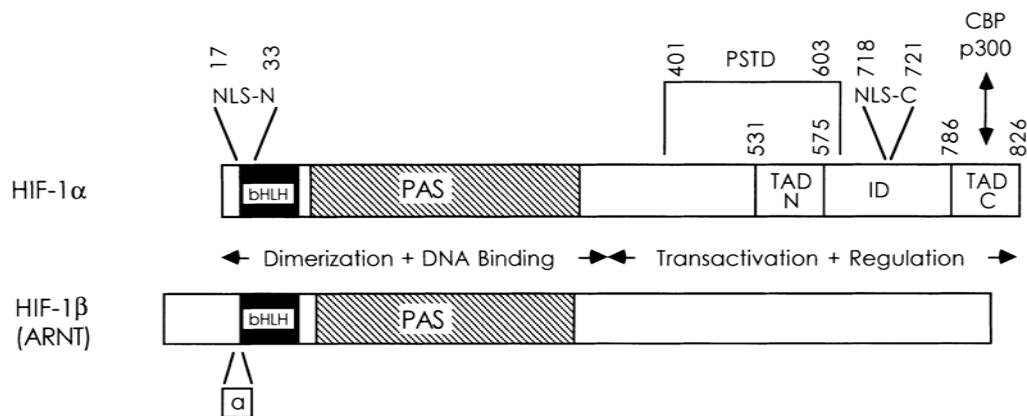


Figure 1.4. Domain structure of Hif1 protein (Courtesy: Ref 88)

(b) Hif1, p300 and their roles in cancer progression

Hif1 plays a very crucial role in cancer progression by regulating expression of several downstream effector molecules involved in EMT and metastasis. Angiogenesis is a critical phenomenon that leads to cancer progression. Hif1 binds to the hypoxia response element (HRE) site of various genes to regulate their function (92). Several pro-angiogenic factors such as VEGF, VEGF receptors FLT-1 and FLK-1, plasminogen activator inhibitor 1 (PAI-1), angiopoietins, platelet-derived growth factor B (PDGF-B), the angiopoietin receptor and matrix metalloproteases (MMP) 2, 7 have HRE sites at their promoter and hence, regulated by Hif1. Apart from that, Hif1 also induces cell proliferation that contributes in the metastasis process (87). p300 is a transcriptional cofactor of Hif1, has histone acetyl transferase (HAT) activity

and is recruited to Hif1 α (93) for its biological functions. p300 acts as a tumor-suppressor by binding with and acetylating p53, which is a major pro-apoptotic protein. p300 also acts as a cellular oncogene by activating several proto-oncogenic factors (94). Autoacetylation induces HAT activity of p300. Both enhanced and suppressed HAT activity in tumor cells can lead to cell cycle arrest and apoptosis (95, 96). Several studies have suggested crucial roles of histone acetylation and deacetylation in gastric cancer progression and invasiveness (97, 98).

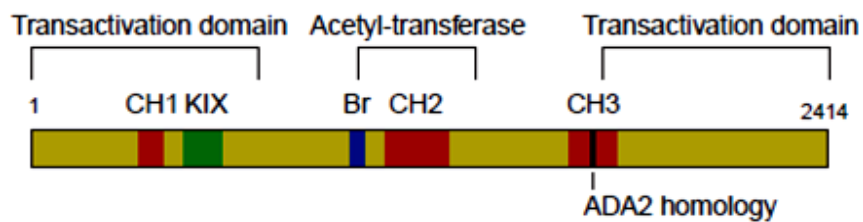


Figure 1.5. Domain structure of p300 protein (Derived from: Ref 98)

The 300 kDa protein, p300, consists of a trans-activation domain and an acetyl transferase domain. In addition, p300 has one bromodomain, three cysteine and histidine rich domains (CH domains) such as CH1, CH2, CH3 and one adenosine deaminase (ADA2) homology domain. The centrally located 380 residue HAT domain (99, 100) is very important for the biological activity of p300. The bromodomain of p300 recognizes several acetylated motifs. The HAT domain lies in the central region of the protein and can autoacetylate itself as well as other histone molecules (100). Inhibition of p300 HAT function influences several biological processes. For example, a specific inhibitor of p300 HAT, C646, blocks cell cycle progression, induces cellular senescence and inhibits the DNA damage response in melanoma cells (101). So, the study of p300-mediated EMT and metastasis regulation by Hif1 in hypoxic as well as *H. pylori*-infected GECs might be important to further elucidate the molecular mechanisms involved in gastric cancer.

Section B. Apoptosis as a negative-regulator of metastasis progression

1.B.1. Apoptosis: An overview

Apoptosis is the programmed cell death pathway by which multicellular organisms maintain their body homeostasis. Defects in the apoptotic pathways leads to generation of neoplastic cells since mutated cells keep on living instead of dying. Metastatic cells show malignant property and resistance to apoptosis by losing their contact with extracellular matrix as well within the cells (102). So apoptotic cell death acts as a check point for spreading of metastatic cells (103). Apoptosis can proceed through two pathways, i.e. the extrinsic pathway and the intrinsic pathway (104). The extrinsic pathway starts with recruitment of death receptors on cell surface followed by activation of caspase 8/caspase 10. The intrinsic pathway is operated through mitochondria in response to several apoptotic stimuli like UV radiation, chemotherapy or hypoxia. Cytochrome *c* (Cvt *c*) release and apoptosis-activating factor 1 (APAF1) complex formation followed by formation of cleaved caspase 9 are the hallmarks of the intrinsic cell death pathway. Both of these pathways activate executioner caspase 3 which cleaves death substances and results in apoptosis (38, 105).

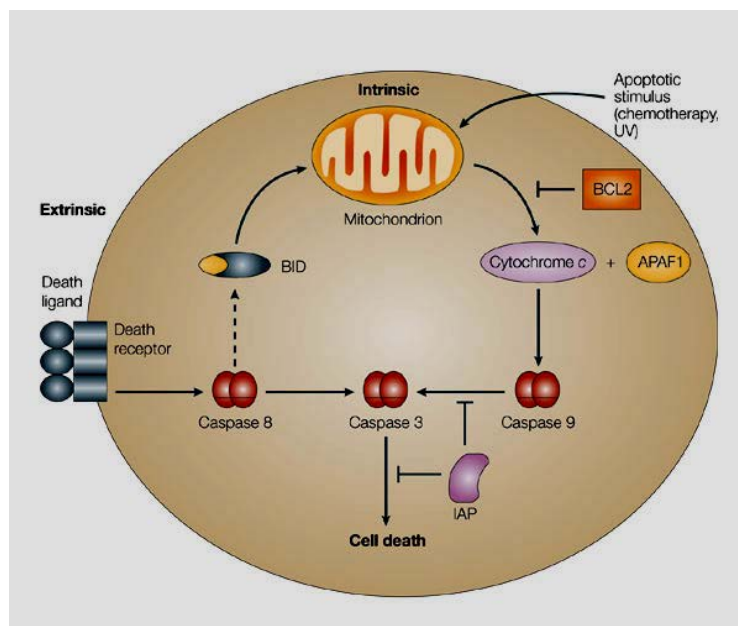


Figure 1.6. Apoptosis pathways (Courtesy: Ref 100)

The intrinsic apoptotic pathway is controlled by both pro as well as antiapoptotic proteins (106). These proteins are encoded by the B-cell lymphoma 2 (Bcl-2) family genes. Balance between these proapoptotic and antiapoptotic genes determines the cell fate. These Bcl-2 family proteins have 1-4 Bcl-2 homology domains (BH1, BH2, BH3, BH4). Several proapoptotic proteins have only BH3 domain which help in their interaction with antiapoptotic counterparts and thereby suppress functions of the antiapoptotic proteins (107). For example, the BH3 protein Noxa is considered to be an apoptosis sensitizer protein which degrades the prosurvival protein Mcl1 leading to induction of apoptosis (108). Likewise, other proapoptotic proteins such as Bax, Bad, Bid, Bak etc. are involved in the intrinsic apoptotic pathway and any functional deregulation of these proteins leads to cancer progression. For example, loss of function mutation of *bax* gene is observed in several tumors (109). Antiapoptotic proteins also regulate intrinsic apoptotic pathway by directly antagonizing the function of proapoptotic proteins (110). Noxa-mediated apoptosis induction plays a crucial role in apoptosis and yet, its potential in apoptosis is not fully understood and remains under-rated.

1.B.2. Noxa-mediated apoptosis induction

Noxa {synonyms: immediate-early-response *protein APR* or phorbol-12-myristate-13-acetate-induced protein 1 (PMAIP1)} is one of the Bcl2 homology 3 (BH-3)-only tumor suppressor protein involved in apoptotic cell death. *noxa* has a p53 binding site in its promoter and hence, participates in p53-mediated apoptosis (111). Once activated by stressors such as ER stress, proteasome-inhibitor treatment or genotoxic stress, Noxa gets translocated to mitochondria and interacts with the pro-survival protein Mcl1. Noxa-bound Mcl1 is degraded by proteasomal degradation which induces Bax oligomerization and Cyt *c* release by pore formation in the outer membrane of mitochondria. This finally leads to the intrinsic cell death pathway (112). p53-independent Noxa expression is also observed as a DNA-damage response of the cell (113, 114). Many reports show that *H. pylori* infection and hypoxia can induce Noxa expression by

enhancing Hif1 α binding to the Noxa promoter HRE (86, 115). This Hif1 α -mediated Noxa expression is independent of p53 status of the cell. The prosurvival protein Mcl1 is upregulated by hypoxia and has a HRE at its promoter (116). So, regulation of Noxa and Mcl1 balance in hypoxic as well as *H. pylori*-infected cells could be a major contributor in metastatic progression of gastric cancer. One major finding by Lowman *et al.* describes that the proapoptotic function of Noxa is modified by its phosphorylation (117). The importance of phosphorylation of BH3 family proteins in carcinogenesis is known for some time (118). Noxa phosphorylation by the stress-induced mitogen-activated protein kinase (MAPK) c-Jun-N-terminal kinases (JNK), prevents mitochondrial translocation of Noxa and help in cell survival by upregulating the pro-survival protein Mcl1 (86, 119).

1.B.3. ROS-mediated apoptosis induction

Reactive oxygen species (ROS) are by-products of the cellular metabolic pathways. ROS include oxygen-derived free radicals such as superoxide anions (O₂^{•-}), hydroxyl radicals (HO[•]), peroxy (RO₂[•]), alkoxy (RO[•]) and non-radical such as hydrogen peroxide (H₂O₂), hypochlorous acid (HOCl) etc. (120). The electron transport chain of mitochondria and NADPH-cytochrome P450 reductase in the endoplasmic reticulum are the major sources of ROS generation (121). Peroxisome also acts as a source of ROS generation. ROS are involved in several biological processes such as wound healing, tissue repair, killing of invading pathogens, to name a few. So, deregulation in ROS generation has critical roles in cell survival and cell death (122).

1.B.4. Apoptosis in metastatic cells

Carcinogenesis and apoptosis are apparently two contradictory cellular events. Resistance to apoptosis enhances carcinogenic properties of the cell. Metastatic cells escape from the apoptotic cell death by disrupting the balance between the pro-apoptotic and anti-apoptotic proteins, reduced caspase function and impaired death-receptor signaling (123).

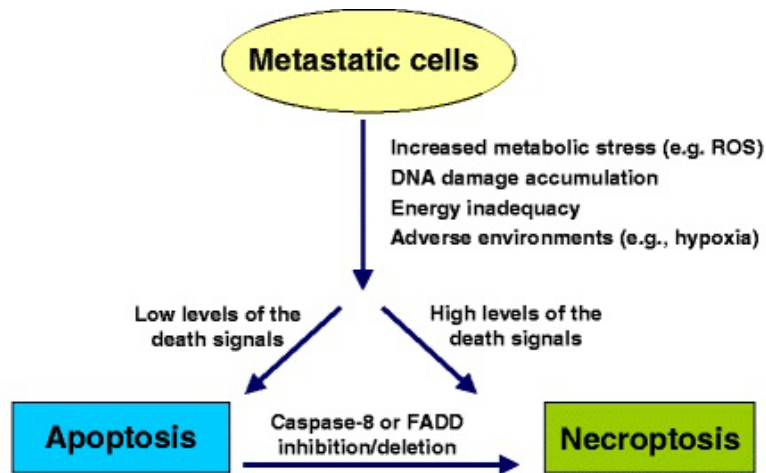


Figure 1.7. Apoptosis acts as a negative regulator of metastasis (Derived from Ref 121)

1.B.5. Apoptosis induction in metastatic cells

Cancer cell proliferation and metastasis can be reversed by apoptosis induction. Contemporary therapeutic approaches like chemotherapy, γ -irradiation, immunotherapy or suicide gene therapy exploits the apoptosis induction mechanism in cancer cells (103, 124). Several chemical compounds are in use for targeted-killing of cancer cells. Some of which are discussed here. Apoptotic cell death can be induced in melanoma cells by photodynamic therapy (125). Inhibition of the cell cycle as well as metastatic property and induction of apoptosis in breast cancer cells are initiated by phytochemicals (126). Mesenchymal properties of hypoxic cancer cells can also be suppressed by hispidulin (127). Current research considers apoptosis induction in metastatic cancer cells as a very potent mechanism to decrease cancer mortality.

1.C. Objectives of the study

Hence, with the above background knowledge, the **objectives** of this study were determined as follows:

1. To decipher apoptosis in hypoxic and invasive gastric epithelial cells (GECs)
2. To study apoptosis mechanisms induced in *H. pylori*-infected GECs that show metastatic behavior

MATERIALS and METHODS

Chapter 2

2.1. MATERIALS

2.1.1. Cell lines and reagents

GECs such as AGS, MKN45, KATO III, NCI-N87 cell lines were procured from University of Virginia, USA. Various stable cell lines were generated in our lab as detailed later. The immortalized human GEC HFE145 was gifted by Dr. Hassan Ashktorab, Department of Medicine, Howard University, Washington, DC, US Clone 39 (HuSH 29 mer shRNA constructs against Hif1 α), Clone 13 (29-mer scrambled shRNA cassette in pGFP-v-RS-vector) and Clone 7 (Hu-SH shRNA GFP cloning vector (empty vector)) were generated by Dr. Asima Bhattacharyya, NISER, Odisha, India.

2.1.2. Constructs and antibodies

List of various constructs and antibodies that were used in the study are shown in appendix I and II, respectively.

2.1.3. Tissue samples

Gastric cancer patients, diagnosed for metastatic stage of cancer were studied. Biopsy sample collection was done following a National Institute of Science Education and Research (NISER) Review Board-approved protocol. Written informed consent was obtained from all patients. Tissue samples were further processed for immunofluorescence microscopy as described in the methodology.

2.2. METHODOLOGY

2.2.1. Maintenance of GECs

AGS, KATO III, MKN-45 and NCI-N87 were regularly maintained in RPMI media (HiMedia, Cat No. AL028A, India) supplemented with 10 % heat-inactivated fetal bovine serum (FBS, HiMedia, Cat No. RM9970, India) in a humidified incubator containing 5% CO₂ and maintaining 37 °C. These cell lines were routinely maintained by subculturing. During subculturing, spent medium was removed from the T-25/T-75 flasks (GENAXY, Cat No.

430639 and 430641 respectively, USA) and pre-warmed trypsin-EDTA solution (HiMedia, Cat No. TCL007, India) was added. After 2-5 min of incubation, cells were gently dislodged from the flask with a sterile pipette and again seeded into a new flask.

2.2.2 Freezing and revival of cell lines

Cells were frozen once confluency was reached (70-80%). Confluent cells were trypsinized and centrifuged (Thermo Scientific, Sorvall Biofuge Stratos, Model No. D35720, USA) after diluting with media containing 10% FBS. Cells were spun down at 150 x g for 5 min at room temperature (RT). Then the cell pellet was diluted with freezing mix {20% dimethyl sulfoxide (DMSO) (HiMedia, Cat No. TC185, India in FBS)} in media. Cells were aliquoted into freezing vials and were first kept at -80 °C for overnight and then shifted to liquid nitrogen for longer preservation.

Revival of frozen cells was done quickly by transferring from liquid nitrogen to a 37 °C water bath. Cells were introduced gently to T-25/T-75 cell culture flasks and put back to the incubator.

2.2.3 Maintenance of *H. pylori* culture

The *cag* (+) *H. pylori* strain 26695 and the *cag* (-) strain 8-1 (American Type Culture Collection, Manassas, VA, USA) were used in our study. *H. pylori* were grown on tripticase soy agar (TSA) plate (Becton Dickinson and Company, Cat No. 221239, USA) while incubating at 37 °C in a microaerophilic atmosphere (90 % N₂, 1% O₂, 10 % CO₂). Cultures were subcultured in every three days by inoculating half the loop of bacterial culture onto another TSA plate. For experiments, *H. pylori* cultures were inoculated into Brucella broth (Difco-BBL, Cat No. 211088, USA) for overnight and then used after optical density (OD) reached more than 0.5.

2.2.4. Cloning, expression and mutagenesis

Cloning and expression of human *nox* gene

Primer design: Cloning and mutagenesis primers were designed for the human *nox* gene. Primers were designed from target sequences by using Integrated DNA Technology (IDT) software (refer appendix III for detail).

Polymerase chain reaction (PCR) and cloning of human *nox* gene: Genomic DNA was isolated from AGS cells using DNeasy Blood & Tissue Kit(QIAGEN, Cat No. 69504, USA) following manufacturer's protocol. *nox* gene (164 bp) was amplified from the genomic DNA in the following manner.

PCR: High fidelity (HIF) Taq polymerase (Thermo Fischer Scientific, Cat No. 11304011, USA) was used for amplification of *nox* from the genomic DNA from AGS cell line.

Reaction Mix (for 25 μ l)

Components	Vol (μ l)
H ₂ O	16.25
10X NEB Taq buffer	2.5
dNTP	0.5
MgCl ₂	2.5
Primer F (10 pmole)	1
Primer R (10 pmole)	1
Genomic DNA	1
HIF Taq polymerase (1X)	0.25

Table 1. Components used for PCR amplification of *nox* gene

Reaction conditions for gradient PCR)

	Temperature °C	Time	No. of Cycles
Initial Denaturation	94°C	2 min	1
Denaturation	94°C	1 min	35
Primer Annealing	62°C- 72°C	1 min	
Primer Extension	72°C	30 sec [#]	
Final Extension	72°C	5 min	1

#2min/kb of plasmid length

Table 2. Reaction conditions for PCR amplification of *nox* gene

The amplified PCR product (164 bp) was run on 1.2% agarose gel and purified by using QIAquick gel extraction kit (QIAGEN, 28706, Germany) .

Agarose gel electrophoresis and gel extraction of the PCR product: Agarose gel electrophoresis was performed for qualitative confirmation of amplified *nox*a construct. 1.2% agarose gels were prepared in 1X TAE buffer (HiMedia, Cat No. ML016, India) with 0.5 µg/ml concentration of ethidium bromide (EtBr, HiMedia, Cat No. MB071, India). The horizontal electrophoresis unit was used to run the gel at 50-100 V for 30 min. Ultraviolet (UV) transilluminator was used to visualize the band position in the gel with respect to the position of molecular weight markers. The band containing the amplified *nox*a was excised by using a scalpel. Three volumes of QG buffer were added to one volume of gel and the gel was incubated at 50 °C for 10 min and allowed to be completely dissolved. The tube containing gel was vortexed for every 2-3 min for complete dissolution. Then one volume of isopropanol was added and mixed properly with the sample. The sample was applied on to the spin column for an incubation period of 2 min followed by centrifugation for 1 min at 16,100×g. Flow through was discarded and 0.5 ml of QG buffer was added to the column followed by incubation for 1 min. Finally, 0.75 ml of buffer PE was added to the column followed by incubation of 2 min and centrifugation at top speed for 1 min. At the last step DNA was eluted into a fresh micro-centrifuge tube by using 30 µl of EB buffer by centrifuging at top speed for 1min. Purification of the PCR product was done using a PCR-purification kit (QIAGEN, Cat No. 28104, Germany).

PCR purification method: Five volumes of buffer PB1 were added to one volume of PCR reaction mix and the sample was applied to QIAquick column and centrifuged at 16,100 × g for 1 min. The flow-through was discarded and 0.75 ml of buffer PE was added to the column followed by centrifugation for 1 min at 16,100 × g. DNA was eluted by adding 30 µl of EB buffer followed by centrifugation at for 1 min at 16,100 × g.

Restriction digestion of purified PCR product: Hind III and Xho I {New England Biolabs (NEB), Cat No. R01045 and R0146S respectively, USA} were used {Hind III (on the F primer) and Xho I (on the R primer)} to clone *nox* in pcDNA3.1⁺ vector. 1 µg of template DNA was used for restriction digestion of the PCR product as well as the vector. Restriction digestion was performed in a 37°C water bath for 3 h.

Components	For Noxa DNA digestion	For pcDNA3.1 ⁺ digestion
10X buffer 2	5 µl	5 µl
Hind III	1 µl	1 µl
Xho I	1 µl	1 µl
H ₂ O	29 µl	42 µl
Template DNA	14 µl	1 µl

Table3. Components used for restriction digestion

Digested DNA was purified by using PCR purification method as mentioned above.

DNA Ligation: Purified digested products were used for ligation by using T4 DNA ligase (NEB, Cat No. M0202S, USA). DNA ligation was performed at 16 °C for 12 h. Amount of the vector and insert used in the reaction was calculated by the ligase calculator software. Vector to insert ratio was 1:6.

Calculation for ligation mix: (10 µl)

Components	Volume
H ₂ O	4.78 µl
10X ligase Buffer	1 µl
Insert (14.2 ng)	0.626 µl
Vector (75 ng)	2.59 µl
Ligase enzyme	1 µl

Table 4. Components used in the ligation reaction

Transformation: 50 µl of DH5a strain of *Escherichia coli* competent cells (Invitrogen, Cat No. 18265017, USA) and 3 µl of ligation mix were added to a pre-chilled microcentrifuge

tube and kept on ice for 30 min. Tubes were incubated in 42 °C water bath for 45 sec. 450 µl of SOC media (Invitrogen, Cat No. 15544034, USA) was added to the cell mix and incubated for 1 h at 37 °C in a shaker. Bacterial suspension was plated on LB agar (HiMedia, Cat No. M1151, India) plate with 75 µg/ml ampicillin (MP Biomedicals, Cat No. 194526, USA) and incubated for overnight at 37 °C.

Selection of positive clones: A single healthy colony was chosen from the plate and inoculated in 4 ml of LB broth with 75µg/ml of ampicillin followed by overnight shaking at 37 °C. Plasmids were extracted from the bacterial culture by alkaline lysis method and recombinant clones were screened by restriction digestion.

Miniprep plasmid isolation (alkaline lysis): The alkaline lysis method was followed to extract plasmids from bacteria.

Composition of solutions used in this protocol

Solution I (Stored at RT)

Tris (25 mM, pH 8.0)

Glucose (50 mM)

EDTA (100 mM, pH 8.0)

Solution II (Stored at RT)

NaOH (0.2 N)

1 % SDS

Solution III (Stored at 4 °C)

Potassium acetate (60 ml)

Glacial acetic acid (11.5 ml)

H₂O (28.5 ml)

Miniprep Protocol: 4 ml of bacterial culture was pelleted down at 16,100×g for 30 sec at 4 °C. The cell pellet was dried and resuspended in 200 µl of ice cold solution I followed by vortexing. 400 µl of freshly prepared solution II was added and the tube was inverted many times to mix. The tube was incubated on ice for 5 min followed by centrifugation at 16,100 × g

for 10 min. Then supernatant was transferred to a fresh tube and an equal amount of phenol:chloroform:isoamylalcohol (25:24:1) mix was added, mixed by inverting several times and then centrifuged at $16,100 \times g$ for 2 min at 4°C . The supernatant was taken in a fresh tube and 2 volume of 100% ethanol was added on top of it, mixed by inverting several times. The tube was then incubated at RT for 2 min followed by centrifugation at maximum speed for 5 min. 1 ml of 70% ethanol was added to the pellet and inverted several times followed by centrifugation at a maximum speed for 2 min. The supernatant was discarded followed by removal of all traces of ethanol from the pellet. The pellet was air-dried and finally resuspended in 50 μl of 1X TE buffer (HiMedia, Cat No. ML012, India) containing 20 $\mu\text{g}/\text{ml}$ DNase-free RNase A and stored at -20°C . Clones were assessed by sequencing (Europhins, India).

Generation of S13A mutant of Noxa by site-directed mutagenesis: Site-directed mutagenesis was carried out by using a single mutagenic primer to insert a single point mutation on the *noxa* plasmid.

The amino acid sequence of *noxa* is:

MPGKKARKNAQPS*PARAPAELEVECATQLRRFG DKLNFRQKLLNLSKLFCSGT

The 13th serine (S^{13}) residue of Noxa (*) was replaced with an alanine residue in the S13A construct.

The mutation is indicated by underlining in the primer shown below.

Primer for *noxa* S13A: 5' AAG AAC GCT CAA CCG GCC CCC GCG CGG GCT CCA 3'

Mutagenesis reaction (25 μ l)

Components	Volume
10X Quik change buffer	2.5 μ l
Quik Solution	0.75 μ l
ds DNA template	1 μ l (100 ng)
Primer	1 μ l (100 ng)
dNTP	1 μ l
Enzyme	1 μ l
H ₂ O	17.75

Table 5. Components of site-directed mutagenesis reaction

Cycling parameters

	Temperature °C	Time	No. of Cycles
Initial denaturation	95 °C	1 min	1
Denaturation	95 °C	1 min	30
Primer annealing	55 °C	1 min	
Primer extension	65 °C	[#] 12 min	
Final extension	65 °C	12 min	1

[#]2min/kb of plasmid length

Table 6. PCR reaction conditions of site-directed mutagenesis reaction

After completion of thermal cycles, the amplified product was treated with 1 μ L (10 U/ μ L) of *Dpn* I enzyme (an endonuclease; targeted sequence: 5'-Gm⁶ATC-3' and is specific for methylated and hemimethylated DNA). This enzyme digests the parental DNA at specific sites, leaving the new strand intact. After addition of this enzyme the tube was incubated at 37 °C for 2 h, followed by transformation into XL10-Gold ultracompetent cells (Agilent, Cat No. 200515, USA), where the mutant closed circle SS-DNA is converted into a duplex form *in vivo* as previously mentioned. Mutants were confirmed by sequencing and positive clones were further amplified by maxi prep method.

Maxiprep: Maxiprep kit (QIAGEN, Cat No. 43776, Germany) was used to amplify the cloned DNA. A healthy colony was chosen from the plate and inoculated in 100 ml LB broth

containing 75 µg/ml of ampicillin followed by overnight shaking at 37 °C. 100 ml of culture was pelleted down at 6000 x g for 15 min at 4 °C. The supernatant was poured off and bacterial pellet was resuspended in 10 ml of buffer P1 (to buffer P1 RNase A & lyseblue reagent were premixed as per manufacturer's instruction). 10 ml of buffer P2 was added to the supernatant, mixed thoroughly by vigorously inverting 4-6 times, and incubated at RT for 5 min. 10 ml of cold buffer P3 was added, mixed thoroughly mixed by vigorously inverting 4-6 times. The lysate was poured into the barrel of the Qiafilter cartridge and incubated at RT for 10 min. Hispeed maxi tip was equilibrated by adding 10 ml Buffer QBT. The column was allowed to drain by gravity flow. The cap was removed from the Qiafilter cartridge outlet nozzle, the plunger was gently inserted into the Qiafilter maxi cartridge and the bacterial lysate was filtered into the previously equilibrated Hispeed tip. The clear lysate was allowed to enter the resin through gravity flow. The Qiagen tip was washed with 60 ml Buffer QC. DNA was eluted by adding 15 ml Buffer QF. The eluate was collected in fresh centrifuge tube. DNA was precipitated with 10.5 ml isopropanol at room-temperature, mixed and incubated for 5 min. The isopropanol mixture was transferred to a 30 ml syringe which is attached to a Qiaprecipitator and placed over a wash bottle. The plunger was inserted and the mixture was filtered through Qiaprecipitator using constant pressure. 2 ml of 70% ethanol was added to the 30 ml syringe and was filtered through Qiaprecipitator. The outlet nozzle of Qiaprecipitator was air-dried to prevent ethanol carryover. The Qiaprecipitator was attached to a 5 ml syringe and 500 µl of TE buffer (37 °C) was added to the syringe. The plunger was inserted to collect DNA from the other side.

2.2.5. Transfection of cell lines

Transient transfection was performed using lipofectamine 2000 reagent (Invitrogen, 11668-019, USA). Cell plating was done one day prior to the transfection for which required number of cells (as mentioned in Table 8) were plated in appropriate volume of growth medium

containing FBS in tissue culture plates, and incubated in an incubator maintaining 37 °C and 5 % CO₂. 1 h prior to transfection, growth medium was gently aspirated from wells and fresh growth medium was added. The required amount of DNA and transfection reagent were diluted in serum free media to the volume indicated in table 8 in separate microcentrifuge tubes followed by an incubation of 5 min at RT. Then both mixtures were mixed together and incubated for 20 min at RT to allow the DNA-Lipofectamine complex formation. Then the transfection mix was immediately added drop-wise onto the cells. Plates were gently swirled to ensure uniform distribution of the complexes. Cells were incubated with the complex at 37 °C and 5 % CO₂ for 36 h to allow gene expression. Cells were treated on the next day according to experimental need.

Culture Vessel	Surface Area Per Well (cm²)	Relative Surface Area (vs. 24-well)	Volume of Plating Medium	DNA (µg) and Dilution Volume (µl)
96-well	0.3	0.2	100 µl	0.2 µg in 25 µl
24-well	2	1	500 µl	0.8µg in 50 µl
12-well	4	2	1 ml	1.6 µg in 100 µl
35-mm	10	5	2 ml	4 µg in 250 µl
6-well	10	5	2 ml	4 µg in 250 µl
60-mm	20	10	5 ml	8 µg in 500 µl
10-cm	60	30	15 ml	24 µg in 1.5 ml

Table 7. Parameters for transient transfection (Adapted from Invitrogen)

2.2.6. Infection of GECs with *H. pylori*

One day prior to infection, *H. pylori* were inoculated in Brucella broth and OD₆₀₀ was assessed after 12-16 h. OD values between 0.5-1 were considered suitable for infection. Transfected or non-transfected GECs were infected with *H. pylori* (in case of transfected groups, cells were used after 24-36 h post-transfection) for various multiplicity of infection (MOI) and time periods.

2.2.7. Exposure of cells to chemical hypoxia induced by CoCl₂.6H₂O, physiological hypoxia and a HAT inhibitor, sodium 4-(3,5-bis(4-hydroxy-3-methoxystyryl)-1H-pyrazol-1-yl)benzoate (CTK7A)

CoCl₂.6H₂O (Sigma-Aldrich, Cat No.255599, USA) was used as a chemical hypoxia-mimetic agent and GasPak™ EZ Anaerobe Pouch System (BD, Cat No. 260683, USA) was used to create physiological hypoxia (1% O₂). Cells were treated with a varied dose of CoCl₂ as indicated in an earlier study (47) or with a fixed dose of 1% O₂ for desired time points. CTK7A, which is a curcumin-derived water-soluble p300/CBP-specific histone acetyltransferase (HAT)/lysine acetyltransferase (KAT) inhibitor (128) was used at a concentration of 100 μM for 24 h, when required.

2.2.8. Whole cell lysate preparation

Following treatment, cells were either trypsinized or scraped off from the culture plate. Then cells were centrifuged at 250 × g for 5 min at 4 °C and the supernatant was discarded. Samples were kept on ice and required amount of protease inhibitor cocktail (HiMedia, Cat No. ML051, India) was added to each tube and then vortexed. 2X Laemmli sample buffer (HiMedia, Cat No. ML-021, India) was added to the lysate at 1:1 ratio followed by vortexing to mix. Finally, samples were kept at 100 °C (dry bath) for 8 min and stored at -80 °C for further use.

2.2.9. Mitochondrial and cytosolic lysate preparation

To study the mitochondrial and the cytosolic distribution of proteins, mitochondrial and cytosolic lysates were isolated. 2×10^6 AGS cells were seeded in six well plates and incubated at 5 % CO₂ and 95 % humidity in a 37 °C incubator. Cells were treated with 200 μM of CoCl₂ and CTK7A or left untreated. In other experimental setup, transfected or pcDNA3.1⁺-transfected cells were used for mitochondrial and cytosolic fraction isolation. After treatment/infection, cells were scraped off the treatment plate followed by collection of lysates in microfuge tubes. The lysates were spun down at $371 \times g$ for 10 min at 4°C. Pellet was resuspended in 150 μl of resuspension buffer {20 mM N-(2-hydroxyethyl) piperazine Na-2-ethanesulfonic acid (HEPES), pH 7.5, 10 mM KCl, 1.5 mM MgCl₂, 1 mM ethylenediaminetetraacetic acid (EDTA), 1 mM ethylene glycol tetraacetic acid (EGTA) + Protease inhibitor cocktail (HiMedia, Cat No. ML-051, India) 10 μl/ml + 150 mM sucrose)}. At this step sodium fluoride (NaF, a phosphatase inhibitor) was added at a concentration of 40 mM). Cells were broken down by 20 passages through 26 gauge needle and were spun at 750 x g for 10 min to remove the nuclei and unbroken cells. The supernatant was taken out and spun at 10000 x g for 15 min at 4 °C. Supernatant collected at this step was the cytosolic fraction. The mitochondria-rich pellet was resuspended in 10 μl of lysis buffer (20 mM Tris-HCl pH 7.4, 150 mM NaCl + protease inhibitor cocktail) and boiled with 10 μl Laemmli sample buffer (HiMedia, Cat No. ML-021, India) followed by heating at 100 °C (dry bath) for 8 min and run on gel for further use.

2.2.10. Nuclear and cytosolic lysate preparation

Nucleus-enriched and cytosolic fractions were prepared by NE-PER Nuclear and Cytoplasmic Extraction Reagents (Thermo Scientific, Cat No. 78833, USA) according to the manufacturer's instruction. 2×10^6 AGS cells were seeded in six well plates and treated with hypoxia and/or CTK7A for 24 h. Cells were pelleted down and NE-PER protocol was followed

for the rest of the processing. Addition of reagents to the cell pellet was based on packed cell volume as mentioned below.

Packed Cell Vol (μl)	CER I (μl)	CER II (μl)	NER (μl)
10	100	5.5	50
20	200	11	100
50	500	27.5	250
100	1000	55	500

2×10^6 cells was considered equivalent to 20 μl packed cell volume.

Table 8. Buffers used in NE-PER isolation (Adapted from NE-PER manual)

Cells were pelleted by centrifugation at 500 x g for 5 min. The supernatant was carefully removed and the pellet was kept dry. CER I buffer was added to the pellet and vortexed vigorously in order to break the pellet followed by an incubation on ice for 10 min. CER II was added to the tubes, vortexed vigorously for 5 sec followed by incubation on ice for 1 min. Tubes were again vortexed for 5 second followed by centrifugation for 5 min at 16000 x g. The supernatant (cytoplasmic extract) was immediately transferred to chilled microcentrifuge tubes and stored at -80°C until used. The insoluble pellet was resuspended in ice cold NER, vortexed at 16000 x g for 15 sec and incubated on ice for 40 min followed by vortexing thrice with 10 min interval. Finally, tubes were centrifuged at maximum speed (~ 16000 x g) in a microcentrifuge tube for 10 min and the nuclear lysate was collected and stored at -80°C .

2.2.11. Sodium dodecyl sulfate polyacrylamide gel electrophoresis (SDS-PAGE)

SDS PAGE is the method of separation of protein samples based on their molecular weight.

Gel components

Solutions: Acrylamide-bisacrylamide (29:1) solution or solution A (Bio-Rad, Cat No. 1610156, USA), separating gel buffer or solution B (pH 8.8) (Bio-Rad, Cat No. 161-0798, USA) and

stacking gel solution or solution C (pH 6.8) (Bio-Rad, Cat No. 161-0799) were purchased from Bio-Rad.

Glycerol: A 50% solution was made by mixing 50 ml glycerol (HiMedia, Cat No. RM1027, India) with 50 ml distilled water.

TEMED: N, N, N', N'-Tetramethylethylenediamine (Bio-Rad, Cat No. 161-0800, USA) was used as a catalyst of polymerization.

Ammonium persulfate (APS): A 10% solution was made by dissolving 10 mg APS (Bio-Rad, Cat No. 161-0700, India) in 100 μ l distilled water. This also acts as a catalyst of polymerization. For best results, APS was prepared fresh.

Working solutions (this calculation is for two gels)

Resolving gel solution: The stock solutions were mixed in the following proportions. Other percentages of gel were achieved by changing the volume of solution A and distilled water appropriately.

Components	7.5%	10%	12.5%	15%
Solution A/Acrylamide: bisacrylamide solution	2.25 ml	3 ml	3.75 ml	4.5 ml
Solution B (Resolving gel solution)	2.25 ml	2.25 ml	2.25 ml	2.25 ml
Distilled water	2 ml	1.25 ml	0.5 ml	No
50% glycerol	2.5ml	2.5ml	2.5ml	2.5ml
TEMED	5 μ l	5 μ l	5 μ l	5 μ l
10% APS	70 μ l	70 μ l	70 μ l	70 μ l

Table 9. Composition of resolving gels

Stacking gel solution: The stock solutions were mixed in the following proportion: (for 2 gels)

Components	Volume
Solution A	900 μ l
Solution C	1.5 ml
DW	3.6 ml
TEMED	6 μ l
APS	36 μ l

Table 10. Composition of stacking gel

APS and TEMED were added to each solution just prior to polymerization.

Electrophoresis buffer: Electrophoresis buffer contained 25 mM Tris-HCl, 190 mM glycine and 0.1 % SDS.

Sample denaturing (Laemmli) buffer: Ready to use 2X Laemmli (HiMedia, Cat No. ML021, India) sample buffer was used for sample preparation.

Casting of the SDS polyacrylamide gel: This is the first step in which the gels were casted between the assembled glass plates. A gel is composed of resolving solution (three fourth of the total height) at the lower region of the glass plate assembly and stacking solution towards the upper region. A 10/15-well comb was inserted into the stacking gel solution. The gel solutions were allowed to polymerize at RT for 20-30 min, after which the comb was gently removed. Electrophoresis buffer was added to the upper surface of the stacking gel and the whole glass plate assembly was kept inside the Mini-PROTEAN gel apparatus (Bio-Rad, Cat No. 165-8003, USA) filled with electrophoresis buffer.

Sample preparation: Samples were already prepared as mentioned above and stored at -80 °C. Samples were taken out at RT and properly thawed before loading.

Sample loading and electrophoresis: Denatured protein samples were loaded into individual wells in the stacking gel following the desired sequence. Standard molecular weight marker (BLUelf prestained protein ladder, BR Biochem, Cat No. BM008-500, India) was loaded to

obtain molecular masses of sample proteins. The electrophoresis chamber was connected to a power pack and electrophoresis was carried out at a constant voltage of 130 V for 15 min followed by 180 V for 1 h, i.e. till the bromophenol blue dye front reached 0.5 cm above the base of the gel.

2.2.12. Immunoblotting

Immunoblotting was performed by using specific antibodies to identify target proteins in the pool of unrelated proteins.

Composition of solutions used in immunoblotting:

Tris-buffered saline (1X TBS): 20 mM Tris, 500 mM NaCl, pH 7.5

4.84 gm Tris, 58.48 gm NaCl were added to 1 L of distilled water and pH was adjusted to 7.5 with HCl. The volume was then made upto 2l.

Phosphate-buffered saline (1X PBS): 10mM Na₂HPO₄, 2 mM KH₂PO₄, 137 mM NaCl and 2.7 mM KCl

8 gm of NaCl, 0.2 gm of KCl, 1.44 gm of Na₂HPO₄ and 0.24 gm of KH₂PO₄ were added in 800ml of distilled water and pH was adjusted to 7.4 with HCl. The volume was made upto 1 L.

Tween-20 wash solution (TBST): 0.1 % (v/v) Tween-20 dissolved in 1X TBS.

Blocking buffer: 3 % (w/v) bovine serum albumin (BSA, Cohn fraction V, HiMedia, Cat No. RM3151, India) in TBST or 5 % non-fat-dry-milk (NFDM, HiMedia, Cat No. RM1254, India) in TBST.

Note: Primary and secondary antibodies were diluted in blocking buffer.

Transfer buffer for polyvinylidene (PVDF) membrane: 48 mM Tris, 39 mM glycine, 0.0375 % SDS, 20 % methanol. 2.904 gm of Tris base, 1.463 gm of glycine, 0.1875 gm of SDS were added to 250 ml of water and pH was adjusted to 8.3, with HCl. 100 ml of methanol was added on top of it and volume was made upto 500 ml.

Procedure for transfer of protein onto PVDF membrane (semi-dry transfer): The semi-dry transfer was performed for the transfer of low molecular weight proteins. Protein samples were run on SDS polyacrylamide gel. After the run was complete, the gels were transferred to chilled transfer buffer for 2-5 min. PVDF membrane (Millipore, Cat No. PVH00010, USA) was pretreated with chilled methanol for 5 min to reduce the hydrophobicity of the membrane followed by water and transfer buffer. Precut thick papers were soaked in transfer buffer. The transfer assembly was prepared by first placing the thick paper on the anode of the transfer apparatus (Bio-Rad Cat No. 170-3940, USA) followed by a PVDF membrane, the electrophoresed gel and another thick paper (towards the cathode). After rolling out air bubbles from the assembly, transfer was carried out at 25 V for 35 min.

Procedure for transfer of proteins onto PVDF membrane (Wet transfer): Wet transfer protocol was followed for transfer of high molecular weight proteins. After completion of SDS gel electrophoresis, the same procedure was followed as that of semidry transfer. For wet transfer, a fiber pad was placed first on the cathode, followed by a thick filter paper, the electrophoresed gel, the pre-soaked PVDF membrane, filter paper and a fiber pad. The whole assembly was made bubble-free by using a roller and was put inside the cassette and then placed inside the tank and connected with power supply of 40 V for 4 h. The whole transfer set up was kept inside the transfer tank filled with transfer buffer. After the transfer process, the membrane was washed with TBS solution (or PBS for non-phospho proteins) and then incubated with blocking solution for 60 min, to prevent non-specific binding. The membrane was probed with specific primary antibody for overnight at 4 °C. Then, membranes were washed with 1X TBST/PBST followed by secondary antibody incubation for 1 h at RT with constant shaking. Membrane was washed thrice with TBST and finally with 1X TBS (5 min for each wash). Super Signal West Femto Chemiluminescent Substrate kit (Thermo Fisher Scientific, Cat No. 34094, USA) was used for blot development and images were taken with Chemi Doc XRS (Bio-Rad

Laboratories, Model No. #1708265, USA) equipped with Quantity One 1-D Analysis software version 4.6.9 (Bio-Rad Laboratories).

Reprobing of the PVDF membrane: Ready to use Restore Plus Western Blot Stripping Buffer (Thermo scientific, Cat No. 46430, USA) was used for stripping the western blotted membranes to probe with different sets of antibodies. One time western-blotted PVDF membrane was kept in the reprobing buffer for 30 min with shaking. Membrane was then washed three times (15 min each) with TBST followed by blocking, primary antibody incubation, washing with TBST, secondary antibody incubation and washing. Finally, membranes were developed as mentioned previously to get desired bands.

2.2.13. Immunoprecipitation (IP) assays

Immunoprecipitation was performed to study interaction between Mcl1 and Noxa in the presence of JNK inhibitor II (SP600125, Calbiochem, Cat No.129-56-6, USA). 2×10^6 cells were seeded in six well plates and treated with JNK inhibitor for 1 h followed by *H. pylori* infection for 5 h. Mitochondrial fraction was isolated as described previously and the IP protocol (described below) was followed. In another set of experiments, interaction between Hif1 α and p300 was studied by immunoprecipitation for which 2×10^6 cells were plated. Cells were treated with CTK7A (100 μ M) and CoCl₂ (200 μ M) in combination or alone for 24 h and whole cell lysates were used for IP assays.

After incubation, cells were scraped from the cell culture plate & collected in microcentrifuge tubes. Cells were centrifuged at 4 °C at 850 x g for 5 min and resuspended in 200 μ l of 1% Triton X-100 and protease inhibitor cocktail (10 μ l/ml)-supplemented TEN buffer (150 mM NaCl, 50 mM Tris pH 7.5, 1 mM EDTA), vortexed, and kept on ice for 30 min for lysis. Then cells were centrifuged at 850 x g at 4°C for 10 min and 800 μ l of 1% Triton X-100 and protease inhibitor cocktail (10 μ l/ml)-supplemented TEN buffer was added to the supernatant in each tube. 10 μ l of protein A/G plus-agarose (Santacruz, Cat No. SC-2003,

USA) was added in each tube and kept at 4 °C for 30 min with shaking followed by centrifugation at 15600 x g for 5 min at 4 °C. Supernatants were collected and IgG B (SantaCruz Biotechnology, Cat No. SC-2762, USA) was added to control IgG-marked tube and specific antibodies (antibody used to pull down) were added to the other tubes as per recommended dilutions followed by overnight incubation at 4 °C with shaking. After 12-14 h, tubes were taken out from the cold room and centrifuged at 2300 x g for 2 min at 4 °C. 15 µl of 50% protein A/G plus-agarose was added to each tube followed by incubation for 3 h with shaking in cold room. Pelleted immunocomplex was washed twice with ice cold 1X PBS (2300 x g for 5 min). Pellet was cooked with sample buffer supplemented with 5% β-mercaptoethanol (HiMedia, Cat No. MB041, India). Lysate was then loaded onto SDS gel as previously explained and desired proteins were detected by western blotting after probing with specific antibodies.

2.2.14. Generation of stable cell lines

Noxa wild type (WT) and mutant (mut) constructs expressing stable cell lines were generated in AGS cells. The protocol for stable cell line generation includes transfection of cells (as described before) with desired constructs and then selection of transformed cells. 28 h post-transfection, cells were trypsinized with 500 µl of trypsin for 5 min. Then cells were distributed in two six well plates, one with 200 µg/ml G418 (Sigma-Aldrich, Cat No. 051M0854, USA) and the other without G418. Cells were kept under selection pressure for 3 days. After 3 days, G418 was added to each well at a concentration of 300 µg/ml. After every 3 days, this selection media was changed and cells were kept fresh selection media for 15 days. Following this, cells were trypsinized and subcultured into media with 300 µg/ml G418.

The same protocol was followed for generation of stable cells expressing pDsRed2-Mito vector (Clontech Laboratories, Cat. No. 63242, USA). This construct was used to fluorescently label mitochondria.

Confirmation of Noxa-expressing stable cells by western blotting: 0.5×10^6 cells were plated for empty vector, Noxa WT and mut constructs. Sample isolation was done after 24 h of plating according to previously-mentioned protocol. The semidry transfer protocol was followed for transfer of proteins.

Confirmation of pDsRed2-Mito expressing stable cells by fluorescence microscopy: 0.16×10^6 pDsRed2-Mito expressing AGS stable cells were seeded on coverslips in 24 well plates. After 24 h of plating, old media was removed from each well and 500 μ l of new media was added to each well with equal amount of paraformaldehyde (PFA) (Sigma-Aldrich, Cat No. SLBCO355V, USA) (1:1 ratio to that of media) and kept at RT for 15 min. Then PFA was removed and samples were washed 3 times with 1X PBS (3 min each) in shaker. Then 4', 6-Diamidino-2-phenylindole, Dihydrochloride (DAPI, Invitrogen, Cat No. D1306, USA) (1:2000) was added to each well and kept for 20 min at RT followed by washing with PBST and allowed to dry. Coverslips were mounted to glass slides with 4 μ l of Fluoromount G (Sigma-Aldrich, Cat No. F-4680, USA) kept for 30 min at RT and detection was done by using Olympus fluorescence microscope (Olympus, Model No. WS-BX51-0169, Japan).

2.2.15. Confocal microscopy

AGS cells were grown on coverslips in 24 well plates and treated with hypoxia and CTK7A alone or in combination for the desired time periods. For another experimental setup, Noxa WT and S13A mutant or empty vector constructs were transfected in pDsRed2-stably expressing AGS cells followed by infection with *H. pylori* for 9 h. Cells were fixed with paraformaldehyde (1:1 ratio to that of the media) and kept at RT for 15 min. Fixed cells were then washed with 1X PBS followed by treatment with triton X-100 for 5 min. Coverslips were washed with 1X PBST and blocked for 1 h with 5% BSA followed by washing and incubation with primary antibody for overnight at 4 °C. After primary antibody incubation, cells were washed with PBST followed by secondary antibody treatment for 2 h. Nuclei of cells were counterstained

by DAPI for 20 min, washed with PBS and coverslips were mounted to slides by using 4 μ l of Fluoromount G. Mitochondrial appearance was assessed by a laser scanning confocal microscope (LSM 780, Carl Zeiss, Jena, Germany) with argon laser 488 excitation and a 63X/1.4 NA oil objective (Carl Zeiss). LSM-TPMT camera system (Carl Zeiss) and ZEN 2010 software (Carl Zeiss) were used for image capturing. Image analysis was performed by using LSM software (Carl Zeiss) and processing was done by Adobe Photoshop CS4. Mitochondrial fragmentation (represented by the length, circularity and roundness) was quantified by ImageJ software (NIH, Bethesda, MD, USA).

(Refer appendix II for detail of antibodies used)

2.2.16. Sectioning of gastric biopsy tissue samples

Biopsy samples were stored in 4% PFA for overnight and then transferred to 25% of sucrose solution at 4 °C. Tissue samples were mounted over glass slides coated with poly-L-lysine (Sigma-Aldrich, Cat No. SLBB7119, USA) and kept at 37 °C for 30 min. Samples were then placed on the holder and dipped into mounting media (Sigma-Aldrich, Cat No. F4680, USA) inside the cryostat (Leica Biosystems, Model No. LEICA CM3050 S, Germany). Sectioning was done for the control as well as patient samples with a thickness of 10 μ m. Immunofluorescence staining was performed as described in the next section.

2.2.17. Immunofluorescence microscopy

Fluorescence microscopy was performed to study the expression of various EMT markers in gastric biopsy tissue samples (described later) and AGS cells. Samples were washed with 1X PBS followed by Triton-X-100 (0.5%) treatment for 15 min. Samples were blocked with 3% FBS for 1 h at RT followed by overnight incubation with primary antibody at 4 °C. Slides were washed 3 times with 1X PBST for 5 min each and incubated with fluorescently conjugated secondary antibodies such as Alexa Fluor 488 goat anti-mouse (Invitrogen, Cat No. A-11001, USA) and Alexa Fluor 488-goat-anti-rabbit (Invitrogen, Cat No. A-11034, USA) for 2 h at RT.

Finally, slides were washed with 1X PBS twice and mounted with Fluoromount G mixed with DAPI (1:2000). Slides were analyzed by a fluorescence microscope (refer appendix II for detail of antibodies used).

2.2.18. Flow cytometry

Apoptosis in untreated as well as treated experimental groups were quantitated by flow cytometry. AGS cells were treated with CoCl₂ alone or in combination with CTK7A for 24 h or left untreated. Similarly, in another set of experiment, AGS cells were transfected with Noxa WT, S13A mutant or empty vector-transfected cells followed by infection with *H. pylori* for 10 h or left uninfected. For both experimental setups cell pellets were washed twice with chilled PBS and cells were stained with Annexin V PE/7 AAD (BD Biosciences, Cat No. 556422 and 559925, respectively) according to the manufacturer's instruction. 10000 cells were taken during acquisition by using FACSCalibur Flow Cytometer (BD Biosciences, Model No. 342976, USA). Results were analyzed by using CellQuest Pro software (BD Biosciences).

2.2.19. Trypan blue dye-exclusion assay

Cell viability was measured by using trypan blue stain (Hyclone, Cat No. SV30084.01, USA). 20 µl of the cell suspension was mixed with 180 µl of trypan blue. Within five minutes of mixing, the cells were counted under an inverted microscope (Olympus, Model no. CKX 41SF, Japan) by using Neubauer hemocytometer (Merienfed, Germany). Viable cells were detected by their dye-exclusion property.

2.2.20. Detection of reactive oxygen species (ROS)

Generation of intracellular ROS was measured by staining cells with 5-(and 6)-chloromethyl-2, 7-dichlorodihydrofluorescein diacetate, acetyl ester (CM-H₂-DCFDA; Invitrogen, Cat No. C6827, USA). This is a chloromethyl derivative of H₂DCFDA which can passively enter into the cell. CM-H₂DCFDA is widely used to measure oxidative stress in cells. CM-H₂DCFDA is resistant to oxidation, but when taken up by cells, is de-acetylated by intracellular esterases to

form the more hydrophilic non-fluorescent reduced dye dichlorofluorescein DCFH, which then is rapidly oxidized to form a two-electron oxidation product, the highly fluorescent DCF in a reaction with the oxidizing species. To do this, 0.166×10^6 AGS cells were grown on 9 mm coverslips in a 24 well cell culture plate. These cells were treated with hypoxia alone or in combination with CTK7A or left untreated for 24 h. Cells were stained with $1\mu\text{M}$ CM-H₂-DCFDA and incubated for 10 min at 37 °C in the dark. Cells were fixed with 4% PFA for 10 min at RT and viewed with fluorescence microscope.

2.2.21. Soft agar assay

The soft agar assay is the technique to study anchorage-independent nature of cells. In this experiment cells were plated in between two layers of agar and treatment was done for desired time.

Preparation of the bottom agar (0.6%): 1.2% Bacto Agar (MP Biomedicals, Cat No. 199835, USA) was prepared by autoclaving 1.2 gm agar in 100 ml of distilled H₂O and continuously maintained at 50 °C to avoid solidification. Dulbecco's Modified Eagle Medium/ Nutrient Mixture F-12 Ham (DMEM/ F12, 1:1 mixture) media (HiMedia, Cat No. AT140A, India) and equal volume of 1.2% agar were mixed properly. 1 ml of the mix was poured on each plate and kept in the CO₂ incubator for 30 min.

Preparation of the top agar (0.3%): Top agar was prepared by adding 2X media (DMEM/ F12, 1:1 mixture), 1.2 % agar, cell suspension (containing 10000 cells) and MilliQ H₂O.

0.3% top agar were plated over 0.6 % bottom agar in 6 well cell culture plates. These plates were treated with CoCl₂ and CTK7A for 30 days at an interval of 3 days. Cells were maintained in humidified 37 °C incubators containing 5% CO₂. At the end of the incubation period, visible colonies on the top agar were counted and colony sizes were compared between various treatment groups.

2.2.22. Scratch assay or wound-healing assay

Scratch assay was performed to study the wound-healing property of cells. 1×10^6 AGS cells were seeded in 35 mm cell culture plates and incubated for 24 h to create a monolayer of cells. Cell layer was scratched with a 200 μ l pipette tip and new media was added to each well. Dislodged cells were washed off and fresh RPMI media was added to wells. Cells were treated with CoCl_2 (200 μ M) and CTK7A (100 μ M) in combination or alone or left untreated for 24 h. A bright field inverted microscope (Carl Zeiss, Primo Vert, Germany) as used to study the wound closure between two boundaries. The migration distance was assessed using Image J 1.43 software (NIH).

2.2.23. Transwell migration and invasion assay

Transwell migration and invasion assay were performed to study metastatic properties of GECs after treatment with CoCl_2 and the HAT inhibitor, CTK7A. In another set of experiment, AGS cells were tested for their invasion and migration potential in *H. pylori*-infected and HAT inhibitor-treated GECs. Cell migration and invasion assays were performed by using 8- μ m pore size transwell biocoat control inserts (migration assay, BD, Cat No. 353097, USA) or matrigel-coated inserts (BD, Cat No. 354483, USA) as per manufacturer's instruction. Transwell inserts were arranged over 24 well plates and 5×10^4 AGS cells dissolved in serum free RPMI were seeded on the upper surface while the lower chamber was filled with 10% FBS-containing media. After completion of treatments as mentioned above for different experimental groups, upper surfaces of the transwell were scraped off by using a cotton swab to remove the non-invading cells. Cells in the lower surface were fixed for 30 min with 4% PFA after a wash with 1X PBST followed by permeabilization with 0.5% tween-20. Inserts were stained for 30 min with haematoxylin (Fischer Scientific, Cat No. 38803, USA). After a final wash with 1X PBS a drying period of 60 min was allowed. Finally, membranes were cut from the inserts and mounted over a glass slide keeping the lower side down. Migrated and invaded cells were

counted (from five different fields) under a bright field inverted microscope (Carl Zeiss, Primo Vert, Germany).

2.2.24. Densitometric and statistical analysis

Densitometric analyses of western blot images as well as flow cytometry data were done by Image J 1.43 software (NIH). Values are given as means \pm SEM. Student's *t*-test was performed for comparisons of two groups. Statistical significance was determined at **P*<0.05. Statistical analysis was also performed by using GraphPad Prism 5 (Prism, V5.04, USA) for confocal analyses. For multiple comparisons, Two-way ANOVA was performed and Turkey test was applied for *post hoc* comparisons.

RESULTS

(Chapters3-5)

3. Apoptosis induction in hypoxic GECs expressing EMT markers and showing invasive properties

3.1. Hif1 α and metastatic markers are upregulated in CoCl₂-treated GECs

CoCl₂.6H₂O is a chemical inducer of hypoxia which has similar biochemical responses as of physiological hypoxia with respect to Hif1 α induction (46). To investigate the role of chemically-induced hypoxia on GECs, dose and time point of CoCl₂ was standardized (Figure 3.1A). For this, AGS cells were treated with 50 μ M, 100 μ M, 200 μ M and 300 μ M of CoCl₂ for 24 h. Hif1 α expression increased dose-dependently and showed equal expression at 200 μ M as well as 300 μ M concentrations. Hif1 α miRNA expression in CoCl₂-exposed cells is also reported in the literature (129). No change in p300 expression was observed with increasing dose of CoCl₂. But as 300 μ M concentration is considered to be beyond the physiological limits (130, 131), this dose was not found suitable for further use. Therefore, 200 μ M of CoCl₂ concentration was considered as the optimum dose for the rest of the experiments. The effect of CoCl₂ on the EMT marker expression pattern was studied with 200 μ M of CoCl₂ for various time points which showed induced expression of Hif1 α , Twist1 and N-cadherin, the major EMT markers expressed in metastatic cells (Figure 3.1B). As AGS cells are E-cadherin null (132), E-cadherin bands were not found upon CoCl₂ exposure.

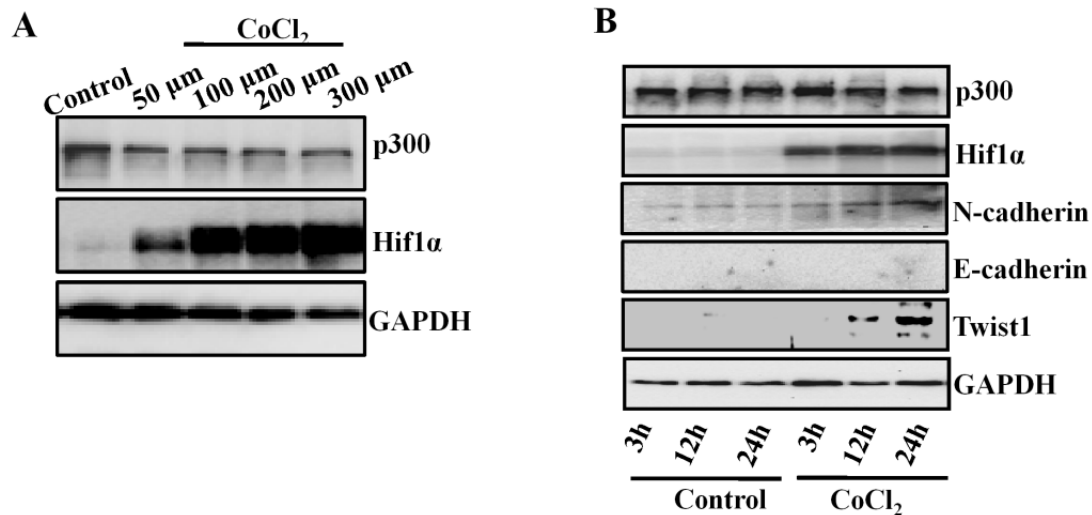


Figure 3.1. Induced expression of Hif1α and EMT markers in CoCl₂-treated GECs. (A) Western blot analysis (n=3) of whole cell lysates isolated from AGS cells after treatment with 50 μM, 100 μM, 200 μM and 300 μM concentrations of CoCl₂ for 24 h. GAPDH was used as a loading control. (B) Expression of Hif1α and various metastatic factors in AGS cells was assessed by western blotting (n=3) at 3 h, 12 h, 24 h after treatment with 200 μM of CoCl₂. GAPDH was used as a loading control.

3.2. Hif1α and EMT markers are upregulated in metastatic gastric cancer biopsy samples

Expression of EMT markers in gastric cancer biopsy samples was studied. Gastric cancer metastatic biopsy samples were collected from metastatic gastric adenocarcinoma patients and compared with adjacent noncancerous areas. Biopsy tissues were sectioned and immunofluorescence staining was performed to study expression of various EMT markers. Remarkably higher expression of Hif1α as well as Twist1 and N-cadherin were observed in metastatic samples as compared to their matched controls while E-cadherin expression was downregulated (Figure 3.2).

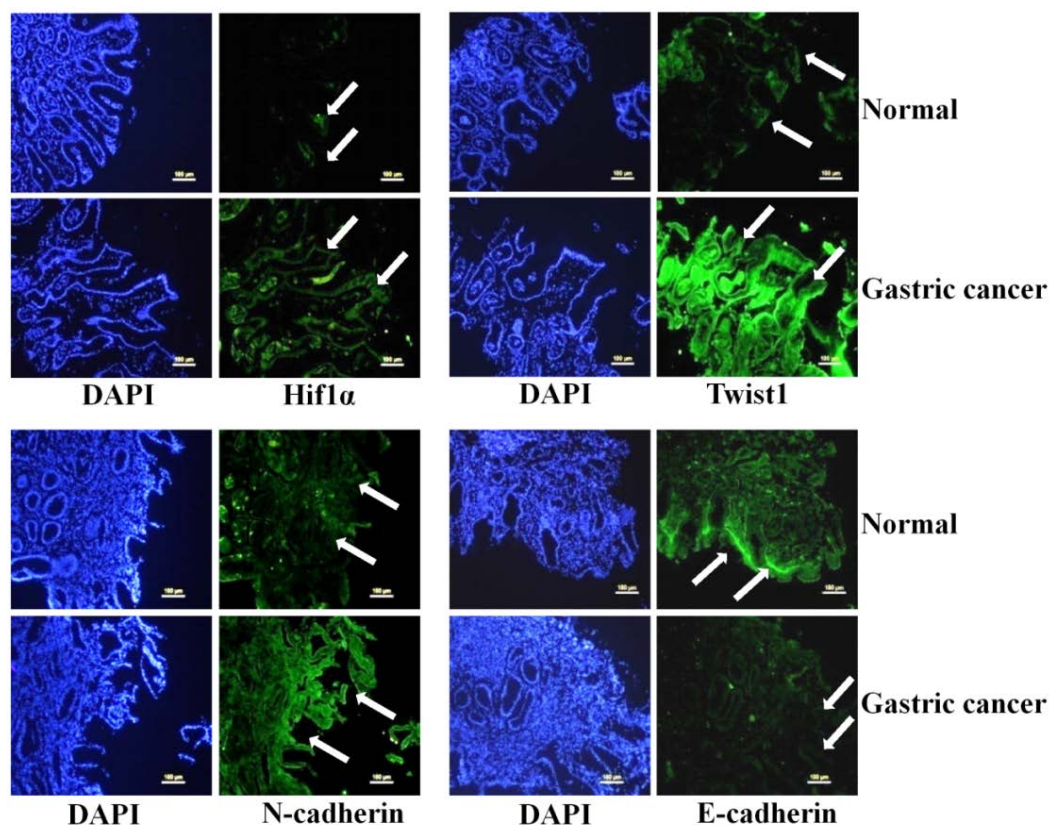


Figure 3.2. Expression pattern of metastatic factors in metastatic gastric cancer biopsy samples. Metastatic gastric cancer biopsy samples and adjacent noncancerous gastric tissue samples ($n=4$ in each group) were immuno stained with fluorescently labeled Hif1 α , Twist1 and N-cadherin antibodies. Nuclear staining was performed with DAPI stain. Scale bar 100 μm .

3.3. Inhibition of HAT activity downregulates expression of Hif1 α in CoCl₂-treated GECs

Hif1 α is one of the major regulatory molecules expressed during EMT and metastasis progression in hypoxic GECs (133). To study the status of Hif1 α under chemical hypoxia, AGS cells were treated with CoCl₂ alone or in combination with one curcumin-derived HAT/KAT inhibitor CTK7A (128) or left untreated for 24 h. Western blot results indicated decrease in Hif1 α expression in CTK7A and CoCl₂-treated GECs. Acetylation of p300 was also reduced in CTK7A and CoCl₂-treated cells (Figure 3.3A). As Hif1 α is a nuclear protein, Hif1 α status was further investigated in the nuclear fraction of GECs and Hif1 α expression was found to be

decreased in HAT inhibitor and CoCl_2 -treated GECs (Figure 3.3B). Further IP were performed to find interaction between Hif1 α and p300. An interaction between p300 and Hif1 α was observed only in CoCl_2 treated cells which was drastically reduced after CTK7A treatment (Figure 3.3C).

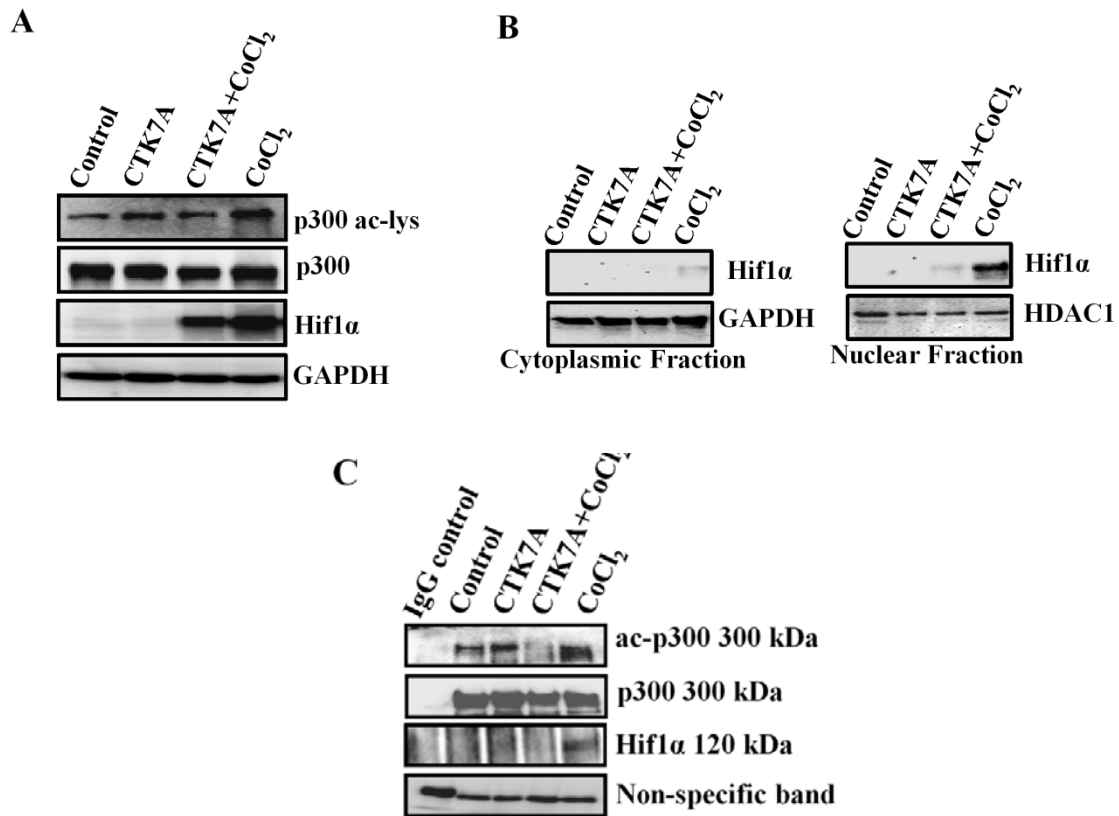


Figure 3.3. Effect of HAT inhibition on Hif1 α expression in CoCl_2 -treated GECs.

(A) Western blot analysis ($n=3$) of whole cell lysates from AGS cells treated with 200 μM of CoCl_2 and/or 100 μM of CTK7A for 24 h. Blots were probed with Hif1 α , p300 and Pan-acetyl lysine antibody. GAPDH was used as a loading control. (B) Western blot ($n=3$) experiments showing Hif1 α expression in the nuclear and cytosolic fractions of CTK7A (100 μM) and/or 200 μM CoCl_2 -treated GECs for 24 h. HDAC1 and GAPDH were used as loading controls for the nuclear and cytosolic fractions, respectively. (C) Interaction between p300 and Hif1 α were assessed by immunoprecipitation experiment with whole cell lysates prepared from CTK7A and CoCl_2 -treated AGS cells. A non-specific band was used to estimate protein loading.

3.4. HAT inhibition downregulates EMT marker expression in chemically-induced and physiological hypoxia

Twist1 is a transcription factor and a hallmark of metastasis in GECs and one of the major metastatic markers expressed during hypoxia exposure (134-136). N-cadherin is another important marker expressed during EMT progression (137). Twist1 and N-cadherin expression was next studied in hypoxic GECs by western blotting and confocal microscopy. Induced expression of Twist1 and N-cadherin was observed in CoCl₂ treated cells, which was inhibited after treatment with CTK7A for 24 h (Figure 3.4A, 3.4B). Similar results were observed in MKN45 cells. p53 null KATO III cells also showed reduced expression of Hif1 α , Twist1 and N-cadherin in CTK7A and CoCl₂ treated cells (Figure 3.4C). Further, effect of CTK7A in physiological hypoxia was studied by exposing GECs to normoxia (21% O₂) and hypoxia (1.0% O₂) for 24 h in the presence or absence of CTK7A. Whole cell lysates were immunoblotted and probed with antibodies for Hif1 α and EMT markers such as N-cadherin and Twist1. Our results confirmed that, CTK7A had the same effect on Hif1 α , N-cadherin and Twist1 expression in 1% O₂-treated cells as it was found in CoCl₂-treated cells (Figure 3.4D). Therefore, majority of our experiments were performed using CoCl₂ unless stated specifically about exposing cells to 1% O₂.

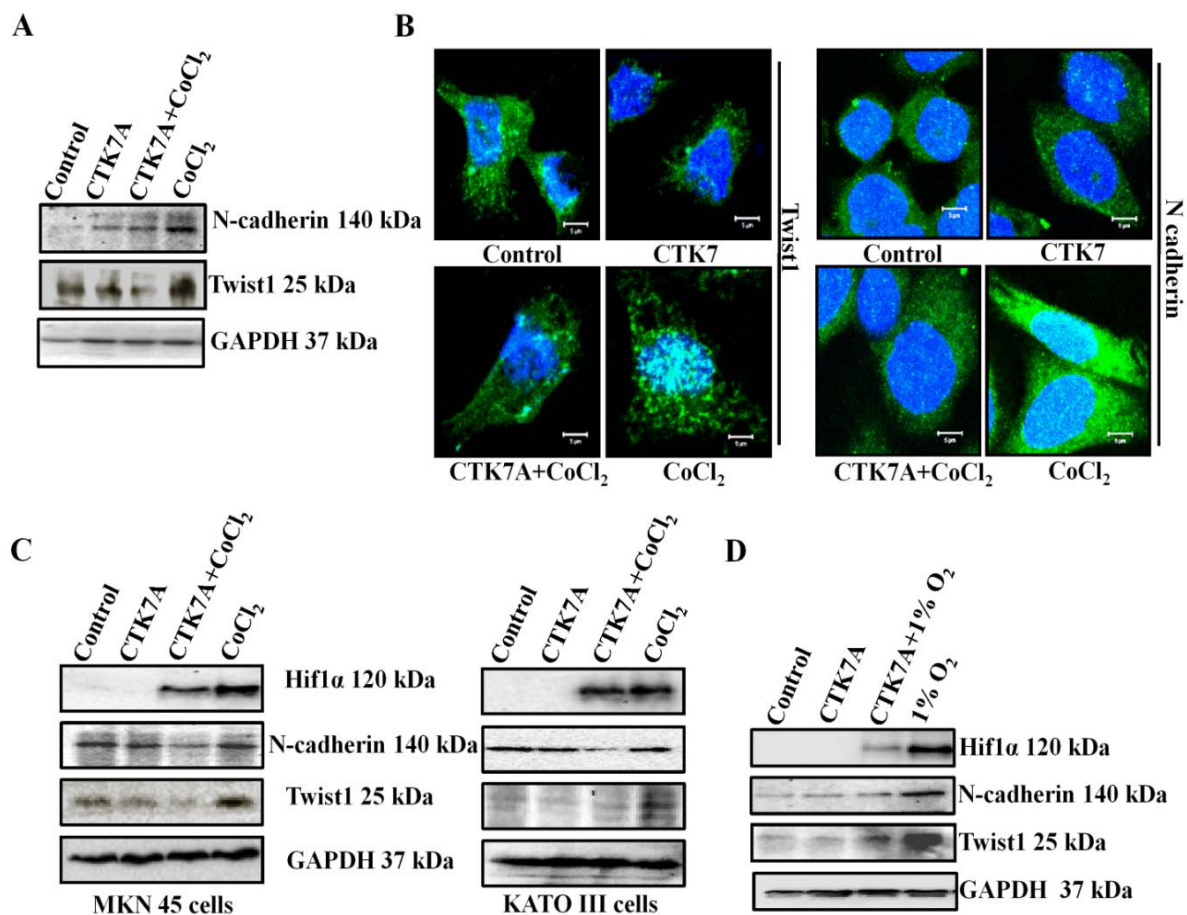
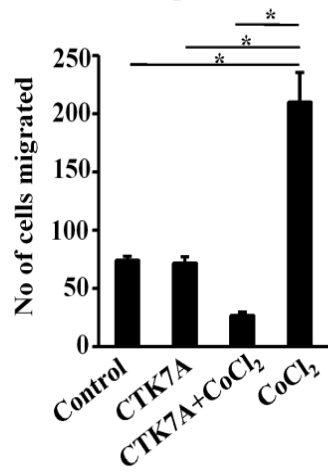
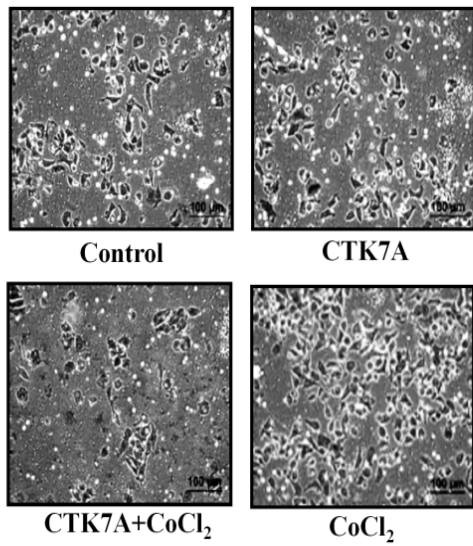
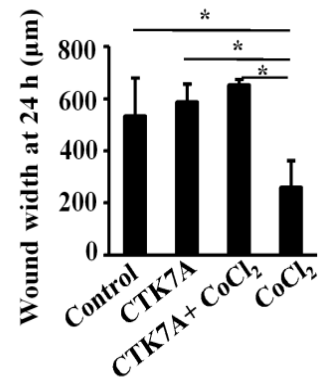
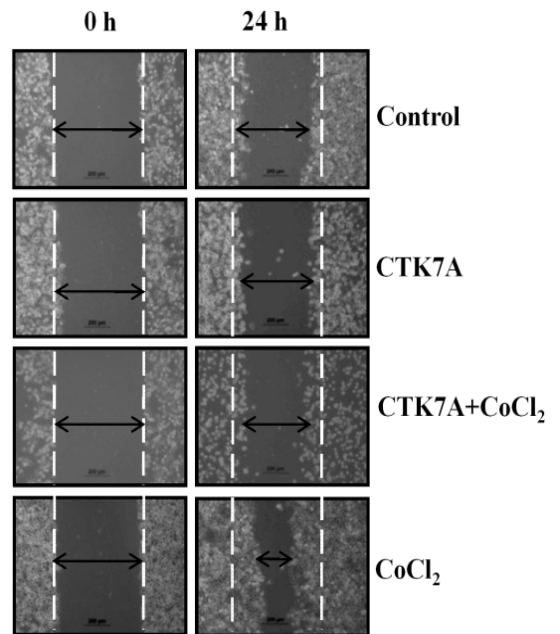


Figure 3.4. Effect of HAT inhibition on EMT marker expression in chemically-induced and physiological hypoxia. (A) A representative western blot analysis ($n=3$) of whole cell lysates from AGS cells after treatment with $200 \mu\text{M}$ of CoCl_2 and/or $100 \mu\text{M}$ of CTK7A for 24 h. GAPDH was used as a loading control. (B) A representative confocal microscopy image of AGS cells treated with CoCl_2 ($200 \mu\text{M}$) alone or in combination with CTK7A ($100 \mu\text{M}$) showed expression pattern of EMT markers Twist1 and N-cadherin. Scale bar $5 \mu\text{m}$. (C) Western blot analysis ($n=3$) of whole cell lysates isolated from MKN-45 cells and KATO III cells after treatment with $200 \mu\text{M}$ of CoCl_2 and/or $100 \mu\text{M}$ of CTK7A for 24 h. GAPDH was used as a loading control. (D) Immunoblotting ($n=3$) of whole cell lysates from AGS cells after a hypoxia ($1\% \text{O}_2$) exposure alone or with CTK7A. GAPDH was used as a loading control.

3.5. Metastatic property of GECs are suppressed in CoCl₂ and HAT inhibitor-treated cells

Role of hypoxia in inducing invasive properties of GECs is well established (138, 139). The effect of HAT inhibition on metastatic properties of CoCl₂-treated GECs was assessed by migration assay, invasion assay, wound-healing assay and anchorage independent growth assay. Migration ability of GECs was evaluated by transwell migration assay and wound healing assay. Our result confirmed a significant reduction in CoCl₂-induced migration upon CTK7A treatment (Figure 3.5A). In another experiment, cell migration ability was measured by filling of the gap which was made in the uniform lawn of cells. Higher migration rate was observed in only CoCl₂-treated wells as compared to CTK7A and CoCl₂-treated wells (Figure 3.5B). Invasiveness of GECs was measured by matrigel invasion assay in which a significant reduction in invasiveness was observed in CoCl₂ plus CTK7A-treated GECs as compared to only CoCl₂-treated cells (Figure 3.5C). Anchorage-independent growth of CoCl₂-treated GECs was evaluated after CTK7A treatment by soft agar assay. A significant reduction in the number of foci was observed in CTK7A-treated cells as compared to only CoCl₂-treated cells (Figure 3.5D).

A**B**

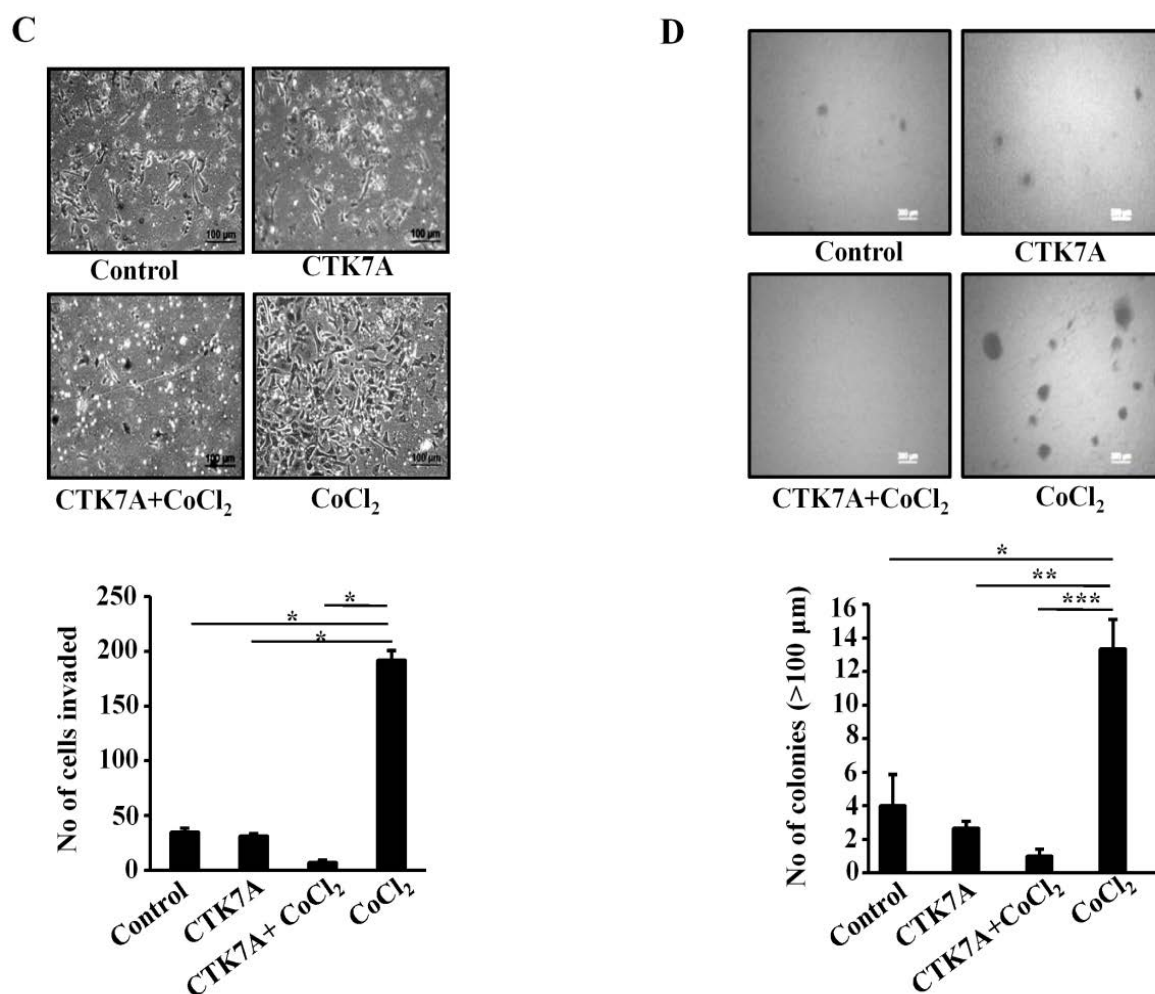


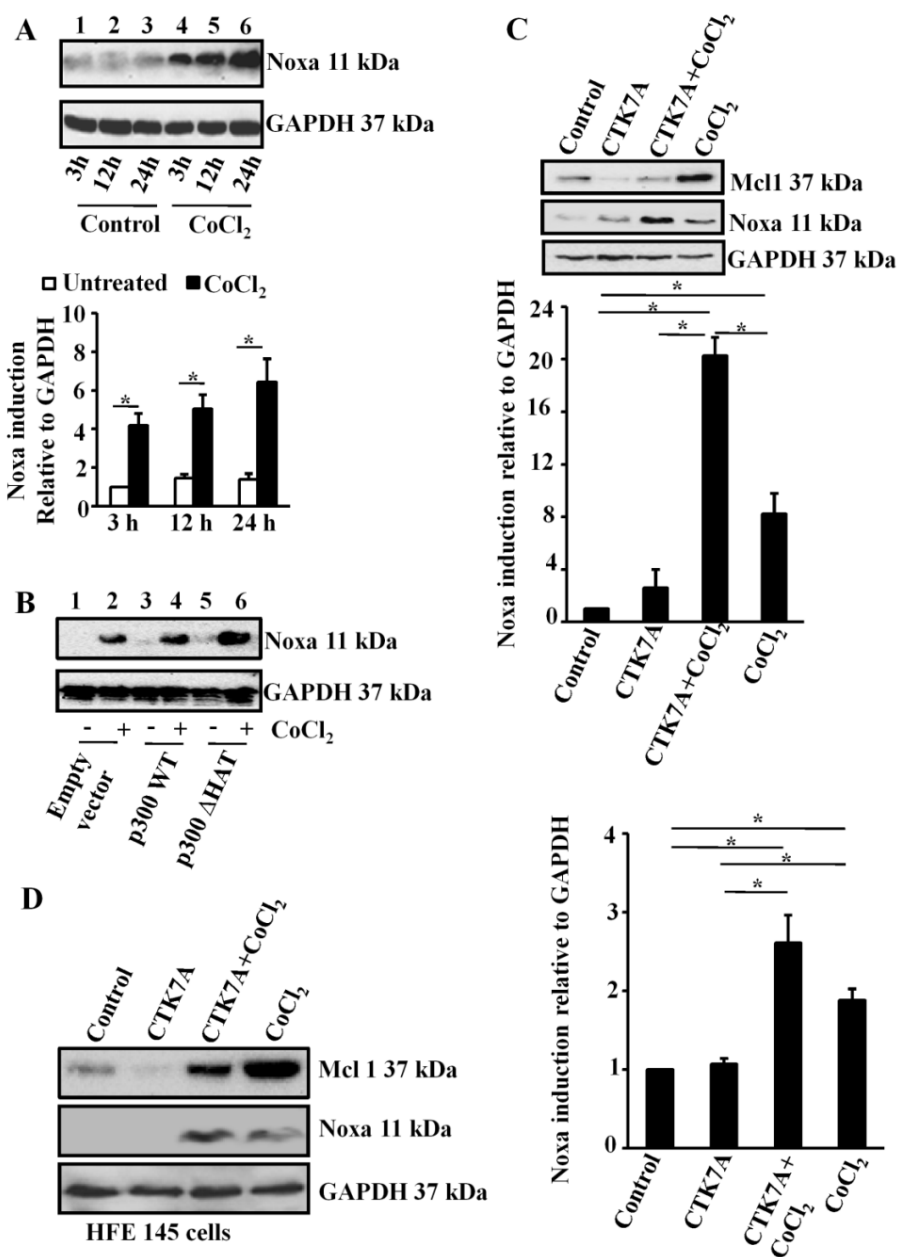
Figure 3.5. HAT inhibition suppresses metastatic properties in CoCl₂-treated GECs. (A) Transwell migration assay was performed by using 24 well inserts in which the upper chamber contains AGS cells suspended in serum-free media while lower chambers had 10% FBS-enriched media. After 24 h of treatment, inserts were stained with haematoxylin and migrated cells were counted using an inverted microscope. Scale =50 μm. Bars represent the count of cells migrated from three independent experiments (mean±SEM). *P< 0.05. (B) Wound healing assay or scratch assay was performed by formation of a wound of uniform width over the monolayer culture of AGS cells followed by treatment with CoCl₂ (200 μM) alone or in combination with CTK7A (100 μM). One untreated experimental setup was used as a control. After 24 h of treatment, wound closure property of cells was measured in terms of change in wound width (n=4 independent experiments, *P<0.05) by using an inverted microscope

equipped with camera (Primo Vert Carl Zeiss, Germany). Scale bar 200 μm . (C) Matrigel-pre-coated Transwell invasion assay was performed to study the invasive property of AGS cells after treatment with CoCl_2 (200 μM) alone or in combination with CTK7A (100 μM) for 24 h. Number of invading cells were stained with haematoxylin and counted ($n=3$ independent experiments, $*P<0.05$) by using an inverted microscope. (D) AGS cells were treated with 200 μM CoCl_2 and/or CTK7A (100 μM) for 24 h or left untreated. After 21 days of incubation, anchorage-independent growth of CTK7A and CoCl_2 -treated hypoxic cells were measured by counting number of colonies over the upper layer of agar surface by using an inverted microscope. Scale bar 300 μm . Student's *t*-test was used for quantification of anchorage-independent growth ($n=3$); $*P<0.05$, $**P<0.01$, $***P<0.001$.

3.6. Inhibition of HAT activity induces Noxa expression in CoCl_2 -treated hypoxic GECs

Noxa is one of the Hif1 α -induced proteins and a major contributor in apoptosis (115). To find out the optimum time for Noxa expression after 200 μM CoCl_2 treatment, AGS cells were treated for 3 h, 12 h and 24 h. A gradual increase in Noxa expression was observed in hypoxic GECs (Figure 3.6A). In order to study the effect of p300HAT on Noxa expression, AGS cells were transfected with pcDNA3.1⁺ empty vector, p300 WT and p300 HAT mutant constructs followed by CoCl_2 (200 μM) treatment for 24 h. A significant increment in Noxa expression was observed in HAT mutant-transfected cells (Figure 3.6B). Role of p300 HAT activity on Noxa expression was validated by using HAT inhibitor CTK7A. AGS cells were treated with CoCl_2 alone or in-combination with CTK7A for 24 h and immunoblotting was performed to validate the status of Noxa. A significant upregulation in Noxa expression was observed in CTK7A and CoCl_2 -treated cells. Antiapoptotic protein Mcl1 remained suppressed in CoCl_2 plus CTK7A-treated cells as compared to only CoCl_2 -treated AGS cells (Figure 3.6C). Further, the effect of CTK7A on non-malignant, immortalized HFE-145 cells was studied in the presence and absence of CoCl_2 . A similar effect of CTK7A on Noxa expression was found in HFE-145

cells but at a lesser magnitude as compared to AGS cells (Figure 3.6D). Two other GECs, KATO III and MKN 45, showed similar Noxa expression pattern as that of AGS cells in the above mentioned experimental conditions (Figure 3.6F). Effect of hypoxia (1% O₂) on GECs after HAT inhibition was further validated by western blotting. AGS cells were exposed to normoxia and hypoxia in the presence or absence of CTK7A. Our results showed that Noxa expression was significantly more in CTK7A and 1% O₂ exposed cells as compared to only 1% O₂-treated cells (Figure 3.6F).



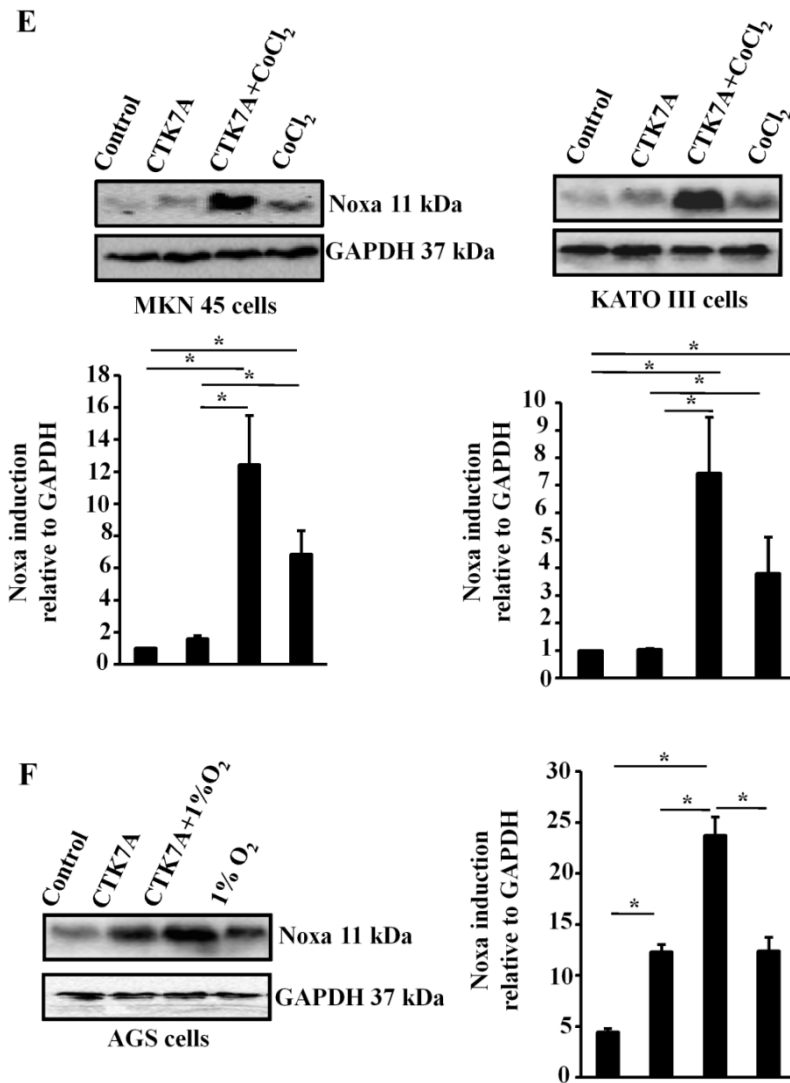


Figure 3.6. Noxa induction in CTK7A-treated and hypoxic GECs. (A) Immunoblot analysis of whole cell lysates ($n=3$) isolated from hypoxia-treated (3 h, 12 h, 24 h with 200 μM of CoCl_2). AGS cells showed time-dependent increment of Noxa expression. GAPDH was used as a loading control. Bar diagrams represent graphical presentation of western blot data (mean \pm SEM, $n=3$), $*P<0.05$. (B) A representative western blot analysis of whole cell lysates of Noxa protein in AGS cells after transfection with empty vector, p300 WT, p300 ΔHAT constructs followed by treatment with 200 μM of CoCl_2 for 24 h ($n=3$). GAPDH was used as a loading control. (C) Immunoblotting of whole cell lysate isolated from AGS cells after treatment with CoCl_2 (200 μM) and/or CTK7A (100 μM) for 24 h showed status of Mcl1 and Noxa proteins. GAPDH was used as a loading control. Significant increment in Noxa expression in

*CTK7A+CoCl₂-treated groups was graphically represented. (mean ± SEM, n = 3), *P<0.05.*

*(D) Whole cell lysates were prepared from immortalized human GEC HFE145 after treatment with CoCl₂ (200 μM) alone or in combination with CTK7A (100 μM) and western blotted by using Noxa and Mcl1 antibodies. GAPDH was used as a loading control. Noxa expression normalized to GAPDH was depicted by bar diagrams (mean ± SEM, n = 3), *P<0.05. (E) Immunoblot analysis (n=3) of whole cell lysates isolated from CoCl₂ (200 μM) and CTK7A (100 μM)-treated KATO III and MKN 45 cells showed induced expression of Noxa protein. GAPDH was used as a loading control. Student's t test was used for graphical presentation of the data. Bars represent mean ± SEM, n = 3, *P<0.05. (F) AGS cells were treated with hypoxia (1% O₂) alone or in combination with CTK7A (100 μM) for 24 h. Whole cell lysates were isolated and probed with Noxa antibody. GAPDH was used as a loading control. Bars represent mean ± SEM, n = 3, *P<0.05.*

3.7. HAT inhibition induces Noxa translocation to mitochondria and Cyt c release in CoCl₂-treated GECs

Noxa is translocated to mitochondria during apoptosis induction (140). Effect of HAT inhibition on Noxa expression was studied in CoCl₂-treated hypoxic GECs. A significant increment in mitochondrial Noxa translocation was observed in CTK7A and CoCl₂-treated GECs (Figure 3.7A). Confocal microscopy also confirmed enhanced Noxa translocation to the mitochondria in CTK7A and CoCl₂-treated AGS cells stably-expressing pDsRed2 construct (Figure 3.7B).

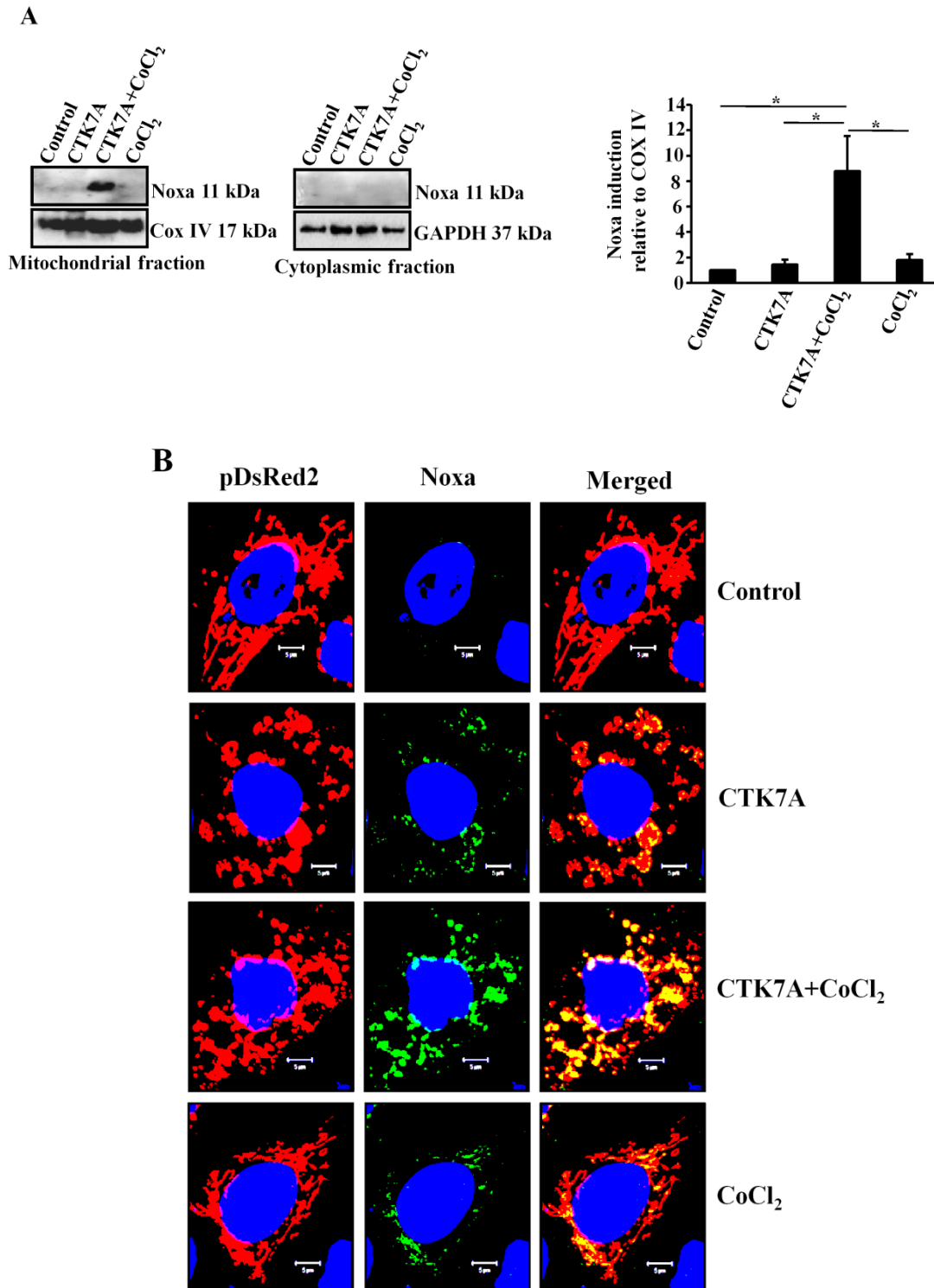


Figure 3.7. CTK7A induced mitochondrial translocation of Noxa in CoCl₂-treated GECs. (A) Mitochondrial and cytosolic lysates of AGS cells treated with CoCl₂ (200 μM) alone or in combination with CTK7A (100 μM) for 24 h were isolated and western blotted (n=3) to study Noxa expression. COX IV and GAPDH were used as loading controls for the mitochondrial

and cytosolic fractions, respectively. Bars depict Noxa expression normalized to COX IV in the mitochondrial fraction (mean \pm SEM, n=3), *P<0.05. **(B)** Confocal microscopy of AGS cells stably-expressing pDsRed2 (n=3) were treated with CoCl₂ (200 μ M) and/or CTK7A (100 μ M) for 24 h showed significant Noxa translocation into the mitochondria. Nuclei were stained with DAPI. Scale bar 10 μ m.

As Noxa translocation was followed by Cyt *c* (140) release, our next aim was to study the status of Cyt *c* in CTK7A and CoCl₂-treated AGS cells. To achieve this goal, confocal microscopy was performed by using pDsRed2 stably-expressing AGS cells, treated with CTK7A (100 μ M) and CoCl₂ (200 μ M) alone or in combination with CTK7A. Our results confirmed that a drastic reduction in mitochondrial retention of Cyt *c* occurred in CTK7A plus CoCl₂-treated cells as compared to control cells, only CTK7A-treated and only CoCl₂-treated cells.

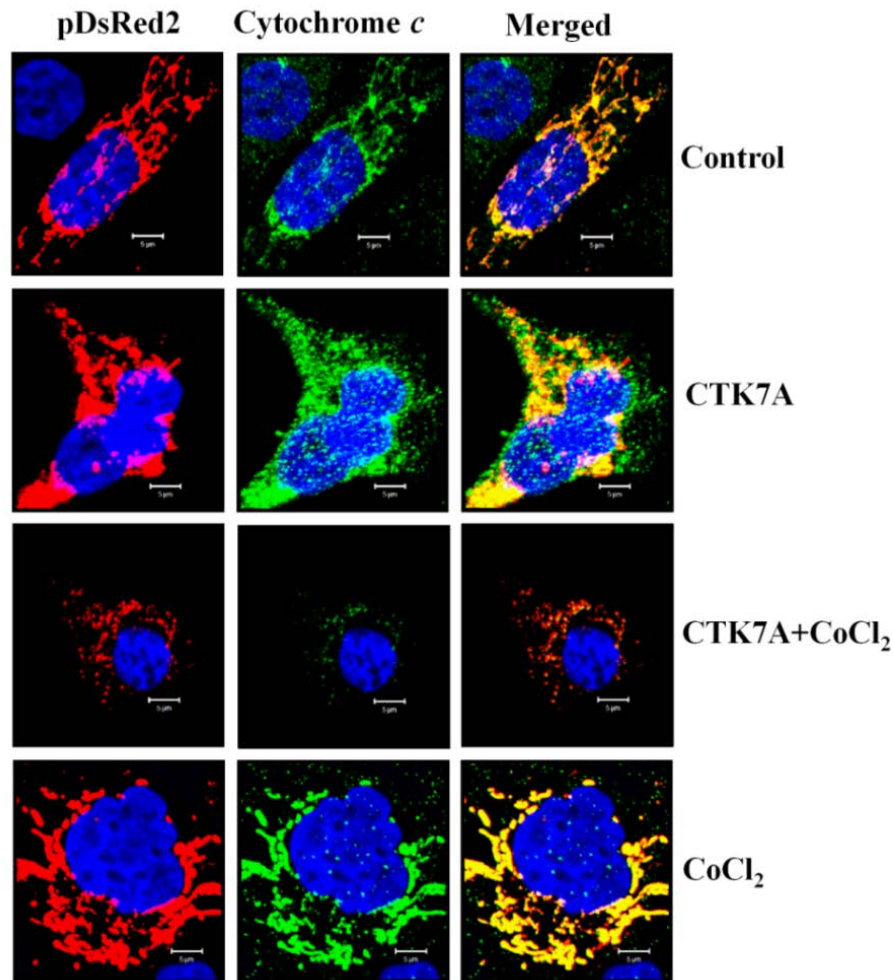


Figure 3.8. *CTK7A induced Cyt c release in CoCl₂-treated GECs. Confocal microscopy data showed that maximum Cyt c release occurred in CTK7A and CoCl₂-treated AGS cells stably-expressing pDsRed2 construct. DAPI staining was used to stain the nucleus. Scale bar 10 μm.*

3.8. Induction of intrinsic apoptotic pathway in CoCl₂ and CTK7A-treated GECs

Mitochondrial fragmentation is one of the important events during intrinsic apoptosis progression (141). Effect of CTK7A and CoCl₂ treatment on mitochondrial stress was studied by confocal microscopy. pDsRed2 stably-expressing AGS cells were used for this experiment. These cells were treated with CTK7A alone or in combination with CoCl₂ for 24 h. Fragmented mitochondrial morphology (spheroidal/punctated) was observed in CTK7A and CoCl₂-treated hypoxic GECs while the tubular network of healthy mitochondria was maintained in control as well as only CoCl₂-treated cells (Figure 3.9 A and B).

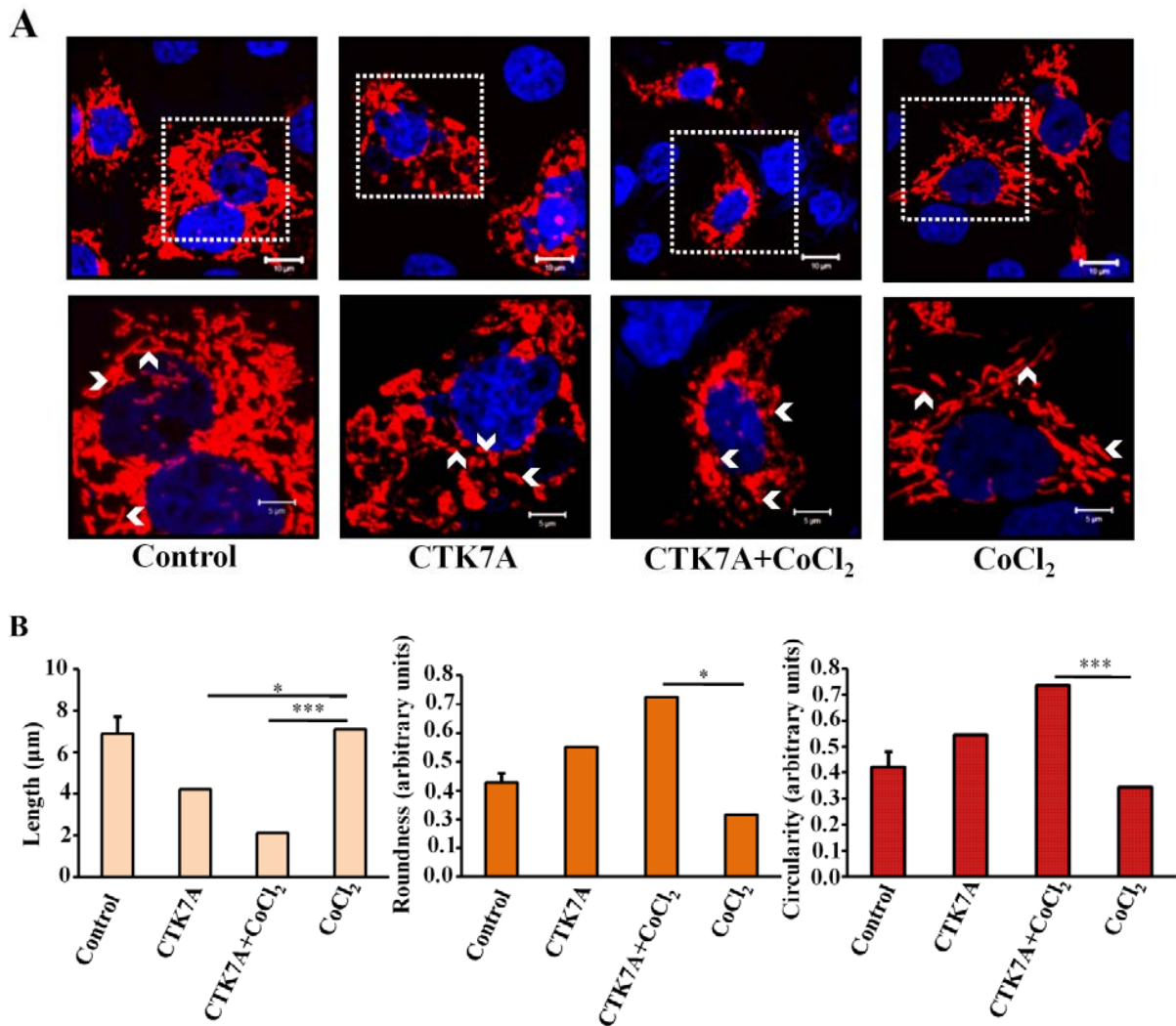


Figure 3.9. Mitochondrial morphology of HAT inhibitor and CoCl₂-treated GECs.

(A) *pDsRed2* stably-expressing AGS cells were treated with CoCl₂ (200 μM) alone or in combination with CTK7A (100 μM) for 24 h and mitochondrial morphology was examined by confocal microscopy. Upper panel: Images taken at lower magnification. Scale bar 10 μm. Lower panel: Zoomed-in images of the selected areas shown in the upper panel. Scale bar 5 μm. (B) Mitochondrial length, roundness and circularity were the important parameters measured from four cells (from four independent experiments). Statistically analysis was done by considering the mean length of five mitochondria from each cell. Circular and round

mitochondrial morphology was observed in CoCl_2 plus CTK7A-treated cells which indicated for more mitochondrial stress (mean \pm SEM, $n=4$), * $P<0.05$, ** $P<0.001$.

As caspase 9 and 3 are induced in mitochondria-mediated intrinsic cell death pathway, western blotting experiment was performed to study the expression of caspase 9 and its downstream effector caspase 3 in the whole cell lysates isolated from CTK7A and hypoxia-treated AGS cells. Maximal expression of cleaved caspase 9 and cleaved caspase 3 were observed in CTK7A-treated hypoxic AGS cells as compared to the single treatment groups or the control cells (Figure 3.9A, 3.9B).

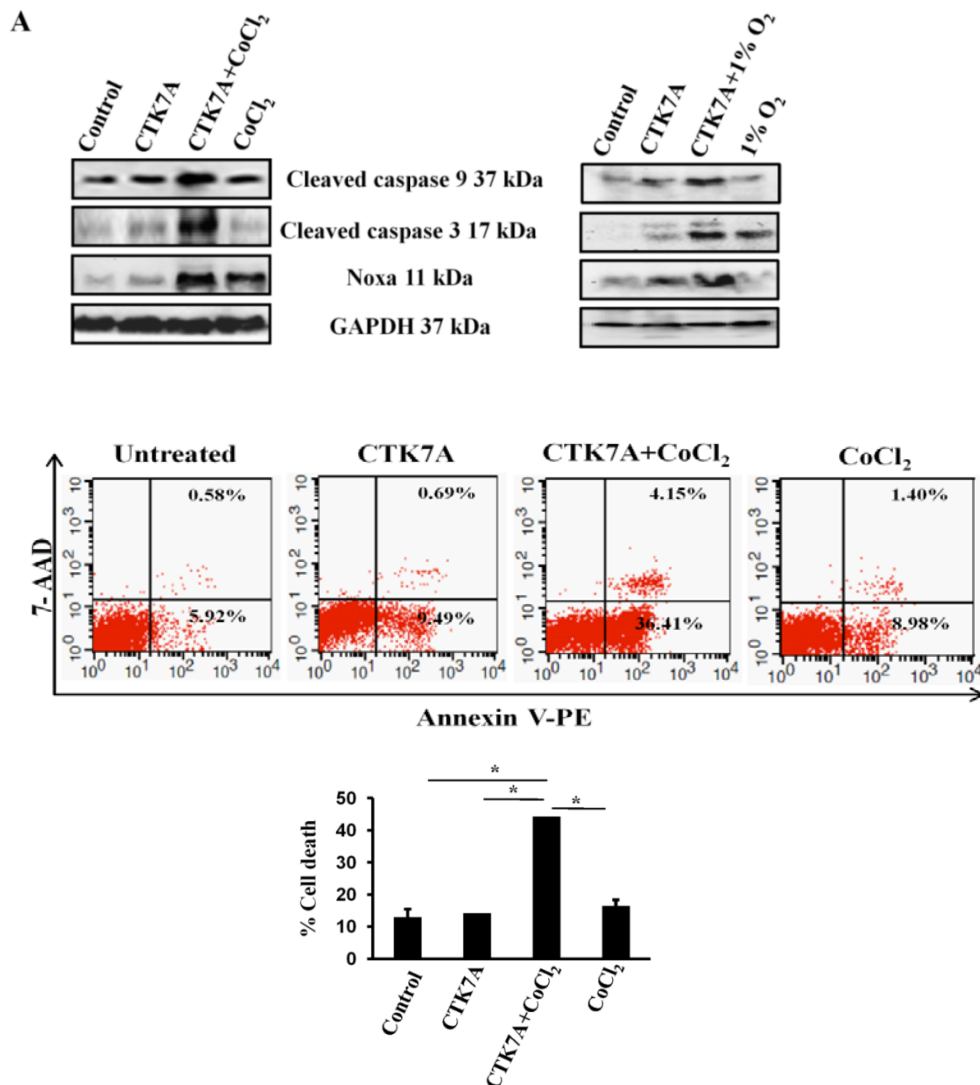


Figure 3.10. Intrinsic apoptotic cell death in CTK7A and CoCl_2 -treated GECs. (A) Whole cell lysates were isolated from AGS cells after treatment with CoCl_2 (200 μM) or hypoxia (1% O_2)

alone or with CTK7A (100 μ M) for 24 h. Western blot analysis ($n=3$) of Noxa, cleaved caspase 9 and cleaved caspase 3 showed their significant upregulation in CTK7A and hypoxia-treated GECs as compared to the single treatment groups. GAPDH was used as a loading control. (B) AGS cells were treated with 200 μ M CoCl₂ alone or in combination with CTK7A (100 μ M) for 24 h or left untreated. After completion of the incubation period cells were harvested and stained with Annexin V PE/7-AAD dyes. Flow cytometry analysis showed maximum apoptotic cell death in CTK and CoCl₂ treated cells. % cell death, in all four experimental groups were depicted by bar diagrams. (mean \pm SEM, $n=4$), * $P<0.05$.

3.9. Noxa upregulation is independent of Hif1 α expression in CTK7A and CoCl₂-treated hypoxic GECs

Binding of Hif1 α to Noxa is facilitated by HRE site in the Noxa promoter region (86). As both Hif1 α and Noxa proteins were upregulated by hypoxia exposure (115), the effect of Hif1 α on Noxa expression after CTK7A treatment in CoCl₂-exposed GECs was studied. AGS cells stably transfected with shRNA against Hif1 α cloned in pGFP-V-RS plasmid or with scrambled control shRNA or with empty pGFP-V-RS plasmid were treated with CTK7A (100 μ M) alone or in combination with CoCl₂ (200 μ M) for 24 h. Our results confirmed of a significant suppression of Hif1 α in Hif1 α -knockdown cells in the presence of CoCl₂, while the empty vector and scrambled shRNA-expressing cells had high expression of Hif1 α following CoCl₂-treatment. However, in spite of a drastic suppression of Hif1 α in Hif1 α suppressed cells, Noxa expression remained unaltered as that of empty vector or scrambled shRNA-transfected cells (Figure 3.11A). To study the effect of Hif1 α overexpression, AGS cells were transfected with Hif1 α overexpression constructs along with empty vector construct followed by CTK7A and CoCl₂ treatment for 24 h. Noxa was upregulated equivalently in empty vector as well as Hif1 α -transfected cells which indicated of Hif1 α -independent Noxa expression in CTK7A and CoCl₂-treated cells (Figure 3.11B).

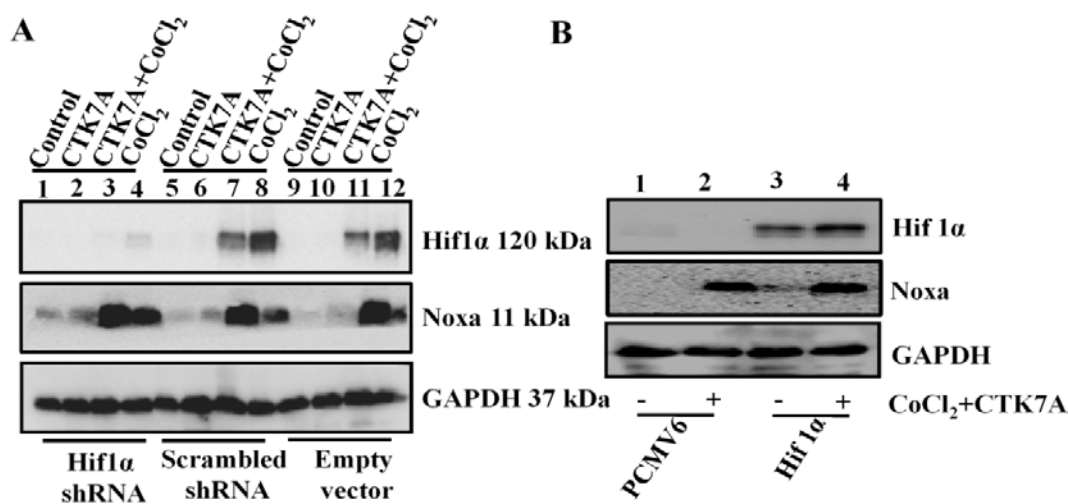


Figure 3.11. Noxa upregulation is independent of Hif1 α status in CTK7A and CoCl₂-treated hypoxic GECs. (A) Whole cell lysates were isolated from empty vector, scrambled negative control shRNA and Hif1 α -shRNA stably-expressing AGS cells treated with CoCl₂ (200 μ M) and/or CTK7A (100 μ M) for 24 h. Lysates were immunoblotted (n=3) and probed with Hif1 α , Noxa antibody. GAPDH was used as a loading control. (B) Western blot analysis (n=3) of whole cell lysates showed equal expression in Hif1 α overexpressed as well as empty vector transfected cells after treatment with hypoxia (200 μ M of CoCl₂) and/or CTK7A (100 μ M) for 24 h. GAPDH was used as a loading control.

3.10. HAT inhibition induces H₂O₂ generation in CoCl₂-treated GECs

Several reports correlated HAT activity with ROS generation (48, 142). Curcumin was reported to have differential effects on HAT function depending on dose. It decreased ROS generation and exerted anticancer effects when used at low concentration. But at higher dose, it killed cells by more ROS production (143). As CTK7A was derived from curcumin, the effect of CTK7A on ROS generation was next assessed. AGS cells were treated with superoxide dismutase (SOD, 200 units/ml for 4 h) to find out the involvement of superoxide (O₂⁻) in Noxa induction followed by treatment with CoCl₂ alone or in combination with CTK7A for 24 h. Whole cell lysates were western blotted and probed with Noxa antibody. There was no change in Noxa and Hif1 α expression after SOD treatment which indicated that neither CTK7A nor CoCl₂ or their

combination had any role on $O_2^{\cdot-}$ generation (Figure 3.12A). In another experiment, AGS cells were treated with a H_2O_2 scavenger, catalase (350 units/ml), for 4 h followed by a 24 h treatment with $CoCl_2$ (200 μ M) alone or in combination with CTK7A (100 μ M). Whole cell lysates were prepared and western blotted. A marked reduction in Noxa level was observed without changing Hif1 α level (Figure 3.12B). ROS generation was further confirmed by using CM- H_2 -DCFDA at a dose of 1 μ M for 10 min to assess intracellular ROS. Fluorescence microscopy data revealed a maximum ROS generation in CTK7A plus $CoCl_2$ -treated cells as compared to other experimental groups which was scavenged after pretreatment with catalase. Altogether, our findings summarized that H_2O_2 -mediated Noxa upregulation in CTK7A and $CoCl_2$ -treated GECs, was independent of cellular O_2 status (Figure 3.12C).

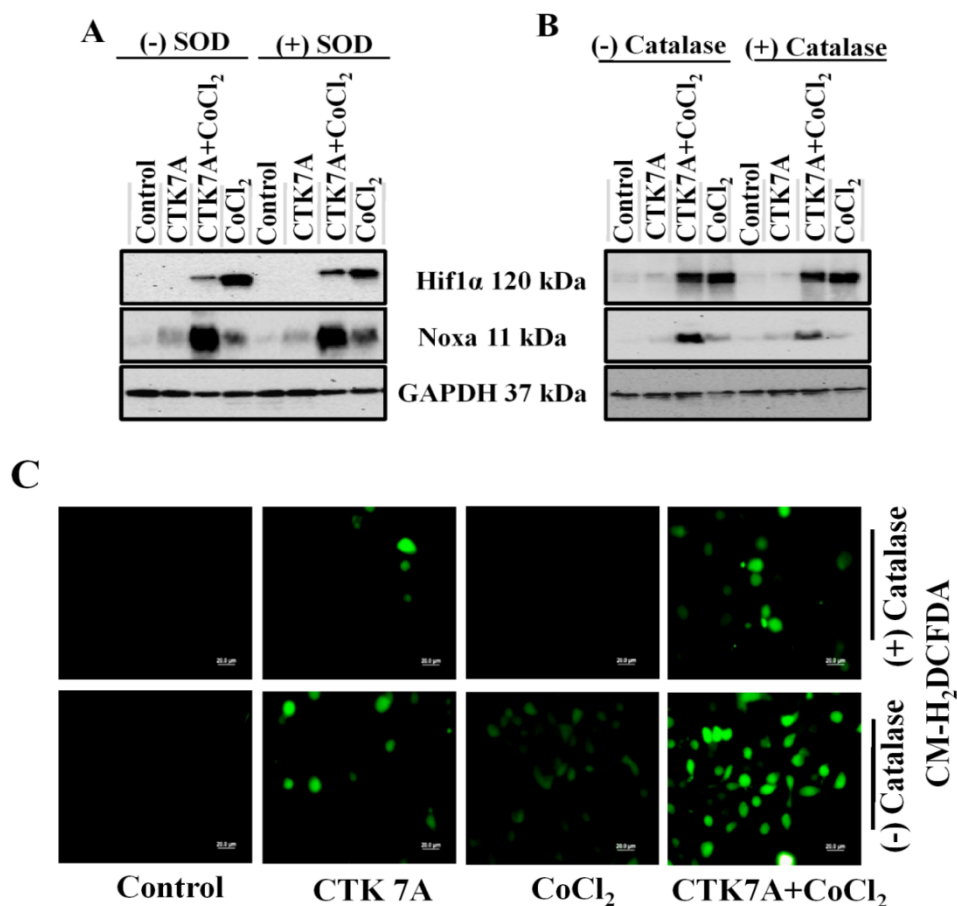


Figure 3.12. CTK7A-mediated ROS generation in $CoCl_2$ -treated GECs leads to increased Noxa expression. (A) AGS cells were pretreated with SOD for 4 h followed by a treatment with

CoCl₂ (200 μM) and/or CTK7A (100 μM) for 24 h. Whole cell lysates were isolated and run on gel. A representative western blotting (n=3) showed status of Noxa and Hif1α. GAPDH was used as a loading control. (B) Immunoblotting (n=3) of whole cell lysates after pretreatment with catalase (350 units/ml) for 4 h followed by treatment with CTK7A (100 μM) and CoCl₂ (200 μM) alone or in combination for 24 h. Blots were probed with antibody for Noxa and Hif1α. GAPDH as the loading control. (C) AGS cells were treated with CoCl₂ (200 μM) alone or combination with CTK7A (100 μM) for 24 h with or without catalase pretreatment (350 units/ml, 4 h). Cells were then incubated with fluorescence probe CM-H₂DCFDA at a final concentration of 1 μM for 10 min followed by fixation with paraformaldehyde at 37°C for 20 min. ROS generation was measured under a fluorescence microscope (Olympus, Japan). Scale bar, 20 μm.

3.11. H₂O₂ induces p38 MAPK-mediated Noxa induction in CTK7A and CoCl₂-treated GECs

Existing reports suggest ROS mediated activation of MAPK and Noxa upregulation (144-147). Status of MAPKs upon hypoxia and CTK7A-exposure alone or in combination for 24 h was studied and upregulation of all three MAPKs i.e. p38, ERK and JNK were observed. Expression of phosphorylated-p38 MAPK (P-p38 MAPK) and P-JNK along with Noxa expression was reduced after catalase treatment while Hif1α expression remained unchanged. There was no change in P-ERK level after catalase treatment (Figure 3.13A). Further, the effect of JNK and p38 MAPK on Noxa expression was studied. For this, cells were pre-treated with JNK or p38 MAPK inhibitors for 1 h followed by treatment with hypoxia (200 μM of CoCl₂) alone or in combination with CTK7A (100 μM) for 24 h. Whole cell lysates were assessed by western blotting to study the status of Noxa in JNK and p38 MAPK inhibitor-treated cells and observed a remarkable downregulation of Noxa in CTK7A and CoCl₂-treated cells with SB203580(p38 MAPK inhibitor)-pretreatment but not in SP600125 (JNK inhibitor) pretreated

CTK7A plus CoCl₂-treated cells. This result established that p38 MAPK-mediated Noxa expression in CTK7A-treated cells (Figure 3.13 B and C).

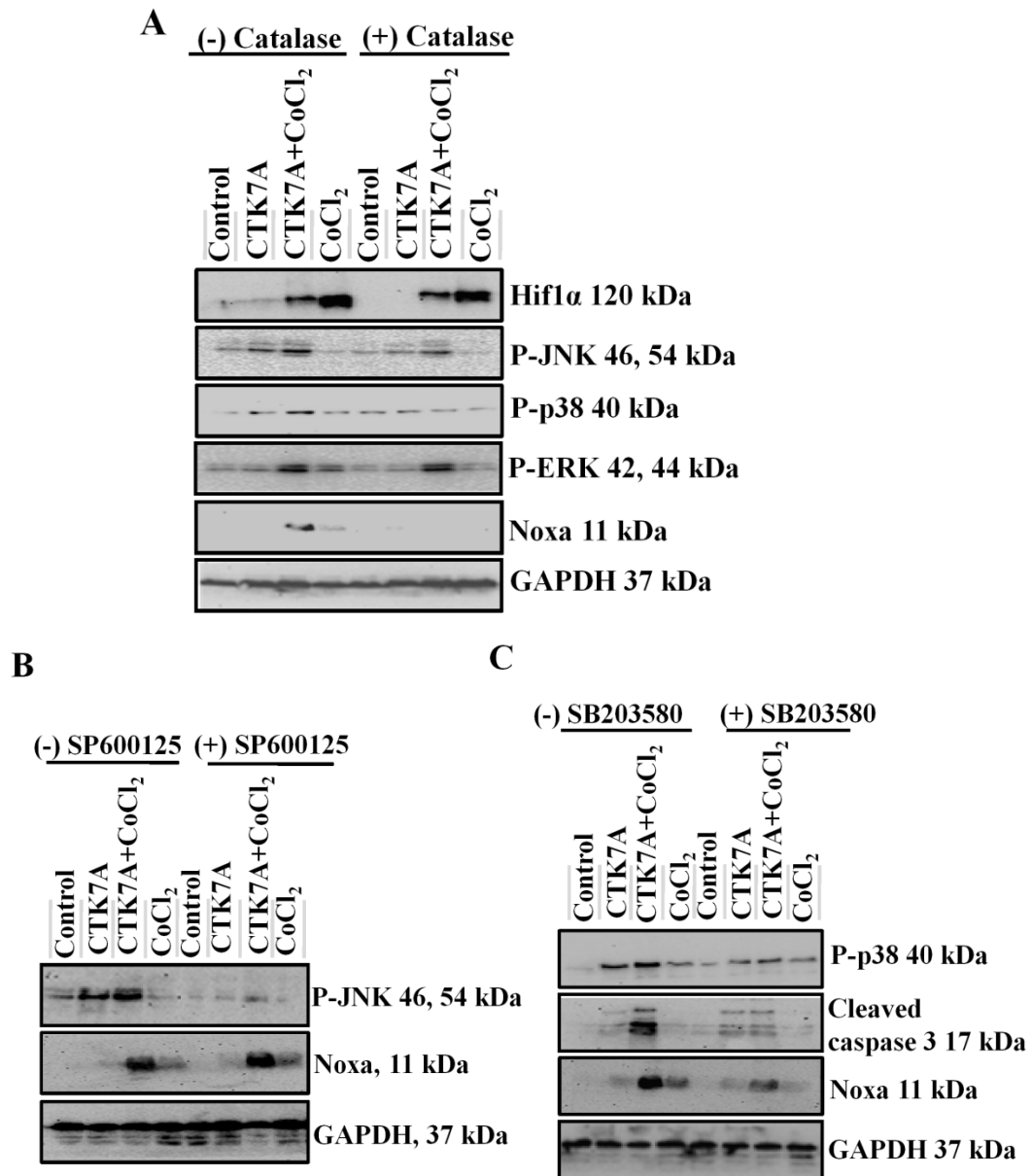


Figure 3.13. H₂O₂ induces p38 MAPK-mediated Noxa upregulation in CTK7A and CoCl₂-treated GECs. (A) AGS cells were pre-treated with catalase (350 units/ml) for 4 h followed by treatment with hypoxia (200 μM of CoCl₂) alone or in combination with CTK7A (100 μM) for 24 h. Whole cell lysates were western blotted (n=3) and probed for Noxa, Hif1α and various MAPKs. GAPDH was used as a loading control. (B) Western blotting (n=3) of whole cell lysates after pretreatment with 25 μM JNK inhibitor II (SP600125) for 1 h followed by CoCl₂

(200 μM) and CTK7A (100 μM) treatment for 24 h showed the status of P-JNK and Noxa. GAPDH was used as a loading control. (C) Whole cell lysates were isolated from AGS cells after pretreatment with 25 μM of p38 MAPK inhibitor (SB203580) for 1 h followed by treatment with CoCl₂ (200 μM) and/or CTK7A (100 μM) for 24 h. Western blot (n=3) showed the effect of p38 MAPK inhibition on cleaved caspase 3 and Noxa expression. GAPDH was a loading control.

3.12. Discussion

Hypoxic environment inside the solid tumor is created by unequal angiogenesis and poor blood supply to parts of the tumor mass which drive cells to be more malignant (133). Treatment resistance and metastatic property are more frequent in hypoxic cancer cells than in non-hypoxic cells. Hif1 α expression is noticed in neoplastic gastric cancer tissues (Panel A of Figure S5 in (47)). It is the major transcription factor which modulates metastasis by regulating downstream effector molecules involved in angiogenesis (148, 149). As also revealed by this study, Hif1 α enhanced EMT and metastasis in hypoxic GECs. This study suggested a novel mechanism which explained the role of HAT inhibitor CTK7A, in regulation of invasiveness, EMT and apoptosis induction. This compound selectively killed hypoxic gastric cancer cells but spared non-hypoxic cells from apoptotic death to a significant extent. Downregulation of EMT marker expression and invasiveness in CTK7A-treated hypoxic GECs was also noticed. Hypoxia-induced invasiveness of GECs was reversed by treatment with CTK7A. Moreover, GECs showed apoptotic cell death to a greater extent after treatment with CTK7A in hypoxic condition. This cell death involved activation of Noxa-mediated intrinsic pathway.

We suggested a novel mechanism of cell death induction in CTK7A-treated hypoxic GECs which was regulated by ROS generation but not by Hif1 α . As Hif1 α is a transcriptional activator for both *noxa* and *mcl1* in *H. pylori*-infected GECs (85, 86), Mcl1 and Noxa expression was studied in hypoxic GECs and Hif1 α -independent Noxa induction mechanism was found to be active in CTK7A-treated hypoxic cells.

Current therapeutic methods exploit the mechanism of ROS-mediated cellular damage in cancerous cells to treat cancer (122, 150, 151). Association between MAPKs and apoptosis is well established in ROS-generating cells. For example, cisplatin-mediated ROS induction had been associated with JNK activation and apoptosis of various types of cells including GECs (152). Another report explained the role of curcumin-mediated ROS generation and activation

of JNK signaling which induced apoptosis in human GECs (145). Apoptosis induction and ROS-mediated p38 activation was well established in the literature (153). Studies also supported involvement of histone acetylation in cancer progression and therapy. Inhibition of p300 HAT activity as well as autoacetylation by CTK7A was earlier shown to substantially reduce the xenografted oral cancer progression in mice (128). Our results confirmed that CTK7A treatment produces a substantially higher amount of ROS specifically H₂O₂ in hypoxic cells than in non-hypoxic or normoxic GECs. Enhanced H₂O₂ generation in hypoxic CTK7A-treated cells induce p38 MAPK-mediated induction of Noxa. Noxa translocation to mitochondria causes significantly higher mitochondrial apoptosis in hypoxic CTK7A-treated cells. Our results showed significantly higher Noxa expression in hypoxic CTK7A-treated GECs as compared to their CTK7A-untreated counterparts. Thus, the potential therapeutic advantage of CTK7A was revealed by our work which might have a better effect over contemporary anticancer remedies.

Altogether, our study put a new insight to understand the detailed mechanism of HAT inhibition-mediated apoptosis induction in GECs exposed to chemically-induced or physiological hypoxia. However, effect of CTK7A on other type of cancers need to be evaluated.

Chapter 4

4. Role of *H. pylori* in inducing antiapoptotic pathways in GECs

4.1. *H. pylori* infection induces Noxa expression without downregulating Mcl1 in human GECs

Mcl1 is a major antiapoptotic protein expressed in cancer tissues and Noxa acts as an antiapoptotic molecule in Mcl1-expressing cells by regulating degradation of Mcl1 (108). The balance between both *mcl1* and *noxa* are Hif1-inducible. Mcl1 and Noxa have crucial roles in determining the life span of a cell (111). The effect of *H. pylori* infection on Noxa and Mcl1 expression in GECs were next investigated. AGS cells were infected with a *cag* PAI (+) *H. pylori* strain 26695 at a multiplicity of infection (MOI) of 200 for various time periods (3 h, 5 h, 8 h and 12 h) (Figure 4.1A). Induced expression of both Mcl1 and Noxa was observed in a time dependent manner which reached the maximal expression level at 5 h post-infection. Hif1 α was equally induced by MOI 200 and 300 t {lower MOIs were earlier reported to have no significant effect on Hif1 α expression (85)}. So, MOI 200 of the strain 26695 was used for all future experiments with the standardized infection time of 5 h, unless stated otherwise. Both Mcl1 and Noxa were equally induced in other GECs, MKN-45, NCI-N87 and Kato III (Figure 4.1B). This was surprising to observe simultaneous Mcl1 and Noxa expression in GECs since Noxa was known to degrade Mcl1.

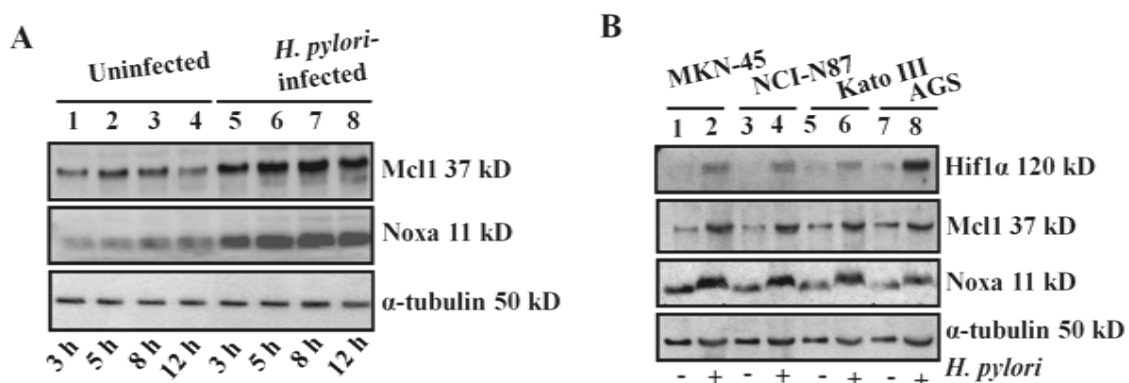


Figure 4.1. Concurrent expression of Noxa and Mcl1 in *H. pylori*-infected GECs. (A) AGS cells were infected with an MOI of 200 of *H. pylori* for various time points (3, 5, 8 and 12 h) or

left uninfected. Whole cell lysates were isolated and western blotted to study Mcl1 and Noxa status. α -Tubulin was used as a loading control. (B) Immunoblot analysis ($n=3$) of whole cell lysates prepared from uninfected or *H. pylori*-infected (an MOI of 200; 5 h) MKN-45, NCI-N87, KATO III, and AGS cells. α -Tubulin was kept as a loading control.

4.2. *H. pylori* infection induces Noxa phosphorylation at S¹³ residue in GECs

To solve the puzzle of simultaneous expression of Noxa and Mcl1 in *H. pylori*-infected GECs, phosphorylation of Noxa was studied since Noxa phosphorylation by Cdk5 was earlier reported to decrease apoptosis in leukaemia cell lines (117). Maximum Noxa phosphorylation at S¹³ residues was observed after 5 h of *H. pylori* infection (Figure 4.2A). *cag* PAI of *H. pylori* encodes proteins for a type IV secretion system (T4SS) which injects virulence factor CagA into infected host cell cytoplasm upon *H. pylori* infection. CagA enhances infected host cell mortality upon phosphorylation (154). But this study confirmed that Noxa phosphorylation was a *cag* PAI-independent event (Figure 4.2B) since equal enhancement in Noxa phosphorylation occurred by *cag* (+)/ (-) strains. As expected, CagA expression and its phosphorylation were noticed in 26695-infected cells but not in cells infected with 8-1 strain confirming the integrity of CagA in 26695 strain (Figure 4.2C). Our next goal was to study potential phosphorylation sites and kinases involved in Noxa phosphorylation, for which GPS2.1 prediction software was used (155) (Figure 4.4D). The analysis predicted about involvement of Cdk5 and JNK in Noxa phosphorylation at S¹³ residue, while p38 MAPK and ERK had much lesser predicted effect. However, expression of Cdk5 was not observed in GECs which corroborated with the other studies that showed no expression of Cdk5 in the human stomach (156, 157).

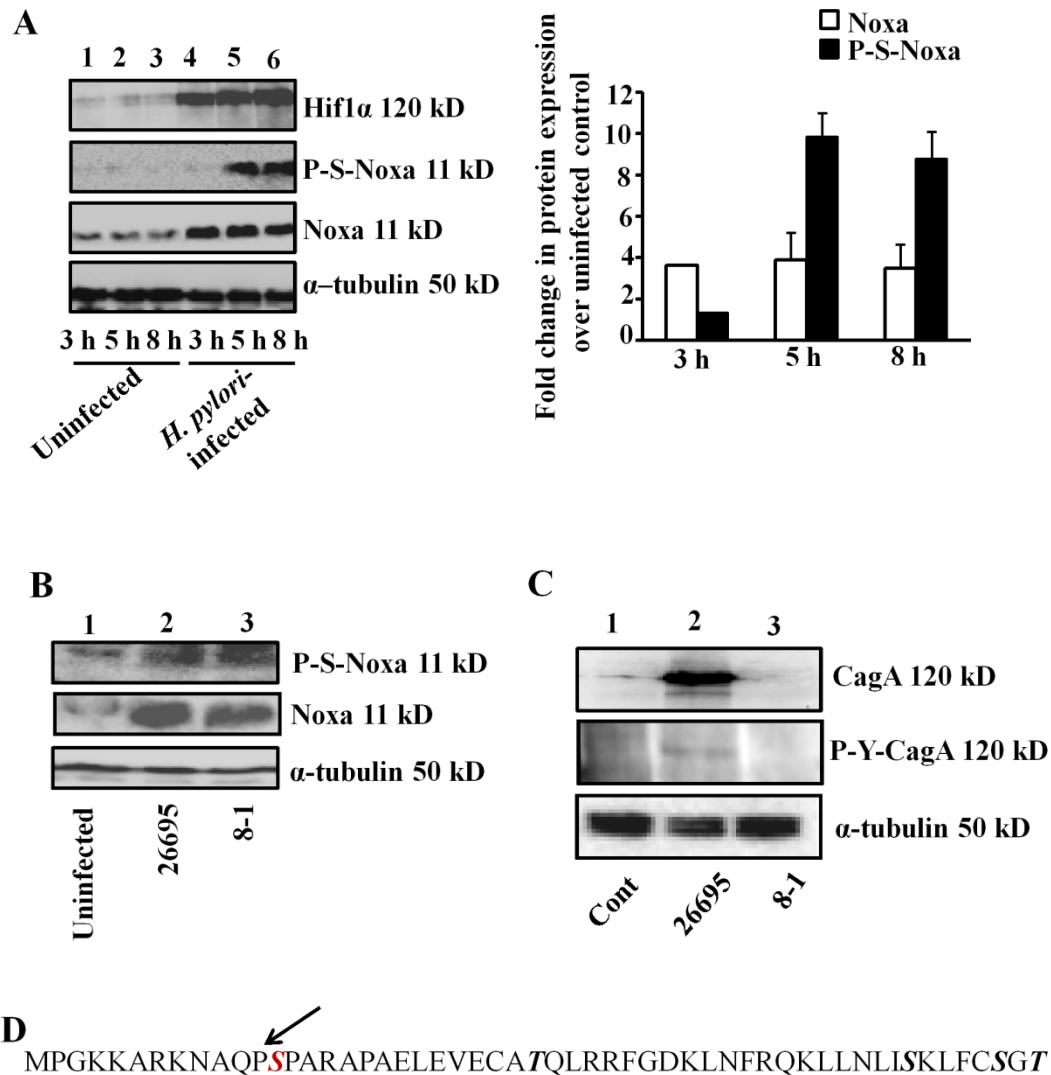


Figure 4.2. Noxa phosphorylation by *H. pylori* is independent of CagA status. (A) Whole cell lysates prepared from AGS cells infected with an MOI of 200 of *H. pylori* for 3 h, 5 h and 8 h. Lysates were run on gel and western blotted to study expression status of phosphor-serine-Noxa, Noxa and Hif1 α proteins. α -Tubulin served as a loading control. Bar diagrams depicted fold change in Noxa and P-Noxa with respect to control (mean \pm SEM, $n = 3$). (B) AGS cells were infected with MOI 200 of *H. pylori* cag PAI (+) strain 26695 and (-) strain (8-1) for 5 h or left uninfected. Western blot analysis of whole cell lysates showed cag PAI-independent expression of P-S-Noxa and Noxa. α -Tubulin was used as a loading control. (C) Immunoblot analysis ($n=3$) of whole cell lysates after infection with cag PAI (+) strain 26695 or (-) strain

8-1. Blots were probed to study CagA expression and its phosphorylation pattern by both the strains. α -Tubulin was used as a loading control. (D) Potential kinase-target site of Noxa protein was analyzed by GPS2.1 software and only S^{13} site appeared to be a potential kinase-target within the five residues which can be phosphorylated (S and T, boldfaced and in italics, S^{13} has been indicated with an arrow).

4.3. Cloning, expression and S13A mutation of *noxa* gene

noxa gene was amplified and cloned in pcDNA3.1⁺ vector (Figure 4.3A). Transformation of DH5 α competent cells was done with the construct for further amplification. Amplified constructs were purified, and transiently transfected to GECs. After 32 h of transfection, whole cell lysates were isolated and run on a gel. Western blot results confirmed *noxa* overexpression as compared to the empty vector-transfected cells (Figure 4.3B). As discussed in the previous section, S^{13} residue of Noxa seemed to be the phosphorylated residue, we attempted to generate a S13A mutant of Noxa by site-directed mutagenesis kit. Construct was confirmed by sequencing. AGS cells were transfected with WT or mut constructs followed by *H. pylori* infection. Whole cell lysates were western blotted and probed with P-serine antibody and Noxa antibody. We have observed a significant Noxa phosphorylation in WT Noxa construct transfected cells as compared to the mut and empty vector-transfected cells while total Noxa remained the same in both samples (Figure 4.3C).

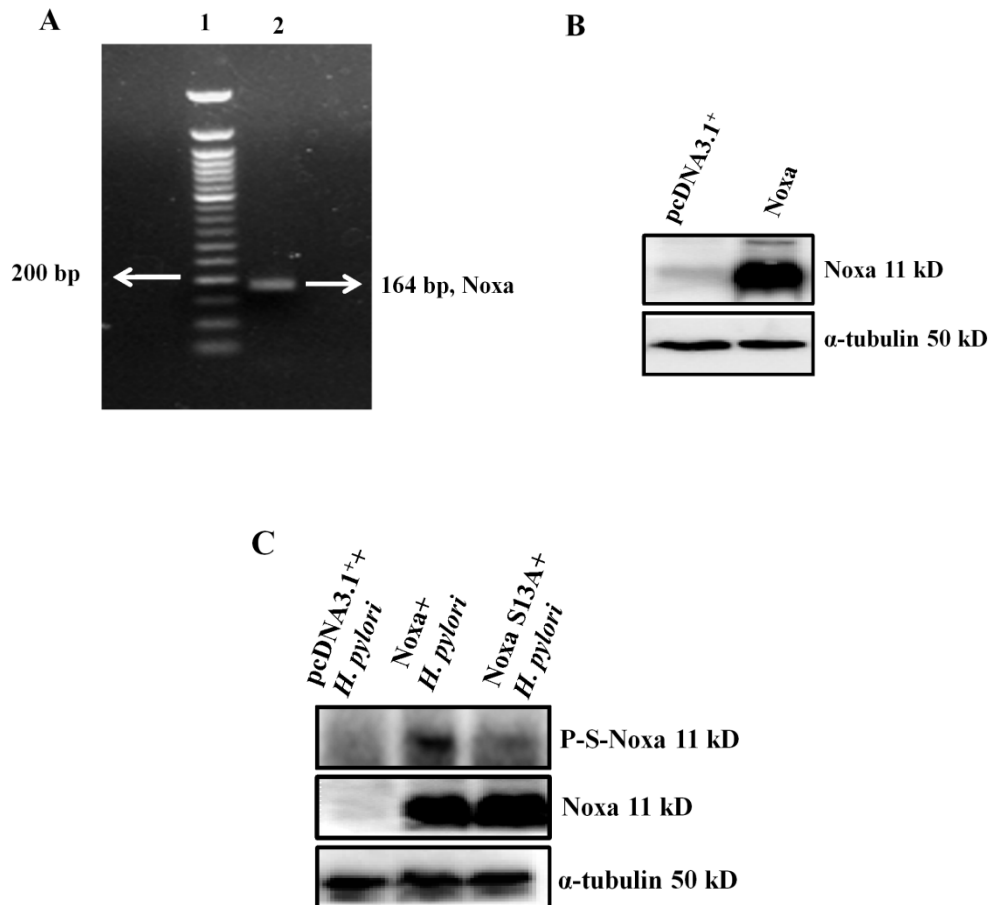


Figure 4.3. Cloning, expression and mutation of noxa. (A) Amplification of human noxa gene. Lane1: 200 bp marker, Lane 2: PCR product showing noxa band at 164 bp (B) Western blot analysis of whole cell lysates isolated from Noxa construct and empty vector-transfected GECs. α -Tubulin served as a loading control. (C) AGS cells were transfected with noxa WT and S13A mut constructs and infected with *H. pylori*. Whole cell lysates were western blotted for P-S-Noxa and Noxa expression. α -Tubulin was kept as a loading control.

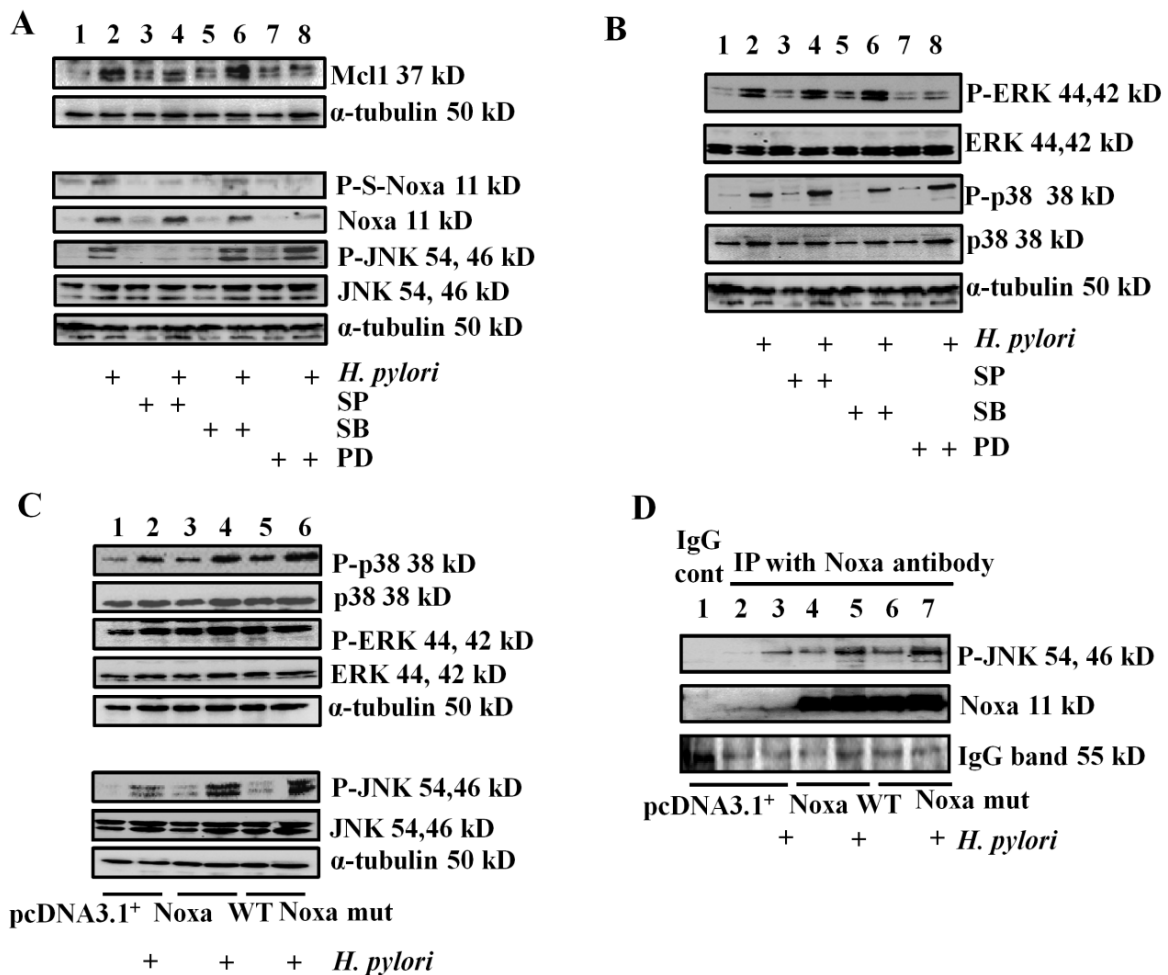
4.4. JNK phosphorylation induces Noxa phosphorylation at S¹³ residue in *H. pylori*-infected GECs

MAPKs are widely distributed throughout the tissue and express in a context dependent manner. As per reports, ERK1/2, p38 MAPK and JNK phosphorylation start at 30 min after *H. pylori* infection and continues till 24 h (158). *H. pylori* at MOI 200 induced MAPKs in infected GECs at 5 h of infection (Figure 4.4A and B). In order to identify which MAPKs played crucial

role in Noxa phosphorylation, cells were pre-treated with the MEK1 inhibitor PD98059 (25 μ M) or p38 MAPK inhibitor SB203580 (25 μ M) for 1 h prior to infection and this pretreatment caused partial suppression of total Noxa and P-S-Noxa. This result matched with findings from previous studies which reported about marked reduction in Noxa expression after ERK and p38 MAPK inhibition (159). Surprisingly, JNK II inhibitor SP600125 (25 μ M, 1 h pre-treatment) inhibited only P-S-Noxa without altering Noxa expression. This result established a correlation between JNK and Noxa phosphorylation in *H. pylori*-infected GECs (Figure 4.4A and B).

JNK-mediated phosphorylation, stabilization and antiapoptotic function of Mcl1 were previously reported (160). So, we assumed that inhibition of JNK phosphorylation would reduce Mcl1 protein expression in *H. pylori*-infected AGS cells. As activation of JNK and p38 MAPK by Noxa has been previously reported (111), the effect of WT and S13A mut Noxa on MAPKs was examined. For this, AGS cells were first transfected with WT and S13A Noxa constructs followed by infection with *H. pylori* (200 MOI) or were left uninfected. Results confirmed that WT and S13A construct equally enhanced *H. pylori*-mediated JNK phosphorylation. But these overexpressions had little effect on p38 MAPK phosphorylation and no effect on ERK1/2 phosphorylation (Figure 4.4C). To study the interaction between Noxa and P-JNK in *H. pylori*-infected GECs, WT and S13A Noxa were ectopically expressed and whole cell lysates were generated. Immunoprecipitation was performed with Noxa antibody and blots were probed for P-JNK and total Noxa. Data showed that P-JNK interaction with Noxa was not affected by the mutation (Figure 4.4D). Effect of JNK overexpression on Noxa phosphorylation at S¹³ was evaluated by western blotting for which AGS cells were transfected with WT Noxa along with JNK1 or JNK2 constructs or S13A Noxa with JNK1 or JNK2 constructs followed by *H. pylori* infection for 5 h or cells were left uninfected. Results confirmed that overexpression of JNK1 or JNK2 enhanced WT Noxa phosphorylation but did not phosphorylate the S13A mutant (Figure 4.4E) in infected GECs (lanes 2, 4, 6 vs lanes 8, 10,

12). Altogether, these findings summarized that Noxa and P-JNK interaction was independent of S¹³ phosphorylation status but JNK-mediated Noxa phosphorylation was drastically affected in Noxa S13A-expressing cells. These results established the importance of the S¹³ residue in JNK-mediated Noxa phosphorylation. Further, we wanted to study the importance of *cag* PAI on JNK phosphorylation for which GECs were infected with *cag* PAI (+) and (-) strains 26695 and 8-1, respectively. Western blotting confirmed about equivalent JNK phosphorylation by *cag* PAI (+) and (-) strains (Figure 4.4F).



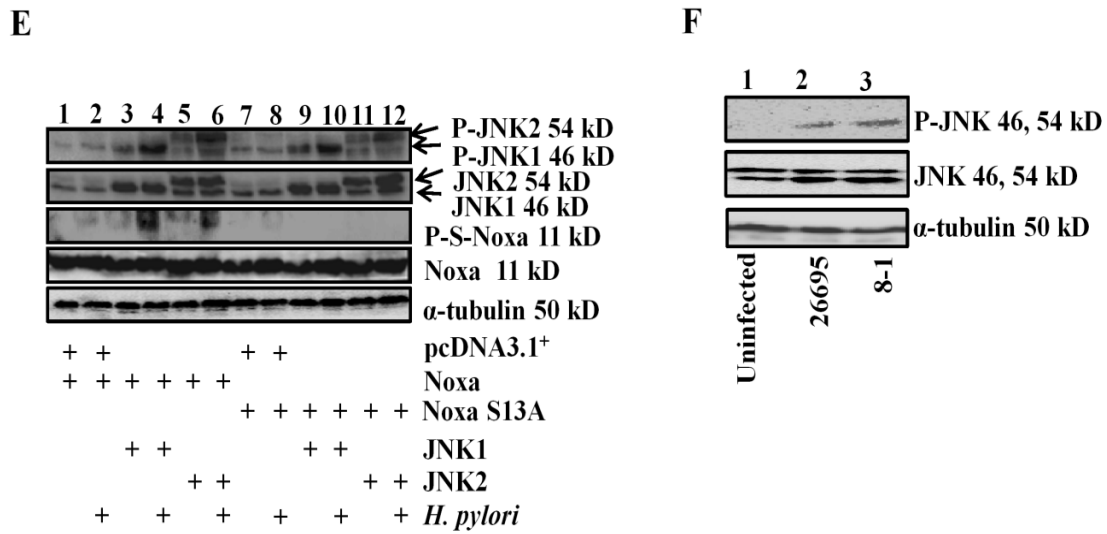


Figure 4.4. Noxa phosphorylation at S¹³ residue was induced by JNK1 and JNK2 in *H. pylori*-infected GECs. (A) AGS cells were pre-treated with 25 μ M JNK inhibitor II [SP600125 (SP)], 25 μ M p38 MAPK inhibitor [SB203580 (SB)] and 25 μ M MEK 1/2 inhibitor [PD98039 (PD)] followed by infection with *H. pylori* (200 MOI) for 5 h. Whole cell lysates were isolated and western blotted to show the status of P-JNK and JNK. α -Tubulin was a loading control. (B) Expression pattern of P-ERK, P-p38 MAPK, ERK and p38 MAPK in AGS cells infected (5 h) with 200 MOI of *H. pylori* was evaluated by western blotting. Pre-treatment with 25 μ M JNK inhibitor II (SP600125), 25 μ M p38 MAPK inhibitor (SB203580) and MEK 1/2 inhibitor (PD98039) were done as indicated. α -Tubulin served as a loading control. (C) Western blot analysis of AGS cells after transfecting with overexpression construct of WT and nonphosphorylatable Noxa S13A mutant followed by infection with *H. pylori* with an MOI of 200 for 5 h showed ERK and p38 MAPK phosphorylation in GECs. α -Tubulin was used as a loading control. (D) Whole cell lysates were prepared from empty vector or WT Noxa or S13A Noxa-transfected and *H. pylori*-infected (MOI 200, 5 h) AGS cells. Lysates were immunoprecipitated with Noxa antibody and probed with P-JNK and Noxa antibody. (E) AGS cells were transfected with JNK1 or JNK2 constructs along with empty vector, WT, or S13A

mutant constructs of Noxa followed by infection with an MOI of 200 of H. pylori for 5 h. Western blot analysis showed JNK mediated Noxa phosphorylation at S¹³ residue. α -Tubulin was used as a loading control. (F) AGS cells were infected with an MOI of 200 of H. pylori cag PAI (+) strain 26695 and (-) strain 8-1 or left uninfected for 5 h. Whole cell lysates were isolated and western blotted for P-JNK and JNK. α -Tubulin was a loading control.

4.5. Inhibition of Noxa phosphorylation at S¹³ induces Mcl1 degradation and mitochondria-mediated intrinsic apoptotic pathway in *H. pylori*-infected GECs

The next study assessed the effect of Noxa phosphorylation on Mcl1. Western blot results confirmed that *H. pylori*-mediated Mcl1 expression was significantly decreased in S13A Noxa construct-transfected cells as compared to the control vector and WT Noxa-transfected in cells (Figure 4.5A). Correlation between Mcl1 downregulation and mitochondria-mediated apoptosis induction are well-studied (161) but the regulation of Mcl1-Noxa interaction is relatively less understood. So, the next study aimed at understanding the effect of JNK on Mcl1-Noxa interaction in *H. pylori*-infected GECs. To achieve this, mitochondrial lysates were prepared from vehicle (DMSO)-treated, *H. pylori*-infected or JNK inhibitor II pre-treated and infected AGS cells. IP experiment was performed with Mcl1 antibody. Results confirmed that Mcl1-Noxa interaction occurred only in JNK-inhibitor-treated and *H. pylori*-infected mitochondria but not in mitochondria isolated from cells which were not treated with the inhibitor (Figure 4.5B). This experiment also identified abrogation of Mcl1-Bax interaction in JNK inhibitor II-treated cells which was not observed in inhibitor-untreated *H. pylori*-infected AGS cells.

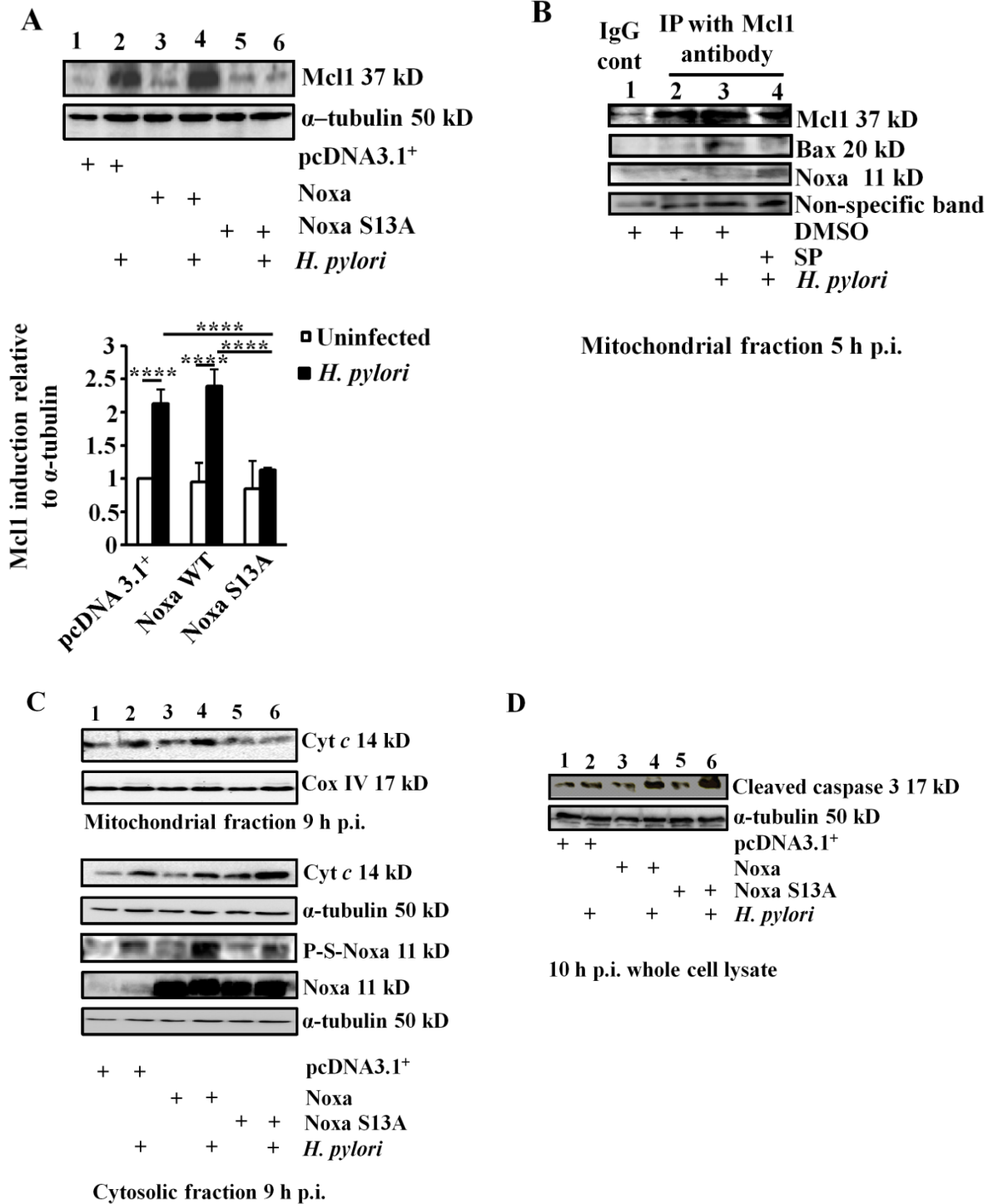


Figure 4.5. Effect of S13A Noxa mutant on intrinsic apoptotic pathway. (A) Immunoblot analysis of whole cell lysates isolated from AGS cells transfected with empty vector, Noxa WT or Noxa S13A construct followed by infection with *H. pylori* (5 h with an MOI of 200) and probed with Mcl1 antibody. Data were analyzed by 2-way ANOVA with Tukey's post hoc test

(n=4). Error bars, SEM. ****P <0.0001. (B) Mitochondrial lysates were immunoprecipitated with Mcl1 antibody after pretreatment with JNK inhibitor II followed by *H. pylori* infection for 5 h. Blots were probed with Mcl1 and Noxa antibodies to assess the Mcl1-Noxa interaction. Further, Mcl1-Bax interaction was studied in the same experimental setup. A nonspecific band was used to show protein loading. (C) Western blot analysis of cytosolic and mitochondrial fractions showed the phosphorylation status of Noxa and Cyt c in *H. pylori*-infected AGS cells expressing either empty vector or Noxa WT or Noxa S13A. α -Tubulin and Cox IV were used as loading controls for cytosolic and mitochondrial fractions, respectively. (D) Whole cell lysates were immunoblotted to study the status of cleaved caspase-3 in WT and S13A Noxa-transfected and infected (MOI of 200 of *H. pylori*, 10 h) AGS cells. α -Tubulin was used as a loading control.

Noxa translocation to mitochondria is a very crucial step in intrinsic apoptotic pathway (162). Noxa displaces apoptotic effectors such as Bak and Bax from pro-survival protein Mcl1 which is followed by Bax or Bak oligomerization resulting in Cyt c release (163). The effect of Noxa phosphorylation on Cyt c release was validated in *H. pylori*-infected GECs by western blotting. Mitochondria-enriched and cytosolic fractions of *H. pylori*-infected AGS cells (already transfected with WT Noxa, S13A Noxa or the empty vector), were western blotted and probed for Noxa and Cyt c. S13A-expressing *H. pylori*-infected cells showed remarkably more Cyt c release as compared to the WT Noxa-transfected cells (Figure 4.5C) which confirmed the significance of Noxa phosphorylation on negatively regulating apoptosis. Cyt c release is accompanied by activation of cleaved caspase-3, the effector caspase which leads to apoptotic cell death (164). We found maximum cleaved caspase 3 accumulation in S13A mutant-expressing cells as compared to empty vector and WT Noxa-transfected groups upon *H. pylori* infection (Figure 4.5D).

4.6. Phosphorylation deficient Noxa S¹³ mutant induces mitochondrial fragmentation in *H. pylori*-infected GECs

Analysis of mitochondrial structure is very crucial to judge the physiological status of a cell. Healthy AGS cells have small, tubular mitochondrial structure and this mitochondrial network is easily destroyed with mitochondrial stress (165). Mitochondrial morphology of pDsRed2 stably-expressing AGS cells was studied by confocal microscopy. These cells were either transiently transfected with empty vector or Noxa WT or S13A mutants followed by infection with *H. pylori* for 8 h or left uninfected. Fragmented mitochondrial structure was noticed in S13A-expressing cells, whereas the reticulotubular network of healthy mitochondria remained unaltered in empty vector-transfected cells but became partially disintegrated in WT construct-transfected and infected cells (Figure 4.6A). Mitochondrial structural integrity was measured in terms of length, circularity and roundness. These parameters were calculated by using image J software and a perfect circle was represented by a circularity value of 1 (Figure 4.6B).

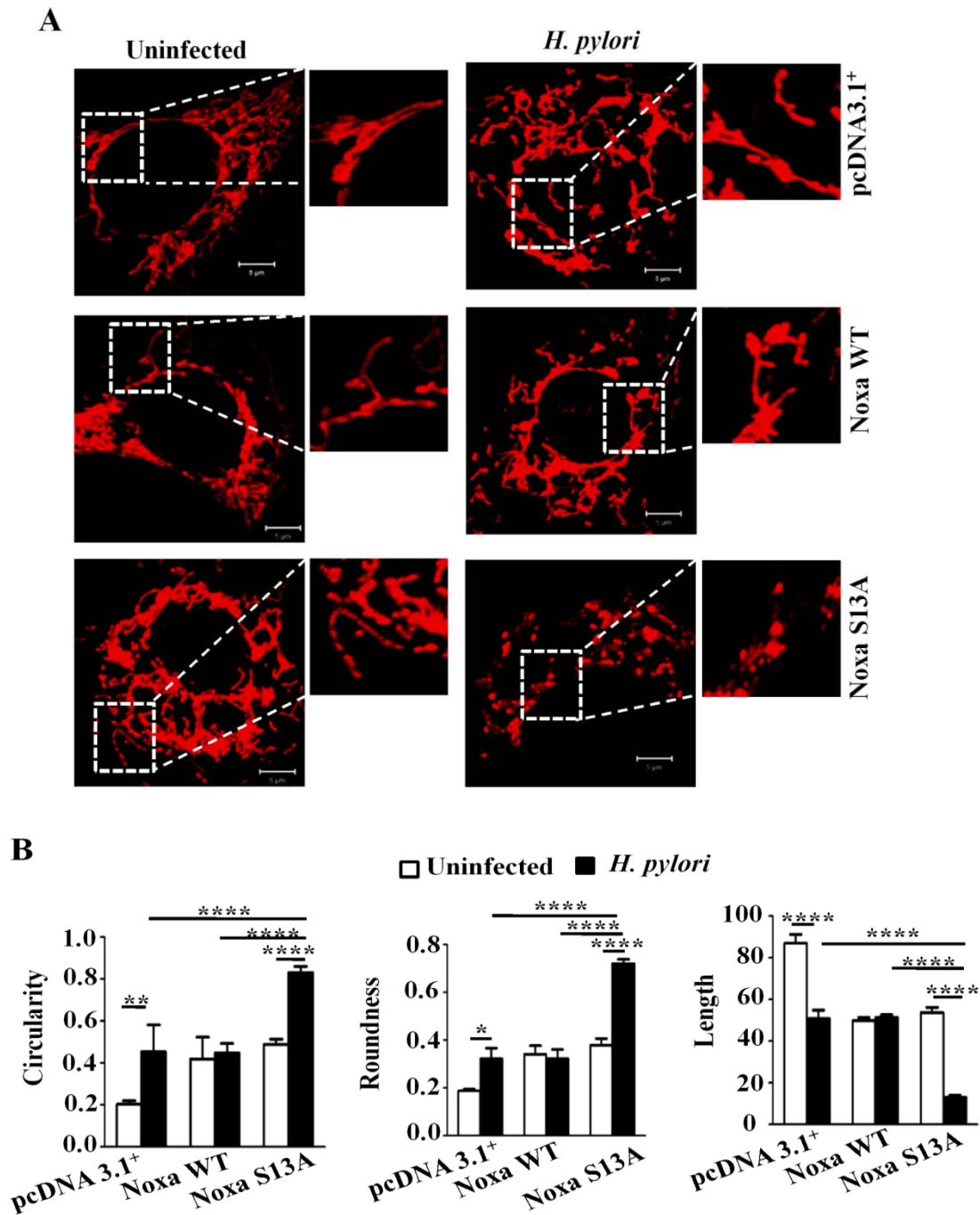


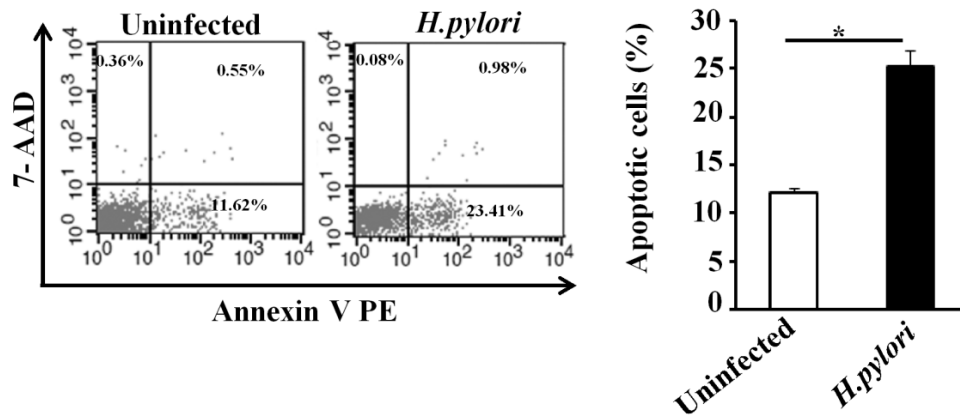
Figure 4.6. Noxa S13A mutant transfection enhances mitochondrial fragmentation in *H. pylori*-infected GECs. (A) Confocal microscopy was done to study mitochondrial morphology in pDsRed2 stably-expressing AGS cells transfected with empty vector (pcDNA3.1⁺), Noxa WT, and Noxa S13A constructs and infected with *H. pylori* (8 h, with an MOI of 200). Scale bars, 5 μ m. (B) Mitochondrial morphology in terms of length, roundness, and circularity was analyzed

from 4 cells (from 4 independent experiments), and 5 mitochondria were taken into account measured from each cell for statistical analysis. 2-way ANOVA with Tukey's post hoc test was used for data analysis. Error bars, SEM. * $P < 0.05$; ** $P < 0.01$; **** $P < 0.0001$.

4.7. Effect of Noxa dephosphorylation on apoptosis of *H. pylori*-infected GECs

Flow cytometric analysis was performed to study the effect of S13A mutation on apoptotic cell death. For this, AGS cells were infected with MOI 200 of *H. pylori* for 10 h. Cells were stained with Annexin V/PE to detect apoptotic cells and 7-AAD to detect necrotic population. Significant apoptosis induction was observed in *H. pylori*-infected GECs (Figure 4.8A). The effect of Noxa WT and S13A mutant on apoptosis induction was further studied in *H. pylori*-infected GECs. Apoptosis induction was significantly more in S13A-transfected and *H. pylori*-infected cells as compared to the empty vector- and Noxa WT-transfected groups (Figure 4.8B).

A



B

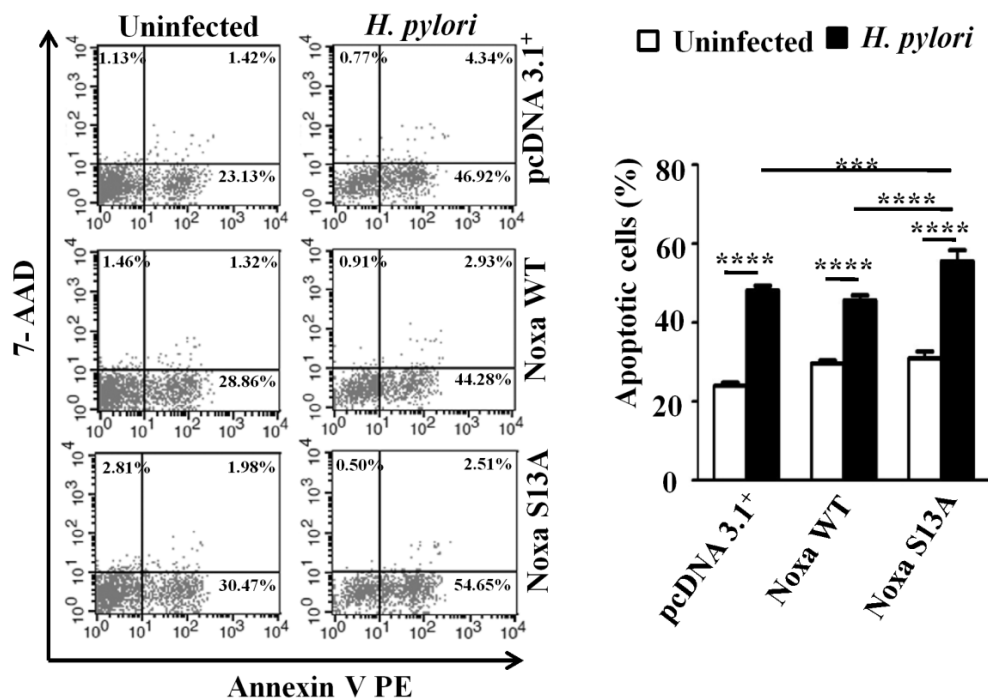


Figure 4.7. S13A-mutated Noxa enhances *H. pylori*-mediated apoptosis in AGS cells. (A) AGS cells were harvested and stained with Annexin V PE/7-AAD dyes for detection of *H. pylori*-mediated apoptosis. The lower-right quadrant showed *H. pylori*-induced apoptosis in infected cells ($n = 6$). Graphical analysis of the data shown in figure 4.8A was performed by Student's *t* test (mean \pm SEM, $n=6$), $*P<0.05$. (B) Noxa WT or Noxa S13A plasmid constructs or empty vector were transfected in AGS cells followed by infection with *H. pylori* for 10 h. *H. pylori*-induced apoptosis was represented by dot plot which showed a marked increase in *H.*

pylori-mediated apoptosis in S13A Noxa construct-transfected cells as compared to WT and empty vector-transfected cells (n=6). The percentage of apoptotic cell death in various transfected groups were compared with two way ANOVA with Tukey's post hoc test. (mean±SEM, n =6), ***P<0.001, ****P<0.0001.

4.8. Discussion

H. pylori-mediated apoptosis as well as proliferation of GECs are regulated by accumulation of mutations and balance between these two events are very much necessary for the survival of the host cell (166). Proapoptotic as well as antiapoptotic proteins play a very crucial role in *H. pylori*-mediated carcinogenesis. BH3-only apoptotic protein Noxa interacts with antiapoptotic protein Mcl1 and leads to its proteasomal degradation. Thus, Mcl1/Noxa balance is a critical regulator of apoptosis (167). This work is the first report showing simultaneous upregulation of proapoptotic protein Noxa and antiapoptotic protein Mcl1 in *H. pylori*-infected GECs. Coexistence of both of these proteins was extensively studied in the present work and JNK-mediated Noxa phosphorylation is found to be responsible for prevention of Noxa-mediated Mcl1 degradation.

H. pylori- mediated gastric epithelial ROS generation and apoptosis induction has been well-documented in the literature (168). Release of Cyt *c* is strongly associated with interaction between pro and antiapoptotic proteins. According to the indirect activation model, conformational change in the multi-BH domain-containing proteins Bax and Bak leads to their auto-oligomerization and pore formation in the outer mitochondrial membrane. This is followed by Cyt *c* release due to the interaction between the BH3-only proteins and their antiapoptotic partners (169). Lowman *et al.* (117) have shown the importance of Noxa S¹³ phosphorylation in leukemia cells under glucose stress. The failure of generating S13A-stably expressing Jurkat cells by Lowman *et al.* support enhanced proapoptotic activity of this mutant which is further validated by unsuccessful attempt by our group to generate GECs with Noxa S13A mutation (86). These results further confirms antiapoptotic potential of Noxa protein by its phosphorylation (170).

H. pylori infection also plays a crucial role in several cellular processes including cell cycle, proliferation and apoptosis by inducing MAPKs activation (159). Significance of JNK

activation in inducing intrinsic apoptotic pathway has been previously reported (171). This study reveals the role of JNK-mediated Noxa phosphorylation in regulating the apoptotic potential of *H. pylori*-infected GECs. Since JNK can induce invasiveness and motility of *H. pylori*-infected cells (172), we assume JNK-mediated Noxa phosphorylation might be helpful for survival of invasive gastric cancer cells. But detailed studies are needed to justify the hypothesis.

Role of *H. pylori*-mediated Bax translocation and mitochondrial fragmentation is well established in the literature (165) but Mcl1-Bax direct interaction is rare to find. A study has demonstrated that Mcl1 can indirectly inhibit Bax-mediated cell death but has not identified a direct Mcl1-Bax interaction as a requirement for that (173). But another group has discussed about the existence of Mcl1-Bax interaction (174). This study confirms that a direct interaction between Mcl1 with Bax occurs in *H. pylori*-infected cells. An enhanced Mcl1-Noxa interaction in JNK inhibitor-treated and *H. pylori*-infected gastric epithelium is also noted. This study further shows that the absence of Noxa phosphorylation at S¹³ residue enhances its binding affinity towards Mcl1 by displacing Bax followed by Bax oligomerization and Cyt *c* release leading to intrinsic cell death (175, 176). As *H. pylori* infection induces Noxa and enhances its phosphorylation in GECs and non-P-Noxa shows significantly high apoptotic potential than P-Noxa, a nonphosphorylatable mutation of Noxa in gastric epithelial cells will only ensure impairment of apoptosis after *H. pylori* infection. Further studies are required to identify the prevalence of Noxa S¹³ mutation and P-JNK expression pattern in *H. pylori*-infected gastric biopsy samples. We have also studied Hif1 α -mediated Noxa induction in *H. pylori*-infected GECs (86). As chemoresistance of gastric cancer cells can be individually attributed to Hif1 α (146) and *H. pylori* (177), a detailed study on *H. pylori*-mediated Noxa phosphorylation and Hif1 α upregulation might help in finding a potential therapeutic strategy to treat treatment-resistant gastric cancer.

In brief, this work establishes the role of Noxa phosphorylation in regulation of apoptosis in *H. pylori*-infected GECs. As *H. pylori* infection modulates both cell survival and cell death mechanism by regulating balance between proapoptotic protein Noxa and antiapoptotic protein Mcl1, this finding might be helpful in understanding Noxa mediated apoptosis in *H. pylori*-infected GECs. The next part of my study depicts the role of p300 HAT function on Noxa-mediated apoptosis in *H. pylori*-infected GECs.

Chapter 5

5. Effect of HAT/KAT inhibition in *H. pylori*-infected metastatic GECs

5.1. HAT/KAT inhibition suppresses *H. pylori*-mediated expression of EMT markers in GECs

Role of *H. pylori* in EMT progression is well established (80, 178, 179). We found Hif1 α -mediated Noxa expression in *H. pylori*-infected GECs (86). p300 is a transcriptional coactivator of Hif1 α . p300 HAT activity is very crucial for its biological functions and hence, has been studied elaborately (94). The first aim of this study was to identify the effect of *H. pylori* on the expression of EMT markers and secondly, to study the effect of inhibition on EMT and metastasis of *H. pylori*-infected GECs. AGS cells were treated with the HAT inhibitor CTK7A (100 μ M, an already standardized dose) followed by *H. pylori* infection (200 MOI) for 24 h. Western blotting of whole cell extracts (Figure 5.1A) showed upregulation of EMT markers, Twist1 and N-cadherin in *H. pylori*-infected GECs which were further suppressed upon HAT inhibition. Expression of EMT markers was further validated by confocal microscopy, which showed downregulation of *H. pylori*-induced N-cadherin and Twist1 expression upon CTK7A treatment (Figure 5.1B and C).

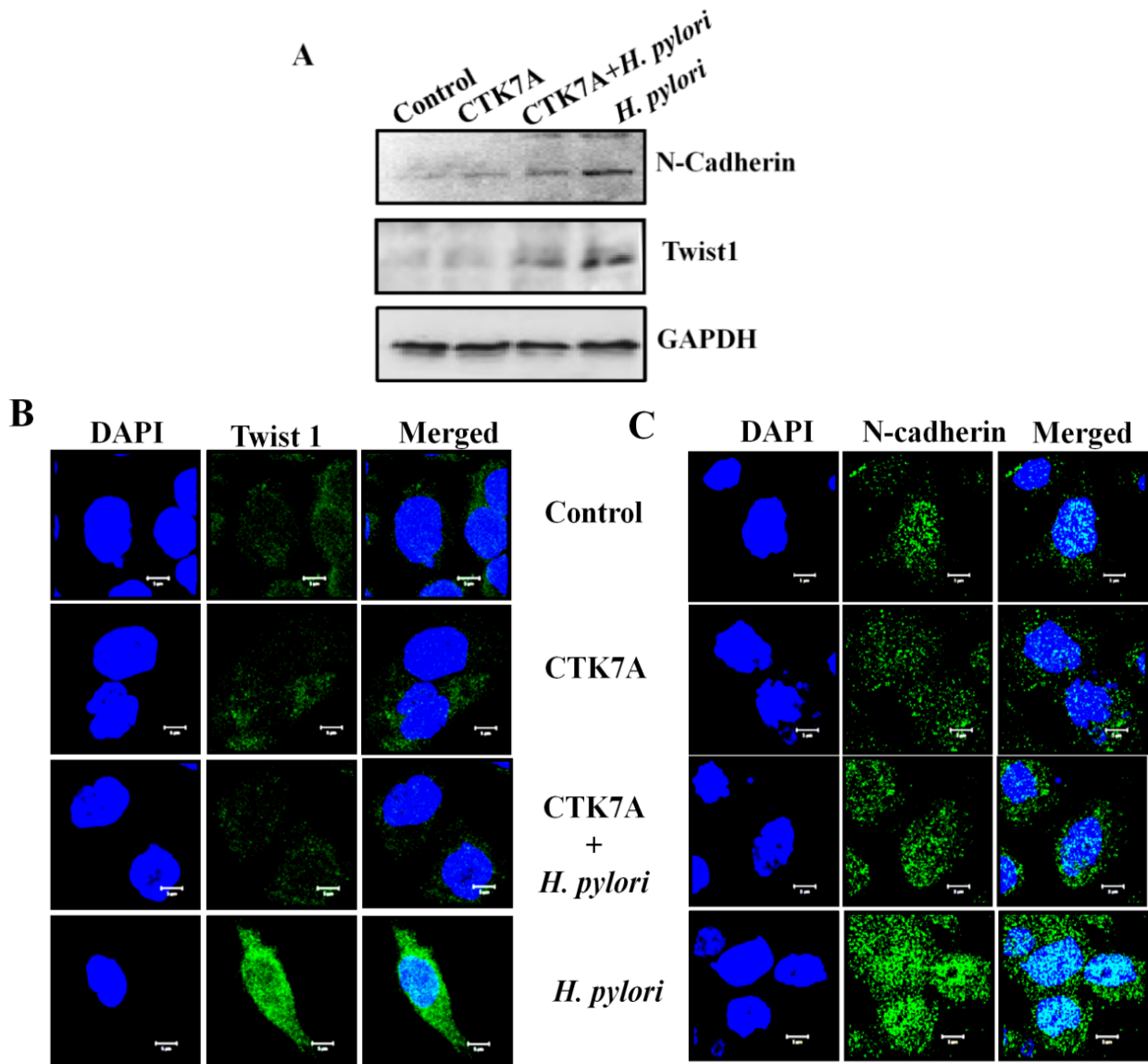


Figure 5.1. Effect of HAT/KAT inhibition on *H. pylori*-induced EMT marker expression. (A) A representative western blot ($n=3$) of whole cell lysates prepared from CTK7A-treated and *H. pylori*-infected AGS cells showed suppressed expression of EMT markers selectively in CTK7A plus *H. pylori*-exposed GECs. GAPDH was used as a loading control (B) A representative confocal microscopy image ($n=3$) of AGS cells infected with *H. pylori* at an MOI of 200 alone or in combination with CTK7A (100 μ M) for 24 h showed status of Twist1 expression. Scale bar, 5 μ m. (C) AGS cells were cells infected with *H. pylori* (MOI 200) alone or in combination with CTK7A (100 μ M) for 24 h and confocal microscopy was performed to study N-cadherin status. Scale bar, 5 μ m.

5.2. *H. pylori*-mediated enhancement in GEC invasion and migration are downregulated by HAT inhibition

To evaluate the effect of HAT inhibition on *H. pylori*-induced metastasis progression, transwell migration and invasion assays were performed. For transwell migration assay, AGS cells were seeded on the upper side of the inserts in a 24 well plate and infected with *H. pylori* (200 MOI) with/without co-treatment with CTK7A (100 μ M) for 24 h. Migrated cells were stained with hematoxylin and studied under a microscope. *H. pylori*-induced cell migration was significantly downregulated with treatment of CTK7A (Figure 5.2 A). Further, invasiveness of GECs was measured by matrigel invasion assay in which a significant reduction in *H. pylori*-mediated invasiveness of GECs was observed with CTK7A co-treatment (Figure 5.2B).

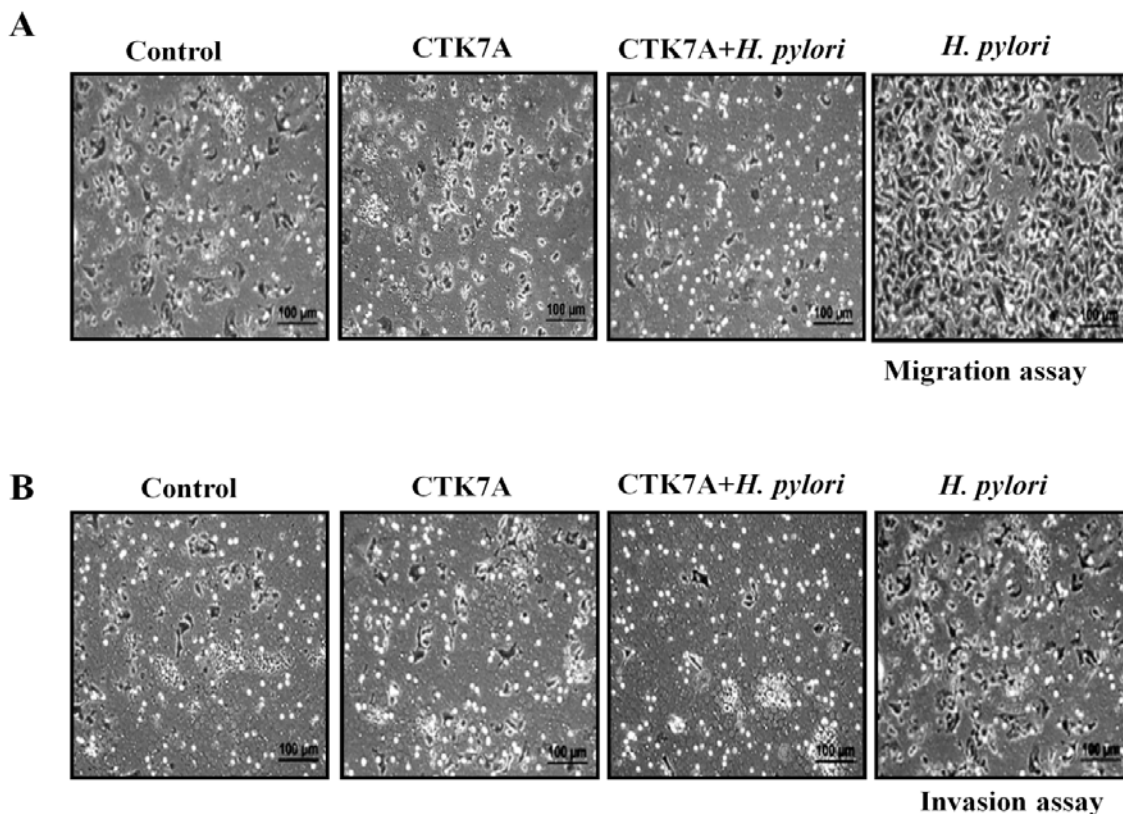


Figure 5.2. *Metastatic properties of H. pylori*-infected GECs were downregulated by HAT inhibition. (A) AGS cells were suspended in serum-free media and were seeded onto the upper chamber of 24 well inserts while the lower chamber had 10% FBS-enriched media. After *H.*

pylori (200 MOI) infection alone or in combination with CTK7A (100 μ M) for 24 h, migrated cells were stained with haematoxylin and counted by using an inverted microscope. Scale =100 μ m. (B) Invasiveness of GECs was studied by matrigel-pre-coated transwells after *H. pylori* infection (200 MOI) with/without CTK7A (100 μ M) treatment for 24 h. Invading cells were stained with haematoxylin and counted by using an inverted microscope. Scale =100 μ m.

5.3. Noxa expression is induced in HAT inhibitor-treated and *H. pylori*-infected GECs

Apoptotic protein Noxa gets induced in *H. pylori*-infected GECs (86). But the effect of p300 HAT inhibition on Noxa expression in *H. pylori*-infected GECs has not been studied. So, the level of Noxa in HAT inhibitor-treated and *H. pylori*-infected GECs was next examined. A significant increase in Noxa expression was observed in CTK7A-treated and *H. pylori*-infected GECs as compared to only *H. pylori*-infected GECs (Figure 5.3A). Mitochondrial translocation of Noxa was remarkably high in *H. pylori*-infected GECs as compared to CTK7A plus *H. pylori* exposed GECs (Figure 5.3B). Confocal microscopy data also corroborated with the western blot result (Figure 5.3C).

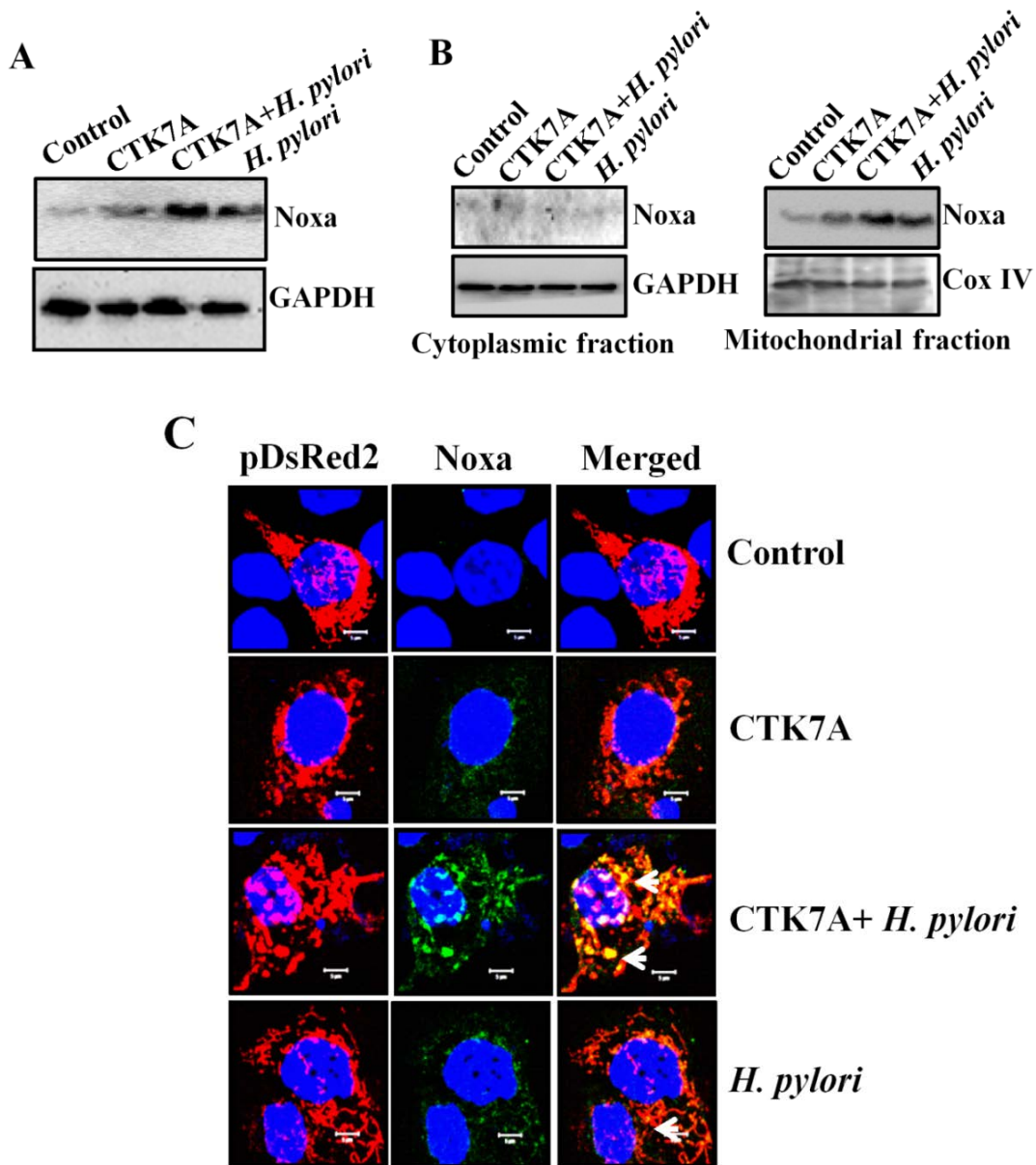


Figure 5.3. Status of Noxa in CTK7A-treated and *H. pylori*-infected GECs.(A) A representative western blot of whole cell lysates prepared from AGS cells infected with *H. pylori* (200 MOI, 24 h) alone or in combination with CTK7A (100 μ M) (n=3). GAPDH was used as a loading control. (B) Mitochondrial and cytosolic fractions of AGS cells were isolated from *H. pylori*-infected and CTK7A-treated GECs and western blotted. GAPDH and Cox IV were used as loading controls for cytosolic and mitochondrial fractions, respectively. (C) *H. pylori*-infected (200 MOI) AGS cells stably-expressing pDsRed2 constructs were treated with

CTK7A (100 μM) for 24 h and confocal microscopy was performed to study Noxa expression. Nuclei were stained with DAPI. Scale bar 10 μm.

5.4. Induction of the intrinsic apoptotic pathway in CTK7A-treated and *H. pylori*-infected GECs

Cyt *c* release and caspase activation are crucial steps in the intrinsic apoptotic pathway (180). Cyt *c* release from the mitochondria was studied in pDsRed2 stably-expressing AGS cells infected for 24 h with *H. pylori* (at an MOI of 200) in presence or absence of CTK7A (100 μM). Confocal microscopy result clearly indicated that mitochondrial retention of Cyt *c* was drastically reduced in CTK7A- plus *H. pylori*-exposed cells (indicating maximal Cyt *c* release into the cytosol) while control cells, only CTK7A-treated and only *H. pylori*-infected cells were able to retain Cyt *c* in the mitochondria (Figure 5.4A). Cleaved caspase 9 and its downstream effector caspase, cleaved caspase 3, were accumulated in CTK7A-treated and *H. pylori*-infected GECs as compared to only *H. pylori*-infected or CTK7A-treated cells (Figure 5.4B).

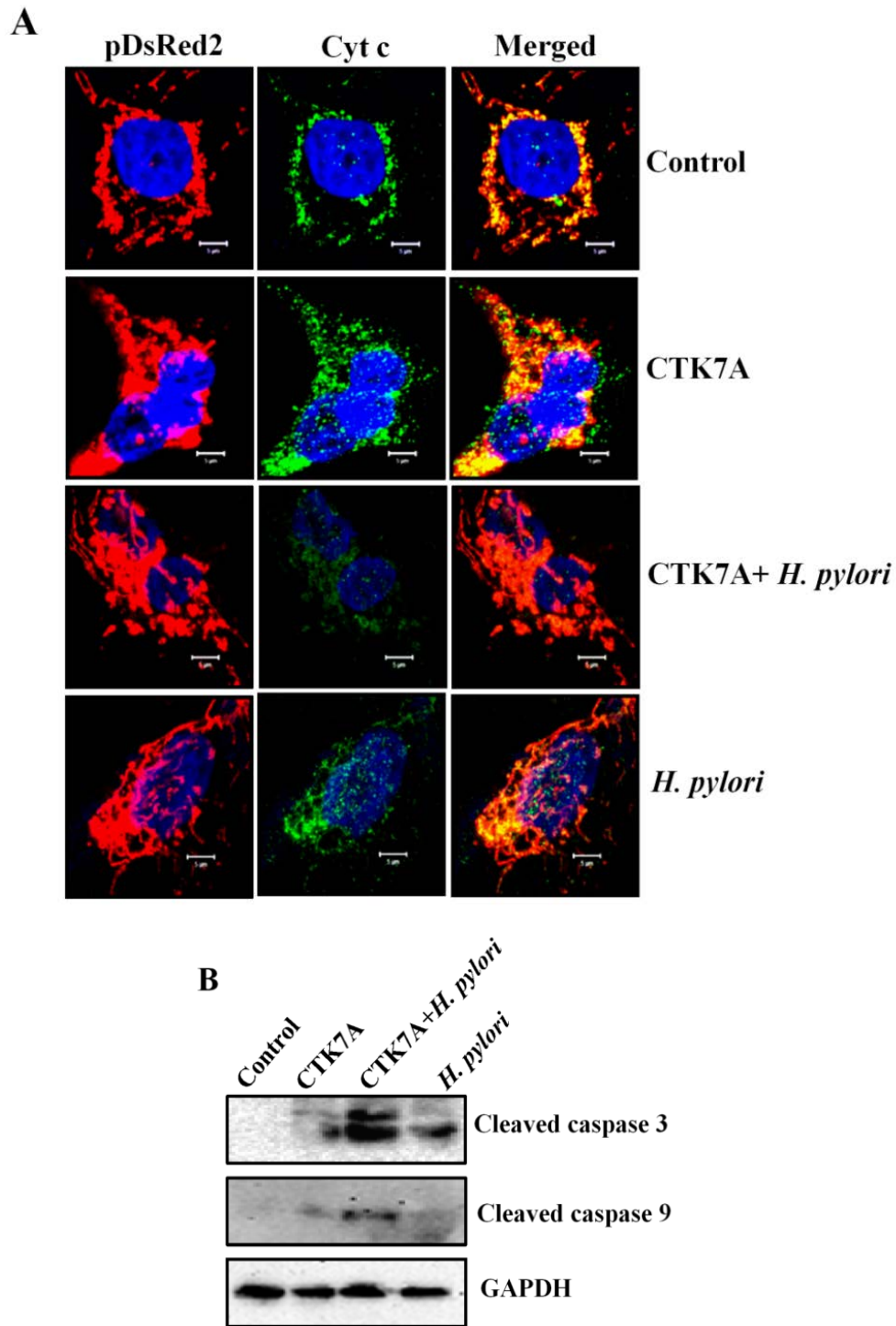


Figure 5.4. Activation of intrinsic apoptotic pathway in HAT inhibitor-treated *H. pylori*-infected GECs. (A) Confocal microscopy of AGS cells stably-expressing pDsRed2 construct and treated with CTK7A (100 μ M) followed by *H. pylori* infection(200 MOI) for 24 h showed maximum Cyt c release in CTK7A treated and *H. pylori*-infected GECs. Nuclei were stained with DAPI. Scale bar 10 μ m. (B) Whole cell lysates prepared from AGS cells after *H. pylori*

(200 MOI) infection alone or in combination with CTK7A (100 μ M) for 24 h. These lysates were immunoblotted (n=3) to study the status of cleaved caspase 9 and cleaved caspase 3. GAPDH was used as a loading control.

5.5. Discussion

H. pylori infection-mediated EMT progression is an interesting field of research (78, 181). *H. pylori* infection induces invasiveness of GECs by suppressing normal epithelial differentiation, cell adhesion, cell polarity maintenance and hence, is involved in metastasis progression (73). The present study revealed upregulation of EMT markers and metastatic property in *H. pylori*-infected GECs. p300 acts as the transcriptional coactivator of Hif1 α which is upregulated by *H. pylori* infection, and has HAT activity. The significance of p300 HAT activity in *H. pylori*-infected GECs had not been studied at all. This study confirmed that inhibition of HAT activity by CTK7A led to suppression of EMT marker expression and metastatic nature of *H. pylori*-infected GECs. This finding was supported by one previous report which explained the tumor-suppressive role of CTK7A in the mouse model of oral cancer (128). So, these new findings might be helpful in controlling EMT progression in *H. pylori*-infected GECs.

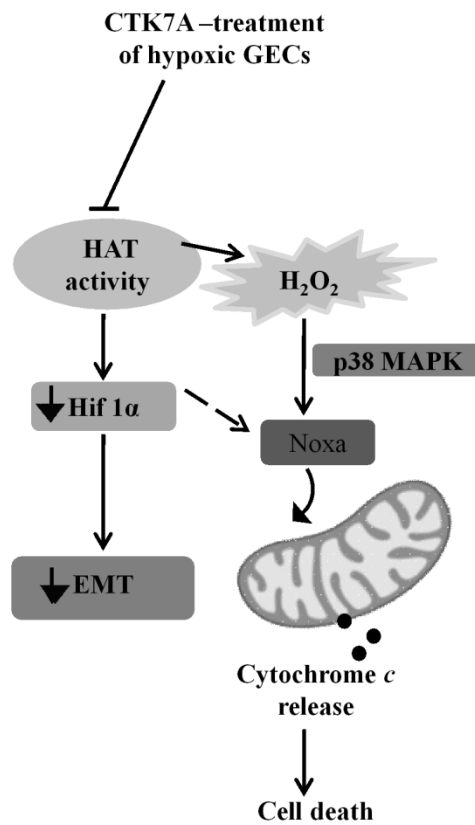
Apoptosis induction in *H. pylori*-infected metastatic GECs is a challenging issue. Several reports have previously shown apoptosis induction in metastatic cells by using various chemical compounds (125, 126). But apoptosis induction in *H. pylori*-infected GECs by HAT inhibitor was not studied altogether. Remarkable upregulation in proapoptotic protein Noxa was observed in *H. pylori*-infected GECs after treatment with HAT inhibitor (CTK7A). Noxa translocation to mitochondria, Cyt *c* release, followed by cleaved caspase 9 and 3 accumulation indicated a significant increase in the intrinsic apoptotic pathway in CTK7A treated and *H. pylori*-infected GECs.

The finding of CTK7A-mediated apoptosis induction selectively in *H. pylori*-infected GECs, therefore, is extremely significant especially because this gives the hope of finding better treatment options for even metastatic gastric cancer with curcumin-derived drugs which will have less side-effects.

SUMMARY AND CONCLUSION

Chapter 6

6.1. Pictorial depiction of selective apoptosis induction in hypoxic GECs expressing EMT markers and invasive property.



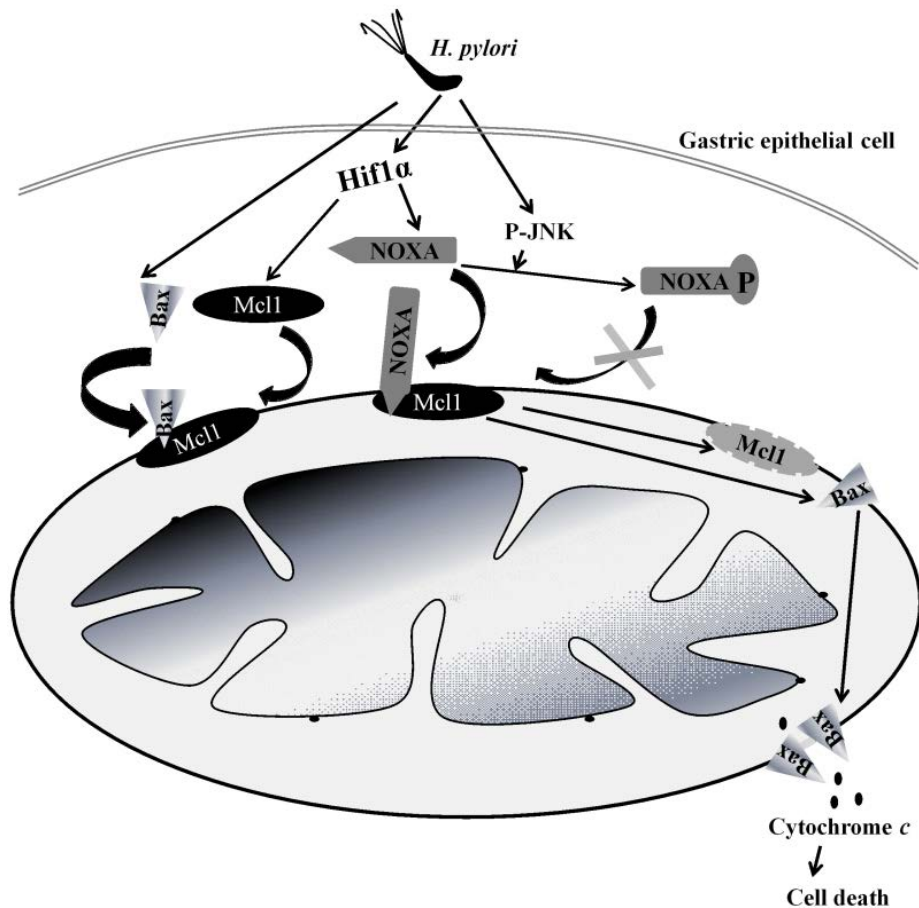
Curved arrow= mitochondrial translocation; solid-headed downward arrow= down-regulation; → dotted arrow= minor pathway, arrow-headed= activation; blunt end-headed= inhibition.

The above picture summarizes the following:

- ❖ Inhibition of HAT activity by CTK7A downregulates Hif1α expression and reduces expression of EMT markers leading to suppression of metastatic property of hypoxic GECs.

- ❖ HAT inhibition induces H₂O₂ generation and activation of p38 MAPK, which subsequently increases Noxa expression. Noxa is translocated to mitochondria and induces intrinsic apoptosis pathway selectively in hypoxic GECs.

6.2. Regulation of Noxa-mediated apoptosis in *H. pylori*-infected GECs.



Curved arrow= translocation

This figure summarizes the following:

- ❖ *H. pylori* infection induces Hif1 α expression in GECs which enhances Noxa expression. *H. pylori* infection also induces mitochondrial translocation of Noxa followed by its interaction with Mcl1.
- ❖ Noxa phosphorylation at S¹³ residue is induced by JNK phosphorylation in *H. pylori*-infected GECs which inhibits its mitochondrial translocation resulting in impairment of apoptosis.

- ❖ Non-phosphorylated form of Noxa has higher mitochondrial translocation potential which further displaces Bax from Mcl1 and induces Mcl1 degradation followed by Bax oligomerization and Cyt *c* release resulting in apoptosis induction.

6.3. HAT inhibition selectively kills *H. pylori*-infected GECs expressing EMT markers

- ❖ *H. pylori* infection induces EMT marker expression and metastasis of GECs.
- ❖ HAT inhibitor CTK7A downregulates expression of EMT markers, anchorage-independent growth as well as invasiveness of *H. pylori*-infected GECs.
- ❖ HAT inhibition upregulates proapoptotic protein Noxa which particularly induces mitochondria-mediated intrinsic cell death pathway by Cyt *c* release and caspase 9, 3 activation.

In conclusion, this thesis work emphasizes on the crucial roles of hypoxia and *H. pylori* infection in inducing metastatic properties of GECs. This work further suggests that Noxa-mediated apoptosis induction is possible in HAT inhibitor-treated hypoxic and *H. pylori*-infected GECs even if these cells show invasive nature.

BIBLIOGRAPHY

1. Parkin, D. M., Bray, F., Ferlay, J., and Pisani, P. (2005) Global cancer statistics, 2002. *CA. Cancer J. Clin.* **55**, 74-108
2. Karimi, P., Islami, F., Anandasabapathy, S., Freedman, N. D., and Kamangar, F. (2014) Gastric cancer: descriptive epidemiology, risk factors, screening, and prevention. *Cancer Epidemiol. Biomarkers Prev.* **23**, 700-713
3. Dikshit, R. P., Mathur, G., Mhatre, S., and Yeole, B. B. (2011) Epidemiological review of gastric cancer in India. *Indian journal of medical and paediatric oncology : official journal of Indian Society of Medical & Paediatric Oncology* **32**, 3-11
4. Fox, J. G., and Wang, T. C. (2007) Inflammation, atrophy, and gastric cancer. *J. Clin. Invest.* **117**, 60-69
5. Nagini, S. (2012) Carcinoma of the stomach: A review of epidemiology, pathogenesis, molecular genetics and chemoprevention. *World journal of gastrointestinal oncology* **4**, 156-169
6. Zabaleta, J. (2012) Multifactorial etiology of gastric cancer. *Methods Mol. Biol.* **863**, 411-435
7. Kusters, J. G., van Vliet, A. H., and Kuipers, E. J. (2006) Pathogenesis of *Helicobacter pylori* infection. *Clin. Microbiol. Rev.* **19**, 449-490
8. Suerbaum, S., and Michetti, P. (2002) *Helicobacter pylori* infection. *N. Engl. J. Med.* **347**, 1175-1186
9. Umehara, S., Higashi, H., Ohnishi, N., Asaka, M., and Hatakeyama, M. (2003) Effects of *Helicobacter pylori* CagA protein on the growth and survival of B lymphocytes, the origin of MALT lymphoma. *Oncogene* **22**, 8337-8342

10. Lahner, E., Bernardini, G., Santucci, A., and Annibale, B. (2010) Helicobacter pylori immunoproteomics in gastric cancer and gastritis of the carcinoma phenotype. *Expert review of proteomics* **7**, 239-248
11. Leber, M. F., and Efferth, T. (2009) Molecular principles of cancer invasion and metastasis (review). *Int. J. Oncol.* **34**, 881-895
12. Chaffer, C. L., and Weinberg, R. A. (2011) A perspective on cancer cell metastasis. *Science* **331**, 1559-1564
13. Valastyan, S., and Weinberg, R. A. (2011) Tumor metastasis: molecular insights and evolving paradigms. *Cell* **147**, 275-292
14. Nguyen, D. X., Bos, P. D., and Massague, J. (2009) Metastasis: from dissemination to organ-specific colonization. *Nature reviews. Cancer* **9**, 274-284
15. Reymond, N., d'Agua, B. B., and Ridley, A. J. (2013) Crossing the endothelial barrier during metastasis. *Nature reviews. Cancer* **13**, 858-870
16. Yang, J., and Weinberg, R. A. (2008) Epithelial-mesenchymal transition: at the crossroads of development and tumor metastasis. *Developmental cell* **14**, 818-829
17. Yao, D., Dai, C., and Peng, S. (2011) Mechanism of the mesenchymal-epithelial transition and its relationship with metastatic tumor formation. *Molecular cancer research : MCR* **9**, 1608-1620
18. Furue, M. (2011) Epithelial tumor, invasion and stroma. *Annals of dermatology* **23**, 125-131

19. Cai, C., Yu, J. W., Wu, J. G., Lu, R. Q., Ni, X. C., Wang, S. L., and Jiang, B. J. (2013) [CD133 promotes the invasion and metastasis of gastric cancer via epithelial-mesenchymal transition]. *Zhonghua wei chang wai ke za zhi = Chinese journal of gastrointestinal surgery* **16**, 662-667
20. Chang, H. L., Gillett, N., Figari, I., Lopez, A. R., Palladino, M. A., and Derynck, R. (1993) Increased transforming growth factor beta expression inhibits cell proliferation in vitro, yet increases tumorigenicity and tumor growth of Meth A sarcoma cells. *Cancer Res.* **53**, 4391-4398
21. Li, Y., Tan, B. B., Zhao, Q., Fan, L. Q., Wang, D., and Liu, Y. (2014) ZNF139 promotes tumor metastasis by increasing migration and invasion in human gastric cancer cells. *Neoplasma* **61**, 291-298
22. Ren, Y. H., Liu, K. J., Wang, M., Yu, Y. N., Yang, K., Chen, Q., Yu, B., Wang, W., Li, Q. W., Wang, J., Hou, Z. Y., Fang, J. Y., Yeh, E. T., Yang, J., and Yi, J. (2014) De-SUMOylation of FOXC2 by SENP3 promotes the epithelial-mesenchymal transition in gastric cancer cells. *Oncotarget* **5**, 7093-7104
23. Liu, N., Wang, Y., Zhou, Y., Pang, H., Zhou, J., Qian, P., Liu, L., and Zhang, H. (2014) Kruppel-like factor 8 involved in hypoxia promotes the invasion and metastasis of gastric cancer via epithelial to mesenchymal transition. *Oncol. Rep.* **32**, 2397-2404
24. Liu, Z., Han, G., Cao, Y., Wang, Y., and Gong, H. (2014) Calcium/calmodulindependent protein kinase II enhances metastasis of human gastric cancer by upregulating nuclear factor-kappaB and Akt-mediated matrix metalloproteinase-9 production. *Molecular medicine reports* **10**, 2459-2464

25. Zhao, H., Wang, Y., Yang, L., Jiang, R., and Li, W. (2014) MiR-25 promotes gastric cancer cells growth and motility by targeting RECK. *Mol. Cell. Biochem.* **385**, 207-213
26. Yang, C., Xu, Y., Zhou, H., Yang, L., Yu, S., Gao, Y., Huang, Y., Lu, L., and Liang, X. (2015) Tetramethylpyrazine protects CoCl₂-induced apoptosis in human umbilical vein endothelial cells by regulating the PHD2/HIF/1 α -VEGF pathway. *Molecular medicine reports*
27. Wei, B., Huang, Q. Y., Huang, S. R., Mai, W., and Zhong, X. G. (2015) MicroRNA34a attenuates the proliferation, invasion and metastasis of gastric cancer cells via downregulation of MET. *Molecular medicine reports* **12**, 5255-5261
28. Semenza, G. L. (2014) Oxygen sensing, hypoxia-inducible factors, and disease pathophysiology. *Annual review of pathology* **9**, 47-71
29. Brown, J. M., and Wilson, W. R. (2004) Exploiting tumour hypoxia in cancer treatment. *Nature reviews. Cancer* **4**, 437-447
30. Helmlinger, G., Yuan, F., Dellian, M., and Jain, R. K. (1997) Interstitial pH and pO₂ gradients in solid tumors in vivo: high-resolution measurements reveal a lack of correlation. *Nat. Med.* **3**, 177-182
31. Dang, C. V., and Semenza, G. L. (1999) Oncogenic alterations of metabolism. *Trends Biochem. Sci.* **24**, 68-72
32. Circu, M. L., and Aw, T. Y. (2010) Reactive oxygen species, cellular redox systems, and apoptosis. *Free Radic. Biol. Med.* **48**, 749-762

33. Shimizu, S., Eguchi, Y., Kamiike, W., Itoh, Y., Hasegawa, J., Yamabe, K., Otsuki, Y., Matsuda, H., and Tsujimoto, Y. (1996) Induction of apoptosis as well as necrosis by hypoxia and predominant prevention of apoptosis by Bcl-2 and Bcl-XL. *Cancer Res.* **56**, 2161-2166
34. Subarsky, P., and Hill, R. P. (2003) The hypoxic tumour microenvironment and metastatic progression. *Clin. Exp. Metastasis* **20**, 237-250
35. Brown, L. F., Detmar, M., Claffey, K., Nagy, J. A., Feng, D., Dvorak, A. M., and Dvorak, H. F. (1997) Vascular permeability factor/vascular endothelial growth factor: a multifunctional angiogenic cytokine. *EXS* **79**, 233-269
36. Murakami, M., and Simons, M. (2008) Fibroblast growth factor regulation of neovascularization. *Curr. Opin. Hematol.* **15**, 215-220
37. Gilkes, D. M., Semenza, G. L., and Wirtz, D. (2014) Hypoxia and the extracellular matrix: drivers of tumour metastasis. *Nature reviews. Cancer* **14**, 430-439
38. Nicotera, P., and Melino, G. (2004) Regulation of the apoptosis-necrosis switch. *Oncogene* **23**, 2757-2765
39. Malhotra, R., Lin, Z., Vincenz, C., and Brosius, F. C., 3rd (2001) Hypoxia induces apoptosis via two independent pathways in Jurkat cells: differential regulation by glucose. *American journal of physiology. Cell physiology* **281**, C1596-1603
40. Greijer, A. E., and van der Wall, E. (2004) The role of hypoxia inducible factor 1 (HIF-1) in hypoxia induced apoptosis. *J. Clin. Pathol.* **57**, 1009-1014

41. Zhang, L., Xing, Q., Qian, Z., Tahtinen, M., Zhang, Z., Shearier, E., Qi, S., and Zhao, F. (2015) Hypoxia Created Human Mesenchymal Stem Cell Sheet for Prevascularized 3D Tissue Construction. *Advanced healthcare materials*
42. Michiels, C. (2004) Physiological and pathological responses to hypoxia. *Am. J. Pathol.* **164**, 1875-1882
43. Li, H., Satriano, J., Thomas, J. L., Miyamoto, S., Sharma, K., Pastor-Soler, N. M., Hallows, K. R., and Singh, P. (2015) Interactions between HIF-1alpha and AMPK in the regulation of cellular hypoxia adaptation in chronic kidney disease. *American journal of physiology. Renal physiology* **309**, F414-428
44. Lee, S. G., Lee, H., and Rho, H. M. (2001) Transcriptional repression of the human p53 gene by cobalt chloride mimicking hypoxia. *FEBS Lett.* **507**, 259-263
45. Ji, Z., Yang, G., Shahzidi, S., Tkacz-Stachowska, K., Suo, Z., Nesland, J. M., and Peng, Q. (2006) Induction of hypoxia-inducible factor-1alpha overexpression by cobalt chloride enhances cellular resistance to photodynamic therapy. *Cancer Lett.* **244**, 182-189
46. Jeon, E. S., Shin, J. H., Hwang, S. J., Moon, G. J., Bang, O. Y., and Kim, H. H. (2014) Cobalt chloride induces neuronal differentiation of human mesenchymal stem cells through upregulation of microRNA-124a. *Biochem. Biophys. Res. Commun.* **444**, 581-587
47. Rath, S., Anand, A., Ghosh, N., Das, L., Kokate, S. B., Dixit, P., Majhi, S., Rout, N., Singh, S. P., and Bhattacharyya, A. (2016) Cobalt chloride-mediated protein kinase Calpha (PKCalpha) phosphorylation induces hypoxia-inducible factor 1alpha

- (HIF1alpha) in the nucleus of gastric cancer cell. *Biochem. Biophys. Res. Commun.* **471**, 205-212
48. Kang, J., Chen, J., Shi, Y., Jia, J., and Zhang, Y. (2005) Curcumin-induced histone hypoacetylation: the role of reactive oxygen species. *Biochem. Pharmacol.* **69**, 1205-1213
49. Li, S., Zhang, J., Yang, H., Wu, C., Dang, X., and Liu, Y. (2015) Copper depletion inhibits CoCl₂-induced aggressive phenotype of MCF-7 cells via downregulation of HIF-1 and inhibition of Snail/Twist-mediated epithelial-mesenchymal transition. *Scientific reports* **5**, 12410
50. Chu, C. Y., Jin, Y. T., Zhang, W., Yu, J., Yang, H. P., Wang, H. Y., Zhang, Z. J., Liu, X. P., and Zou, Q. (2016) CA IX is upregulated in CoCl₂-induced hypoxia and associated with cell invasive potential and a poor prognosis of breast cancer. *Int. J. Oncol.* **48**, 271-280
51. Fu, O. Y., Hou, M. F., Yang, S. F., Huang, S. C., and Lee, W. Y. (2009) Cobalt chloride-induced hypoxia modulates the invasive potential and matrix metalloproteinases of primary and metastatic breast cancer cells. *Anticancer Res.* **29**, 3131-3138
52. Fei, F., Zhang, D., Yang, Z., Wang, S., Wang, X., Wu, Z., Wu, Q., and Zhang, S. (2015) The number of polyploid giant cancer cells and epithelial-mesenchymal transition-related proteins are associated with invasion and metastasis in human breast cancer. *J. Exp. Clin. Cancer Res.* **34**, 158
53. Lopez-Sanchez, L. M., Jimenez, C., Valverde, A., Hernandez, V., Penarando, J., Martinez, A., Lopez-Pedreria, C., Munoz-Castaneda, J. R., De la Haba-Rodriguez, J.

- R., Aranda, E., and Rodriguez-Ariza, A. (2014) CoCl₂, a mimic of hypoxia, induces formation of polyploid giant cells with stem characteristics in colon cancer. *PloS one* **9**, e99143
54. Triantafyllou, A., Liakos, P., Tsakalof, A., Georgatsou, E., Simos, G., and Bonanou, S. (2006) Cobalt induces hypoxia-inducible factor-1alpha (HIF-1alpha) in HeLa cells by an iron-independent, but ROS-, PI-3K- and MAPK-dependent mechanism. *Free Radic. Res.* **40**, 847-856
55. Tan, X. L., Huang, X. Y., Gao, W. X., Zai, Y., Huang, Q. Y., Luo, Y. J., and Gao, Y. Q. (2008) CoCl₂-induced expression of p300 promotes neuronal-like PC12 cell damage. *Neurosci. Lett.* **441**, 272-276
56. Peek, R. M., Jr., and Blaser, M. J. (2002) Helicobacter pylori and gastrointestinal tract adenocarcinomas. *Nature reviews. Cancer* **2**, 28-37
57. Montecucco, C., and Rappuoli, R. (2001) Living dangerously: how Helicobacter pylori survives in the human stomach. *Nature reviews. Molecular cell biology* **2**, 457-466
58. Vale, F. F., and Vitor, J. M. (2010) Transmission pathway of Helicobacter pylori: does food play a role in rural and urban areas? *Int. J. Food Microbiol.* **138**, 1-12
59. Telford, J. L., Covacci, A., Rappuoli, R., and Chiara, P. (1997) Immunobiology of Helicobacter pylori infection. *Curr. Opin. Immunol.* **9**, 498-503
60. Bui, D., Brown, H. E., Harris, R. B., and Oren, E. (2015) Serologic Evidence for Fecal-Oral Transmission of Helicobacter pylori. *Am. J. Trop. Med. Hyg.*

61. Aziz, R. K., Khalifa, M. M., and Sharaf, R. R. (2015) Contaminated water as a source of *Helicobacter pylori* infection: A review. *Journal of advanced research* **6**, 539-547
62. Safaei, H. G., Rahimi, E., Zandi, A., and Rashidipour, A. (2011) *Helicobacter pylori* as a zoonotic infection: the detection of *H. pylori* antigens in the milk and faeces of cows. *Journal of research in medical sciences : the official journal of Isfahan University of Medical Sciences* **16**, 184-187
63. Marshall, B. J., and Warren, J. R. (1984) Unidentified curved bacilli in the stomach of patients with gastritis and peptic ulceration. *Lancet* **1**, 1311-1315
64. Ilver, D., Arnqvist, A., Ogren, J., Frick, I. M., Kersulyte, D., Incecik, E. T., Berg, D. E., Covacci, A., Engstrand, L., and Boren, T. (1998) *Helicobacter pylori* adhesin binding fucosylated histo-blood group antigens revealed by retagging. *Science* **279**, 373-377
65. Bourzac, K. M., Satkamp, L. A., and Guillemin, K. (2006) The *Helicobacter pylori* *cag* pathogenicity island protein CagN is a bacterial membrane-associated protein that is processed at its C terminus. *Infect. Immun.* **74**, 2537-2543
66. Ta, L. H., Hansen, L. M., Sause, W. E., Shiva, O., Millstein, A., Ottemann, K. M., Castillo, A. R., and Solnick, J. V. (2012) Conserved transcriptional unit organization of the *cag* pathogenicity island among *Helicobacter pylori* strains. *Frontiers in cellular and infection microbiology* **2**, 46
67. Backert, S., and Selbach, M. (2008) Role of type IV secretion in *Helicobacter pylori* pathogenesis. *Cellular microbiology* **10**, 1573-1581

68. Truong, B. X., Mai, V. T., Tanaka, H., Ly le, T., Thong, T. M., Hai, H. H., Van Long, D., Furumatsu, K., Yoshida, M., Kutsumi, H., and Azuma, T. (2009) Diverse characteristics of the CagA gene of *Helicobacter pylori* strains collected from patients from southern vietnam with gastric cancer and peptic ulcer. *J. Clin. Microbiol.* **47**, 4021-4028
69. Quiding-Jarbrink, M., Lundin, B. S., Lonroth, H., and Svennerholm, A. M. (2001) CD4+ and CD8+ T cell responses in *Helicobacter pylori*-infected individuals. *Clin. Exp. Immunol.* **123**, 81-87
70. Buti, L., Spooner, E., Van der Veen, A. G., Rappuoli, R., Covacci, A., and Ploegh, H. L. (2011) *Helicobacter pylori* cytotoxin-associated gene A (CagA) subverts the apoptosis-stimulating protein of p53 (ASPP2) tumor suppressor pathway of the host. *Proc. Natl. Acad. Sci. U. S. A.* **108**, 9238-9243
71. Lamb, A., Yang, X. D., Tsang, Y. H., Li, J. D., Higashi, H., Hatakeyama, M., Peek, R. M., Blanke, S. R., and Chen, L. F. (2009) *Helicobacter pylori* CagA activates NF-kappaB by targeting TAK1 for TRAF6-mediated Lys 63 ubiquitination. *EMBO reports* **10**, 1242-1249
72. Tsang, Y. H., Lamb, A., Romero-Gallo, J., Huang, B., Ito, K., Peek, R. M., Jr., Ito, Y., and Chen, L. F. (2010) *Helicobacter pylori* CagA targets gastric tumor suppressor RUNX3 for proteasome-mediated degradation. *Oncogene* **29**, 5643-5650
73. Brandt, S., Kwok, T., Hartig, R., Konig, W., and Backert, S. (2005) NF-kappaB activation and potentiation of proinflammatory responses by the *Helicobacter pylori* CagA protein. *Proc. Natl. Acad. Sci. U. S. A.* **102**, 9300-9305

74. Varon, C., Dubus, P., Mazurier, F., Asencio, C., Chambonnier, L., Ferrand, J., Giese, A., Senant-Dugot, N., Carlotti, M., and Megraud, F. (2012) Helicobacter pylori infection recruits bone marrow-derived cells that participate in gastric preneoplasia in mice. *Gastroenterology* **142**, 281-291
75. Wei, J., Nagy, T. A., Vilgelm, A., Zaika, E., Ogden, S. R., Romero-Gallo, J., Piazuelo, M. B., Correa, P., Washington, M. K., El-Rifai, W., Peek, R. M., and Zaika, A. (2010) Regulation of p53 tumor suppressor by Helicobacter pylori in gastric epithelial cells. *Gastroenterology* **139**, 1333-1343
76. Das, L., Kokate, S. B., Rath, S., Rout, N., Singh, S. P., Crowe, S. E., Mukhopadhyay, A. K., and Bhattacharyya, A. (2016) ETS2 and Twist1 promote invasiveness of Helicobacter pylori-infected gastric cancer cells by inducing Siah2. *Biochem. J.*
77. Wang, F., Meng, W., Wang, B., and Qiao, L. (2014) Helicobacter pylori-induced gastric inflammation and gastric cancer. *Cancer Lett.* **345**, 196-202
78. Bessede, E., Staedel, C., Acuna Amador, L. A., Nguyen, P. H., Chambonnier, L., Hatakeyama, M., Belleanne, G., Megraud, F., and Varon, C. (2014) Helicobacter pylori generates cells with cancer stem cell properties via epithelial-mesenchymal transition-like changes. *Oncogene* **33**, 4123-4131
79. Bagnoli, F., Buti, L., Tompkins, L., Covacci, A., and Amieva, M. R. (2005) Helicobacter pylori CagA induces a transition from polarized to invasive phenotypes in MDCK cells. *Proc. Natl. Acad. Sci. U. S. A.* **102**, 16339-16344
80. Choi, Y. J., Kim, N., Chang, H., Lee, H. S., Park, S. M., Park, J. H., Shin, C. M., Kim, J. M., Kim, J. S., Lee, D. H., and Jung, H. C. (2015) Helicobacter pylori-induced

epithelial-mesenchymal transition, a potential role of gastric cancer initiation and an emergence of stem cells. *Carcinogenesis* **36**, 553-563

81. Ramos, P. S., Sardinha, A., Nardi, A. E., and de Araujo, C. G. (2014) Cardiorespiratory optimal point: a submaximal exercise variable to assess panic disorder patients. *PloS one* **9**, e104932
82. Wang, P., Mei, J., Tao, J., Zhang, N., Tian, H., and Fu, G. H. (2012) Effects of *Helicobacter pylori* on biological characteristics of gastric epithelial cells. *Histol. Histopathol.* **27**, 1079-1091
83. Zhu, Y., Jiang, Q., Lou, X., Ji, X., Wen, Z., Wu, J., Tao, H., Jiang, T., He, W., Wang, C., Du, Q., Zheng, S., Mao, J., and Huang, J. (2012) MicroRNAs up-regulated by CagA of *Helicobacter pylori* induce intestinal metaplasia of gastric epithelial cells. *PloS one* **7**, e35147
84. Zabaleta, J. (2012) MicroRNA: A Bridge from *H. pylori* Infection to Gastritis and Gastric Cancer Development. *Frontiers in genetics* **3**, 294
85. Bhattacharyya, A., Chattopadhyay, R., Hall, E. H., Mebrahtu, S. T., Ernst, P. B., and Crowe, S. E. (2010) Mechanism of hypoxia-inducible factor 1 alpha-mediated Mcl1 regulation in *Helicobacter pylori*-infected human gastric epithelium. *American journal of physiology. Gastrointestinal and liver physiology* **299**, G1177-1186
86. Rath, S., Das, L., Kokate, S. B., Pratheek, B. M., Chattopadhyay, S., Goswami, C., Chattopadhyay, R., Crowe, S. E., and Bhattacharyya, A. (2015) Regulation of Noxa-mediated apoptosis in *Helicobacter pylori*-infected gastric epithelial cells. *FASEB J.* **29**, 796-806

87. Rankin, E. B., and Giaccia, A. J. (2008) The role of hypoxia-inducible factors in tumorigenesis. *Cell Death Differ.* **15**, 678-685
88. Semenza, G. L. (2002) HIF-1 and tumor progression: pathophysiology and therapeutics. *Trends in molecular medicine* **8**, S62-67
89. Park, J. H., Kim, T. Y., Jong, H. S., Chun, Y. S., Park, J. W., Lee, C. T., Jung, H. C., Kim, N. K., and Bang, Y. J. (2003) Gastric epithelial reactive oxygen species prevent normoxic degradation of hypoxia-inducible factor-1alpha in gastric cancer cells. *Clin. Cancer Res.* **9**, 433-440
90. Semenza, G. L. (2000) HIF-1: mediator of physiological and pathophysiological responses to hypoxia. *J Appl Physiol (1985)* **88**, 1474-1480
91. Schofield, C. J., and Ratcliffe, P. J. (2004) Oxygen sensing by HIF hydroxylases. *Nature reviews. Molecular cell biology* **5**, 343-354
92. Miyazaki, K., Kawamoto, T., Tanimoto, K., Nishiyama, M., Honda, H., and Kato, Y. (2002) Identification of functional hypoxia response elements in the promoter region of the DEC1 and DEC2 genes. *J. Biol. Chem.* **277**, 47014-47021
93. Freedman, S. J., Sun, Z. Y., Poy, F., Kung, A. L., Livingston, D. M., Wagner, G., and Eck, M. J. (2002) Structural basis for recruitment of CBP/p300 by hypoxia-inducible factor-1 alpha. *Proc. Natl. Acad. Sci. U. S. A.* **99**, 5367-5372
94. Goodman, R. H., and Smolik, S. (2000) CBP/p300 in cell growth, transformation, and development. *Genes Dev.* **14**, 1553-1577
95. Kawamura, T., Hasegawa, K., Morimoto, T., Iwai-Kanai, E., Miyamoto, S., Kawase, Y., Ono, K., Wada, H., Akao, M., and Kita, T. (2004) Expression of p300 protects

- cardiac myocytes from apoptosis in vivo. *Biochem. Biophys. Res. Commun.* **315**, 733-738
96. Clarke, A. S., Lowell, J. E., Jacobson, S. J., and Pillus, L. (1999) Esa1p is an essential histone acetyltransferase required for cell cycle progression. *Mol. Cell. Biol.* **19**, 2515-2526
97. Ishihama, K., Yamakawa, M., Semba, S., Takeda, H., Kawata, S., Kimura, S., and Kimura, W. (2007) Expression of HDAC1 and CBP/p300 in human colorectal carcinomas. *J. Clin. Pathol.* **60**, 1205-1210
98. Yang, W. Y., Gu, J. L., and Zhen, T. M. (2014) Recent advances of histone modification in gastric cancer. *Journal of cancer research and therapeutics* **10 Suppl**, 240-245
99. Liu, X., Wang, L., Zhao, K., Thompson, P. R., Hwang, Y., Marmorstein, R., and Cole, P. A. (2008) The structural basis of protein acetylation by the p300/CBP transcriptional coactivator. *Nature* **451**, 846-850
100. Chan, H. M., and La Thangue, N. B. (2001) p300/CBP proteins: HATs for transcriptional bridges and scaffolds. *J. Cell Sci.* **114**, 2363-2373
101. Yan, G., Eller, M. S., Elm, C., Larocca, C. A., Ryu, B., Panova, I. P., Dancy, B. M., Bowers, E. M., Meyers, D., Lareau, L., Cole, P. A., Taverna, S. D., and Alani, R. M. (2013) Selective inhibition of p300 HAT blocks cell cycle progression, induces cellular senescence, and inhibits the DNA damage response in melanoma cells. *J. Invest. Dermatol.* **133**, 2444-2452

102. Zornig, M., Hueber, A., Baum, W., and Evan, G. (2001) Apoptosis regulators and their role in tumorigenesis. *Biochim. Biophys. Acta* **1551**, F1-37
103. Su, Z., Yang, Z., Xu, Y., Chen, Y., and Yu, Q. (2015) Apoptosis, autophagy, necroptosis, and cancer metastasis. *Molecular cancer* **14**, 48
104. Andersen, M. H., Becker, J. C., and Straten, P. (2005) Regulators of apoptosis: suitable targets for immune therapy of cancer. *Nature reviews. Drug discovery* **4**, 399-409
105. Weinmann, M., Jendrossek, V., Handrick, R., Guner, D., Goecke, B., and Belka, C. (2004) Molecular ordering of hypoxia-induced apoptosis: critical involvement of the mitochondrial death pathway in a FADD/caspase-8 independent manner. *Oncogene* **23**, 3757-3769
106. Reed, J. C. (2000) Mechanisms of apoptosis. *Am. J. Pathol.* **157**, 1415-1430
107. Shamas-Din, A., Brahmabhatt, H., Leber, B., and Andrews, D. W. (2011) BH3-only proteins: Orchestrators of apoptosis. *Biochim. Biophys. Acta* **1813**, 508-520
108. Nakajima, W., Hicks, M. A., Tanaka, N., Krystal, G. W., and Harada, H. (2014) Noxa determines localization and stability of MCL-1 and consequently ABT-737 sensitivity in small cell lung cancer. *Cell death & disease* **5**, e1052
109. Rampino, N., Yamamoto, H., Ionov, Y., Li, Y., Sawai, H., Reed, J. C., and Perucho, M. (1997) Somatic frameshift mutations in the BAX gene in colon cancers of the microsatellite mutator phenotype. *Science* **275**, 967-969
110. Portt, L., Norman, G., Clapp, C., Greenwood, M., and Greenwood, M. T. (2011) Anti-apoptosis and cell survival: a review. *Biochim. Biophys. Acta* **1813**, 238-259

111. Hassan, M., Alaoui, A., Feyen, O., Mirmohammadsadegh, A., Essmann, F., Tannapfel, A., Gulbins, E., Schulze-Osthoff, K., and Hengge, U. R. (2008) The BH3-only member Noxa causes apoptosis in melanoma cells by multiple pathways. *Oncogene* **27**, 4557-4568
112. Kalimuthu, S., and Se-Kwon, K. (2013) Cell survival and apoptosis signaling as therapeutic target for cancer: marine bioactive compounds. *International journal of molecular sciences* **14**, 2334-2354
113. Naik, E., Michalak, E. M., Villunger, A., Adams, J. M., and Strasser, A. (2007) Ultraviolet radiation triggers apoptosis of fibroblasts and skin keratinocytes mainly via the BH3-only protein Noxa. *J. Cell Biol.* **176**, 415-424
114. Huelsemann, M. F., Patz, M., Beckmann, L., Brinkmann, K., Otto, T., Fandrey, J., Becker, H. J., Theurich, S., von Bergwelt-Baildon, M., Pallasch, C. P., Zahedi, R. P., Kashkar, H., Reinhardt, H. C., Hallek, M., Wendtner, C. M., and Frenzel, L. P. (2015) Hypoxia-induced p38 MAPK activation reduces Mcl-1 expression and facilitates sensitivity towards BH3 mimetics in chronic lymphocytic leukemia. *Leukemia* **29**, 981-984
115. Kim, J. Y., Ahn, H. J., Ryu, J. H., Suk, K., and Park, J. H. (2004) BH3-only protein Noxa is a mediator of hypoxic cell death induced by hypoxia-inducible factor 1alpha. *J. Exp. Med.* **199**, 113-124
116. Koshikawa, N., Maejima, C., Miyazaki, K., Nakagawara, A., and Takenaga, K. (2006) Hypoxia selects for high-metastatic Lewis lung carcinoma cells overexpressing Mcl-1 and exhibiting reduced apoptotic potential in solid tumors. *Oncogene* **25**, 917-928

117. Lowman, X. H., McDonnell, M. A., Kosloske, A., Odumade, O. A., Jenness, C., Karim, C. B., Jemmerson, R., and Kelekar, A. (2010) The proapoptotic function of Noxa in human leukemia cells is regulated by the kinase Cdk5 and by glucose. *Mol. Cell* **40**, 823-833
118. Cartron, P. F., Loussouarn, D., Campone, M., Martin, S. A., and Vallette, F. M. (2012) Prognostic impact of the expression/phosphorylation of the BH3-only proteins of the BCL-2 family in glioblastoma multiforme. *Cell death & disease* **3**, e421
119. Karim, C. B., Michel Espinoza-Fonseca, L., James, Z. M., Hanse, E. A., Gaynes, J. S., Thomas, D. D., and Kelekar, A. (2015) Erratum: Structural Mechanism for Regulation of Bcl-2 protein Noxa by phosphorylation. *Scientific reports* **5**, 15872
120. Liou, G. Y., and Storz, P. (2010) Reactive oxygen species in cancer. *Free Radic. Res.* **44**, 479-496
121. Mates, J. M., and Sanchez-Jimenez, F. M. (2000) Role of reactive oxygen species in apoptosis: implications for cancer therapy. *Int. J. Biochem. Cell Biol.* **32**, 157-170
122. Bhattacharyya, A., Chattopadhyay, R., Mitra, S., and Crowe, S. E. (2014) Oxidative stress: an essential factor in the pathogenesis of gastrointestinal mucosal diseases. *Physiol. Rev.* **94**, 329-354
123. Wong, R. S. (2011) Apoptosis in cancer: from pathogenesis to treatment. *J. Exp. Clin. Cancer Res.* **30**, 87
124. Fulda, S., and Debatin, K. M. (2006) Extrinsic versus intrinsic apoptosis pathways in anticancer chemotherapy. *Oncogene* **25**, 4798-4811

125. Ketabchi, A., MacRobert, A., Speight, P. M., and Bennett, J. H. (1998) Induction of apoptotic cell death by photodynamic therapy in human keratinocytes. *Arch. Oral Biol.* **43**, 143-149
126. Ouhtit, A., Gaur, R. L., Abdraboh, M., Ireland, S. K., Rao, P. N., Raj, S. G., Al-Riyami, H., Shanmuganathan, S., Gupta, I., Murthy, S. N., Hollenbach, A., and Raj, M. H. (2013) Simultaneous inhibition of cell-cycle, proliferation, survival, metastatic pathways and induction of apoptosis in breast cancer cells by a phytochemical super-cocktail: genes that underpin its mode of action. *Journal of Cancer* **4**, 703-715
127. Xie, J., Gao, H., Peng, J., Han, Y., Chen, X., Jiang, Q., and Wang, C. (2015) Hispidulin prevents hypoxia-induced epithelial-mesenchymal transition in human colon carcinoma cells. *American journal of cancer research* **5**, 1047-1061
128. Arif, M., Vedamurthy, B. M., Choudhari, R., Ostwal, Y. B., Mantelingu, K., Kodaganur, G. S., and Kundu, T. K. (2010) Nitric oxide-mediated histone hyperacetylation in oral cancer: target for a water-soluble HAT inhibitor, CTK7A. *Chem. Biol.* **17**, 903-913
129. Bensellam, M., Duvillie, B., Rybachuk, G., Laybutt, D. R., Magnan, C., Guiot, Y., Pouyssegur, J., and Jonas, J. C. (2012) Glucose-induced O₂ consumption activates hypoxia inducible factors 1 and 2 in rat insulin-secreting pancreatic beta-cells. *PloS one* **7**, e29807
130. Balaiya, S., Khetpal, V., and Chalam, K. V. (2012) Hypoxia initiates sirtuin1-mediated vascular endothelial growth factor activation in choroidal endothelial cells through hypoxia inducible factor-2alpha. *Mol. Vis.* **18**, 114-120

131. Xie, L., and Collins, J. F. (2013) Transcription factors Sp1 and Hif2alpha mediate induction of the copper-transporting ATPase (Atp7a) gene in intestinal epithelial cells during hypoxia. *J. Biol. Chem.* **288**, 23943-23952
132. Oliveira, M. J., Costa, A. M., Costa, A. C., Ferreira, R. M., Sampaio, P., Machado, J. C., Seruca, R., Mareel, M., and Figueiredo, C. (2009) CagA associates with c-Met, E-cadherin, and p120-catenin in a multiproteic complex that suppresses Helicobacter pylori-induced cell-invasive phenotype. *J. Infect. Dis.* **200**, 745-755
133. Vaupel, P. (2004) The role of hypoxia-induced factors in tumor progression. *Oncologist* **9 Suppl 5**, 10-17
134. Gort, E. H., van Haften, G., Verlaan, I., Groot, A. J., Plasterk, R. H., Shvarts, A., Suijkerbuijk, K. P., van Laar, T., van der Wall, E., Raman, V., van Diest, P. J., Tijsterman, M., and Vooijs, M. (2008) The TWIST1 oncogene is a direct target of hypoxia-inducible factor-2alpha. *Oncogene* **27**, 1501-1510
135. Liu, K., Sun, B., Zhao, X., Wang, X., Li, Y., Qiu, Z., Gu, Q., Dong, X., Zhang, Y., Wang, Y., and Zhao, N. (2015) Hypoxia induced epithelial-mesenchymal transition and vasculogenic mimicry formation by promoting Bcl-2/Twist1 cooperation. *Exp. Mol. Pathol.* **99**, 383-391
136. Martin, A., and Cano, A. (2010) Tumorigenesis: Twist1 links EMT to self-renewal. *Nature cell biology* **12**, 924-925
137. Nakajima, S., Doi, R., Toyoda, E., Tsuji, S., Wada, M., Koizumi, M., Tulachan, S. S., Ito, D., Kami, K., Mori, T., Kawaguchi, Y., Fujimoto, K., Hosotani, R., and Imamura, M. (2004) N-cadherin expression and epithelial-mesenchymal transition in pancreatic carcinoma. *Clin. Cancer Res.* **10**, 4125-4133

138. Xing, F., Okuda, H., Watabe, M., Kobayashi, A., Pai, S. K., Liu, W., Pandey, P. R., Fukuda, K., Hirota, S., Sugai, T., Wakabayashi, G., Koeda, K., Kashiwaba, M., Suzuki, K., Chiba, T., Endo, M., Mo, Y. Y., and Watabe, K. (2011) Hypoxia-induced Jagged2 promotes breast cancer metastasis and self-renewal of cancer stem-like cells. *Oncogene* **30**, 4075-4086
139. Zhong, H., De Marzo, A. M., Laughner, E., Lim, M., Hilton, D. A., Zagzag, D., Buechler, P., Isaacs, W. B., Semenza, G. L., and Simons, J. W. (1999) Overexpression of hypoxia-inducible factor 1alpha in common human cancers and their metastases. *Cancer Res.* **59**, 5830-5835
140. Woo, H. N., Seo, Y. W., Moon, A. R., Jeong, S. Y., Choi, E. K., and Kim, T. H. (2009) Effects of the BH3-only protein human Noxa on mitochondrial dynamics. *FEBS Lett.* **583**, 2349-2354
141. Cereghetti, G. M., Costa, V., and Scorrano, L. (2010) Inhibition of Drp1-dependent mitochondrial fragmentation and apoptosis by a polypeptide antagonist of calcineurin. *Cell Death Differ.* **17**, 1785-1794
142. Kang, J., Zhang, Y., Chen, J., Chen, H., Lin, C., Wang, Q., and Ou, Y. (2003) Nickel-induced histone hypoacetylation: the role of reactive oxygen species. *Toxicol. Sci.* **74**, 279-286
143. Chen, J., Wanming, D., Zhang, D., Liu, Q., and Kang, J. (2005) Water-soluble antioxidants improve the antioxidant and anticancer activity of low concentrations of curcumin in human leukemia cells. *Pharmazie* **60**, 57-61

144. Fischer, S., Wiesnet, M., Renz, D., and Schaper, W. (2005) H₂O₂ induces paracellular permeability of porcine brain-derived microvascular endothelial cells by activation of the p44/42 MAP kinase pathway. *Eur. J. Cell Biol.* **84**, 687-697
145. Liang, T., Zhang, X., Xue, W., Zhao, S., and Pei, J. (2014) Curcumin induced human gastric cancer BGC-823 cells apoptosis by ROS-mediated ASK1-MKK4-JNK stress signaling pathway. *International journal of molecular sciences* **15**, 15754-15765
146. Nakamura, J., Kitajima, Y., Kai, K., Mitsuno, M., Ide, T., Hashiguchi, K., Hiraki, M., and Miyazaki, K. (2009) Hypoxia-inducible factor-1alpha expression predicts the response to 5-fluorouracil-based adjuvant chemotherapy in advanced gastric cancer. *Oncol. Rep.* **22**, 693-699
147. Nys, K., Van Laethem, A., Michiels, C., Rubio, N., Piette, J. G., Garmyn, M., and Agostinis, P. (2010) A p38(MAPK)/HIF-1 pathway initiated by UVB irradiation is required to induce Noxa and apoptosis of human keratinocytes. *J. Invest. Dermatol.* **130**, 2269-2276
148. Kitajima, Y., and Miyazaki, K. (2013) The Critical Impact of HIF-1a on Gastric Cancer Biology. *Cancers* **5**, 15-26
149. Lin, M. T., Kuo, I. H., Chang, C. C., Chu, C. Y., Chen, H. Y., Lin, B. R., Sureshbabu, M., Shih, H. J., and Kuo, M. L. (2008) Involvement of hypoxia-inducing factor-1alpha-dependent plasminogen activator inhibitor-1 up-regulation in Cyr61/CCN1-induced gastric cancer cell invasion. *J. Biol. Chem.* **283**, 15807-15815
150. Chen, W., Zhao, Z., Li, L., Wu, B., Chen, S. F., Zhou, H., Wang, Y., and Li, Y. Q. (2008) Hispolon induces apoptosis in human gastric cancer cells through a ROS-mediated mitochondrial pathway. *Free Radic. Biol. Med.* **45**, 60-72

151. Matsunaga, T., Tsuji, Y., Kaai, K., Kohno, S., Hirayama, R., Alpers, D. H., Komoda, T., and Hara, A. (2010) Toxicity against gastric cancer cells by combined treatment with 5-fluorouracil and mitomycin c: implication in oxidative stress. *Cancer Chemother. Pharmacol.* **66**, 517-526
152. Bae, I. H., Kang, S. W., Yoon, S. H., and Um, H. D. (2006) Cellular components involved in the cell death induced by cisplatin in the absence of p53 activation. *Oncol. Rep.* **15**, 1175-1180
153. Chung, K. S., Han, G., Kim, B. K., Kim, H. M., Yang, J. S., Ahn, J., Lee, K., Song, K. B., and Won, M. (2013) A novel antitumor piperazine alkyl compound causes apoptosis by inducing RhoB expression via ROSmediated cAbl/p38 MAPK signaling. *Cancer Chemother. Pharmacol.* **72**, 1315-1324
154. Jones, K. R., Whitmire, J. M., and Merrell, D. S. (2010) A Tale of Two Toxins: Helicobacter Pylori CagA and VacA Modulate Host Pathways that Impact Disease. *Frontiers in microbiology* **1**, 115
155. Xue, Y., Ren, J., Gao, X., Jin, C., Wen, L., and Yao, X. (2008) GPS 2.0, a tool to predict kinase-specific phosphorylation sites in hierarchy. *Molecular & cellular proteomics : MCP* **7**, 1598-1608
156. Iseki, H., Ko, T. C., Xue, X. Y., Seapan, A., Hellmich, M. R., and Townsend, C. M., Jr. (1997) Cyclin-dependent kinase inhibitors block proliferation of human gastric cancer cells. *Surgery* **122**, 187-194; discussion 194-185
157. Tsai, L. H., Takahashi, T., Caviness, V. S., Jr., and Harlow, E. (1993) Activity and expression pattern of cyclin-dependent kinase 5 in the embryonic mouse nervous system. *Development* **119**, 1029-1040

158. Ding, S. Z., Smith, M. F., Jr., and Goldberg, J. B. (2008) Helicobacter pylori and mitogen-activated protein kinases regulate the cell cycle, proliferation and apoptosis in gastric epithelial cells. *J. Gastroenterol. Hepatol.* **23**, e67-78
159. Tromp, J. M., Geest, C. R., Breij, E. C., Elias, J. A., van Laar, J., Luijckx, D. M., Kater, A. P., Beaumont, T., van Oers, M. H., and Eldering, E. (2012) Tipping the Noxa/Mcl-1 balance overcomes ABT-737 resistance in chronic lymphocytic leukemia. *Clin. Cancer Res.* **18**, 487-498
160. Kodama, Y., Taura, K., Miura, K., Schnabl, B., Osawa, Y., and Brenner, D. A. (2009) Antiapoptotic effect of c-Jun N-terminal Kinase-1 through Mcl-1 stabilization in TNF-induced hepatocyte apoptosis. *Gastroenterology* **136**, 1423-1434
161. Nijhawan, D., Fang, M., Traer, E., Zhong, Q., Gao, W., Du, F., and Wang, X. (2003) Elimination of Mcl-1 is required for the initiation of apoptosis following ultraviolet irradiation. *Genes Dev.* **17**, 1475-1486
162. Schuler, M., Maurer, U., Goldstein, J. C., Breitenbucher, F., Hoffarth, S., Waterhouse, N. J., and Green, D. R. (2003) p53 triggers apoptosis in oncogene-expressing fibroblasts by the induction of Noxa and mitochondrial Bax translocation. *Cell Death Differ.* **10**, 451-460
163. Willis, S. N., and Adams, J. M. (2005) Life in the balance: how BH3-only proteins induce apoptosis. *Curr. Opin. Cell Biol.* **17**, 617-625
164. Porter, A. G., and Janicke, R. U. (1999) Emerging roles of caspase-3 in apoptosis. *Cell Death Differ.* **6**, 99-104

165. Ashktorab, H., Frank, S., Khaled, A. R., Durum, S. K., Kifle, B., and Smoot, D. T. (2004) Bax translocation and mitochondrial fragmentation induced by *Helicobacter pylori*. *Gut* **53**, 805-813
166. Matsumoto, Y., Marusawa, H., Kinoshita, K., Endo, Y., Kou, T., Morisawa, T., Azuma, T., Okazaki, I. M., Honjo, T., and Chiba, T. (2007) *Helicobacter pylori* infection triggers aberrant expression of activation-induced cytidine deaminase in gastric epithelium. *Nat. Med.* **13**, 470-476
167. Alves, N. L., Derks, I. A., Berk, E., Spijker, R., van Lier, R. A., and Eldering, E. (2006) The Noxa/Mcl-1 axis regulates susceptibility to apoptosis under glucose limitation in dividing T cells. *Immunity* **24**, 703-716
168. Domek, M. J., Netzer, P., Prins, B., Nguyen, T., Liang, D., Wyle, F. A., and Warner, A. (2001) *Helicobacter pylori* induces apoptosis in human epithelial gastric cells by stress activated protein kinase pathway. *Helicobacter* **6**, 110-115
169. Martinou, J. C., and Youle, R. J. (2011) Mitochondria in apoptosis: Bcl-2 family members and mitochondrial dynamics. *Developmental cell* **21**, 92-101
170. Liu, W., Swetzig, W. M., Medisetty, R., and Das, G. M. (2011) Estrogen-mediated upregulation of Noxa is associated with cell cycle progression in estrogen receptor-positive breast cancer cells. *PloS one* **6**, e29466
171. Tournier, C., Hess, P., Yang, D. D., Xu, J., Turner, T. K., Nimmual, A., Bar-Sagi, D., Jones, S. N., Flavell, R. A., and Davis, R. J. (2000) Requirement of JNK for stress-induced activation of the cytochrome c-mediated death pathway. *Science* **288**, 870-874

172. Snider, J. L., Allison, C., Bellaire, B. H., Ferrero, R. L., and Cardelli, J. A. (2008) The beta1 integrin activates JNK independent of CagA, and JNK activation is required for Helicobacter pylori CagA+-induced motility of gastric cancer cells. *J. Biol. Chem.* **283**, 13952-13963
173. Germain, M., Milburn, J., and Duronio, V. (2008) MCL-1 inhibits BAX in the absence of MCL-1/BAX Interaction. *J. Biol. Chem.* **283**, 6384-6392
174. Sedlak, T. W., Oltvai, Z. N., Yang, E., Wang, K., Boise, L. H., Thompson, C. B., and Korsmeyer, S. J. (1995) Multiple Bcl-2 family members demonstrate selective dimerizations with Bax. *Proc. Natl. Acad. Sci. U. S. A.* **92**, 7834-7838
175. Giam, M., Huang, D. C., and Bouillet, P. (2008) BH3-only proteins and their roles in programmed cell death. *Oncogene* **27 Suppl 1**, S128-136
176. Zhang, L., Lopez, H., George, N. M., Liu, X., Pang, X., and Luo, X. (2011) Selective involvement of BH3-only proteins and differential targets of Noxa in diverse apoptotic pathways. *Cell Death Differ.* **18**, 864-873
177. Nardone, G., Rocco, A., Vaira, D., Staibano, S., Budillon, A., Tatangelo, F., Sciulli, M. G., Perna, F., Salvatore, G., Di Benedetto, M., De Rosa, G., and Patrignani, P. (2004) Expression of COX-2, mPGE-synthase1, MDR-1 (P-gp), and Bcl-xL: a molecular pathway of H pylori-related gastric carcinogenesis. *J. Pathol.* **202**, 305-312
178. Lee, D. G., Kim, H. S., Lee, Y. S., Kim, S., Cha, S. Y., Ota, I., Kim, N. H., Cha, Y. H., Yang, D. H., Lee, Y., Park, G. J., Yook, J. I., and Lee, Y. C. (2014) Helicobacter pylori CagA promotes Snail-mediated epithelial-mesenchymal transition by reducing GSK-3 activity. *Nature communications* **5**, 4423

179. Yin, Y., Grabowska, A. M., Clarke, P. A., Whelband, E., Robinson, K., Argent, R. H., Tobias, A., Kumari, R., Atherton, J. C., and Watson, S. A. (2010) Helicobacter pylori potentiates epithelial:mesenchymal transition in gastric cancer: links to soluble HB-EGF, gastrin and matrix metalloproteinase-7. *Gut* **59**, 1037-1045
180. Elmore, S. (2007) Apoptosis: a review of programmed cell death. *Toxicol. Pathol.* **35**, 495-516
181. Yu, H., Zeng, J., Liang, X., Wang, W., Zhou, Y., Sun, Y., Liu, S., Li, W., Chen, C., and Jia, J. (2014) Helicobacter pylori promotes epithelial-mesenchymal transition in gastric cancer by downregulating programmed cell death protein 4 (PDCD4). *PloS one* **9**, e105306

Appendix I

PLASMID CONSTRUCTS USED

Constructs	Description	Source
pcDNA3.1 ⁺ -Noxa	Wild type construct	Self generated
pcDNA3.1 ⁺ -Noxa mut	Noxa (S13A) mutation	Self generated from Noxa wild type
pDsRed2-Mito	<i>Discosoma sp.</i> red fluorescent protein and subunit VIII of human cytochrome oxidase sequence containing plasmid targets mitochondria	Clontech Gifted by Dr. Chandan Goswami, School of Biological Sciences, NISER, India
pCMV-p300	Wild type construct	Gastroenterology. 2009 June ; 136(7): 2258–2269
pCMV-ΔHAT	HAT region is deleted	Gastroenterology. 2009 June; 136(7): 2258–2269
JNK1	Wild type construct	Cell. 1994 Mar 25;76(6); 1025-37
JNK2	Wild type construct	Genes Dev. 1994 Dec 15; 8 (24):2996-3007

Appendix II

ANTIBODIES USED FOR WESTERN BLOTTING AND MICROSCOPY

Antibodies	Clone	Dilution	Company	Catalogue
p300 (WB)	Mouse Monoclonal	1:250	Abcam	ab3164
Anti-HIF1 α (WB)	Mouse Monoclonal	1:2000	Abcam	ab16066
Anti-HIF1 α (IF)	Mouse Monoclonal	1:200	Abcam	ab16066
Anti-p53 (WB)	Rabbit Monoclonal	1:1000	Abcam	ab32049
Acetylated lysine (WB)	Rabbit Polyclonal	1:1000	Cell Signaling Technology	9441
Anti-Twist1 (WB)	Mouse Monoclonal	1:250	Abcam	ab50887
Anti-Twist1 (IF)	Mouse Monoclonal	1:50	Abcam	ab50887
Cleaved caspase 3 (WB)	Rabbit Polyclonal	1:1000	Cell Signaling Technology	9661
Cleaved caspase 9 (WB)	Rabbit Polyclonal	1:1000	Cell Signaling Technology	9501
COX IV (WB)	Rabbit Polyclonal	1:1000	Cell Signaling Technology	4850
Noxa (WB and IF)	Mouse Monoclonal	1:250	Abcam	13654
Cytochrome <i>c</i> (WB)	Rabbit Polyclonal	1:1000	Cell Signaling Technology	4272
Cytochrome <i>c</i> (WB)	Rabbit Polyclonal	1:100	Cell Signaling Technology	4272

Anti-Phosphoserine (WB)	Mouse Monoclonal	1:250	Sigma-Aldrich	P5747
Alpha Tubulin (WB)	Rabbit Monoclonal	1:100000	Abcam	ab52866
N-Cadherin (WB)	Rabbit Polyclonal	1:1000	Cell Signaling Technology	4061
N-Cadherin (IF)	Rabbit Polyclonal	1:100	Cell Signaling Technology	4061
E-Cadherin (WB)	Rabbit Polyclonal	1:1000	Cell Signaling Technology	3195
E-Cadherin (IF)	Rabbit Polyclonal	1:1000	Cell Signaling Technology	3195
Acetyl-p53 (Lys382) (WB)	Rabbit Polyclonal	1:1000	Cell Signaling Technology	2525
Phospho-p44/42-MAPK (Thr202/Tyr204) (WB)	Rabbit Monoclonal	1:1000	Cell Signaling Technology	4370
Phospho-p38MAPK (Thr180/Tyr182) (WB)	Rabbit Monoclonal	1:1000	Cell Signaling Technology	4511
Phospho-SAPK/JNK (Thr183/Tyr185) (WB)	Rabbit Monoclonal	1:1000	Cell Signaling Technology	4668
p44/42 MAPK (WB)	Rabbit Polyclonal	1:1000	Cell Signaling Technology	4695
SAPK/JNK (WB)	Rabbit Polyclonal	1:1000	Cell Signaling Technology	9258
p38MAPK (WB)	Rabbit Polyclonal	1:1000	Cell Signaling Technology	9212

Anti-MC11 (WB)	Rabbit Monoclonal	1:1000	Abcam	ab32078
Anti Bax (WB)	Rabbit Polyclonal	1:1000	Abcam	ab10813
p53 (WB)	Mouse Monoclonal	1:1000	Abcam	ab28
CagA (WB)	Mouse Monoclonal	1:100-1:1000	SANTACRUZ BIOTECH	SC-28368
GAPDH (WB)	Mouse Monoclonal	1:500	IMGENEX	IMG-6665A
HDAC1 (WB)	Rabbit Polyclonal	1:1000	Cell Signaling Technology	2062

WB: western blot, IF: immunofluorescence microscopy

Appendix III

PRIMER SEQUENCES USED FOR noxa CLONING

Primers	Sequence
Forward	5' AAA AGC TTC ACC ATG CCT GGG AAG AAG GCG CGC 3'
Reverse	5' G C TCG AGT CAG GTT CCT GAG CAG AAG AGT TTG GAT ATC AGA TTC AG 3'

PRIMER USED FOR noxa S13A MUTATION

Mutagenesis primer	Sequence
	5' AAG AAC GCT CAA CCG <u>GCC</u> CCC GCG CGG GCT CCA 3'

PUBLICATIONS



Contents lists available at ScienceDirect

The International Journal of Biochemistry & Cell Biology

journal homepage: www.elsevier.com/locate/biocel

Inhibition of histone/lysine acetyltransferase activity kills CoCl_2 -treated and hypoxia-exposed gastric cancer cells and reduces their invasiveness



Suvasmita Rath^a, Lopamudra Das^a, Shrikant Babanrao Kokate^a, Nilabh Ghosh^a, Pragyesh Dixit^a, Niranjana Rout^b, Shivaram P. Singh^c, Subhasis Chattopadhyay^a, Hassan Ashktorab^d, Duane T. Smoot^e, Mahadeva M. Swamy^f, Tapas K. Kundu^f, Sheila E. Crowe^g, Asima Bhattacharyya^{a,*}

^a School of Biological Sciences, National Institute of Science Education and Research (NISER) Bhubaneswar, HBNI, P.O. Bimpur-Padanpur, Via Jatni, Dist. Khurda, 752050, Odisha, India

^b Oncopathology, Acharya Harihar Regional Cancer Centre, Cuttack, 753007, Odisha, India

^c Department of Gastroenterology, SCB Medical College, Cuttack, 753007, Odisha, India

^d Department of Medicine, Howard University, Washington, DC, 20059, USA

^e Department of Medicine, Meharry Medical Center, Nashville, TN, 37208, USA

^f Transcription and Disease Laboratory, Molecular Biology and Genetics Unit, JNCASR, Jakkur PO, Bangalore 560064, Karnataka, India

^g School of Medicine, University of California, San Diego, CA, 92093, USA

ARTICLE INFO

Article history:

Received 19 July 2016

Received in revised form 23 October 2016

Accepted 21 November 2016

Available online 23 November 2016

Keywords:

Apoptosis

Cancer metastasis

CTK7A

HAT

Hif1 α

Hypoxia

ABSTRACT

Hypoxia enhances immortality and metastatic properties of solid tumors. Deregulation of histone acetylation has been associated with several metastatic cancers but its effect on hypoxic responses of cancer cells is not known. This study aimed at understanding the effectiveness of the hydrazinocurcumin, CTK7A, an inhibitor of p300 lysine/histone acetyltransferase (KAT/HAT) activity, in inducing apoptosis of gastric cancer cells (GCCs) exposed to cobalt chloride (CoCl_2), a hypoxia-mimetic chemical, or 1% O_2 . Here, we show that CTK7A-induced hydrogen peroxide (H_2O_2) generation in CoCl_2 -exposed and invasive gastric cancer cells (GCCs) leads to p38 MAPK-mediated Noxa expression and thereafter, mitochondrial apoptotic events. Noxa induction in normal immortalized gastric epithelial cells after CTK7A and hypoxia-exposure is remarkably less in comparison to similarly-treated GCCs. Moreover, hypoxia-exposed GCCs, which have acquired invasive properties, become apoptotic after CTK7A treatment to a significantly higher extent than normoxic cells. Thus, we show the potential of CTK7A in sensitizing hypoxic and metastatic GCCs to apoptosis induction.

© 2016 Elsevier Ltd. All rights reserved.

Abbreviations: Ac, acetylated; BH3, Bcl2 homology 3; CM-H₂-DCFDA, 5-(and 6)-chloromethyl-2,7-dichlorodihydrofluorescein diacetate acetyl ester; $\text{CoCl}_2 \cdot 6\text{H}_2\text{O}$, cobalt chloride hexahydrate; Cyt c, cytochrome c; DAPI, (4',6-Diamidino-2-phenylindole) Dilactate; ERK, extracellular signal-regulated kinases; GCC, gastric cancer cell; HAT, histone acetyltransferase; H_2O_2 , hydrogen peroxide; Hif1, hypoxia-inducible factor 1; HRE, hypoxia-responsive element; IP, immunoprecipitation; JNK, c-Jun N-terminal kinase; MAPK, mitogen-activated protein kinase; PAGE, polyacrylamide gel electrophoresis; ROS, reactive oxygen species; SDS, sodium dodecyl sulphate; SOD, superoxide dismutase; WT, wild type.

* Corresponding author.

E-mail address: asima@niser.ac.in (A. Bhattacharyya).

1. Introduction

Solid tumors are different from normal tissues in terms of their oxygen supply and consumption. The core of solid tumors become hypoxic due to inefficient blood supply (Karakashev and Reginato, 2015; Rankin and Giaccia, 2008). Hypoxia provides the ideal microenvironment for promoting metastasis (Sullivan and Graham, 2007). Naturally, like other solid tumors, gastric cancer malignancy and treatment resistance are largely, if not solely, determined by hypoxia (Vaupel and Mayer, 2007). Thus, selective therapeutic targeting of hypoxic metastatic gastric cancer cells is a challenging area of research.

Hypoxic cells undergo several hypoxia-adaptations. The master regulatory protein expressed in hypoxic cells is hypoxia-inducible

factor1 (Hif1). Hif1 is a heterodimeric protein having two subunits, α and β . While Hif1 α gets degraded in normoxia and hypoxia stabilizes it, Hif1 β is constitutively expressed and its stability is not regulated by cellular oxygenation status (Huang et al., 1998). Hif1 α dimerizes with Hif1 β and transcriptionally activates a number of hypoxia-responsive genes by binding to the hypoxia-responsive elements (HREs) (Rohwer et al., 2009). p300 acts as a transcriptional coactivator of Hif1. p300 has an intrinsic histone or lysine (K) acetyltransferase (HAT or KAT) activity and functions as a protein scaffold (Chan and La Thangue, 2001; Santer et al., 2011). Autoacetylation induces acetyltransferase activity of p300. Both enhanced and suppressed (HAT) activity in tumor cells can lead to cell cycle arrest and apoptosis (Clarke et al., 1999; Kawamura et al., 2004). It is evident from the literature that the relation of HAT activity with cancer is tissue and context-dependent. Dysregulation of histone acetylation and deacetylation have been associated with gastric cancer progression and invasiveness (Yang et al., 2014). Studies have found expression of Hif1 α in gastric cancer and have associated Hif1 α with aggressive metastasis and treatment resistance (Liu et al., 2008; Rohwer and Cramer, 2010; Urano et al., 2006). Induction of apoptotic cell death in invasive cancer cells is a highly desired goal to achieve for cancer therapists. Cellular apoptosis is orchestrated by two separate signaling pathways- the mitochondria-mediated intrinsic pathway and the death receptor-mediated extrinsic pathway (Cotter, 2009). Chemo and radiotherapy induce the former pathway by involving the Bcl2 family proteins. A Bcl2 homology 3 (BH3)-only tumor suppressor protein Noxa is transcriptionally induced by Hif1 and induces mitochondria mediated intrinsic apoptotic pathway (Gomez-Bougie et al., 2011).

In this study, we investigated the role of p300 HAT activity on Noxa-mediated apoptosis in CoCl₂-treated and 1% O₂-exposed GCCs. We showed that downregulation of HAT activity significantly induced reactive oxygen species (ROS) generation as well as Noxa-mediated apoptosis selectively in hypoxic GCCs but not in non-hypoxic GCCs. In addition, the expression of metastatic markers in CoCl₂-treated GCCs was also downregulated after suppression of HAT activity by the hydrazinocurcumin, CTK7A. Thus, this study revealed a previously undescribed mechanism for how CTK7A can induce apoptosis in hypoxia-exposed invasive GCCs and further enriched our understanding of its antitumor effects.

2. Methods

2.1. Cell lines

GCCs AGS, MKN 45, KATO III were cultured and maintained as previously described (Bhattacharyya et al., 2009). Immortalized human GCC cell HFE145 and pDsRed2 (Clontech, CA, USA)-expressing AGS stable cells were maintained in 10% heat-inactivated FBS-supplemented RPMI 1640. Most of the studies were performed using non-metastatic AGS cells so that metastasis induction could be clearly identified. HFE145 cells were used to study properties of non-malignant human gastric epithelial cells. *hif1 α* knockdown cells were prepared as described previously (Rath et al., 2015).

2.2. Chemicals and reagents

Cobalt chloride hexahydrate (CoCl₂·6H₂O) (Sigma-Aldrich, MO, USA) or 1% O₂ was used to induce hypoxia in AGS cells as per standard methods (Rath et al., 2016; Wu and Yotnda, 2011). CTK7A at 100 μ M dose (Arif et al., 2010) either alone or in combination with CoCl₂ (200 μ M) was used for 24 h treatment. ERK1/2 inhibitor PD98059, p38 MAPK inhibitor SB203580, and JNK inhibitor II SP600125 (all from Calbiochem, CA, USA) were used at 25 μ M dose

for 1 h prior to CoCl₂ and CTK7A treatment. Superoxide dismutase (SOD) and catalase (CAT) (both from Sigma Aldrich) were used at 200 units/ml and 350 units/ml dose, respectively, for 4 h prior to treatment with CoCl₂ and CTK7A. 5-(and 6)-chloromethyl-2,7-dichlorodihydrofluorescein diacetate, acetyl ester (CM-H₂-DCFDA; Invitrogen, CA, USA) was used to detect intracellular ROS generation.

2.3. Whole cell, nuclear, cytosolic and mitochondrial lysate preparation

Whole cell lysates were prepared by standard protein isolation protocol. Nuclear and cytoplasmic fractions were isolated using NEPER Kit following manufacturer's instruction (Thermo Scientific, IL, USA). Mitochondrial lysates were prepared following a previously described protocol (Rath et al., 2015).

2.4. Western blots, antibodies and immunoprecipitation

Proteins were separated by sodium dodecyl sulphate polyacrylamide gel electrophoresis (SDS-PAGE) followed by western blotting. Membranes were probed with specific antibodies for p300, acetylated lysine, Hif1 α , Noxa, Twist1 (Abcam, MA, USA), caspase 3, caspase 9, Cytochrome c, N cadherin, E cadherin, phospho p38 MAPK, phospho ERK and phospho JNK (Cell Signaling Technology, MA, USA). GAPDH (Imgenex Corporation, CA, USA) and Cox IV (Cell Signaling Technology, MA, USA) antibodies were used as loading controls for the cytosolic fraction and mitochondrial fractions, respectively. Proteins were detected by using Super Signal West Femto kit (Thermo scientific). Images were taken with Chemidoc XRS (Bio-Rad Laboratories, CA, USA) equipped with Quantity One-4.6.9 software.

2.5. Flow cytometry

Apoptosis was quantified by flow cytometry. AGS cells were treated with CoCl₂ (Sigma-Aldrich) alone and/or CTK7A for 24 h or left untreated. Cell pellets were washed twice with chilled PBS and stained with Annexin V PE/7-AAD (BD Biosciences, CA, USA) according to manufacturer's instruction. 1×10^4 cells were acquired per sample using FACSCalibur Flow Cytometer (BD Biosciences). Results were analyzed by CellQuest Pro software (BD Biosciences).

2.6. Confocal microscopy

pDsRed2 (Clontech)-expressing AGS stable cells were used for confocal microscopy. These cells were treated with CoCl₂ and/or CTK7A or left untreated for 24 h. Noxa translocation to mitochondria and cytochrome c release from mitochondria were studied in the above experimental condition. Cells were fixed with 4% paraformaldehyde at 37 °C for 15 min followed by incubation with DAPI (4', 6-Diamidino-2-Phenylindole, Dilactate (Invitrogen) for 20 min. Mitochondrial morphology was studied as described earlier (Rath et al., 2015). Fragmentation of mitochondria, as assessed by roundness, circularity and length, was measured by ImageJ software (NIH, MD, USA). Roundness [$4 \times (\text{surface area}) / (\pi \times \text{major axis}^2)$] and circularity [$4\pi \times (\text{surface area} / \text{perimeter}^2)$] together represented mitochondrial sphericity (sphericity value 1 = perfect spheroid).

2.7. Transwell migration and invasion assay

Cell migration and invasion assays were performed using 8- μ m pore size Transwell Biocoat control inserts (migration assay)

or matrigel-coated inserts, as per manufacturer's instruction (Becton Dickinson, MA, USA). 5×10^4 AGS cells in serum free media were seeded on the upper surface of 24 well transwell plate and 10% FBS-containing media was added to the lower chamber. Cells were treated with CoCl_2 or 1% O_2 alone and/or CTK7A for 24 h or left untreated. After completion of the incubation, upper surfaces of transwell were scraped off and cells in the lower surface were fixed for 30 min with 4% paraformaldehyde, and stained for 30 min with haematoxylin. Migrated and invaded cells were counted (from five different fields) under an inverted microscope (Primo Vert, Carl Zeiss, Jena, Germany).

2.8. Wound healing assay

1×10^6 AGS cells were seeded in 35 mm plates and wound healing assays were performed as described earlier were kept for 24 h to create a monolayer of cells. Multiple uniform wounds of constant diameter were made on the monolayer culture. Detached cells were washed followed by 24 h treatment of CoCl_2 and/or CTK7A or were left untreated. Imaging was done by an inverted microscope equipped with camera (Primo Vert, Carl Zeiss).

2.9. Soft agar assay

AGS cells were harvested and 1×10^3 cells were mixed with 0.3% top agar and plated onto 0.6% bottom agar in 6 cm cell culture plates. Cells were treated with CoCl_2 (50 μM) and/or CTK7A (100 μM) for 24 h. These plates were fed twice weekly with the above treatment condition and maintained for 3 weeks in a humidified incubator containing 5% CO_2 . At the end of the incubation period, visible colonies on the top agar were directly counted and colony sizes were compared between various treatment groups.

2.10. Human gastric biopsy specimen collection and fluorescence microscopy

Biopsy samples from the antral gastric mucosa were collected from patients suffering from metastatic gastric cancer and undergoing diagnostic esophagogastroduodenoscopy following a National Institute of Science Education and Research (NISER) Review Board-approved protocol. Written informed consent was obtained from all patients. Gastric biopsy samples were embedded in optimal cutting temperature (OCT) compound (VWR International, Lutterworth, UK). Cryosectioning was performed at 10 μm (Leica, Wetzlar, Germany). Sections were stained with Hif1 α , Twist1, E-cadherin and N-cadherin primary antibodies followed by incubation with fluorescently labelled secondary antibodies (Alexa Fluor 488 anti-rabbit and anti mouse from Molecular Probes, Invitrogen, Paisley). The sections were examined by a fluorescence microscope (Olympus, Tokyo, Japan).

2.11. Reactive oxygen species (ROS) measurement

ROS was measured by staining cells with a membrane-permeable dye, 5-(and 6)-chloromethyl-2,7-dichlorodihydrofluorescein diacetate, acetyl ester (CM-H₂-DCFDA; Invitrogen). 0.166×10^6 AGS cells were grown on 9 mm coverslips in 24 well cell culture plates. After treatment, cells were stained with 1 μM CM-H₂-DCFDA and incubated for 10 min at 37 °C in the dark. Cells were fixed with 4% paraformaldehyde for 10 min at room temperature and viewed by fluorescence microscope (Olympus).

2.12. Statistics

Values are given as mean \pm SEM. Student's *t*-test was performed for comparison between groups. Statistical significance was deter-

mined at $P < 0.05$. 2-way ANOVA was performed to compare various transfected groups. Bonferroni test was applied for *post hoc* analysis. Colocalization analysis of confocal images was performed by ImageJ plugin Coloc 2.

3. Results

3.1. CoCl_2 and 1% O_2 treatment enhances expression of metastatic factors in AGS cells

Cobalt chloride (CoCl_2) mimics hypoxia, induces ROS generation and promotes mitochondria-mediated apoptosis (Torii et al., 2011; Wang et al., 2000). CoCl_2 has the same biochemical response as that of physiological hypoxia (Bae et al., 2012; Lee et al., 2001) and induces Hif1 α expression in GCCs (Rath et al., 2016). In contrast, several reports have also shown that CoCl_2 -induced Hif1 α inhibits apoptosis (Piret et al., 2005, 2002) and enhances metastatic potential (Zhang et al., 2013). In order to study the expression of metastatic factors in GCCs after treatment with 200 μM cobalt chloride hexahydrate ($\text{CoCl}_2 \cdot 6\text{H}_2\text{O}$) for various time periods, western blotting were performed. Although GAPDH is a Hif1-target gene, we used GAPDH as a loading control since GAPDH was not found to be regulated by hypoxia in the gastric cancer cell lines AGS (Xiao et al., 2012), MGS-803 and SGC-7901 (Luo et al., 2010) as well as in other hypoxic cancer cells studied *in vitro* (Jung et al., 2014; Said et al., 2007, 2009). Western blot data ($n = 3$) showed that although Hif1 α was significantly induced as early as 3 h of treatment and it was maintained up to 24 h, Hif1 α -dependent metastasis-inducing transcription factor Twist1 was noticeably enhanced only at 12 and 24 h of CoCl_2 treatment (Fig. 1A). The mesenchymal marker N-cadherin was highly upregulated at 24 h of CoCl_2 treatment. Therefore, we used 200 μM CoCl_2 and 100 μM CTK7A [(Sodium 4-(3,5-bis (4-hydroxy-3-methoxystyryl)-1H-pyrazol-1-yl) benzoate], a curcumin-derived water soluble HAT/KAT and p300 autoacetylation inhibitor treatment for 24 h for the rest of our experiments. As AGS cells do not express the invasion-suppressor epithelial marker E-cadherin (Oliveira et al., 2009), we did not observe the other component of "cadherin switch" associated with metastasis, the E-cadherin degradation (Gheldof and Berx, 2013) in CoCl_2 -treated hypoxic AGS cells. p300, however, remained equally expressed at all time points. We also performed immunofluorescence microscopy on human metastatic gastric cancer biopsies and compared with matched controls from adjacent noncancerous areas. Metastatic samples ($n = 4$), which showed substantial high expression of Hif1 α , also had high Twist1 and N-cadherin but showed much lower E-cadherin expression compared to their matched controls ($n = 4$) (Fig. S1A).

In an attempt to understand the effect of HAT function inhibition on the expression of Hif1 α and the above-mentioned metastasis markers, AGS cells were incubated for 24 h with 100 μM of CTK7A in the presence or absence of 200 μM CoCl_2 or were left untreated. Western blotting ($n = 3$) of whole cell lysates showed that CoCl_2 -mediated induced expression of Hif1 α , Twist1 and N-cadherin was substantially inhibited by CTK7A (Fig. 1B). We also noticed that acetylated p300 (ac-p300) remained suppressed in CoCl_2 plus CTK7A-treated cells as compared to the other three treatment groups. p300 expression was not altered by CTK7A treatment. Twist1 and N-cadherin expression in CTK7A-treated and untreated CoCl_2 -exposed AGS cells were further assessed by confocal microscopy ($n = 3$) (Fig. S1B). Confocal images complemented our findings shown in Fig. 1B. As protein expression varies from cell to cell, we tested Hif1 α , N-cadherin and Twist1 expression in CoCl_2 and CTK7A-treated MKN45 and Kato III cells. Data ($n = 3$) confirmed that as in AGS cells, CoCl_2 -induced expression of Hif1 α , N-cadherin and Twist1 in MKN45 and Kato III cells was significantly inhibited

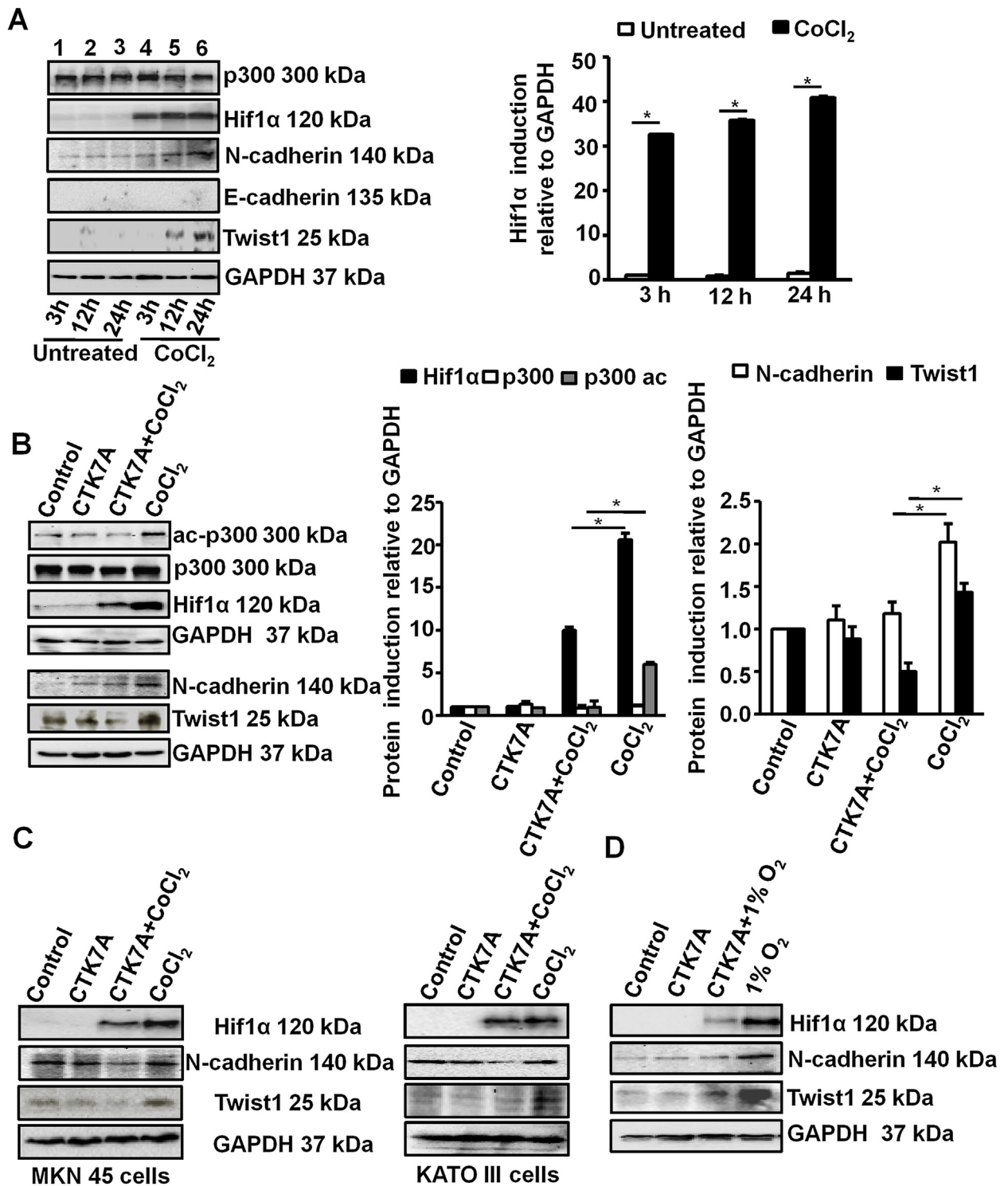


Fig. 1. HAT inhibition downregulated CoCl_2 and 1% O_2 -induced expression of metastatic markers in GCCs. (A) Expression of various metastatic factors was assessed at 3 h, 12 h, 24 h after treatment with 200 μM of CoCl_2 by western blotting ($n=3$). GAPDH was used as a loading control. Graphical presentation of western blot data clearly showed significant induction of Hif1 α from 3 h to 24 h of CoCl_2 treatment (mean \pm SEM, $n=3$, $*P<0.05$). (B) Western blot analysis ($n=3$) of whole cell lysates from AGS cells after treatment with 200 μM of CoCl_2 and/or 100 μM of CTK7A for 24 h. Bar diagrams represent status of EMT markers (mean \pm SEM). $*P<0.05$ (C) Western blot analysis ($n=3$) indicated downregulation of metastatic markers N-cadherin, Twist1, Hif1 α in metastatic gastric cancer cell lines KATO III and MKN 45 after CoCl_2 and CTK7A treatment. (D) Western blot analysis ($n=3$) of whole cell lysates from AGS cells after a hypoxia (1% O_2) exposure alone or with CTK7A. GAPDH was used as a loading control.

ited by CTK7A treatment (Figs. 1C and S2A). To study the effect of CTK7A in hypoxic environment, GCCs were exposed to normoxia (21% O_2) and hypoxia (1% O_2) for 24 h in the presence or absence of CTK7A. Whole cell lysates were immunoblotted ($n=3$) to detect the expression of EMT markers. CTK7A showed the same effect on

Hif1 α , N-cadherin and Twist1 expression in 1% O_2 -treated cells as it was found in CoCl_2 -treated cells (Figs. 1D and S2B). Therefore, majority of our experiments were performed using CoCl_2 unless we stated specifically about treating cells with 1% O_2 .

3.2. CTK7A decreases migration and invasion properties in CoCl₂ as well as 1% O₂-treated GCCs

Hypoxia plays a positive role in gastric cancer invasion and migration (Xing et al., 2011; Zhong et al., 1999). In order to assess the effect of HAT inhibition on migrating ability of hypoxic GCCs, we performed transwell migration assay and wound healing assay. Cells were seeded in inserts for transwell migration assay and were treated with CTK7A and CoCl₂ or 1% O₂ for 24 h. Migrated cells were stained with hematoxylin and studied under a microscope. A significant reduction in hypoxia-induced migration was observed upon CTK7A treatment (Fig. 2A and B) (n = 4, *P < 0.05). For further validation of our data, wound healing assay was performed. Confluent layers of AGS cells were wounded and exposed to CTK7A and CoCl₂. After 24 h, we found that control and only CTK7A-treated cells were comparable to CoCl₂ and CTK7A-treated cells with respect to their poor wound-healing ability but CoCl₂-treated cells had significantly high (n = 4, *P < 0.05) wound-healing ability than other groups (Fig. S3A). Invasiveness of GCCs was measured by matrigel invasion assay which showed significant (n = 4, *P < 0.05) reduction of invasive property in hypoxia plus CTK7A-treated GCCs as compared to only hypoxia exposed cells (Fig. 2C and D). The change in clonogenic potential of CoCl₂-treated AGS cells after CTK7A treatment was examined by soft agar assay (n = 3). We found that the number of foci was significantly (*P < 0.05, **P < 0.01, ***P < 0.001) increased by CoCl₂ exposure as compared to control cells, CTK7A plus CoCl₂-exposed cells showed significantly less foci formation than only CoCl₂-treated cells (Fig. S3B).

3.3. Inhibition of HAT activity induces Noxa in hypoxic GCCs in a Hif1 α -independent manner

Hif1 α depletion in gastric cancer cell line induces apoptosis under hypoxia (Tanaka et al., 2015). Noxa is a mediator of apoptosis in hypoxic cells and is induced by Hif1 α (Kim et al., 2004). In an attempt to assess Noxa expression pattern in hypoxic cells, AGS cells were treated with 200 μ M CoCl₂ for 3 h, 12 h and 24 h. Western blot data (n = 3) revealed a time-dependent enhancement in Noxa expression in CoCl₂-treated cells (*P < 0.05) (Fig. 3A). We next assessed Noxa expression in control and CoCl₂-treated AGS cells with or without CTK7A treatment by performing western blotting (n = 3) of whole cell lysates. Although CTK7A and CoCl₂ independently induced Noxa expression, CTK7A treatment resulted in a far higher (*P < 0.05) Noxa expression in CoCl₂-treated cells than in untreated cells (Fig. 3B). Treatment of normal immortalized HFE-145 cells with CTK7A showed a much lower magnitude of Noxa induction in CTK7A plus CoCl₂-treated cells than their AGS counterparts (Fig. 3C). MKN45 and KATO III cells, two other GCCs with metastatic properties, were also tested for their Noxa expression pattern. Noxa expression in these cells showed the same trend as in AGS cells (n = 3, *P < 0.05) (Fig. 3D). In order to assess Noxa expression by hypoxia and CTK7A, AGS cells were exposed to normoxia and hypoxia (1% O₂) in the presence or absence of CTK7A. Noxa expression was significantly high in CTK7A and 1% O₂ co-treated cells as compared to only 1% O₂-treated cells (Fig. 3E). Noxa expression is known to be induced by the transcription factor Hif1. Our data always showed significantly high Hif1 α expression in only CoCl₂ (or 1% O₂)-exposed GCCs as compared to CoCl₂ (or 1% O₂) and CTK7A-treated cells (Fig. 1B, C, E and F). Noxa expression was always high in CoCl₂ (or 1% O₂) and CTK7A-treated GCCs as compared to only CoCl₂ (or 1% O₂)-treated hypoxic GCCs (Fig. 3C–F). To find out the role of Hif1 α on Noxa expression in the presence of CTK7A, AGS cells were stably transfected with Hif1 α shRNA (Rath et al., 2015). The knockdown of Hif1 α significantly suppressed CoCl₂-mediated Hif1 α protein expression than empty vector and scrambled shRNA-expressing cells but did not change the pattern of

CTK7A-induced Noxa expression in CoCl₂-treated AGS cells. These data confirmed that Noxa regulation in hypoxic CTK7A-treated GCCs was not dependent on Hif1 α (Fig. 3F).

3.4. CTK7A induces mitochondrial translocation of Noxa and intrinsic apoptosis events in hypoxic GCCs

Since mitochondrial translocation of Noxa is required for its apoptotic activity (Lowman et al., 2010; Rath et al., 2015), we examined mitochondrial Noxa status after CTK7A treatment. Western blotting (n = 3) of mitochondrial and cytoplasmic fractions of AGS cells showed significantly higher (*P < 0.05) mitochondrial expression and localization of Noxa in CTK7A plus CoCl₂-treated cells as compared to control, only CTK7A-treated or only CoCl₂-treated cells (Fig. 4A). Confocal microscopy (n = 4) of the same set of cells (Fig. 4B) corroborated western blot results. As cytochrome c (Cyt c) release is the hallmark of the intrinsic apoptotic pathway, we examined mitochondrial Cyt c status before and after CTK7A and CoCl₂ treatment. For this, AGS cells stably expressing pDsRed2 were treated with CTK7A and CoCl₂ or left untreated. Results (n = 4) clearly indicated that mitochondrial retention of Cyt c was drastically reduced in CTK7A plus CoCl₂-treated cells (indicating maximal Cyt c release into the cytosol) while control cells, CTK7A-treated and CoCl₂-treated cells were able to retain mostly all their Cyt c in the mitochondria (Fig. 4C). Colocalization analysis of Noxa-pDsRed2 and Cyt c-pDsRed2 were performed and the data (Figs. S4A and S4B, respectively) showed significantly high Noxa but significantly less Cyt c in the CTK7A + CoCl₂-treated mitochondria as compared to the other three treatment groups (n = 4, *P < 0.05). These data clearly showed that CTK7A + CoCl₂ treated cells were undergoing maximal apoptotic stress. During intrinsic apoptosis, mitochondria undergo fragmentation (appears spheroidal/punctated) before releasing Cyt c into the cytosol. Confocal microscopy was performed to find out whether any mitochondrial stress was induced by CTK7A treatment. pDsRed2 stably-expressing AGS cells were treated with CTK7A in the presence or absence of CoCl₂. The tubular network of healthy mitochondria observed in control and CoCl₂-treated cells was found to be damaged in cells treated with CTK7A. However, mitochondria appeared significantly (n = 4, *P < 0.05, **P < 0.001) smaller, disintegrated and had increased roundness and circularity in CTK7A plus CoCl₂-treated cells when compared with other treatment groups (Fig. S5A and S5B).

Next, we sought to examine the expression of caspase 9, a key factor representing the intrinsic apoptotic pathway and the downstream effector caspase 3 in relation to Noxa expression. Western blotting (n = 3) of total cell lysates showed that CoCl₂ or 1% O₂ plus CTK7A-treated cells had maximal expression of cleaved caspase 9 and cleaved caspase 3 (17, 19 kDa) indicating that these cells were undergoing apoptotic cell death to the greatest extent (Fig. 4D). Graphical representation of Noxa and cleaved caspase 3 (the catalytically active 17 kDa form) identified significantly high expression of these two factors in CoCl₂ or 1% O₂ plus CTK7A-treated cells as compared to the other treatment groups (n = 3, *P < 0.05). The degree of apoptosis induction in CTK7A plus CoCl₂-treated AGS cells was next determined. To detect apoptotic cells, control, CoCl₂-treated, CTK7A alone and CTK7A plus CoCl₂-treated AGS cells were stained with Annexin V-PE and necrotic population was determined by 7-AAD staining (n = 4). Flow cytometric analysis of the lower-right quadrant showed that CTK7A plus CoCl₂-treated cells underwent significantly higher cell death (*P < 0.05) compared to the control, CTK7A-treated and only CoCl₂-treated cells (Fig. 4E). These data altogether confirmed that CTK7A was a potent inducer of apoptosis selectively in CoCl₂ and CTK7A-treated GCCs.

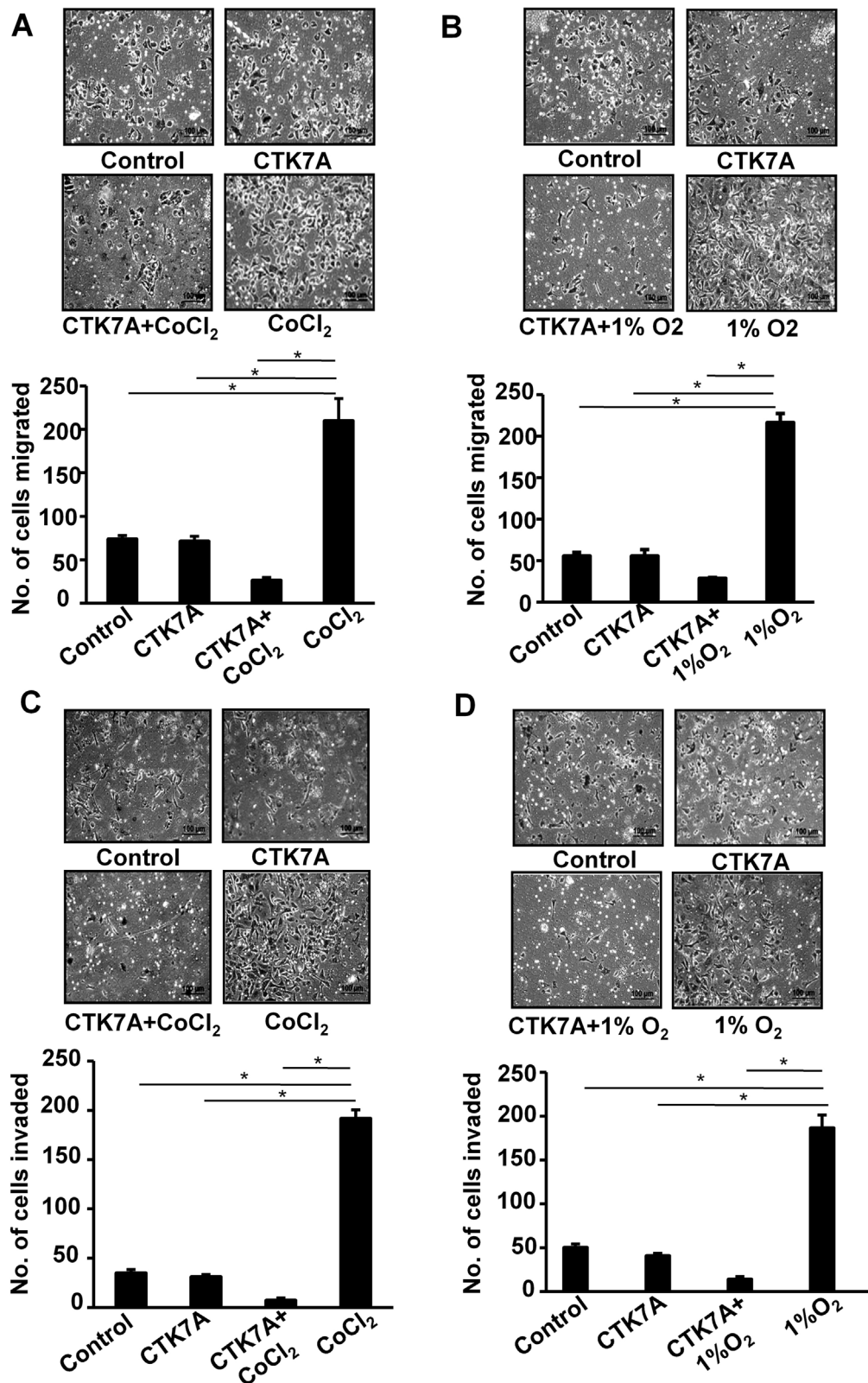


Fig. 2. CTK7A reduced metastatic properties in CoCl₂-exposed and 1% O₂-treated GCCs. (A) AGS cells were suspended in serum-free media and were seeded onto upper chambers of 24 well inserts while lower chambers had 10% FBS-enriched media. After treatment, migrated cells were stained with haematoxylin and counted using an inverted microscope. Scale=50 μ m. Bars represent count of cells migrated from three independent experiments (n=4, mean \pm SEM). **P*<0.05. (B) AGS cells were treated with 1% O₂ alone or in combination with CTK7A (100 μ M) or left untreated for 24 h and migration ability of these cells was assessed by counting the number of migrated cells (n=4, mean \pm SEM). **P*<0.05. Photographs were taken using an inverted microscope equipped with camera (Primo Vert Carl Zeiss, Germany). Scale bar 200 μ m. (C) Invasiveness of GCCs was studied by using matrigel-precoated Transwell after treatment with CoCl₂ (200 μ M) alone or in combination with CTK7A (100 μ M) for 24 h. Number of invading cells were stained with haematoxylin and counted (n=4, mean \pm SEM), **P*<0.05) by using an inverted microscope. (D) Invasiveness of GCCs was studied by using matrigel-precoated Transwell after treatment with 1% O₂ alone or in combination with CTK7A (100 μ M) for 24 h. Invading cells were stained with haematoxylin and counted (mean \pm SEM, n=4, **P*<0.05) by using an inverted microscope.

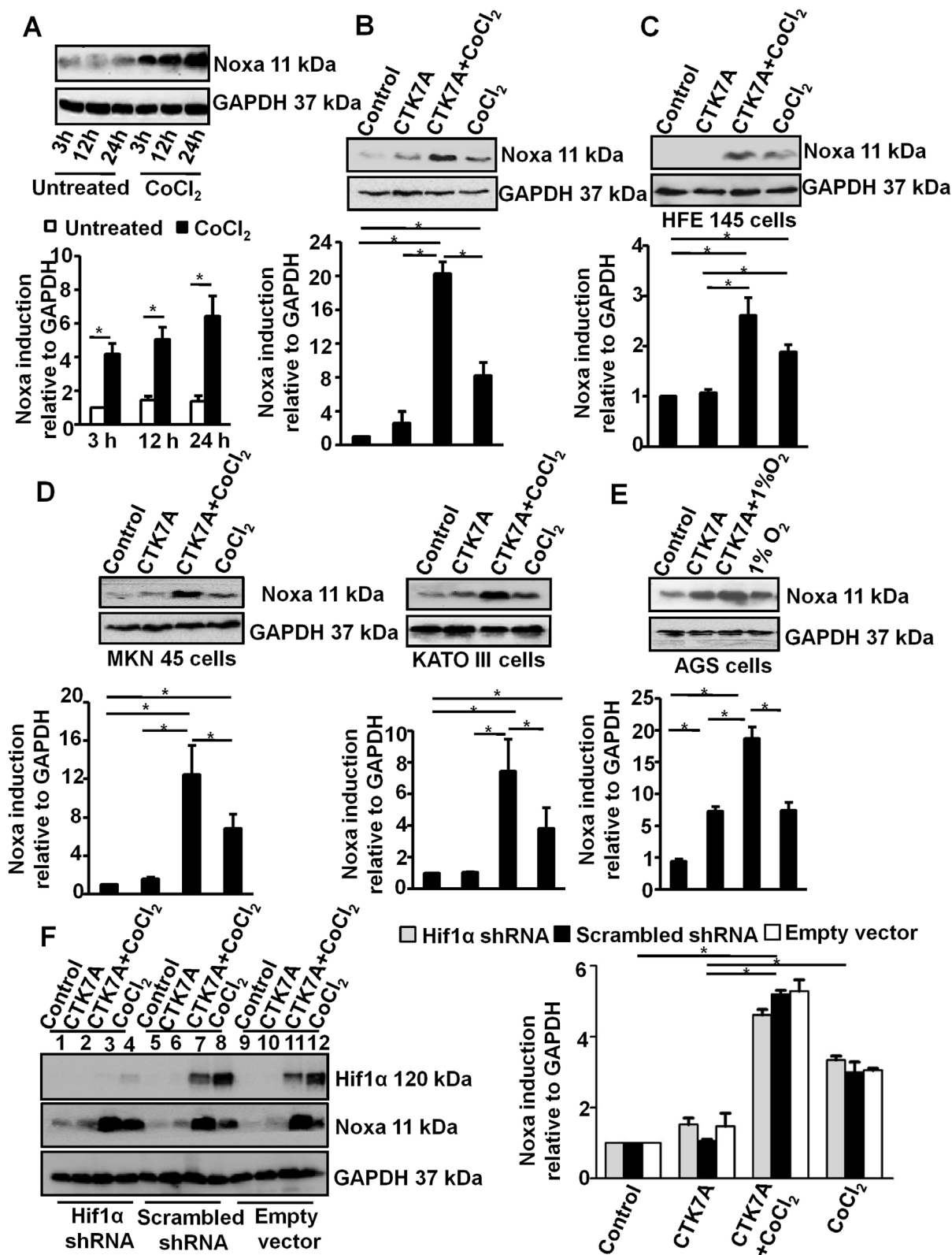


Fig. 3. Inhibition of HAT induces Noxa expression in hypoxia-treated GCCs. (A) A representative western blot of whole cell lysates ($n=3$) prepared from CoCl₂-treated (3 h, 12 h, 24 h with 200 μ M of CoCl₂) AGS cells showed time-dependent induced expression of Noxa. GAPDH was used as a loading control. Graphical presentation of western blot data clearly indicated increment in Noxa expression with time (mean \pm SEM, $n=3$), $*P<0.05$. (B) Expression of Noxa was analyzed by immunoblotting of cell lysates prepared from AGS cells treated with CoCl₂ (200 μ M) and/or CTK7A (100 μ M) for 24 h. GAPDH was used as a loading control. Graphical presentation of western blot data confirmed significant increase in Noxa expression in CTK7A+CoCl₂-treated groups as compared to other groups (mean \pm SEM, $n=3$), $*P<0.05$. (C) Immunoblot analysis of whole cell lysates prepared from immortalized human GCC HFE145 treated with CoCl₂ (200 μ M) alone or in combination with CTK7A (100 μ M) showed induced expression of Noxa in CTK7A+CoCl₂ combination treatment. GAPDH was used as a loading control. Bars depict Noxa expression normalized to GAPDH (mean \pm SEM, $n=3$), $*P<0.05$. (D) Noxa expression in CoCl₂ (200 μ M) and CTK7A (100 μ M)-treated KATO III and MKN 45 cells. Analysis of data by Student's *t*-test clearly showed a significant increase in Noxa expression in CTK7A+CoCl₂-treated cells as compared to other groups. Bars represent mean \pm SEM,

3.5. CTK7A-mediated Noxa induction in CoCl₂-treated GCCs is mediated by H₂O₂ generation

Earlier reports correlated HAT activity with ROS generation (Kang et al., 2005). Curcumin, at low concentration, was shown to exert anticancer activity in leukemia by decreasing ROS generation whereas at high dose it killed cells through more ROS production (Chen et al., 2005). As CTK7A was derived from curcumin, we sought to assess the effect of CTK7A on ROS generation. To find out the involvement of superoxide (O₂^{•-}) in Noxa induction, we performed western blotting (n = 3) using AGS cell lysates prepared from control cells, only CTK7A-treated cells, CoCl₂-treated cells or CTK7A + CoCl₂-treated cells in the presence or absence of 200 units/ml superoxide-dismutase (SOD). (-)SOD group and (+)SOD group showed no difference in Hif1α and Noxa expression which indicated that neither CTK7A nor CoCl₂ alone or in combination had any role on O₂^{•-} generation (Fig. 5A). In contrast, a 4 h pretreatment of cells with 350 units/ml of catalase, a H₂O₂ scavenger, markedly suppressed Noxa expression induced by CTK7A + CoCl₂ treatment (*P < 0.05) (Fig. 5B) while catalase had no suppressive effect on Hif1α expression (n = 3). Chloromethyl-H₂DCFDA (CM-H₂DCFDA) was used at a dose of 1 μM for 10 min to visualize ROS generation in GCCs after CTK7A and CoCl₂ treatment. Fluorescence microscopy revealed that although CTK7A or CoCl₂ slightly induced ROS generation compared to control (Fig. 5C), CTK7A + CoCl₂ treatment induced maximal ROS generation. Pretreatment with catalase notably scavenged that effect. These results suggested that H₂O₂, but not O₂^{•-}, was the main mediator in CTK7A-induced Noxa expression in CoCl₂-treated AGS cells.

3.6. CTK7A-induced H₂O₂ generation in CoCl₂-treated GCCs causes p38 MAPK-mediated Noxa upregulation

Our data established that CTK7A in CoCl₂ or 1% O₂-exposed cells caused Noxa-mediated cell death. It is known that ROS can mediate Noxa induction (Fischer et al., 2005) and MAPK activation (Bae et al., 2006; Chung et al., 2013; Liang et al., 2014). In order to find out the effect of H₂O₂ on MAPK activation, we treated AGS cells with catalase prior to treatment with CoCl₂ and CTK7A. Whole cell lysates were prepared and western blot data (n = 3) revealed that CoCl₂ plus CTK7A-treatment induced maximal JNK, p38 MAPK as well as ERK1/2 phosphorylation compared to control, CTK7A alone or CoCl₂-alone (Fig. 6A). Catalase had no suppressive effect on ERK phosphorylation; JNK phosphorylation was partially suppressed and p38 MAPK phosphorylation was noticeably decreased in CTK7A plus CoCl₂-treated cells as compared to other treatment groups. This data provided an important direction that p38 MAPK and JNK were mediating Noxa induction in CTK7A and CoCl₂-cotreated cells. To find out the role of JNK and p38 MAPK activation on CTK7A-mediated Noxa induction in CoCl₂-treated cells, AGS cells were pretreated with SP600125 and SB203580, respectively. Data (n = 3) revealed that JNK inhibition had no effect on Noxa (Fig. 6B) but p38 MAPK inhibition drastically reduced Noxa and the downstream effector molecule, cleaved caspase 3 in CTK7A and CoCl₂-treated cells. (Fig. 6C). Altogether, we established that HAT inhibition in CoCl₂-treated cells induced Noxa expression which was triggered by ROS-mediated p38 MAPK activation.

4. Discussion

Hypoxic regions remain scattered inside solid tumors as a resultant effect of heterogeneous angiogenesis and poor blood supply to certain parts of the tumor. Cancer cells thrive and progress towards malignancy in hypoxic environments (Vaupe, 2004). Hypoxic cancer cells metastasize very aggressively and become treatment-resistant (Kitajima and Miyazaki, 2013; Lin et al., 2008). The novelty of this work lies in the finding that CTK7A, a hydrazinocurcumin compound, selectively kills hypoxia-exposed and CoCl₂-treated GCCs but spares non-hypoxic and CoCl₂-untreated cells from apoptotic death to a significant extent. Cancer cells generally are under oxidative stress and further increment in ROS by therapeutic attempts make cancer cells susceptible to ROS-induced cell-damages. Gastric cancer tissues express significant amount of ROS (Bhattacharyya et al., 2014) and therefore, therapeutic interventions of gastric cancer also exploits the ROS-generating machinery (Chen et al., 2008; Matsunaga et al., 2010). This study confirms that CTK7A treatment produces substantially higher amount of ROS in hypoxic cells than in untreated GCCs. Our finding is supported by few other reports which state induced ROS generation in hypoxic cells (Clanton, 2007; Sabharwal and Schumacker, 2014). As CoCl₂ also induces ROS generation (Guan et al., 2015) and acts as a chemical hypoxia-inducer (Rath et al., 2016), its role in ROS generation in p300 HAT inhibitor treated cells might have a good therapeutic advantage. Enhanced ROS in CoCl₂ plus CTK7A-treated cells induce p38 MAPK-mediated Noxa expression. Noxa translocation to mitochondria significantly increases mitochondrial apoptosis in CoCl₂ and CTK7A-cotreated cells. Further, we show that Noxa induction in CoCl₂ and CTK7A-co-treated GCCs is dependent on ROS generation. Our analysis also demonstrates that the fold change in Noxa enhancement in hypoxic CTK7A-treated GCCs over the CTK7A-untreated hypoxic cells is much higher than the fold change noticed in their counterparts in non-cancer GCCs. This study further confirms that Noxa induction after CTK7A treatment in hypoxic AGS cells is no longer dependent on Hif1α. This enigma is solved by the finding that Noxa is only slightly induced in CoCl₂-treated cells but the upregulation of Noxa following CTK7A treatment in those cells is mostly induced by H₂O₂. This is in keeping with earlier studies which reported about enhanced apoptosis in ROS-generating cells. Cisplatin-mediated ROS induction has been associated with JNK activation and apoptosis of various types of cells including GCCs (Bae et al., 2006). Curcumin-mediated ROS induction reportedly induced JNK signaling and caused apoptosis of human GCCs (Liang et al., 2014). Similar reports exist for ROS-mediated p38 MAPK activation (Chung et al., 2013). The importance of histone acetylation in cancer progression and therapy has been well documented. Suppression of HAT activity of p300 by CTK7A was earlier shown to substantially reduce the xenografted oral cancer progression in mice (Arif et al., 2010). Thus, our finding of ROS and p38 MAPK-mediated enhancement of Noxa expression mostly in HAT activity-suppressed CoCl₂-treated cells adds a new layer of complexity to the existing understanding on the altered nature of hypoxic cells and offers hope that even hypoxic cells that show metastatic properties can be killed by CTK7A. Although our study provides important information that ROS and p38 MAPK control CTK7A treatment-induced apoptosis of CoCl₂-treated cells, the complete signaling mechanism of ROS upregulation by HAT inhibition remains elusive.

n = 3, *P < 0.05. (E) Immunoblot analysis of whole cell lysates prepared from AGS cells treated with hypoxia (1% O₂) alone or in combination with CTK7A (100 μM) showed markedly induced expression of Noxa in CTK7A + hypoxia group. GAPDH was used as a loading control. (F) Immunoblot analysis (n = 3) showed equal expression of Noxa in the empty vector, scrambled negative control shRNA and Hif1α-shRNA stably-expressing AGS cells treated with 200 μM of CoCl₂ and/or CTK7A (100 μM) for 24 h. GAPDH was used as loading control. Data were further analyzed by 2-way ANOVA with Bonferroni *post hoc* test. Error bars, mean ± SEM. *P < 0.05.

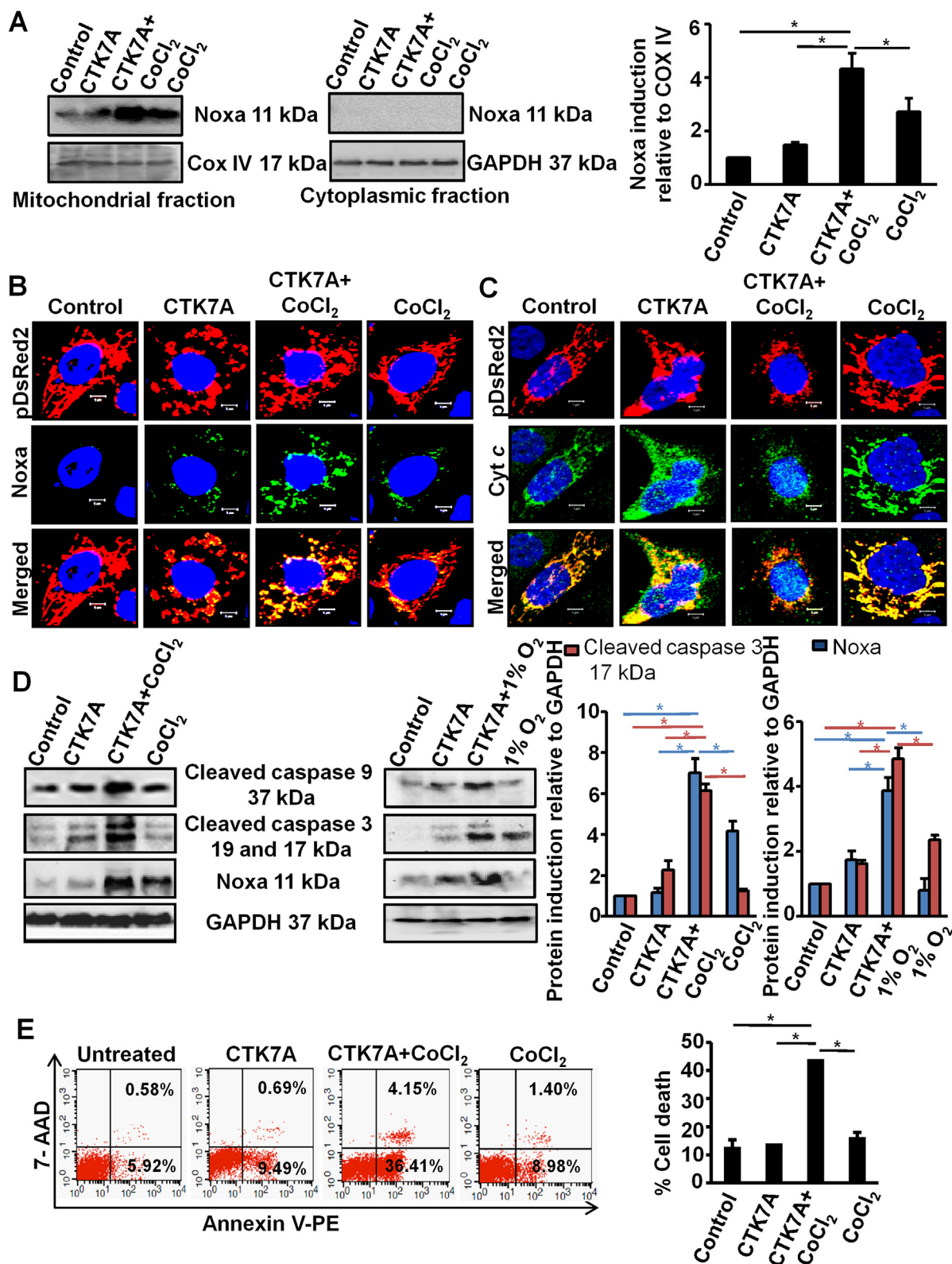


Fig. 4. CTK7A induced intrinsic apoptosis by mitochondrial translocation of Noxa in CoCl₂-treated GCCs. (A) Western blot (n = 3) showing status of Noxa in the mitochondria and cytosolic fraction of AGS cells treated with CoCl₂, 200 μM, or in combination with CTK7A (100 μM) for 24 h. COX IV and GAPDH were used as loading controls for the mitochondrial and cytosolic fractions, respectively. Bars depict Noxa expression normalized to COX IV in the mitochondrial fraction (mean ± SEM, n = 3), *P < 0.05. (B) Confocal microscopy of AGS cells (n = 3) treated with CoCl₂ (200 μM) and/or CTK7A (100 μM) for 24 h showed high Noxa translocation to mitochondria in CTK7A + CoCl₂-treated cells. Nuclei were stained with DAPI. Scale bar 10 μm. (C) Confocal microscopic image showing cytochrome c release from mitochondria in the above mentioned experimental groups. DAPI staining was for nucleus. Scale bar 10 μm. (D) Immunoblotting (n = 3) of whole cell lysates prepared from AGS cells after treatment with CoCl₂ (200 μM) or hypoxia (1% O₂) alone or in combination with CTK7A (100 μM) for 24 h indicated status of Noxa, cleaved caspase 3 and cleaved caspase 9. Error bars, mean ± SEM, n = 3, *P < 0.05. (E) AGS cells were treated with 200 μM CoCl₂ alone or in combination with CTK7A (100 μM) or left untreated. Cells were harvested and stained with Annexin V PE/7-AAD dyes. A representative dot plot (n = 4) indicated striking increase in apoptosis in CTK7A + CoCl₂-treated GCCs as compared to other treatment groups. % cell death were compared between various treatment groups (mean ± SEM, n = 4), *P < 0.05.

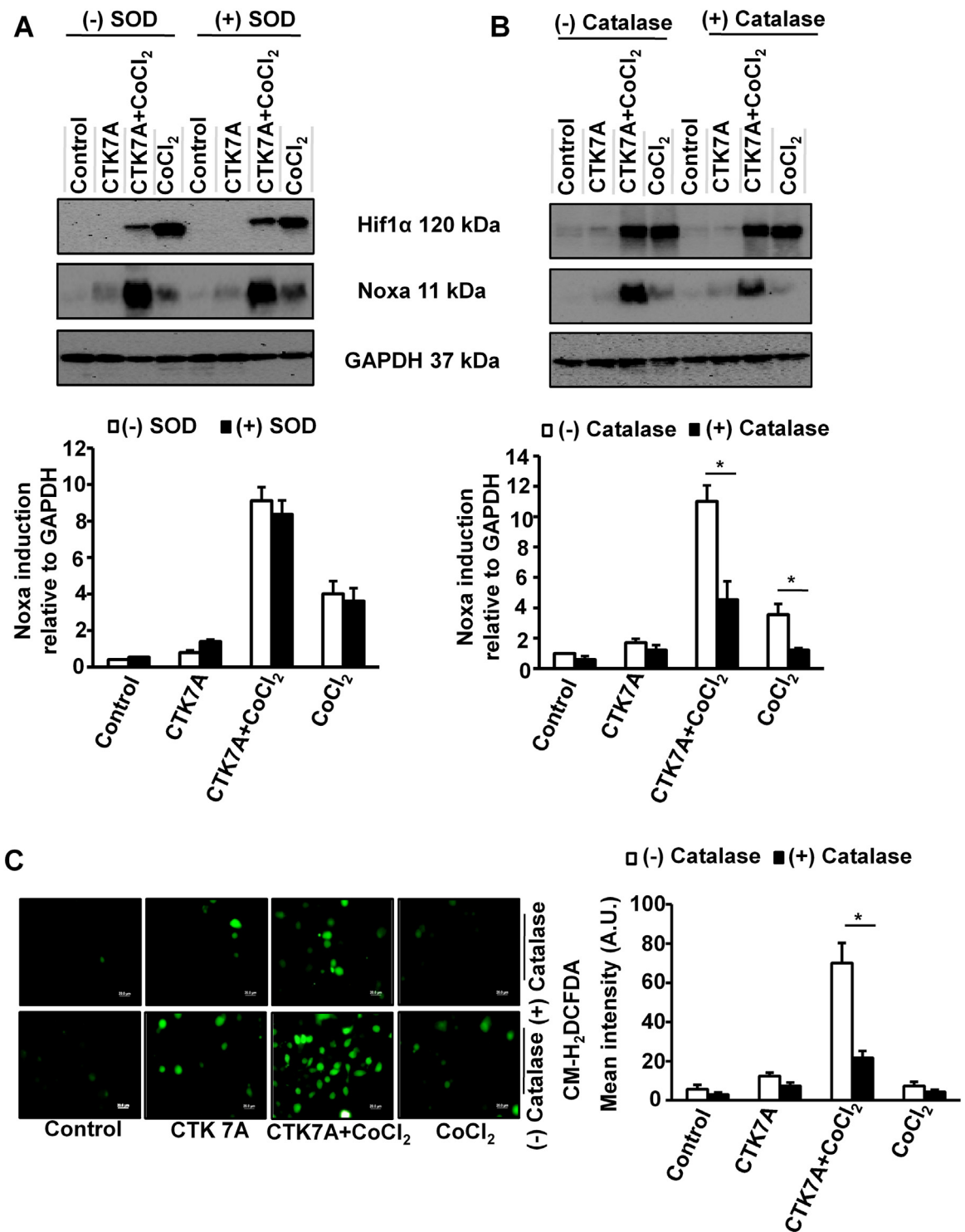


Fig. 5. CTK7A-mediated increase in Noxa expression was regulated by ROS generation in CoCl₂-treated GCCs. (A) Immunoblot analysis (n=3) of AGS cells after treatment with SOD for 4 h followed by treatment with CoCl₂ (200 μM) and/or CTK7A (100 μM) for detection of Noxa and Hif1α expression. GAPDH was used as a loading control. Bars depict Noxa expression normalized to GAPDH (mean ± SEM, n=3), *P<0.05. (B) Western blotting (n=3) of cell lysates after treatment with catalase (350 units/ml) for 4 h followed by above mentioned combination of CTK7A and CoCl₂ for detection of Noxa and Hif1α expression. Graphical presentation of Noxa expression was shown by bar diagrams (mean ± SEM, n=3), *P<0.05. (C) AGS cells were treated with CoCl₂ (200 μM) alone or in combination with CTK7A (100 μM) for 24 h with or without catalase pre-treatment (350 units/ml, 4 h). Cells were then incubated with fluorescence probe CM-H₂DCFDA at a final concentration of 1 μM for 10 min followed by fixation with paraformaldehyde at 37 °C for 20 min. ROS generation was measured under a fluorescence microscope (Olympus, Japan). Scale bar, 20 μm. Bars depict mean fluorescence intensity (mean ± SEM, n=3), *P<0.05.

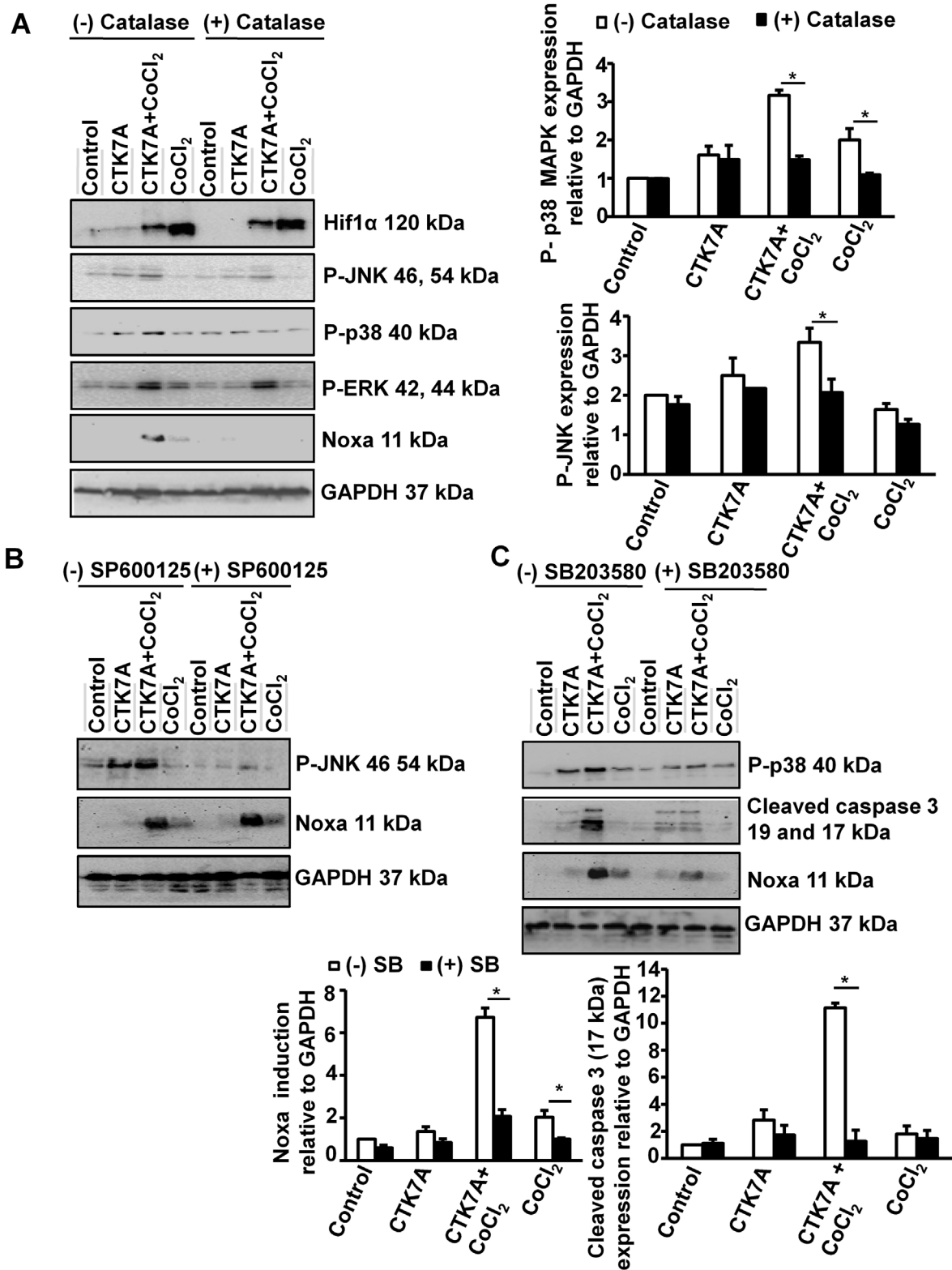


Fig. 6. CTK7A induced p38 MAPK phosphorylation and Noxa upregulation via generation of H_2O_2 in $CoCl_2$ -treated GCCs. (A) Western blot analysis ($n=3$) of whole cell lysates from AGS cells pre-treated with catalase (350 units/ml) for 4 h followed by treatment with 200 μM of $CoCl_2$ alone or in combination with CTK7A for 24 h showed effect of ROS on Noxa, Hif1 α and all MAPKs. Bar diagrams represent status of p38 MAPK and JNK (mean \pm SEM, $n=3$) * $P<0.05$. (B) Western blotting ($n=3$) showed the status of P-JNK and Noxa after pre-treatment with 25 μM JNK inhibitor II (SP600125) for 1 h followed by $CoCl_2$ (200 μM) and/or CTK7A (100 μM) treatment for 24 h. GAPDH was used as a loading control. (C) Immunoblotting ($n=3$) of AGS cell lysates showed the effect of p38 MAPK inhibition on cleaved caspase 3 and Noxa after pre-treatment with 25 μM p38 MAPK inhibitor (SB203580) for 1 h followed by $CoCl_2$ (200 μM) treatment and/or CTK7A (100 μM) for 24 h. Graphs depict expression pattern of Noxa and cleaved caspase 3 normalized to GAPDH (mean \pm SEM, $n=3$), * $P<0.05$.

Altogether, our study elaborates the mechanism of p300 hypoacetylation-mediated antitumor activity in CoCl₂-treated and hypoxic GCCs. The effectiveness of CTK7A in enhancing Noxa-mediated apoptosis via ROS generation and p38 MAPK activation in hypoxic and invasive GCCs supports the possibility that CTK7A may be further exploited for therapeutic purposes. This has further implications since CTK7A shows the promise to avoid widespread toxicity and serious side effects that are commonly associated with cancer therapy. Future studies are required to confirm the effect of CTK7A on other types of cancer.

Competing interests

The authors declare that they have no competing interests.

Acknowledgements

This work was supported by Fast Track Grant SR/FT/LS-38/2010, Science and Engineering Research Board, Govt. of India, to AB; an Indian Council of Medical Research (ICMR) fellowship to SR; fellowships from Department of Atomic Energy (DAE), India, to LD, SBK and PD. The authors thank Mr. Alok Kumar Jena for his assistance in confocal microscopy.

Appendix A. Supplementary data

Supplementary data associated with this article can be found, in the online version, at <http://dx.doi.org/10.1016/j.biocel.2016.11.014>.

References

- Arif, M., Vedamurthy, B.M., Choudhari, R., Ostwal, Y.B., Mantelingu, K., Kodaganur, G.S., Kundu, T.K., 2010. Nitric oxide-mediated histone hyperacetylation in oral cancer: target for a water-soluble HAT inhibitor, CTK7A. *Chem. Biol.* 17 (8), 903–913.
- Bae, I.H., Kang, S.W., Yoon, S.H., Um, H.D., 2006. Cellular components involved in the cell death induced by cisplatin in the absence of p53 activation. *Oncol. Rep.* 15 (5), 1175–1180.
- Bae, S., Jeong, H.J., Cha, H.J., Kim, K., Choi, Y.M., An, I.S., Koh, H.J., Lim, D.J., Lee, S.J., An, S., 2012. The hypoxia-mimetic agent cobalt chloride induces cell cycle arrest and alters gene expression in U266 multiple myeloma cells. *Int. J. Mol. Med.* 30 (5), 1180–1186.
- Bhattacharyya, A., Chattopadhyay, R., Burnette, B.R., Cross, J.V., Mitra, S., Ernst, P.B., Bhakat, K.K., Crowe, S.E., 2009. Acetylation of apurinic/apyrimidinic endonuclease-1 regulates Helicobacter pylori-mediated gastric epithelial cell apoptosis. *Gastroenterology* 136 (7), 2258–2269.
- Bhattacharyya, A., Chattopadhyay, R., Mitra, S., Crowe, S.E., 2014. Oxidative stress: an essential factor in the pathogenesis of gastrointestinal mucosal diseases. *Physiol. Rev.* 94 (2), 329–354.
- Chan, H.M., La Thangue, N.B., 2001. p300/CBP proteins: HATs for transcriptional bridges and scaffolds. *J. Cell Sci.* 114 (Pt. 13), 2363–2373.
- Chen, J., Wanming, D., Zhang, D., Liu, Q., Kang, J., 2005. Water-soluble antioxidants improve the antioxidant and anticancer activity of low concentrations of curcumin in human leukemia cells. *Pharmazie* 60 (1), 57–61.
- Chen, W., Zhao, Z., Li, L., Wu, B., Chen, S.F., Zhou, H., Wang, Y., Li, Y.Q., 2008. Hispolon induces apoptosis in human gastric cancer cells through a ROS-mediated mitochondrial pathway. *Free Radic. Biol. Med.* 45 (1), 60–72.
- Chung, K.S., Han, G., Kim, B.K., Kim, H.M., Yang, J.S., Ahn, J., Lee, K., Song, K.B., Won, M., 2013. A novel antitumor piperazine alkyl compound causes apoptosis by inducing RhoB expression via ROS-mediated cAbl/p38 MAPK signaling. *Cancer Chemother. Pharmacol.* 72 (6), 1315–1324.
- Clanton, T.L., 2007. Hypoxia-induced reactive oxygen species formation in skeletal muscle. *J. Appl. Physiol.* (1985) 102 (6), 2379–2388.
- Clarke, A.S., Lowell, J.E., Jacobson, S.J., Pillus, L., 1999. Esa1p is an essential histone acetyltransferase required for cell cycle progression. *Mol. Cell. Biol.* 19 (4), 2515–2526.
- Cotter, T.G., 2009. Apoptosis and cancer: the genesis of a research field. *Nat. Rev. Cancer* 9 (7), 501–507.
- Fischer, S., Wiesnet, M., Renz, D., Schaper, W., 2005. H₂O₂ induces paracellular permeability of porcine brain-derived microvascular endothelial cells by activation of the p44/42 MAP kinase pathway. *Eur. J. Cell Biol.* 84 (7), 687–697.
- Gheldof, A., Berx, G., 2013. Cadherins and epithelial-to-mesenchymal transition. *Prog. Mol. Biol. Transl. Sci.* 116, 317–336.
- Gomez-Bougie, P., Menoret, E., Juin, P., Dousset, C., Pellat-Deceunynck, C., Amiot, M., 2011. Noxa controls Mule-dependent Mcl-1 ubiquitination through the regulation of the Mcl-1/USP9X interaction. *Biochem. Biophys. Res. Commun.* 413 (3), 460–464.
- Guan, D., Su, Y., Li, Y., Wu, C., Meng, Y., Peng, X., Cui, Y., 2015. Tetramethylpyrazine inhibits CoCl₂-induced neurotoxicity through enhancement of Nrf2/GCLC/GSH and suppression of HIF1alpha/NOX2/ROS pathways. *J. Neurochem.* 134 (3), 551–565.
- Huang, L.E., Gu, J., Schau, M., Bunn, H.F., 1998. Regulation of hypoxia-inducible factor 1alpha is mediated by an O₂-dependent degradation domain via the ubiquitin-proteasome pathway. *Proc. Natl. Acad. Sci. U. S. A.* 95 (14), 7987–7992.
- Jung, D.W., Kim, W.H., Seo, S., Oh, E., Yim, S.H., Ha, H.H., Chang, Y.T., Williams, D.R., 2014. Chemical targeting of GAPDH moonlighting function in cancer cells reveals its role in tubulin regulation. *Chem. Biol.* 21 (11), 1533–1545.
- Kang, J., Chen, J., Shi, Y., Jia, J., Zhang, Y., 2005. Curcumin-induced histone hypoacetylation: the role of reactive oxygen species. *Biochem. Pharmacol.* 69 (8), 1205–1213.
- Karakashev, S.V., Reginato, M.J., 2015. Progress toward overcoming hypoxia-induced resistance to solid tumor therapy. *Cancer Manage. Res.* 7, 253–264.
- Kawamura, T., Hasegawa, K., Morimoto, T., Iwai-Kanai, E., Miyamoto, S., Kawase, Y., Ono, K., Wada, H., Akao, M., Kita, T., 2004. Expression of p300 protects cardiac myocytes from apoptosis in vivo. *Biochem. Biophys. Res. Commun.* 315 (3), 733–738.
- Kim, J.Y., Ahn, H.J., Ryu, J.H., Suk, K., Park, J.H., 2004. BH3-only protein Noxa is a mediator of hypoxic cell death induced by hypoxia-inducible factor 1alpha. *J. Exp. Med.* 199 (1), 113–124.
- Kitajima, Y., Miyazaki, K., 2013. The critical impact of HIF-1a on gastric cancer biology. *Cancers (Basel)* 5 (1), 15–26.
- Lee, S.G., Lee, H., Rho, H.M., 2001. Transcriptional repression of the human p53 gene by cobalt chloride mimicking hypoxia. *FEBS Lett.* 507 (3), 259–263.
- Liang, T., Zhang, X., Xue, W., Zhao, S., Pei, J., 2014. Curcumin induced human gastric cancer GGC-823 cells apoptosis by ROS-mediated ASK1-MKK4-JNK stress signaling pathway. *Int. J. Mol. Sci.* 15 (9), 15754–15765.
- Lin, M.T., Kuo, I.H., Chang, C.C., Chu, C.Y., Chen, H.Y., Lin, B.R., Sureshbabu, M., Shih, H.J., Kuo, M.L., 2008. Involvement of hypoxia-inducing factor-1alpha-dependent plasminogen activator inhibitor-1 up-regulation in Cyr61/CCN1-induced gastric cancer cell invasion. *J. Biol. Chem.* 283 (23), 15807–15815.
- Liu, L., Ning, X., Sun, L., Zhang, H., Shi, Y., Guo, C., Han, S., Liu, J., Sun, S., Han, Z., Wu, K., Fan, D., 2008. Hypoxia-inducible factor-1 alpha contributes to hypoxia-induced chemoresistance in gastric cancer. *Cancer Sci.* 99 (1), 121–128.
- Lowman, X.H., McDonnell, M.A., Kosloske, A., Odumade, O.A., Jenness, C., Karim, C.B., Jemerson, R., Kelekar, A., 2010. The proapoptotic function of Noxa in human leukemia cells is regulated by the kinase Cdk5 and by glucose. *Mol. Cell* 40 (5), 823–833.
- Luo, H.Y., Wei, W., Shi, Y.X., Chen, X.Q., Li, Y.H., Wang, F., Qiu, M.Z., Li, F.H., Yan, S.L., Zeng, M.S., Huang, P., Xu, R.H., 2010. Cetuximab enhances the effect of oxaliplatin on hypoxic gastric cancer cell lines. *Oncol. Rep.* 23 (6), 1735–1745.
- Matsunaga, T., Tsuji, Y., Kaai, K., Kohno, S., Hirayama, R., Alpers, D.H., Komoda, T., Hara, A., 2010. Toxicity against gastric cancer cells by combined treatment with 5-fluorouracil and mitomycin c: implication in oxidative stress. *Cancer Chemother. Pharmacol.* 66 (3), 517–526.
- Oliveira, M.J., Costa, A.M., Costa, A.C., Ferreira, R.M., Sampaio, P., Machado, J.C., Seruca, R., Mareel, M., Figueiredo, C., 2009. CagA associates with c-Met, E-cadherin, and p120-catenin in a multiprotein complex that suppresses Helicobacter pylori-induced cell-invasive phenotype. *J. Infect. Dis.* 200 (5), 745–755.
- Piret, J.P., Mottet, D., Raes, M., Michiels, C., 2002. CoCl₂, a chemical inducer of hypoxia-inducible factor-1, and hypoxia reduce apoptotic cell death in hepatoma cell line HepG2. *Ann. N. Y. Acad. Sci.* 973, 443–447.
- Piret, J.P., Minet, E., Cosse, J.P., Ninane, N., Debacq, C., Raes, M., Michiels, C., 2005. Hypoxia-inducible factor-1-dependent overexpression of myeloid cell factor-1 protects hypoxic cells against tert-butyl hydroperoxide-induced apoptosis. *J. Biol. Chem.* 280 (10), 9336–9344.
- Rankin, E.B., Giaccia, A.J., 2008. The role of hypoxia-inducible factors in tumorigenesis. *Cell Death Differ.* 15 (4), 678–685.
- Rath, S., Das, L., Kokate, S.B., Pratheek, B.M., Chattopadhyay, S., Goswami, C., Chattopadhyay, R., Crowe, S.E., Bhattacharyya, A., 2015. Regulation of Noxa-mediated apoptosis in Helicobacter pylori-infected gastric epithelial cells. *FASEB J.* 29 (3), 796–806.
- Rath, S., Anand, A., Ghosh, N., Das, L., Kokate, S.B., Dixit, P., Majhi, S., Rout, N., Singh, S.P., Bhattacharyya, A., 2016. Cobalt chloride-mediated protein kinase Calpha (PKCalpha) phosphorylation induces hypoxia-inducible factor 1alpha (HIF1alpha) in the nucleus of gastric cancer cell. *Biochem. Biophys. Res. Commun.* 471 (1), 205–212.
- Rohwer, N., Cramer, T., 2010. HIFs as central regulators of gastric cancer pathogenesis. *Cancer Biol. Ther.* 10 (4), 383–385.
- Rohwer, N., Lobitz, S., Daskalow, K., Jons, T., Vieth, M., Schlag, P.M., Kimmner, W., Wiedenmann, B., Cramer, T., Hocker, M., 2009. HIF-1alpha determines the metastatic potential of gastric cancer cells. *Br. J. Cancer* 100 (5), 772–781.
- Sabharwal, S.S., Schumacker, P.T., 2014. Mitochondrial ROS in cancer: initiators, amplifiers or an Achilles' heel? *Nat. Rev. Cancer* 14 (11), 709–721.
- Said, H.M., Hagemann, C., Stojic, J., Schoemig, B., Vince, G.H., Flentje, M., Roosen, K., Vordermark, D., 2007. GAPDH is not regulated in human glioblastoma under hypoxic conditions. *BMC Mol. Biol.* 8, 55.

- Said, H.M., Polat, B., Hagemann, C., Anacker, J., Flentje, M., Vordermark, D., 2009. Absence of GAPDH regulation in tumor-cells of different origin under hypoxic conditions in vitro. *BMC Res. Notes* 2, 8.
- Santer, F.R., Hoschele, P.P., Oh, S.J., Erb, H.H., Bouchal, J., Cavarretta, I.T., Parson, W., Meyers, D.J., Cole, P.A., Culig, Z., 2011. Inhibition of the acetyltransferases p300 and CBP reveals a targetable function for p300 in the survival and invasion pathways of prostate cancer cell lines. *Mol. Cancer Ther.* 10 (9), 1644–1655.
- Sullivan, R., Graham, C.H., 2007. Hypoxia-driven selection of the metastatic phenotype. *Cancer Metastasis Rev.* 26 (2), 319–331.
- Tanaka, T., Kitajima, Y., Miyake, S., Yanagihara, K., Hara, H., Nishijima-Matsunobu, A., Baba, K., Shida, M., Wakiyama, K., Nakamura, J., Noshiro, H., 2015. The apoptotic effect of HIF-1 α inhibition combined with glucose plus insulin treatment on gastric cancer under hypoxic conditions. *PLoS One* 10 (9), e0137257.
- Torii, S., Goto, Y., Ishizawa, T., Hoshi, H., Goryo, K., Yasumoto, K., Fukumura, H., Sogawa, K., 2011. Pro-apoptotic activity of inhibitory PAS domain protein (IPAS), a negative regulator of HIF-1, through binding to pro-survival Bcl-2 family proteins. *Cell Death Differ.* 18 (11), 1711–1725.
- Urano, N., Fujiwara, Y., Doki, Y., Tsujie, M., Yamamoto, H., Miyata, H., Takiguchi, S., Yasuda, T., Yano, M., Monden, M., 2006. Overexpression of hypoxia-inducible factor-1 α in gastric adenocarcinoma. *Gastric Cancer* 9 (1), 44–49.
- Vaupel, P., Mayer, A., 2007. Hypoxia in cancer: significance and impact on clinical outcome. *Cancer Metastasis Rev.* 26 (2), 225–239.
- Vaupel, P., 2004. The role of hypoxia-induced factors in tumor progression. *Oncologist* 9 (Suppl. 5), 10–17.
- Wang, G., Hazra, T.K., Mitra, S., Lee, H.M., Englander, E.W., 2000. Mitochondrial DNA damage and a hypoxic response are induced by CoCl₂ in rat neuronal PC12 cells. *Nucleic Acids Res.* 28 (10), 2135–2140.
- Wu, D., Yotnda, P., 2011. Induction and testing of hypoxia in cell culture. *J. Vis. Exp.*
- Xiao, L., Kovac, S., Chang, M., Shulkes, A., Baldwin, G.S., Patel, O., 2012. Induction of gastrin expression in gastrointestinal cells by hypoxia or cobalt is independent of hypoxia-inducible factor (HIF). *Endocrinology* 153 (7), 3006–3016.
- Xing, F., Okuda, H., Watabe, M., Kobayashi, A., Pai, S.K., Liu, W., Pandey, P.R., Fukuda, K., Hirota, S., Sugai, T., Wakabayashi, G., Koeda, K., Kashiwaba, M., Suzuki, K., Chiba, T., Endo, M., Mo, Y.Y., Watabe, K., 2011. Hypoxia-induced Jagged2 promotes breast cancer metastasis and self-renewal of cancer stem-like cells. *Oncogene* 30 (39), 4075–4086.
- Yang, W.Y., Gu, J.L., Zhen, T.M., 2014. Recent advances of histone modification in gastric cancer. *J. Cancer Res. Ther.* 10 (Suppl), 240–245.
- Zhang, L., Huang, G., Li, X., Zhang, Y., Jiang, Y., Shen, J., Liu, J., Wang, Q., Zhu, J., Feng, X., Dong, J., Qian, C., 2013. Hypoxia induces epithelial-mesenchymal transition via activation of SNAIL by hypoxia-inducible factor-1 α in hepatocellular carcinoma. *BMC Cancer* 13, 108.
- Zhong, H., De Marzo, A.M., Laughner, E., Lim, M., Hilton, D.A., Zagzag, D., Buechler, P., Isaacs, W.B., Semenza, G.L., Simons, J.W., 1999. Overexpression of hypoxia-inducible factor 1 α in common human cancers and their metastases. *Cancer Res.* 59 (22), 5830–5835.

Supplementary Figures

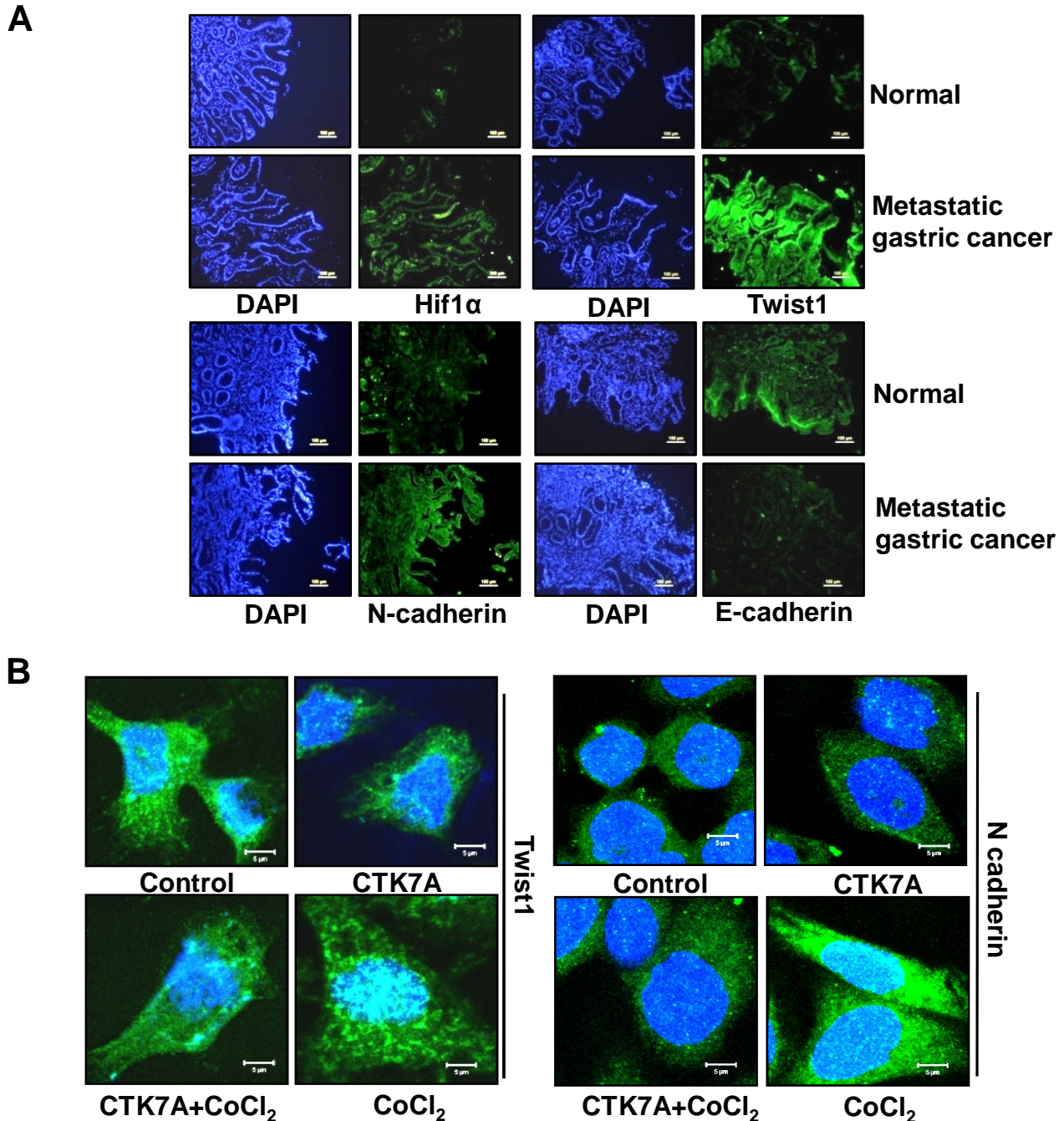


Fig. S1. Metastatic factors expressed in metastatic gastric cancer biopsy samples and in CTK7A and/or CoCl₂-treated GCCs. (A) Immunofluorescence microscopy of metastatic gastric biopsy samples and adjacent non cancerous gastric tissue samples (n=4 from each group) revealed upregulation of Hif1 α , Twist1 and N-cadherin in metastatic samples as compared to paired non-cancerous antral biopsies. DAPI was used for nuclear staining. Scale bar 100 μ m. (B) A representative confocal microscopy image of AGS cells treated with CoCl₂ (200 μ M) alone or in combination with CTK7A (100 μ M) showed downregulation of EMT markers Twist1 and N-cadherin in CTK7A+CoCl₂-treated cells. Scale bar 5 μ m.

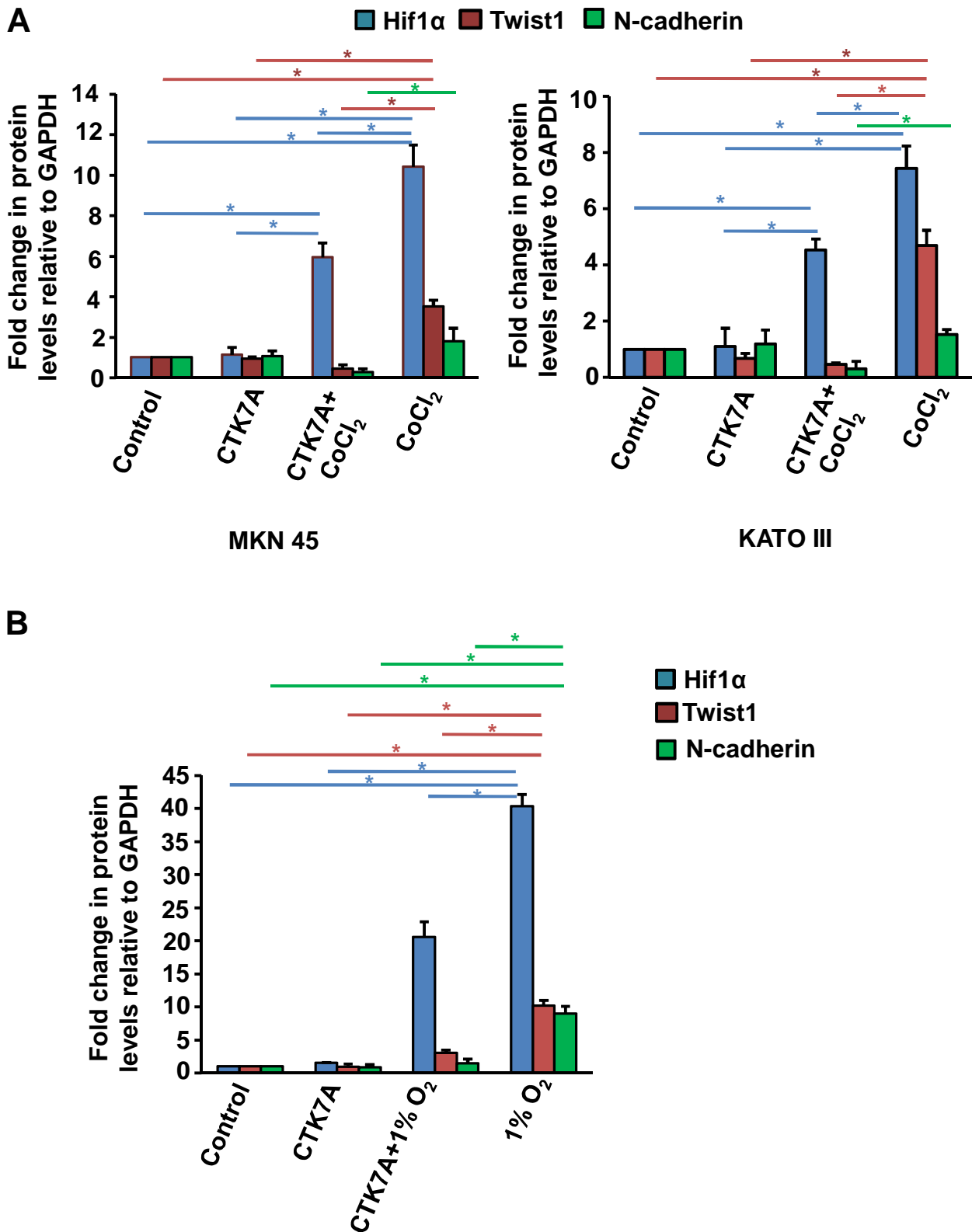


Fig. S2. CTK7A downregulated expression of metastatic markers in hypoxic GCCs. (A) Graphical presentation of data shown in Figure 1C for MKN 45 and KATO III cells by Student's t-test demonstrated expression pattern of metastatic markers in CTK7A and CoCl₂ treated cells as compared to other 3 experimental groups (n=3 independent experiments, *P<0.05). (B) Bar diagram of Figure 1D depicted expression pattern of metastatic markers in the above experimental conditions by Student's t-test (n=3 independent experiments, *P<0.05).

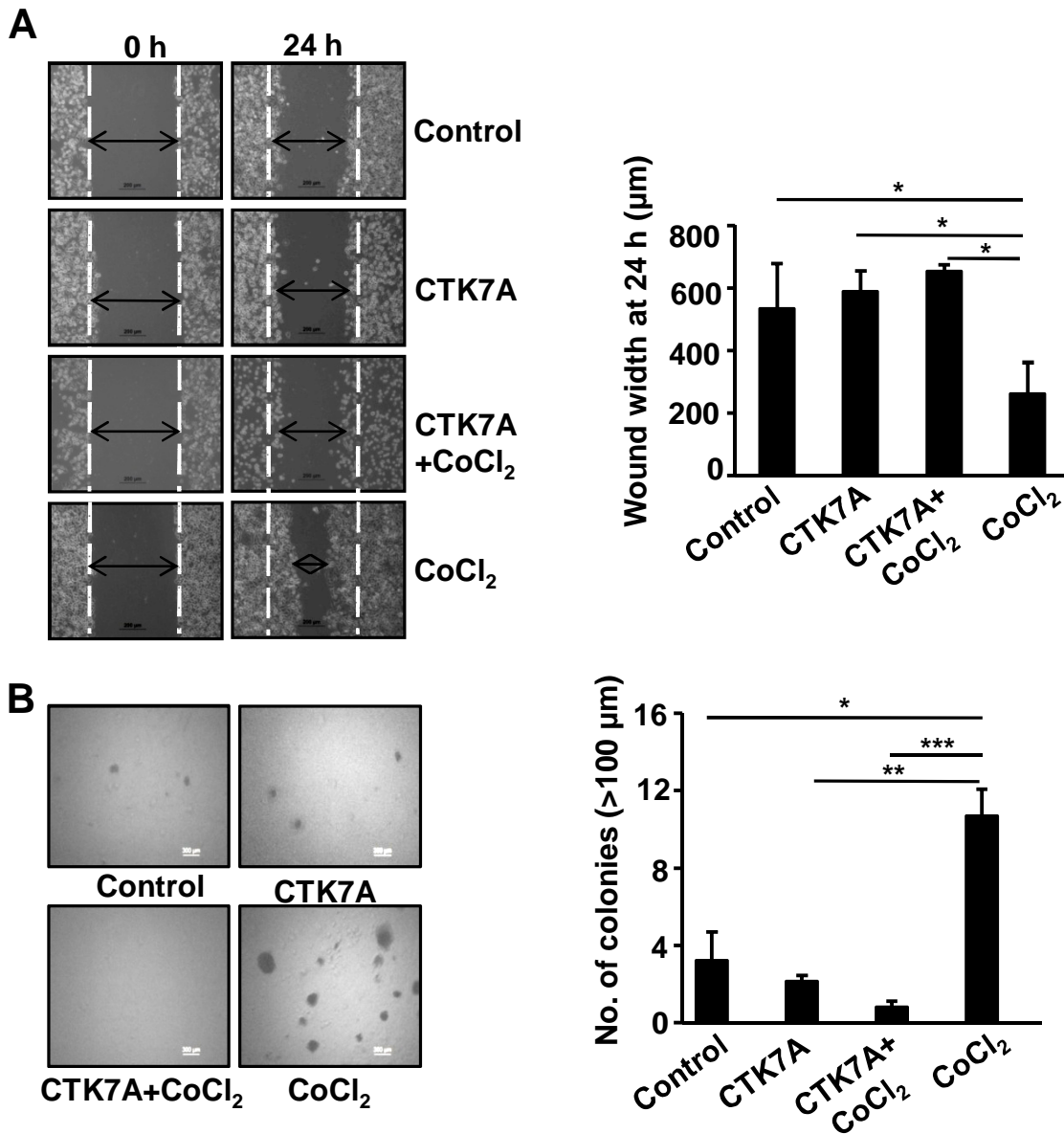


Fig. S3. *CTK7A* downregulated metastatic properties in CoCl_2 -treated GCCs. (A) AGS cells were treated with CoCl_2 (200 μM) alone or in combination with *CTK7A* (100 μM) or left untreated for 24 h and wound healing property of cells was assessed by measuring the wound width ($n=4$ independent experiments, $*P<0.05$). Photographs were taken using an inverted microscope equipped with camera (Primo Vert Carl Zeiss, Germany). Scale bar 200 μm . (B) Anchorage-independent growth of *CTK7A* and CoCl_2 -treated cells was evaluated by soft agar assay. AGS cells were treated with 200 μM CoCl_2 and/or *CTK7A* (100 μM) for 24 h or left untreated. Cells were incubated for 21 days. Colonies were counted by an inverted microscope. Scale bar 300 μm . Bar graphs depict quantification of anchorage-independent growth ($n=3$) by Student's *t*-test; $*P<0.05$, $**P<0.01$, $***P<0.001$.

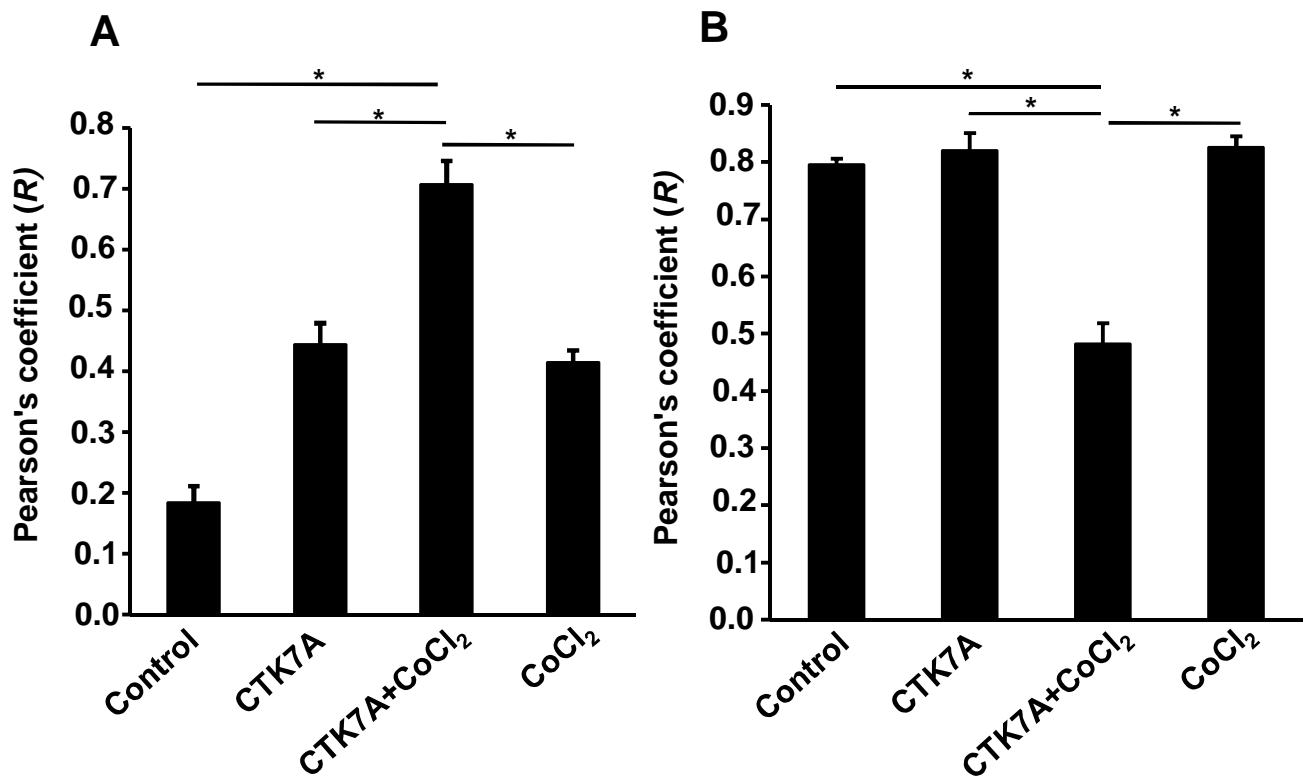


Fig. S4. CTK7A increased Noxa translocation to mitochondria and cytochrome c release in CoCl₂-treated GCCs. (A) Colocalization analysis of figure 4B was performed by ImageJ plugin Coloc 2 considering 4 separate mitochondrial regions in four different cells excluding the nucleus. A representative bar diagram (n=4) indicated significantly high Noxa in mitochondria in the CTK7A+CoCl₂-treated GCCs as compared to the other three treatment groups. (mean±SEM, n=4), *P<0.05 (B) Graphical analysis of figure 4C by using Coloc 2 software demonstrated significantly less Cytochrome c in the CTK7A+CoCl₂-treated mitochondria as compared to the other three experimental groups (mean±SEM, n=4), *P<0.05.

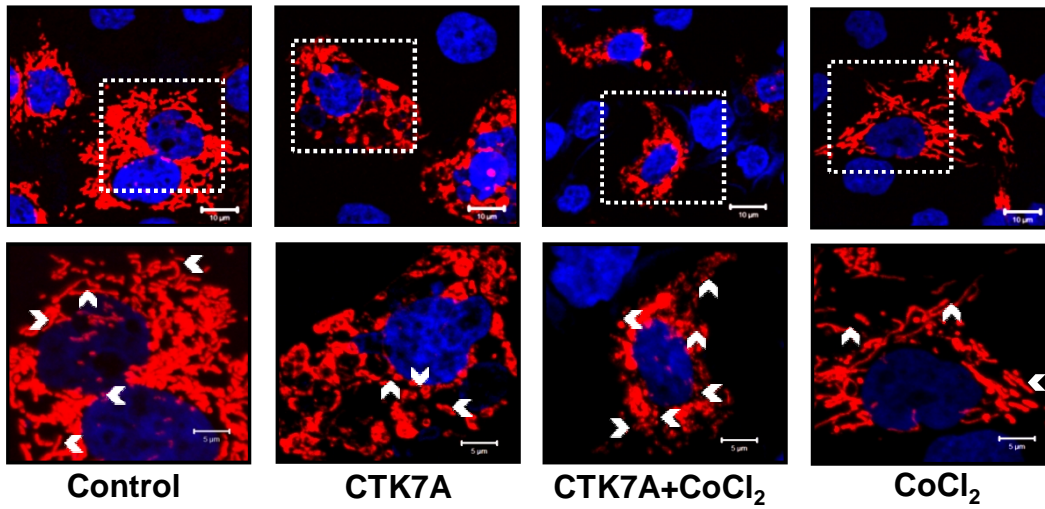
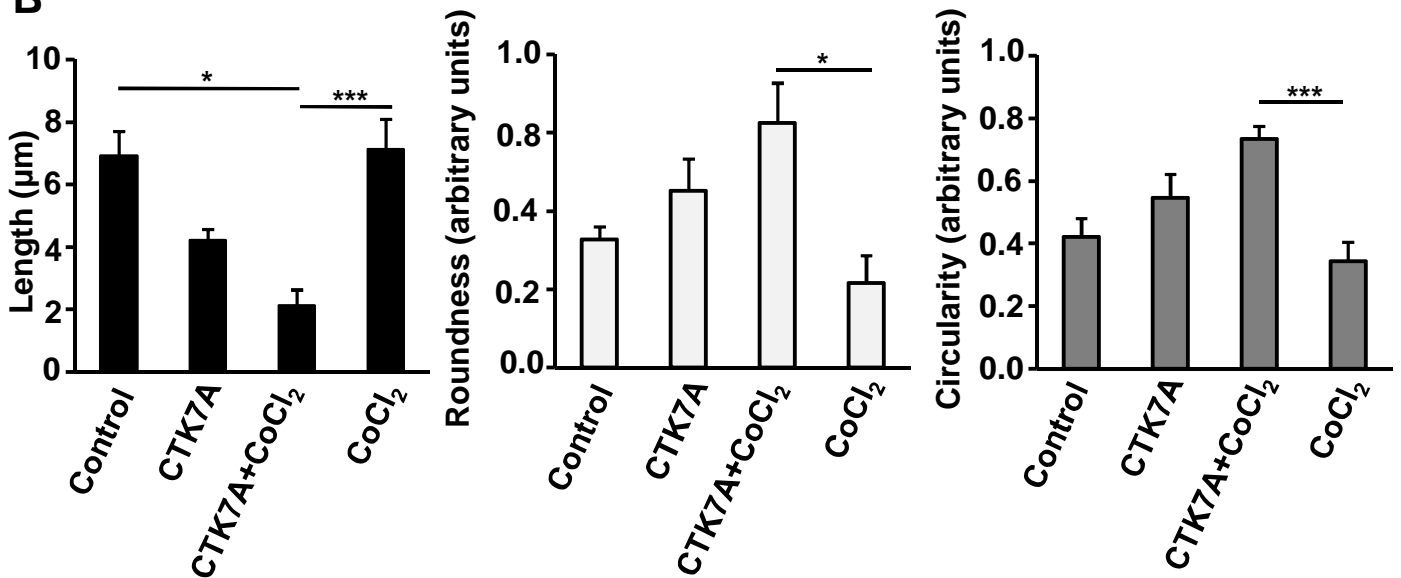
A**B**

Fig. S5. CTK7A induced mitochondrial fragmentation in CoCl₂-treated GCCs. (A) Upper panel: mitochondrial morphology was examined by confocal microscopy after treatment with CoCl₂ (200 µM) alone or in combination with CTK7A (100 µM) for 24 h in p-DsRed2 stably-expressing AGS cells. Scale bar 10 µm. Lower panel: zoomed-in images of the selected areas shown in the upper panel. Scale bar 5 µm. (B) Mitochondrial morphology was analyzed in terms of length, roundness and circularity based on information collected from four cells (from four independent experiments). The mean length of five mitochondria was taken from each cell for statistical analysis. Circular mitochondrial appearance, indicative of mitochondrial stress, was most apparent in CoCl₂+CTK7A treated cells (mean±SEM, n=4), **P*<0.05, ***P*<0.001.



Cobalt chloride-mediated protein kinase C α (PKC α) phosphorylation induces hypoxia-inducible factor 1 α (HIF1 α) in the nucleus of gastric cancer cell



Suvasmita Rath^{a,1}, Aditya Anand^{a,1}, Nilabh Ghosh^a, Lopamudra Das^a, Shrikant B. Kokate^a, Pragyesh Dixit^a, Swetapadma Majhi^a, Niranjan Rout^b, Shivaram P. Singh^c, Asima Bhattacharya^{a,*}

^a National Institute of Science Education and Research (NISER), School of Biological Sciences, PO, Bhipur-Padanpur, Via- Jatni, Dist. Khurda, 752050, Odisha, India

^b Department of Oncopathology, Acharya Harihar Regional Cancer Centre, Cuttack, 753007, Odisha, India

^c Department of Gastroenterology, SCB Medical College, Cuttack, 753007, Odisha, India

ARTICLE INFO

Article history:

Received 10 January 2016

Accepted 22 January 2016

Available online 28 January 2016

Keywords:

Cobalt chloride
Gastric epithelial cell
HIF1 α
Hypoxia
p300
PKC

ABSTRACT

Hypoxia promotes cancer progression, and metastasis. The major protein expressed in hypoxic solid cancer is hypoxia-inducible factor 1 (HIF1). We show that enhanced phosphorylation of a conventional protein kinase C isoform, PKC α , at threonine 638 (T⁶³⁸) by hypoxia-mimetic cobalt chloride induces HIF1 α in nuclei of gastric epithelial cells (GECs). Moreover, phospho-T⁶³⁸-PKC α (P-PKC α) interacts with p300-HIF1 α complex in the nuclei of hypoxic GECs and PKC α phosphorylation at T⁶³⁸ enhances transcriptional activity of HIF1 α . High P-PKC α expression in neoplastic gastric cancer biopsy samples as compared to nonneoplastic samples suggests that P-PKC α might act as an indicator of gastric cancer progression.

© 2016 Elsevier Inc. All rights reserved.

1. Introduction

Hypoxia induces a number of proteins which enable cells to adapt to low-oxygen environment. The master transcriptional regulator in hypoxic cells is a heterodimeric protein hypoxia-inducible factor 1 (HIF1). HIF1 binds to the hypoxia-response element (HRE) of the target gene to induce transcription. It comprises of α and β subunits. The β subunit is constitutively expressed but HIF1 α is only detected in hypoxic cells or in cells that are under oxidative stress [1]. Prolyl hydroxylation of HIF1 α in the normoxic cells catalyzed by prolyl hydroxylases (PHDs) leads to its binding

with the pVHL-E3 ubiquitin ligase complex following degradation. Hypoxia inhibits prolyl hydroxylation of HIF1 α and stabilizes it [2]. Cobalt chloride (CoCl₂·6H₂O) induces biochemical responses similar to hypoxia [3].

Blood circulation is inefficient in solid tumors and as a result, hypoxic regions are common at the core of solid tumors [4]. Prolonged hypoxia induces apoptosis but cells that can survive hypoxic assault, emerge as more drug-resistant and metastatic [5–7]. Besides HIF1, the PKC family of Ser/Thr kinases are also induced by hypoxia that can regulate various cellular functions including cell growth, differentiation and apoptosis [8]. Tissue ischemia or hypoxic stress leads to the activation of various protein kinase C (PKC) family members. PKCs protect against hypoxic injury and are implicated in ischemia-related diseases [9]. The PKC family has ten isoforms grouped in three subfamilies based on their differences in structure and catalytic domains and on their ability to respond to the cofactors Ca⁺⁺ and diacylglycerol (DAG). PKC α is a conventional or classical isoform and requires both Ca⁺⁺ and DAG for activation [10].

PKC α promotes invasiveness of various cancers including gastric

Abbreviations: CoCl₂·6H₂O, Cobalt chloride hexahydrate; DAG, Diacylglycerol; DAPI, 4',6-Diamidino-2-Phenylindole, Dilactate; DN, Dominant negative; GECs, Gastric epithelial cells; HDAC1, Histone-deacetylase 1; HIF1, Hypoxia-inducible factor 1; HRE, Hypoxia-response element; NLS, Nuclear localization signal; PHDs, Prolyl hydroxylases; PKC, Protein kinase C; PVDF, Polyvinylidene fluoride; SDS-PAGE, Sodium dodecyl sulphate-polyacrylamide gel electrophoresis; WT, Wild type.

* Corresponding author.

E-mail address: asima@niser.ac.in (A. Bhattacharya).

¹ Contributed equally.

cancer [11,12]. But contradicting reports on PKC α downregulation in several cancers [11] and PKC α -mediated apoptosis induction in 12-O-tetradecanoyl phorbol-13-acetate-treated human gastric cancer cell lines [13] also exist. Cellular localization of PKCs determines their function and the effect is tissue or cell line-specific. For example, nuclear translocation of PKC δ in C5 cells induces apoptosis whereas its mitochondrial translocation is required for apoptosis in SP1 cells [14–16]. Phosphorylation and dephosphorylation influence PKC-mediated cellular signaling and impart specificities to PKC binding to distinct substrates as well [17]. Subcellular fractionation shows that phosphorylated active PKC α can translocate to the nucleus [18]. So, subcellular localization of PKC α might be the key factor determining its role in cancer progression. However, its expression status and role in hypoxic gastric cancer cells have not yet been studied.

This study identifies that PKC α phosphorylation at T⁶³⁸ is induced in the nucleus of GECs after treatment with CoCl₂. Moreover, this study establishes that T⁶³⁸-phosphorylated PKC α induces expression of HIF1 α after CoCl₂ treatment in GECs. As human gastric neoplasia samples also showed highly-increased expression of P-PKC α as compared to noncancerous samples, P-PKC α might be useful as a molecular marker to study gastric cancer progression. Since fluctuations in blood flow during solid tumor development creates hypoxic state, our results implicate that P-PKC α might be a regulator of HIF1 α activity in aggressively growing solid tumors.

2. Materials and methods

2.1. Cell culture and treatment

Cell lines and reagents used in this work are listed in supplementary materials.

2.2. Plasmids, site-directed mutagenesis and transfection

Wild type (WT) PKC α and its dominant negative (DN) mutant K368R (mutated in the ATP binding cassette and is kinase function-dead) were gifted by Bernard Weinstein (Addgene plasmids # 21232 and #21235, respectively) [19]. PKC α T638A mutant construct was generated from the WT PKC α construct using Quik-Change site directed mutagenesis kit (Agilent Technologies, Santa Clara, CA). Mutagenesis primers and transfection method are described in supplementary materials.

2.3. Immunoprecipitation, western blotting and antibodies

Whole cell lysates were prepared by using standard protocol. Nuclear and cytoplasmic fractions were isolated using NE-PER kit (Thermo scientific, MI). Further details are provided in supplementary materials.

2.4. Immunofluorescence microscopy of gastric cancer biopsies

Immunofluorescence staining was performed to detect HIF1 α , P-PKC α , PKC α proteins in human gastric cancer biopsy samples. Gastric neoplasia and metastatic biopsy samples from the antral gastric mucosa were collected from patients who were undergoing diagnostic esophagogastroduodenoscopy following a NISER Review Board-approved protocol. Biopsy samples from surrounding non-cancerous areas were used as control samples. Research was carried out in accordance with the Declaration of Helsinki (2013) of the World Medical Association. Written informed consent was obtained from all patients prior to the study. Primary antibodies used were HIF1 α , P-PKC α and PKC α (1:500). Digital images were captured using a fluorescence microscope (Carl Zeiss, Jena,

Germany).

2.5. Confocal microscopy

Detailed protocol for confocal microscopy is given in the supplementary materials section.

2.6. Dual luciferase assay

Dual luciferase assay was performed to study the effect of PKC α overexpression on the transcriptional activity of HIF1 α according to manufacturer's instruction (Promega, CA) details of which can be found from the supplementary materials section.

2.7. Statistical analysis

All data were presented as mean \pm SE from three or more independent experiments. Student's *t*-test was performed for statistical comparisons between two experimental groups. Statistical significance was determined at $P < 0.05$.

3. Results

3.1. Short treatment with CoCl₂ induces nuclear P-PKC α expression

Expression of PKC α and P-PKC α was assessed in normoxic (or control) and CoCl₂-treated AGS cells. Comparison of western blots ($n = 3$) of whole cell lysates prepared from control or 30 min, 1 h and 3 h CoCl₂-treated (200 μ M) AGS cells did not show any change in expression of PKC α and P-PKC α (Fig. 1A). CoCl₂ at 200 μ M was not cytotoxic to AGS cells (data not shown). Expression of HIF1 α time-dependently increased with CoCl₂ treatment. Western blot results of the nuclear fractions identified significant ($n = 3$; $P < 0.05$) induction of P-PKC α in the nuclear fraction of CoCl₂-treated AGS cells as compared to control cells. Whereas, equal P-PKC α expression was observed in the cytosol of CoCl₂-treated and control cells at all time points. On the contrary, total PKC α was constitutively expressed in both compartments and was not changed after CoCl₂ treatment (Fig. 1B). GAPDH and HDAC1 immunoblots were used as cytosolic and nuclear loading controls, respectively. We next sought to determine whether 200 μ M CoCl₂ was able to effectively induce P-PKC α expression in another gastric cancer cell line, NCI-N87. Western blot data confirmed that 200 μ M CoCl₂ induced nuclear expression of P-PKC α in NCI-N87 cells as it did in AGS cells (Supplementary Fig. S1). Confocal microscopy data also showed the same trend of P-PKC α and PKC α expression in the nuclear and cytosolic compartments of control and CoCl₂-treated cells (Fig. 1C and Supplementary Fig. S2). Antral biopsy samples obtained from consenting patients were used to study expression of PKC α and P-PKC α proteins in gastric neoplasia. Comparison of fluorescence microscopy images obtained from neoplasia patients with images from non-cancer gastric "control" tissues showed very high P-PKC α expression in neoplasia samples but no difference was observed amongst these groups with respect to PKC α expression (Supplementary Fig. S3). However, we did not observe any difference between metastatic gastric cancer samples ($n = 4$) collected from antrum and adjacent non-cancer "control" samples ($n = 4$) with respect to PKC α expression but P-PKC α expression was substantially less in metastatic samples as compared to control samples (Supplementary Fig. S4). Next, we wanted to examine whether HIF1 α expression differs in metastatic and neoplastic samples. Immunofluorescence microscopy data showed equivalent high expression of HIF1 α in both neoplastic and metastatic gastric cancer tissues as compared to their non-cancer counterparts (Supplementary Fig. S5).

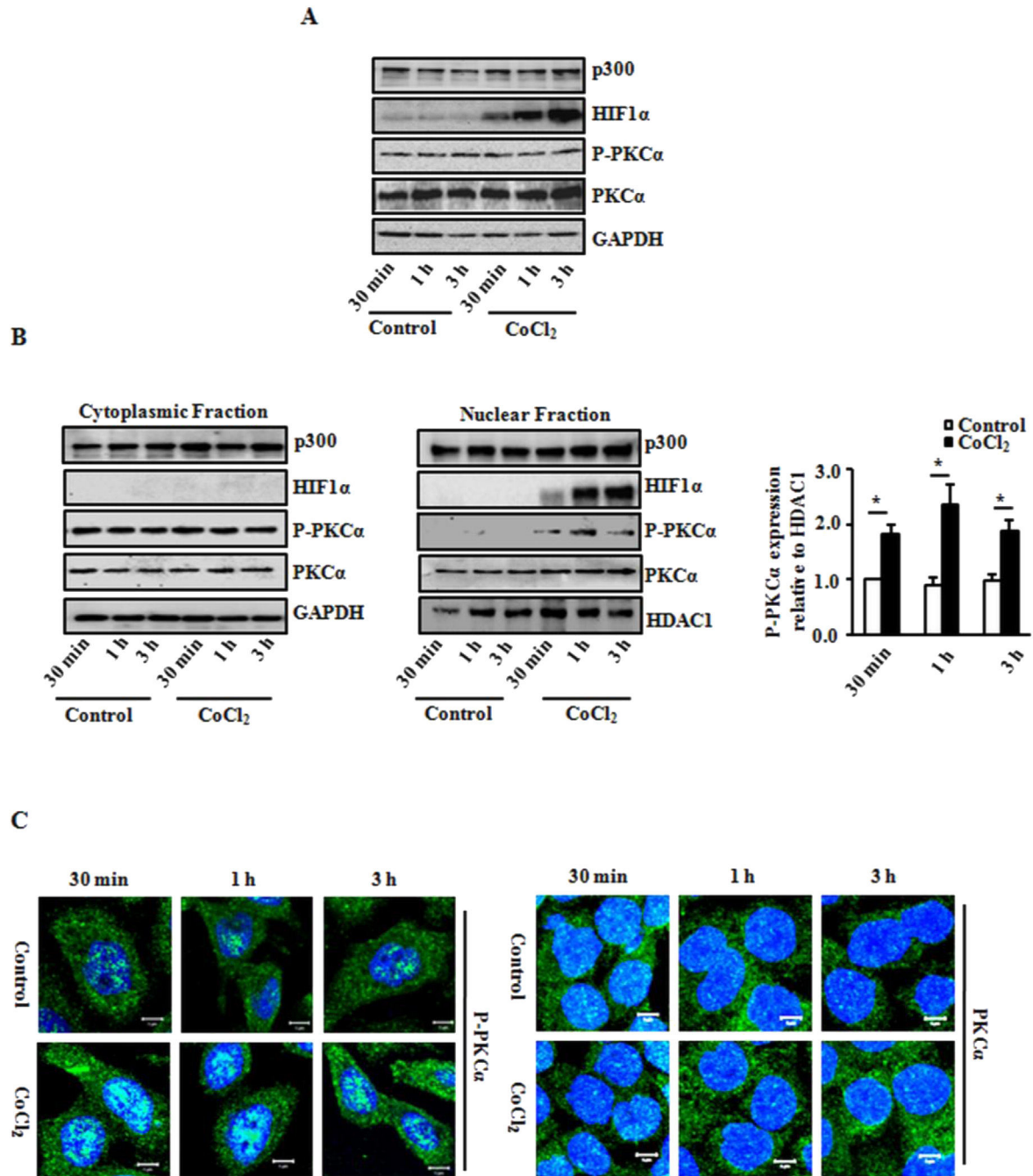


Fig. 1. CoCl_2 induced phosphorylation of $\text{PKC}\alpha$ in the nuclear fraction of GECs. (A) Western blot analysis ($n = 3$) of whole cell lysates prepared from control and $200 \mu\text{M}$ CoCl_2 -treated AGS cells at various time points (30 min, 1 h, 3 h) was done to assess expression of p300, HIF1 α , P-PKC α and PKC α . GAPDH was used as a loading control. (B) Representative western blots ($n = 3$) of cytoplasmic (left panel) and nuclear fractions (right panel) showed time-dependent induced expression of P-PKC α , HIF1 α in CoCl_2 -treated GECs. GAPDH and HDAC1 were kept as a loading control for the cytoplasmic fraction nuclear fraction respectively. A graphical representation of the data showing nuclear P-PKC α induction normalized to HDAC1. Bars depicting normalized data (mean \pm SEM, $n = 3$), * $P < 0.05$. (C) AGS cells were cultured on coverslips and treated with $200 \mu\text{M}$ of CoCl_2 for various time points (30 min, 1 h, and 3 h) or left untreated. Nuclear expression of P-PKC α was visualized by confocal microscope. Nuclei of the AGS cells were stained with DAPI. Scale bar $5 \mu\text{m}$.

3.2. P-PKC α induces HIF1 α expression in the CoCl_2 -treated GECs

Intratumoral hypoxia is a hallmark of solid tumors and helps in cancer progression through activation of HIF1 α . Western blot results shown in Fig. 1B and C proved P-PKC α expression in the nucleus of CoCl_2 -treated cells. As PKC α phosphorylation in the nucleus peaked ahead of nuclear expression of HIF1 α (1 h and 3 h, respectively) (Fig. 1B and Supplementary Fig. S1), we sought to know whether HIF1 α induction was regulated by PKC α . To

determine the effect of PKC α on HIF1 α expression, we transfected AGS cells with either WT PKC α or kinase function-dead dominant negative DN PKC α or the empty vector followed by $200 \mu\text{M}$ CoCl_2 treatment for 1 h. Western blotting of cytosolic and nuclear fractions (Fig. 2A) showed that CoCl_2 -mediated nuclear HIF1 α expression was enhanced in PKC α WT construct-transfected cells as compared to the empty vector or DN construct-transfected cells. It is well-established that hypoxia induces various isoforms of PKC including the classical isoforms and PKC α [20]. As demonstrated in

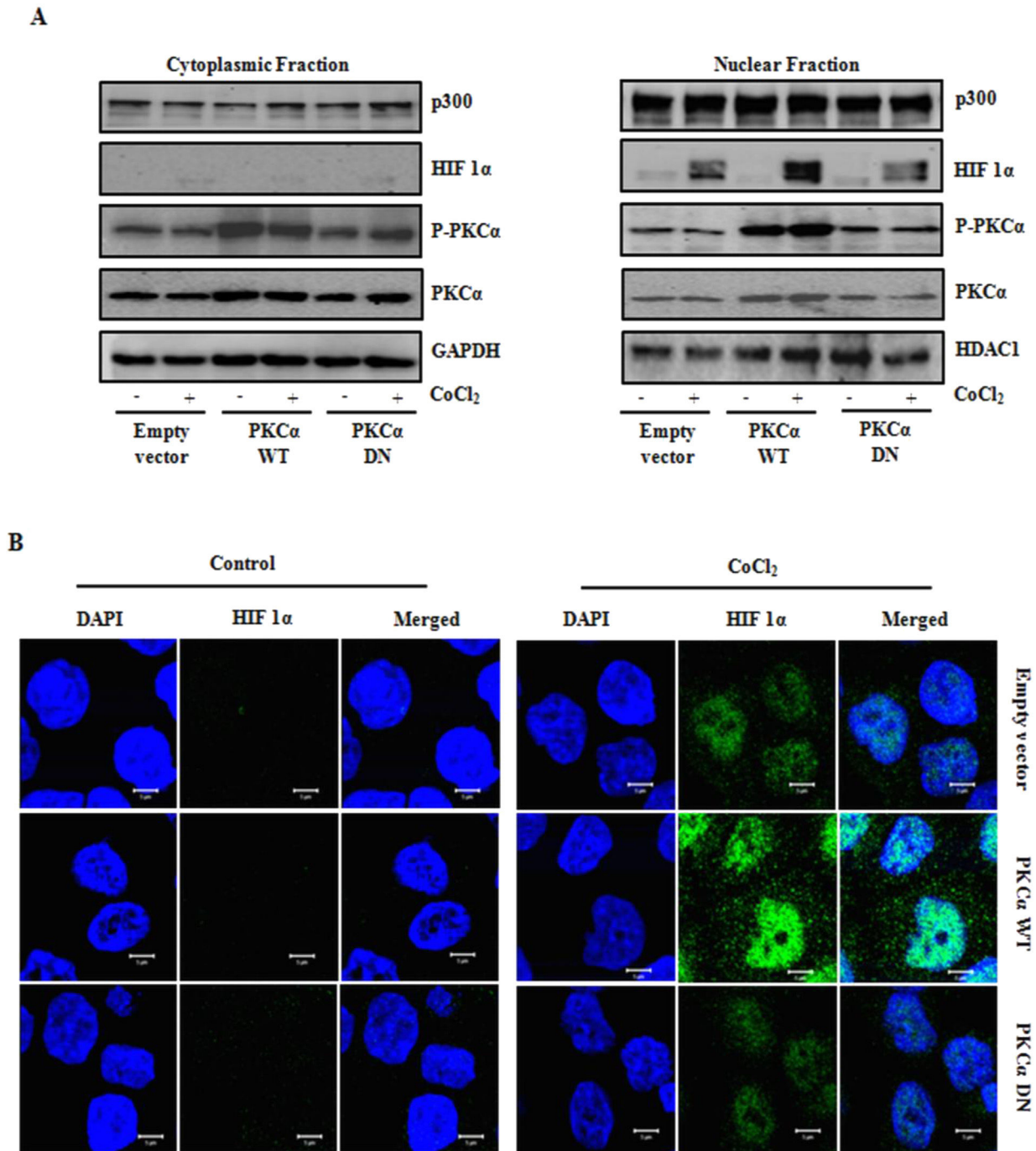


Fig. 2. CoCl₂-mediated PKC α phosphorylation induced expression of HIF1 α in the nuclei of CoCl₂ treated GECs. (A) AGS cells were transfected with empty vector, PKC α WT and PKC α DN constructs followed by exposure to 200 μ M of CoCl₂ for 1 h. Cytoplasmic and nuclear fractions were isolated and status of p300, HIF1 α , P-PKC α and PKC α were analyzed by immunoblotting (n = 3). GAPDH and HDAC1 were used as loading control for the cytoplasmic fraction and the nuclear fraction, respectively. (B) AGS cells were transfected with empty vector, PKC α WT and PKC α DN constructs followed by treatment with 200 μ M of CoCl₂ for 1 h. Cells were fixed and expression of HIF1 α was studied by confocal microscopy. Nuclei were stained with DAPI. Scale bar 5 μ m.

Fig. 2A, the absence of kinase function in the DN PKC α [19] having K368R mutation blocked the HIF1 α -inducing effect shown by PKC α in CoCl₂ treated hypoxic GECs. Confocal microscopy of the above experimental cell groups further confirmed that CoCl₂-induced nuclear expression of HIF1 α was maximal in WT PKC α -overexpressed cells as compared to the empty vector or DN PKC α -transfected cells (Fig. 2B). The effect of PKC α phosphorylation at T⁶³⁸ on CoCl₂-induced HIF1 α expression was assessed by comparing the

empty vector, PKC α WT or T638A mutant-transfected AGS cells. Western blotting of the cytoplasmic and nuclear lysates prepared from control or CoCl₂-treated cells from each transfection group clearly showed significant enhancement of HIF1 α expression in nuclear lysates prepared from WT PKC α -expressing cells but not in PKC α T638A mutant-expressing cells after CoCl₂ treatment (Fig. 3A). As T638A PKC α reduces PKC α stability [21,22], we observed decreased expression of PKC α protein in T638A construct-

transfected cells as compared to the WT construct-expressed cells. Confocal microscopy results supported that CoCl₂-mediated induction of nuclear expression of HIF1 α was further enhanced by WT PKC α overexpression but overexpression of the T638A construct had no such effect on HIF1 α (Fig. 3B).

3.3. PKC α interacts with HIF1 α -p300 complex in CoCl₂-treated GECs

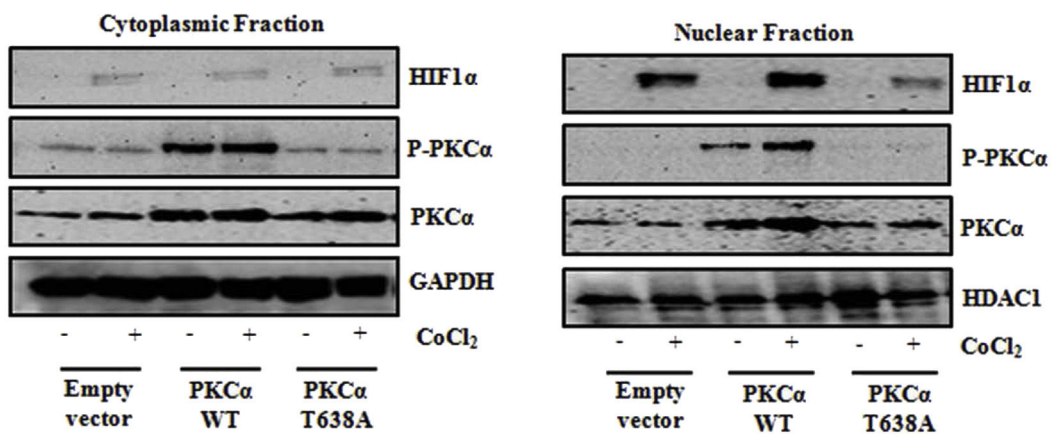
Next, we sought to identify whether PKC α or P-PKC α interacted with HIF1 α in CoCl₂-treated AGS cells. For this, nuclear lysates from CoCl₂-treated and control cells were immunoprecipitated with HIF1 α antibody and western blotting was performed using PKC α , P-PKC α and HIF1 α primary antibodies. PKC α or P-PKC α did not

interact with HIF1 α (Fig. 4A) directly. HIF1 α needs to interact with its transcriptional coactivator p300/CBP to be transcriptionally active [23,24]. As no interaction of PKC α with HIF1 α might be due to epitope unavailability, we performed another immunoprecipitation assay using p300 antibody. p300 interacted with both HIF1 α and P-PKC α only in CoCl₂-treated nuclear lysates. Whereas, binding of PKC α with p300 was independent of CoCl₂ (Fig. 4B). More P-PKC α interacted with p300 at 1 h of CoCl₂ treatment as compared to 3 h.

3.4. PKC α activity and phosphorylation at T⁶³⁸ is required to induce HIF1 α transcriptional activity

A dual luciferase assay was performed to determine the optimal

A



B

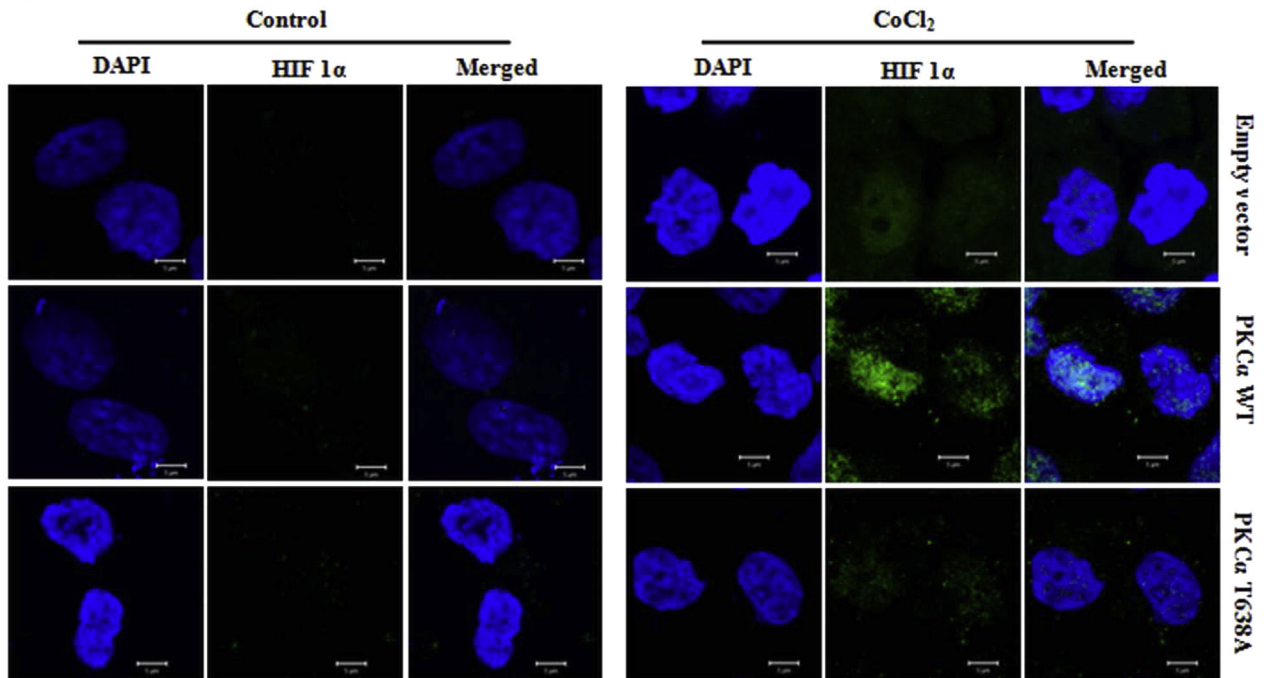


Fig. 3. CoCl₂-induced phosphorylation of PKC α at T⁶³⁸ enhanced HIF1 α expression in the nuclei of GECs. (A) Immunoblot analysis (n = 3) of cytoplasmic and nuclear lysates prepared from AGS cells transfected with empty vector, PKC α WT and PKC α T638A constructs and treated with 200 μ M of CoCl₂ for 1 h. GAPDH and HDAC1 were used as loading control for cytosolic and nuclear fractions, respectively. (B) AGS cells were transfected with empty vector, PKC α WT and PKC α T638A constructs followed by treatment with 200 μ M CoCl₂ for 1 h. Cells were fixed, immunostained with anti-HIF1 α antibody and expression of nuclear HIF1 α was studied by confocal microscopy. DAPI was used to stain nuclei. Scale bar 5 μ m.

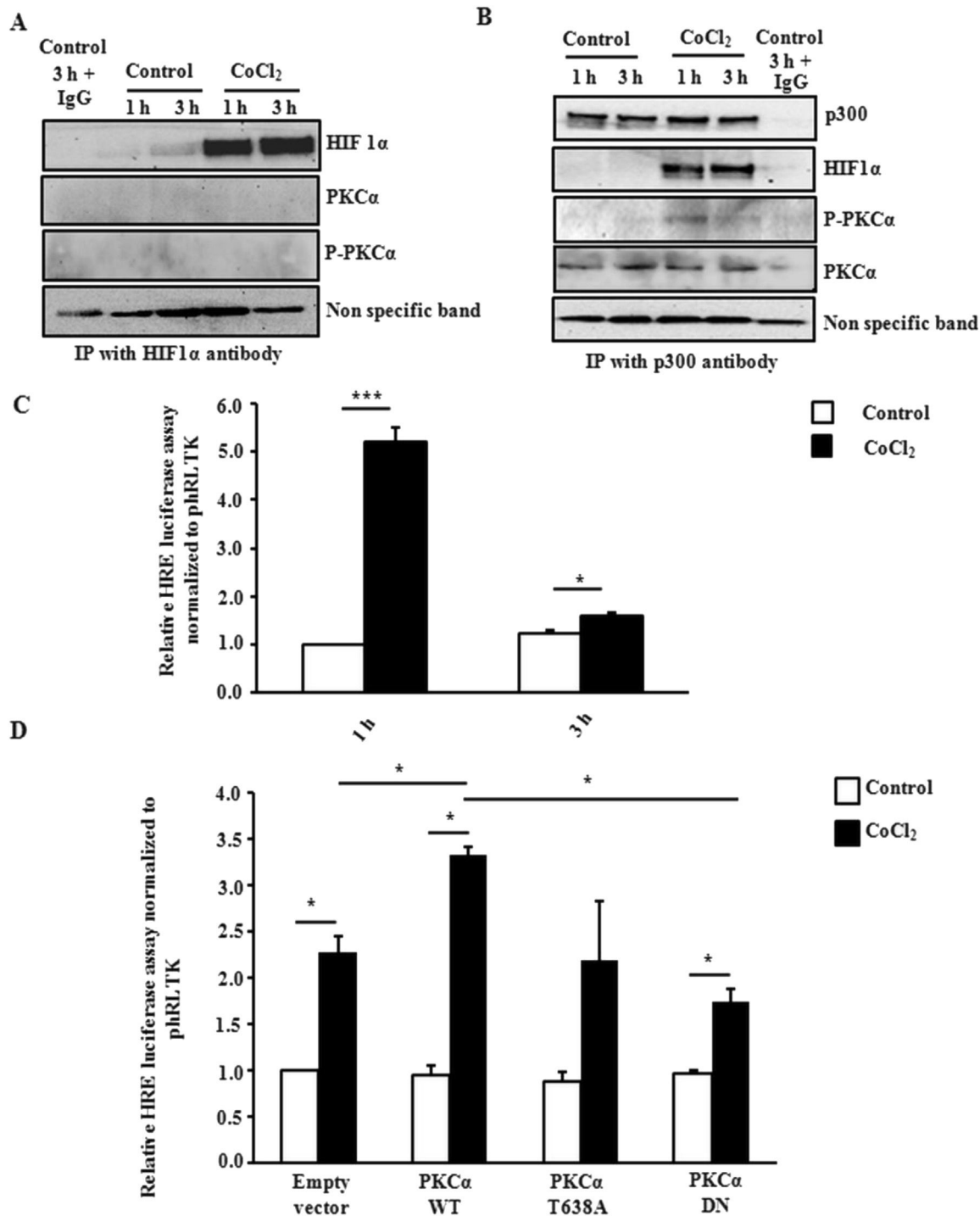


Fig. 4. CoCl₂ induced P-PKC α interaction with HIF1 α -p300 complex and enhanced transcriptional activity of HIF1 after phosphorylation at T⁶³⁸ residue in the nuclear fraction of GECs. (A) Immunoprecipitation experiment was performed to study interaction between HIF1 α and PKC α in the nuclear fraction of AGS cells. Nuclear extracts prepared from 200 μ M CoCl₂ treated cells (1 h and 3 h) were immunoprecipitated using HIF1 α antibody. A non-specific band was used to ensure equal protein loading. (B) AGS cells were treated 200 μ M CoCl₂ for 1 h and 3 h followed by immunoprecipitation of nuclear lysates using p300 antibody. A non-specific band was used to estimate protein loading. (C) Dual luciferase assay was performed in AGS cells to assess optimal time of transcriptional activity of HIF1 α in PKC α WT construct ectopically expressed and CoCl₂ treated cells (mean \pm SEM, n = 3), ***P < 0.001; P < 0.05. (D) Dual luciferase assay (mean \pm SEM, n = 3) showing HRE-luciferase activity in empty vector, PKC α WT, DN and T638A construct-transfected cells.

time of transcriptional activation of HIF1 α following CoCl₂ treatment. For this, AGS cells were cotransfected with a *Renilla* luciferase construct and a HRE luciferase construct along with PKC α WT construct. Cell lysates were prepared following CoCl₂ treatment and dual luciferase assay was performed. Data showed (means \pm SE, n = 3) that HRE luciferase activity was significantly increased

(P < 0.05) at 1 h of CoCl₂ treatment (Fig. 4C). In another attempt to identify the effect of PKC α on transcriptional activity of HIF1 α , AGS cells were transiently transfected with HRE and *Renilla* luciferase construct along with the empty vector, PKC α WT, T638A or DN construct. Although significant enhancement (P \leq 0.05) of HIF1 α HRE activation was observed in CoCl₂-treated cells of each

transfected group (means \pm SE, $n = 3$) as compared to control (except for the T638A group), WT PKC α was found to maximally induce HRE activity after CoCl₂ treatment suggesting that WT PKC α potentiated transcriptional activity of HIF1 α in CoCl₂ treated hypoxic GECs (Fig. 4D).

4. Discussion

Signaling events in hypoxia determine cancer progression, metastasis, drug resistance properties and overall treatment outcome in solid cancer. Research spanning the past two decades has implicated PKC α in various solid cancers [25,26]. However, the role of PKC α in CoCl₂-treated GECs has not been studied at all. We show that CoCl₂ induces P-PKC α expression at T⁶³⁸ residue in the nuclei of GECs. Moreover, we report that CoCl₂-induced P-PKC α enhances HIF1 α expression and transcriptional activity. Our data further implicates that phosphorylation-dephosphorylation of PKC α might act as on-off regulators for HIF1 α expression and transcriptional activation in hypoxic tissues.

Various isoforms of PKC can be translocated and retained in the nucleus (despite of the fact that PKCs lack nuclear localization signal) or PKCs can be residents within the nucleus. PKC translocation to the nucleus varies from isotype to isotype [27]. Nuclear PKC α -binding partners have been identified by various groups [28]. Hypoxia induces translocation of PKC α to the nucleus and enhances its phosphorylation [29]. PKC α requires phosphorylation at T⁴⁹⁷ (activation loop), T⁶³⁸ (turn motif), and S⁶⁵⁷ (hydrophobic domain) for its activation [30]. Phosphorylation of the activation loop of PKC α causes autophosphorylation in the turn motif and hydrophobic domain, thus turning PKC α into a catalytically active, stable and mature molecule [31]. As T⁶³⁸ is a priming phosphorylation site in PKC α required for its complete catalytic activation [30,32], dephosphorylation and mutation at this residue inactivates PKC α enzyme [10,33]. We report here for the first time that phosphorylation of PKC α at T⁶³⁸ is induced by CoCl₂-mediated hypoxia. Further, we report that P-PKC α expression in the cytoplasm of GECs does not depend on CoCl₂ but its expression in the nucleus is significantly induced by CoCl₂.

PKC α -mediated HIF1 α expression and transactivation are known to occur in various experimental conditions [34,35]. Naturally, the PKC inhibitor Gö6976 treatment results in attenuation of HIF1 α expression under hypoxia [36]. Our data shows that both HIF1 α and P-PKC α are maximally expressed in WT PKC α -transfected hypoxic cells as compared to the empty vector or PKC α DN or T638A mutant-transfected cells. Suppression of HIF1 α transcriptional activity in T638A mutant or empty vector-transfected hypoxic cells as compared to the WT PKC α -transfected cells further establishes the role of P-PKC α in inducing the transcriptional activity of HIF1 α . The study to understand the molecular mechanism of P-PKC α -mediated HIF1 α induction is being pursued in our laboratory. Although we know that p300 gene alteration is very common in gastric carcinoma [37], we still do not know how p300 gene alteration or inactivating mutations would modulate the molecular interaction of P-PKC α with p300-HIF1 α complex in gastric cancer which also warrants further experimentation.

Our data shows that overexpression of the kinase function-dead K368R mutant (the DN construct has the mutation in the activation loop) of PKC α also blocks the priming phosphorylation at the turn motif at T⁶³⁸ under the influence of CoCl₂. As both DN and T638A constructs show similar effects on HIF1 α expression and transcriptional function, we predict that P-PKC α might show similar effects on HIF1 α in cancers which show upregulation of nuclear PKC α . As P-PKC α expression is high in neoplastic but not in metastatic biopsy samples while HIF1 α expression remains high in both types of gastric cancer tissues, we speculate that PKC α -HIF1 α

interaction differs depending on gastric cancer staging. The data further indicates that PKC α phosphorylation is differentially regulated in neoplastic and metastatic gastric cancer tissues. Therefore, P-PKC α appears to be a potential molecular marker determining the staging of gastric cancer. Extensive research is required to find out whether high P-PKC α expression is exclusive for neoplasia and how that affects various stages of cancer progression.

In conclusion, this work identifies induced expression of nuclear P-PKC α in the CoCl₂ treated hypoxic GECs. The finding that PKC α phosphorylation in hypoxic GECs enhancing HIF1 α expression and transcriptional activity suggests that hypoxia-mediated induction of P-PKC α might be a major contributor in hypoxia-induced gastric cancer progression.

Conflict of interest

The authors declare no conflict of interests.

Acknowledgment

This work was partly supported by a grant to Asima Bhattacharyya (Sanction No. SR/FT/LS-38/2010), Science and Engineering Research Board (SERB), Govt. of India and institutional funding from NISER, Bhubaneswar. We acknowledge Mr. Alok Kumar Jena for his assistance with confocal imaging.

Appendix A. Supplementary data

Supplementary data related to this article can be found at <http://dx.doi.org/10.1016/j.bbrc.2016.01.140>.

References

- [1] A. Bhattacharyya, R. Chattopadhyay, S. Mitra, S.E. Crowe, Oxidative stress: an essential factor in the pathogenesis of gastrointestinal mucosal diseases, *Physiol. Rev.* 94 (2014) 329–354.
- [2] S.N. Greer, J.L. Metcalf, Y. Wang, M. Ohh, The updated biology of hypoxia-inducible factor, *EMBO J.* 31 (2012) 2448–2460.
- [3] E.S. Jeon, J.H. Shin, S.J. Hwang, G.J. Moon, O.Y. Bang, H.H. Kim, Cobalt chloride induces neuronal differentiation of human mesenchymal stem cells through upregulation of microRNA-124a, *Biochem. Biophys. Res. Commun.* 444 (2014) 581–587.
- [4] J.M. Brown, A.J. Giaccia, The unique physiology of solid tumors: opportunities (and problems) for cancer therapy, *Cancer Res.* 58 (1998) 1408–1416.
- [5] G. Melillo, Targeting hypoxia cell signaling for cancer therapy, *Cancer Metastasis Rev.* 26 (2007) 341–352.
- [6] N. Chaudary, R.P. Hill, Hypoxia and metastasis, *Clin. Cancer Res.* 13 (2007) 1947–1949.
- [7] K.L. Bennewith, S. Dedhar, Targeting hypoxic tumour cells to overcome metastasis, *BMC cancer* 11 (2011) 504.
- [8] S. Nakashima, Protein kinase C alpha (PKC alpha): regulation and biological function, *J. Biochem.* 132 (2002) 669–675.
- [9] M.E. Barnett, D.K. Madgwick, D.J. Takemoto, Protein kinase C as a stress sensor, *Cell. Signal* 19 (2007) 1820–1829.
- [10] A.C. Newton, Protein kinase C: structural and spatial regulation by phosphorylation, cofactors, and macromolecular interactions, *Chem. Rev.* 101 (2001) 2353–2364.
- [11] G. Martiny-Baron, D. Fabbro, Classical PKC isoforms in cancer, *Pharmacol. Rev.* 55 (2007) 477–486.
- [12] G.K. Schwartz, J. Jiang, D. Kelsen, A.P. Albino, Protein kinase C: a novel target for inhibiting gastric cancer cell invasion, *J. Natl. Cancer Inst.* 85 (1993) 402–407.
- [13] H. Okuda, M. Adachi, M. Miyazawa, Y. Hinoda, K. Imai, Protein kinase Calpha promotes apoptotic cell death in gastric cancer cells depending upon loss of anchorage, *Oncogene* 18 (1999) 5604–5609.
- [14] M.J. Humphries, A.M. Ohm, J. Schaack, T.S. Adwan, M.E. Reyland, Tyrosine phosphorylation regulates nuclear translocation of PKCdelta, *Oncogene* 27 (2008) 3045–3053.
- [15] T.A. DeVries, M.C. Neville, M.E. Reyland, Nuclear import of PKCdelta is required for apoptosis: identification of a novel nuclear import sequence, *EMBO J.* 21 (2002) 6050–6060.
- [16] L. Li, P.S. Lorenzo, K. Bogi, P.M. Blumberg, S.H. Yuspa, Protein kinase Cdelta targets mitochondria, alters mitochondrial membrane potential, and induces apoptosis in normal and neoplastic keratinocytes when overexpressed by an adenoviral vector, *Mol. Cell. Biol.* 19 (1999) 8547–8558.

- [17] D. Breitkreutz, L. Braiman-Wikman, N. Daum, M.F. Denning, T. Tennenbaum, Protein kinase C family: on the crossroads of cell signaling in skin and tumor epithelium, *J. Cancer Res. Clin. Oncol.* 133 (2007) 793–808.
- [18] K. Vijayan, E.L. Szotek, J.L. Martin, A.M. Samarel, Protein kinase C- α -induced hypertrophy of neonatal rat ventricular myocytes, *Am. J. Physiol. Heart Circ. Physiol.* 287 (2004) H2777–H2789.
- [19] J.W. Soh, I.B. Weinstein, Roles of specific isoforms of protein kinase C in the transcriptional control of cyclin D1 and related genes, *J. Biol. Chem.* 278 (2003) 34709–34716.
- [20] M. Goldberg, H.L. Zhang, S.F. Steinberg, Hypoxia alters the subcellular distribution of protein kinase C isoforms in neonatal rat ventricular myocytes, *J. Clin. Invest.* 99 (1997) 55–61.
- [21] F. Bornancin, P.J. Parker, Phosphorylation of threonine 638 critically controls the dephosphorylation and inactivation of protein kinase C α , *Curr. Biol.* 6 (1996) 1114–1123.
- [22] T. Ikenoue, K. Inoki, Q. Yang, X. Zhou, K.L. Guan, Essential function of TORC2 in PKC and Akt turn motif phosphorylation, maturation and signalling, *EMBO J.* 27 (2008) 1919–1931.
- [23] D. Lando, D.J. Peet, D.A. Whelan, J.J. Gorman, M.L. Whitelaw, Asparagine hydroxylation of the HIF transactivation domain a hypoxic switch, *Science* 295 (2002) 858–861.
- [24] Q. Ke, M. Costa, Hypoxia-inducible factor-1 (HIF-1), *Mol. Pharmacol.* 70 (2006) 1469–1480.
- [25] J.K. Schroder, S. Kasimir-Bauer, S. Seeber, M.E. Scheulen, In vitro effect of multidrug resistance modifiers on idarubicin efflux in blasts of acute myeloid leukemia, *J. Cancer Res. Clin. Oncol.* 126 (2000) 111–116.
- [26] T. Yamasaki, A. Takahashi, J. Pan, N. Yamaguchi, K.K. Yokoyama, Phosphorylation of Activation Transcription Factor-2 at Serine 121 by Protein Kinase C Controls c-Jun-mediated activation of transcription, *J. Biol. Chem.* 284 (2009) 8567–8581.
- [27] J.P. Petiti, S. Gutierrez, J.H. Mukdsi, A.L. De Paul, A.I. Torres, Specific subcellular targeting of PKC α and PKC ϵ in normal and tumoral lactotroph cells by PMA-mitogenic stimulus, *J. Mol. Histol.* 40 (2009) 417–425.
- [28] A.M. Martelli, C. Evangelisti, M. Nyakern, F.A. Manzoli, Nuclear protein kinase C, *Biochim. Biophys. Acta* 1761 (2006) 542–551.
- [29] N.M. Hasan, P.J. Parker, G.E. Adams, Induction and phosphorylation of protein kinase C- α and mitogen-activated protein kinase by hypoxia and by radiation in Chinese hamster V79 cells, *Radiat. Res.* 145 (1996) 128–133.
- [30] P.R. Debata, B. Ranasinghe, A. Berliner, G.M. Curcio, S.J. Tantry, E. Ponimaskin, P. Banerjee, Erk1/2-dependent phosphorylation of PKC α at threonine 638 in hippocampal 5-HT(1A) receptor-mediated signaling, *Biochem. Biophys. Res. Commun.* 397 (2010) 401–406.
- [31] T. Seki, H. Matsubayashi, T. Amano, Y. Shirai, N. Saito, N. Sakai, Phosphorylation of PKC activation loop plays an important role in receptor-mediated translocation of PKC, *Genes Cells* 10 (2005) 225–239.
- [32] F. Bornancin, P.J. Parker, Phosphorylation of protein kinase C- α on serine 657 controls the accumulation of active enzyme and contributes to its phosphatase-resistant state, *J. Biol. Chem.* 272 (1997) 3544–3549.
- [33] L.M. Keranen, E.M. Dutil, A.C. Newton, Protein kinase C is regulated in vivo by three functionally distinct phosphorylations, *Curr. Biol.* 5 (1995) 1394–1403.
- [34] C. De Ponti, R. Carini, E. Alchera, M.P. Nitti, M. Locati, E. Albano, G. Cairo, L. Tacchini, Adenosine A2a receptor-mediated, normoxic induction of HIF-1 through PKC and PI-3K-dependent pathways in macrophages, *J. Leukoc. Biol.* 82 (2007) 392–402.
- [35] J.E. Ziello, I.S. Jovin, Y. Huang, Hypoxia-Inducible Factor (HIF)-1 regulatory pathway and its potential for therapeutic intervention in malignancy and ischemia, *Yale J. Biol. Med.* 80 (2007) 51–60.
- [36] A.S. Hui, A.L. Bauer, J.B. Striet, P.O. Schnell, M.F. Czyzyk-Krzeska, Calcium signaling stimulates translation of HIF- α during hypoxia, *FASEB J.* 20 (2006) 466–475.
- [37] N. Koshiishi, J.M. Chong, T. Fukasawa, R. Ikeno, Y. Hayashi, N. Funata, H. Nagai, M. Miyaki, Y. Matsumoto, M. Fukayama, p300 gene alterations in intestinal and diffuse types of gastric carcinoma, *Gastric Cancer Off. J. Int. Gastric Cancer Assoc. Jpn. Gastric Cancer Assoc.* 7 (2004) 85–90.

Supplementary materials

Cobalt chloride-mediated protein kinase C α (PKC α) phosphorylation induces hypoxia-inducible factor 1 α (HIF1 α) in the nucleus of gastric cancer cell

Suvasmita Rath^{1*}, Aditya Anand^{1*}, Nilabh Ghosh¹, Lopamudra Das¹, Shrikant B Kokate¹, Pragyesh Dixit¹, Swetapadma Majhi¹, Niranjan Rout², Shivaram P Singh³, Asima Bhattacharyya^{1#}

¹National Institute of Science Education and Research (NISER), School of Biological Sciences, PO. Bhipur-Padanpur, Via- Jatni, Dist. Khurda, Odisha 752050, India.

²Department of Oncopathology, Acharya Harihar Regional Cancer Centre, Cuttack 753007, Odisha, India. ³Department of Gastroenterology, SCB Medical College, Cuttack 753007, Odisha, India.

*Contributed equally

#Corresponding author

Supplementary materials and methods

1. Cell culture and treatment

Gastric epithelial cancer cells (GECs) AGS, MKN45 or NCI-N87 were cultured and maintained as previously reported [1]. Cobalt chloride induces hypoxic condition similar to physiological hypoxia [2-6], modulates a similar group of genes as physiological hypoxia [7-9] and shows no cytotoxicity [7]. Cobalt chloride hexahydrate ($\text{CoCl}_2 \cdot 6\text{H}_2\text{O}$) (Sigma Aldrich) was used to examine the effect of hypoxia on P-PKC α , PKC α and HIF1 α expression. Experiments were done using AGS cell line, unless mentioned otherwise.

2. Plasmids, site-directed mutagenesis and transfection

QuikChange site directed mutagenesis kit (Agilent Technologies, Santa Clara, CA) was used to generate PKC α T638A mutant construct from the WT PKC α construct. The following mutagenesis primer was used to generate the T638A mutation in the WT PKC α construct- 5'CGAGGACAGCCCGTCTTAGCACCACCTGATCAGCTGGTT3' where ACA (T) was changed to GCA (A). 1×10^6 AGS cells were seeded in six-well cell culture plates 18–24 h before transfection and were transfected with 2 μg of plasmid DNA and 10 μl of Lipofectamine 2000 reagent (Invitrogen, CA). 32 h post-transfection, cells were treated with 200 μM dose of $\text{CoCl}_2 \cdot 6\text{H}_2\text{O}$ for various time periods.

3. Immunoprecipitation, western blotting and antibodies

Whole cell lysates were prepared by using standard protocol. Nuclear and cytoplasmic fractions were isolated using NE-PER kit (Thermo scientific, MI). These lysates were separated by SDS-PAGE followed by western blotting. Membranes were incubated with antibodies against P-PKC α (Abcam, Cambridge, MA), PKC α , HDAC1 (Cell Signaling Technology, MA), HIF1 α and GAPDH (Abcam). GAPDH and HDAC1 antibodies were used for normalization of protein loading for the cytoplasmic and nuclear fractions, respectively. Membranes were detected by using Super Signal West Femto kit (Thermo Scientific, MI).

Chemidoc XRS (Bio-Rad, Hercules, CA) equipped with Quantity One -4.6.9 software was used for visualization of western blots. Immunoprecipitation was performed by using p300 and HIF1 α antibody to determine interaction between p300, PKC α and HIF1 α .

4. *Confocal microscopy*

AGS cells were plated at a density of 0.166×10^6 cells/ well and treated with CoCl₂ for 30 min, 1 h and 3 h. In another experiment, cells were transfected with pcDNA3.1⁺ (empty vector), PKC α WT, PKC α T638A and PKC α DN constructs using Lipofectamine 2000 (Invitrogen) and cells were treated with CoCl₂ for 1 h. Cells were fixed with 4% paraformaldehyde at 37°C for 15 min. Staining was done for P-PKC α , and PKC α followed by DAPI (4', 6-Diamidino-2-Phenylindole, Dilactate (Invitrogen) treatment for 20 min. Cellular distribution of P-PKC α and PKC α was assessed by a laser scanning confocal microscope (LSM 780, Carl Zeiss, Jena, Germany) with argon laser 488 excitation and a 63X/1.4 NA oil objective (Carl Zeiss). The microscope was equipped with LSM-TPMT camera system (Carl Zeiss) and ZEN 2010 software (Carl Zeiss). Images were analyzed using LSM software (Carl Zeiss). All images were acquired at room temperature and images were digitally processed for presentation using Adobe Photoshop CS4.

5. *Dual luciferase assay*

To study the effect of PKC α overexpression and to standardize the time point of CoCl₂ treatment- on the transcriptional activity of HIF1 α , we transfected AGS cells with pGL3-HRE-luciferase construct (containing 4 tandem repeats of human EPO gene HRE) [10] and the *Renilla* luciferase construct phRLTK at a ratio of 24.5:24.5:1 followed by CoCl₂ treatment for 30 min and 1 h. In another set of experiments, cells were transfected with pcDNA3.1⁺ (empty vector) or PKC α -WT or PKC α -T638A or PKC α -DN along with pGL3-HRE-luciferase construct and phRLTK construct for 24 h and then hypoxia was induced by

CoCl₂ treatment for 1 h. Dual luciferase assay was performed according to manufacturer's instruction (Promega, CA).

Supplementary figures and figure legends

Fig. S1.

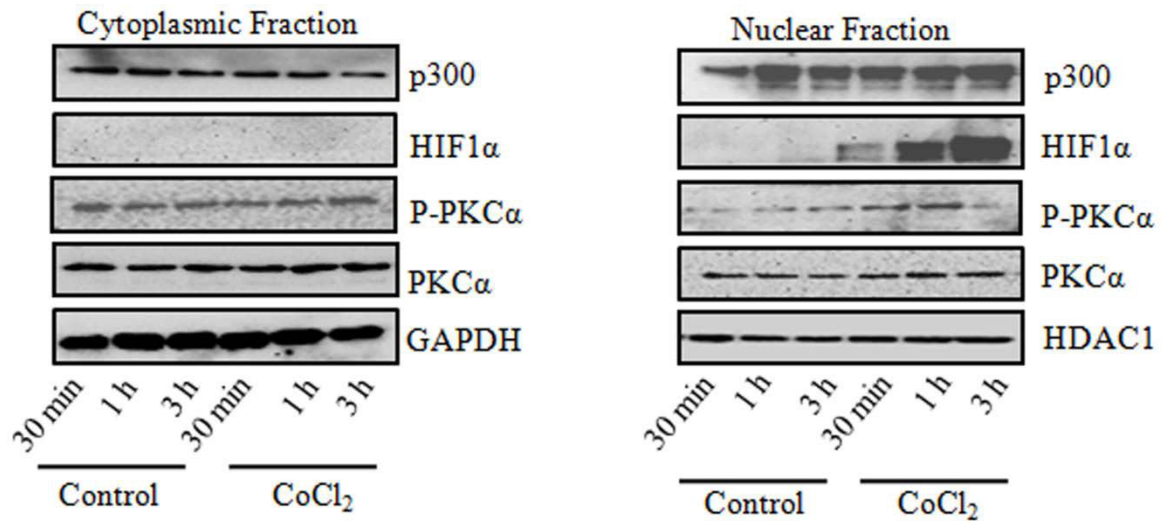


Fig. S1. CoCl₂ induced PKC α phosphorylation in the nucleus of NCI-N87 cell. Representative western blot (n=3) of nuclear and cytosolic lysates prepared from NCI-N87 cells treated with 200 μ M CoCl₂ for various time points (30 mins, 1 h, 3 h). GAPDH was used as a loading control for the cytoplasmic fraction while HDAC1 was used as a loading control for the nuclear fraction.

Fig. S2.

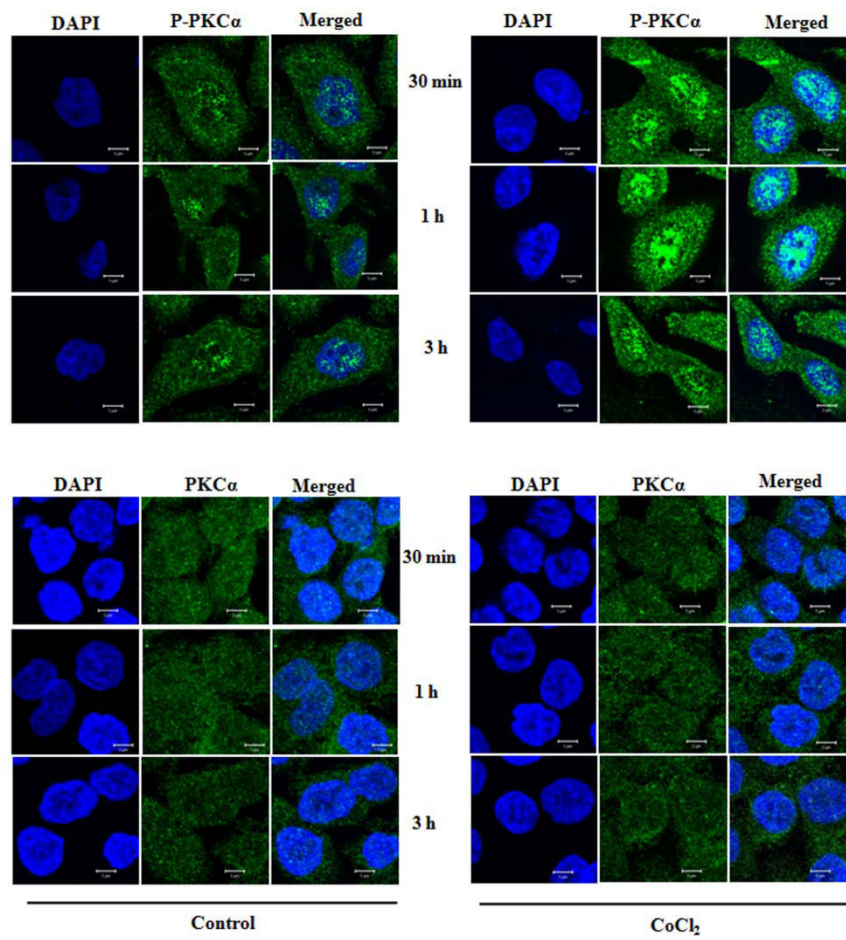


Fig. S2. All panels used to prepare the merged images of Fig. 1C.

Fig. S3.

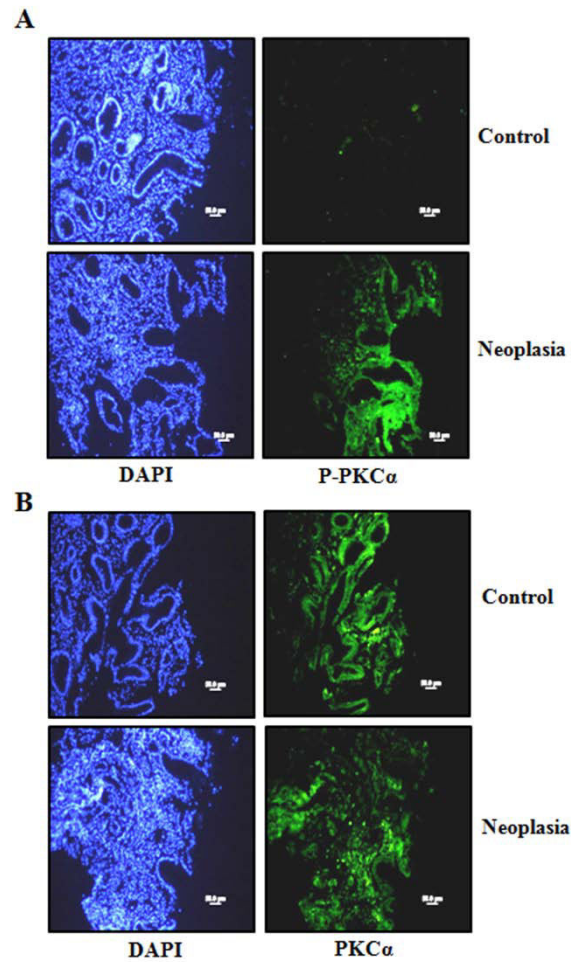


Fig. S3. Fluorescence microscopy of gastric biopsies from gastric neoplasia patients. (A) Comparison of P-PKC α expression in antral neoplastic gastric epithelial biopsy samples with adjacent non-cancer gastric biopsies (control) and (B) comparison of PKC α expression in non-cancer and gastric neoplasia samples (n=4 for each group). Scale 100 μ m.

Fig. S4.

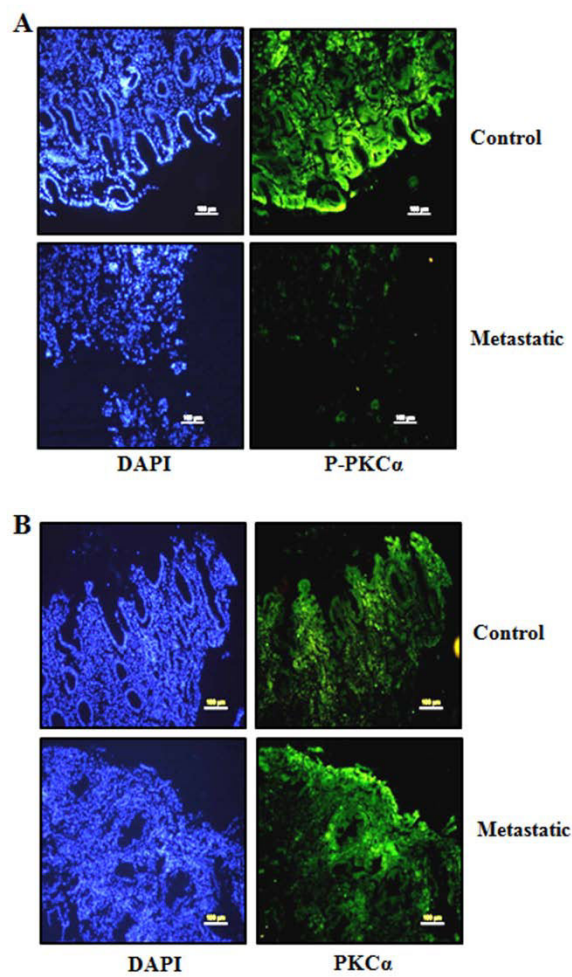


Fig. S4. Fluorescence microscopy of gastric biopsies from metastatic gastric cancer patients. (A) Comparison of metastatic gastric cancer biopsy samples (epithelia) with adjacent non-cancer gastric biopsies (control) for P-PKCa and (B) PKCa expression (n=4 in each group). Scale 100 μ m.

Fig. S5.

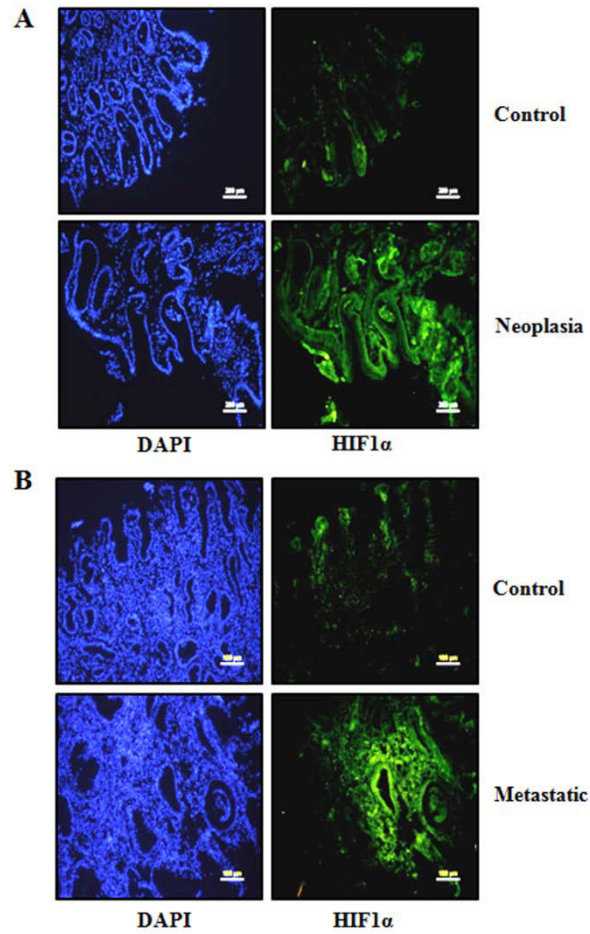


Fig. S5. HIF1 α expression in gastric neoplasia and metastatic cancer samples. (A) Fluorescence microscopy to study HIF1 α expression in neoplastic and (B) metastatic gastric cancer samples along with their respective controls (n=4 in each group). Scale 100 μ m.

Supplementary references:

- [1] A. Bhattacharyya, R. Chattopadhyay, B.R. Burnette, J.V. Cross, S. Mitra, P.B. Ernst, K.K. Bhakat, S.E. Crowe, Acetylation of apurinic/apyrimidinic endonuclease-1 regulates *Helicobacter pylori*-mediated gastric epithelial cell apoptosis, *Gastroenterology* 136 (2009) 2258-2269.
- [2] Y. Huang, K.M. Du, Z.H. Xue, H. Yan, D. Li, W. Liu, Z. Chen, Q. Zhao, J.H. Tong, Y.S. Zhu, G.Q. Chen, Cobalt chloride and low oxygen tension trigger differentiation of acute myeloid leukemic cells: possible mediation of hypoxia-inducible factor-1alpha, *Leukemia* 17 (2003) 2065-2073.
- [3] J.Y. Jung, W.J. Kim, Involvement of mitochondrial- and Fas-mediated dual mechanism in CoCl₂-induced apoptosis of rat PC12 cells, *Neurosci. Lett.* 371 (2004) 85-90.
- [4] S. Bae, H.J. Jeong, H.J. Cha, K. Kim, Y.M. Choi, I.S. An, H.J. Koh, D.J. Lim, S.J. Lee, S. An, The hypoxia-mimetic agent cobalt chloride induces cell cycle arrest and alters gene expression in U266 multiple myeloma cells, *Int. J. Mol. Med.* 30 (2012) 1180-1186.
- [5] B. Ateghang, M. Wartenberg, M. Gassmann, H. Sauer, Regulation of cardiotrophin-1 expression in mouse embryonic stem cells by HIF-1alpha and intracellular reactive oxygen species, *J. Cell Sci.* 119 (2006) 1043-1052.
- [6] E.H. Kim, J.H. Won, I. Hwang, J.W. Yu, Cobalt Chloride-induced Hypoxia Ameliorates NLRP3-Mediated Caspase-1 Activation in Mixed Glial Cultures, *Immune network* 13 (2013) 141-147.
- [7] Z. Ji, G. Yang, S. Shahzidi, K. Tkacz-Stachowska, Z. Suo, J.M. Nesland, Q. Peng, Induction of hypoxia-inducible factor-1alpha overexpression by cobalt chloride

- enhances cellular resistance to photodynamic therapy, *Cancer Lett.* 244 (2006) 182-189.
- [8] S.G. Lee, H. Lee, H.M. Rho, Transcriptional repression of the human p53 gene by cobalt chloride mimicking hypoxia, *FEBS Lett.* 507 (2001) 259-263.
- [9] A. Vengellur, B.G. Woods, H.E. Ryan, R.S. Johnson, J.J. LaPres, Gene expression profiling of the hypoxia signaling pathway in hypoxia-inducible factor 1alpha null mouse embryonic fibroblasts, *Gene Expr.* 11 (2003) 181-197.
- [10] M. Ema, S. Taya, N. Yokotani, K. Sogawa, Y. Matsuda, Y. Fujii-Kuriyama, A novel bHLH-PAS factor with close sequence similarity to hypoxia-inducible factor 1alpha regulates the VEGF expression and is potentially involved in lung and vascular development, *Proc. Natl. Acad. Sci. U. S. A.* 94 (1997) 4273-4278.

Regulation of Noxa-mediated apoptosis in *Helicobacter pylori*-infected gastric epithelial cells

Suvasmita Rath,* Lopamudra Das,* Shrikant Babanrao Kokate,* B. M. Pratheek,* Subhasis Chattopadhyay,* Chandan Goswami,* Ranajoy Chattopadhyay,^{†,1} Sheila Eileen Crowe,^{†,1} and Asima Bhattacharyya^{*,2}

*National Institute of Science Education and Research, School of Biological Sciences, Bhubaneswar, Odisha, India; and [†]Department of Medicine, University of Virginia, Charlottesville, Virginia, USA

ABSTRACT *Helicobacter pylori* induces the antiapoptotic protein myeloid cell leukemia 1 (Mcl1) in human gastric epithelial cells (GECs). Apoptosis of oncogenic protein Mcl1-expressing cells is mainly regulated by Noxa-mediated degradation of Mcl1. We wanted to elucidate the status of Noxa in *H. pylori*-infected GECs. For this, various GECs such as AGS, MKN45, and KATO III were either infected with *H. pylori* or left uninfected. The effect of infection was examined by immunoblotting, immunoprecipitation, chromatin immunoprecipitation assay, *in vitro* binding assay, flow cytometry, and confocal microscopy. Infected GECs, surgical samples collected from patients with gastric adenocarcinoma as well as biopsy samples from patients infected with *H. pylori* showed significant up-regulation of both Mcl1 and Noxa compared with noninfected samples. Coexistence of Mcl1 and Noxa was indicative of an impaired Mcl1-Noxa interaction. We proved that Noxa was phosphorylated at Ser¹³ residue by JNK in infected GECs, which caused cytoplasmic retention of Noxa. JNK inhibition enhanced Mcl1-Noxa interaction in the mitochondrial fraction of infected cells, whereas overexpression of nonphosphorylatable Noxa resulted in enhanced mitochondria-mediated apoptosis in the infected epithelium. Because phosphorylation-dephosphorylation can regulate the apoptotic function of Noxa, this could be a potential target molecule for future treatment approaches for *H. pylori*-induced gastric cancer.—Rath, S., Das, L., Kokate, S. B., Pratheek, B. M., Chattopadhyay, S., Goswami, C., Chattopadhyay, R., Crowe, S. E., Bhattacharyya, A. Regulation of Noxa-mediated apoptosis in *Helicobacter pylori*-infected gastric epithelial cells. *FASEB J.* 29, 796–806 (2015). www.fasebj.org

Key Words: JNK • cytochrome *c* • gastric cancer • myeloid cell leukemia 1 • mitochondrial fragmentation

Abbreviations: *cag*, cytotoxin-associated gene; ChIP, chromatin immunoprecipitation; GEC, gastric epithelial cell; Hif1, hypoxia-inducible factor 1; HRE, hypoxia-response element; IHC, immunohistochemistry; MALT, mucosa-associated lymphoid tissue; Mcl1, myeloid cell leukemia 1; MOI, multiplicity of infection; mut, mutant; PAI, pathogenicity island; p.i., postinfection; P-JNK, phospho-JNK; P-Noxa, phosphorylated Noxa; P-S-Noxa, phospho-Ser-Noxa; ROS, reactive oxygen species; shRNA, short hairpin RNA; UVA, University of Virginia; WT, wild-type

HELICOBACTER PYLORI infects the human stomach leading to gastritis, gastric and duodenal ulcers, gastric carcinoma, and mucosa-associated lymphoid tissue (MALT) lymphoma (1). The risk for gastric cancer is at least 2-fold greater in infected persons than in uninfected individuals. *H. pylori* promotes gastric cancer either *via* its cancer-promoting effects or *via* creating a carcinogenic environment by inducing host inflammatory responses to chronic infection. Signaling events induced in infected host cells play crucial roles in determining disease pathogenesis. One of the major signaling molecules induced in *H. pylori*-infected gastric epithelial cells (GECs) is hypoxia-inducible factor 1 (Hif1), a heterodimeric transcription factor (2, 3). Endogenous or *H. pylori*-induced gastric epithelial reactive oxygen species (ROS) stabilize the oxygen-labile α -subunit of Hif1 in normoxic condition (3, 4), whereas the β -subunit is constitutively expressed (5). Several cellular processes including cell proliferation, apoptosis, and tumor angiogenesis are regulated by Hif1 (5). A Bcl2 family antiapoptotic and tumorigenic protein myeloid cell leukemia 1 (Mcl1) and a proapoptotic Bcl2 homology 3 (BH3)-only tumor suppressor protein Noxa (synonyms are immediate-early response protein *APR* or phorbol 12-myristate 13-acetate-induced protein 1) both contain hypoxia-response elements (HREs) in their promoters (6, 7). *H. pylori* infection augments expression of both Mcl1 (2) and Noxa in the infected GECs (8). Noxa is a unique BH3 protein because it binds only with Mcl1 and A1 pro-survival proteins, whereas other BH3 proteins can interact with any Bcl2 family member. However, a recent finding shows that Noxa can bind to other antiapoptotic and proapoptotic proteins as well (9). Mcl1 has potent antiapoptotic and tumorigenic functions, but in effect, it is an extremely short-lived molecule due to its proteasomal degradation. Noxa imparts its apoptotic function mainly by translocating to mitochondria followed by its binding with Mcl1. Noxa-bound Mcl1 is targeted for proteasomal degradation (10). In the presence of glucose, Noxa

¹ Current affiliation: School of Medicine, University of California, San Diego, San Diego, California, USA.

² Correspondence: National Institute of Science Education and Research, School of Biological Sciences, Bhubaneswar 751005, Odisha, India. E-mail: asima@niser.ac.in
doi: 10.1096/fj.14-257501

This article includes supplemental data. Please visit <http://www.fasebj.org> to obtain this information.

phosphorylation by Cdk5 sequesters the BH3 protein in the cytoplasm and decreases apoptosis of proliferating leukemia cell lines and primary T cells (11). Understanding the regulation of Mcl1 stability by Noxa is important for developing cancer therapeutics, especially for cancers with up-regulated Mcl1 expression. Because Mcl1 is highly induced in gastric cancer and is associated with a poor prognosis (12), studying the Mcl1-Noxa interaction in *H. pylori*-infected GECs would help in designing better treatment strategies for *H. pylori*-induced gastric cancer.

To gain insight into the kinetics of expression of Mcl1 and Noxa in *H. pylori*-infected GECs, we analyzed expression of Mcl1 and Noxa over a time period. Our results show that although *H. pylori* simultaneously up-regulates both Mcl1 and Noxa expression in the infected GECs, Mcl1 is not degraded, suggesting phosphorylation of Noxa. We confirm that Noxa is phosphorylated by JNK, a stress-induced MAPK activated in *H. pylori*-infected GECs. Furthermore, we prove that *H. pylori*-mediated phosphorylation regulates the apoptotic function of Noxa in the infected GEC.

MATERIALS AND METHODS

Cell culture and bacteria

Gastric epithelial cancer cells AGS, MKN-45, NCI-N87, and KATO III, and *H. pylori* strain 26695 and 8-1 [a cytotoxin-associated gene (*cag*) pathogenicity island (PAI) (+) strain (American Type Culture Collection, Manassas, VA, USA) and a *cag* PAI(-) strain, respectively] were cultured and maintained as previously reported (13).

Plasmids, mutagenesis, and transfections

Human wild-type (WT) Noxa sequence and S13A mutant (mut) sequence were cloned in pcDNA3.1⁺ vector (Invitrogen, Carlsbad, CA, USA) by using *Hind*III and *Xho*I as restriction enzymes. Primers used for WT Noxa cloning were 5'-AAAAGCTTCAC-CATGCTGGGAAGAAGGCGCGC-3' (forward primer) and 5'-GCTCGAGTCAGGTTCTGAGCAGAAGAGTTTGGATATCA-GATTCAG-3' (reverse primer). Noxa S13A mut was generated by using Noxa WT construct as a template using the QuikChange Site-Directed Mutagenesis Kit (Agilent Technologies, Santa Clara, CA, USA) following the manufacturer's instructions. The primer used for mutagenesis was 5'-AAGAACGCTCAACCGGCC-(AGC)CCCGCGCGGGCTCCA-3', where the codon for A (underlined and in italics) replaced the Ser¹³ of WT Noxa (in parentheses, original codon). JNK1 and JNK2 constructs used were described earlier (14, 15). A total of 1×10^6 AGS cells were seeded in 6-well cell culture plates 18–24 h before transfection and were transfected with 2 μ g plasmid DNA and 10 μ l Lipofectamine 2000 reagent (Invitrogen). Cells were infected after 24 h of transfections.

Stable *hif1 α* knockdown in AGS cells

hif1 α was stably knocked down using short hairpin RNA (shRNA) using Lipofectamine 2000 reagent. We also derived stable cells expressing empty negative control shRNA and scrambled negative control shRNA-expressing cells. All constructs (HuSH plasmids) were purchased from OriGene Technologies, Incorporated (Rockville, MD, USA).

Infections and treatments

Cells were infected with various multiplicities of infection (MOIs) of *H. pylori* for specified periods. We found that an MOI of 200 for 5 h was optimum to induce Hif1 α and Noxa in GECs. When required, AGS cells were pretreated with 150 nM Echinomycin (Sigma-Aldrich, St. Louis, MO, USA), MEK1/2 inhibitor PD98059, p38 MAPK inhibitor SB203580, and JNK inhibitor II (all from Calbiochem, San Diego, CA, USA) at 25 μ M concentration for 1 h prior to infection.

Human GEC isolation from mucosal biopsy specimens

Gastric biopsy samples from the gastric antral mucosa were collected from individuals undergoing esophagogastroduodenoscopy, as per a University of Virginia (UVA) institutional review board-approved protocol. Epithelial cells were isolated, cultured, and infected with an MOI of 200 of *H. pylori* 26695 or 8-1 for 5 h as mentioned previously (13).

Mitochondrial and cytosolic lysate preparation

A total of 2×10^6 cells were collected by centrifugation at $1300 \times g$ for 3 min at 4°C. Cells were resuspended in 150 μ l ice-cold extraction buffer containing 20 mM 4-(2-hydroxyethyl)piperazine-1-ethanesulfonic acid (pH 7.5), 10 mM KCl, 150 mM sucrose, 1.5 mM MgCl₂, 1 mM EDTA, 1 mM EGTA, and 1 mM DTT supplemented with protease inhibitor cocktail (Sigma-Aldrich) and kept for 10 min at 4°C. Cells were homogenized by 20 passages through a 26-gauge needle. Homogenates were centrifuged at $10,000 \times g$ at 4°C for 5 min to remove nuclei and unbroken cells. Supernatant was centrifuged at $12,000 \times g$ for 30 min at 4°C to obtain the cytosolic fraction in supernatant. The mitochondria-enriched pellet was resuspended in cold 10 μ l lysis buffer containing 20 mM Tris-HCl (pH 7.4), 150 mM NaCl, 1% Nonidet P-40, and 1 mM DTT along with protease inhibitor cocktail followed by 20 min incubation on ice and finally centrifuged at $15,000 \times g$ for 5 min. Mitochondrial lysate was collected and boiled with an equal volume of 2 \times Laemmli buffer (HiMedia, Mumbai, Maharashtra, India).

Immunoprecipitation, Western blotting, and antibodies

Whole-cell lysates were prepared from GECs after treatments and were separated by SDS-PAGE followed by Western blotting. Blots were probed with antibodies to phosphoserine and phosphotyrosine (Sigma-Aldrich), CagA (Santa Cruz Biotechnology, Santa Cruz, CA, USA), caspase-3 (Sigma-Aldrich), Noxa, Hif1 α , Mcl1, and Cdk5 (all from Abcam, Cambridge, MA, USA), p53 (Calbiochem), phospho-JNK, JNK, phospho-ERK, ERK, phospho-p38, p38, cytochrome *c*, phospho-p53 (Ser¹⁵) Cdk5, and Bax (all from Cell Signaling Technology, Danvers, MA, USA). α -Tubulin (Abcam) and histone deacetylase 1 and Cox IV (both from Cell Signaling Technology) antibodies were used for normalization of protein loading. Noxa was immunoprecipitated to analyze interaction between Noxa and JNK. Mcl1 was immunoprecipitated from mitochondrial fraction to assess its interaction with Bax and Noxa. Proteins were detected by using the Thermo Scientific SuperSignal West Femo Chemiluminescent Substrate kit (Thermo Fisher Scientific, Kalamazoo, MI, USA). Western blot images were taken with ChemiDoc XRS (Bio-Rad Laboratories, Hercules, CA, USA) equipped with Quantity One 1-D Analysis software version 4.6.9 (Bio-Rad Laboratories).

Chromatin immunoprecipitation assay

Chromatin immunoprecipitation (ChIP) assay was performed using the QuikChIP Kit (Imgenex, San Diego, CA, USA) as

described before (13). Following treatments, chromatin was sonicated into fragments with an average length of 0.5–3 kb. After centrifugation at $12,000 \times g$ for 10 min, supernatants were diluted in dilution buffer, and immunoprecipitation was performed using Hif1 α antibody (Novus Biologicals, Littleton, CO, USA). ChIP DNA was detected by PCR with the primers 5'-GACGGG-GTTTCACCATATTGGCAAG-3' (forward primer) and 5'-TGA-GAGCCGCTTCATGCTAAGGACTT-3' (reverse primer) targeting a 346 bp region from the *nox*a promoter containing the HRE region. Specificity of the reaction was assessed by using a pair of negative control primers (5'-GCACGTTTCATCAATTTGAA-GAAAGACTGC-3' and 5'-AACAGCAACAACAACA ATGCACT-GAACTGT-3') from the 5'-upstream region of *nox*a promoter. After reversing the DNA-protein cross-links in the immunocomplexes, the *nox*a promoter sequence in the oligonucleotide containing the HRE region (91 bp) was quantitated by real-time PCR using the DNA Engine Opticon continuous fluorescence detector (Bio-Rad Laboratories). Preoptimized FAM-labeled primer-probe sets for *nox*a and 18S rRNA (Applied Biosystems, Foster City, CA, USA) were used for the study.

In vitro binding assay

Nuclear extracts were prepared from treated cells using the Nuclear and Cytoplasmic Extraction Kit (Thermo Fisher Scientific, Rockford, IL, USA). Streptavidin-coated superparamagnetic beads (Dynabeads M-280 Streptavidin, Dynal; Invitrogen) were used to capture 5'-biotinylated double-stranded *nox*a HRE oligonucleotide, and binding assays were performed as described previously (13). The *nox*a HRE WT oligos were 5'-TGGGA TTA-CAGCGTGAGCCACCGCGT-3' and 5'-ACGCGGTGGCT-CACGCCTGTAATCCCA-3', whereas mut primers were 5'-TGGGATTAACAGGCGACAGCCACCGCGT-3' and 5'-ACGCGGTGGCTGTGCCCTGTAATCCCA-3'. These primers were biotinylated at the 5' end. Bound proteins were dissociated by boiling in $1 \times$ Laemmli sample buffer and analyzed by Western blotting.

Immunohistochemistry

Immunohistochemistry (IHC) staining was performed for Hif1 α , Mcl1, and Noxa proteins. Paraffin-embedded infected or uninfected biopsy samples were collected following a UVA institutional review board-approved protocol. Surgical sections of gastric adenocarcinomas were obtained from the UVA Biorepository and Tissue Research Facility. Sections were stained as previously reported (13). Dilutions of primary antibodies were as follows: Hif1 α (Novus Biologicals), Mcl1 (BD Biosciences, Franklin Lakes, NJ, USA), and Noxa (ProSci, Poway, CA, USA). Digital images were captured using the Aperio ScanScope XT Slide Scanner (Aperio Technologies, Vista, CA, USA).

Flow cytometry

AGS cells were either infected with *H. pylori* for 10 h or left uninfected. Cells were harvested and washed twice with chilled PBS. Cells were then stained with Annexin V PE/7-AAD dyes (BD Biosciences) as per manufacturer's instruction. In a separate set of experiments, AGS cells were transfected with either Noxa WT or Noxa S13A plasmid constructs or empty vector followed by infection with *H. pylori* for 10 h. Cells were stained with Annexin V PE/7-AAD dyes. A total of 10,000 cells were acquired by the FACSCalibur Flow Cytometer (BD Biosciences) and analyzed by CellQuest Pro software (BD Biosciences).

Cell viability assay using trypan blue

AGS cells were kept uninfected or infected with *H. pylori* for 10 h. In another set, AGS cells were transfected with either Noxa WT or

Noxa S13A plasmid constructs or empty vector followed by infection with *H. pylori* for 10 h. A total of $20 \mu\text{l}$ cell suspension was mixed with $180 \mu\text{l}$ trypan blue (Invitrogen), and cell counting was done using a Neubauer hemocytometer (Camlab Ltd., Cambridge, United Kingdom).

Confocal microscopy

Noxa WT and S13A mutant or empty vector constructs were transfected in pDsRed2 (Clontech, Mountain View, CA, USA)-expressing AGS stable cells. Cells were fixed with 4% paraformaldehyde at 37°C for 15 min followed by DAPI (dilactate; Invitrogen) treatment for 20 min. Mitochondrial integrity was assessed by a laser-scanning confocal microscope (LSM 780; Carl Zeiss, Jena, Germany) with argon laser 488 excitation and a $63 \times / 1.4$ NA oil objective (Carl Zeiss). The microscope was equipped with an LSM-TPMT camera system and ZEN 2010 software (both from Carl Zeiss). Images were analyzed using LSM software (Carl Zeiss). All images were acquired at room temperature and digitally processed for presentation using Adobe Photoshop CS4 (Adobe Systems Incorporated, San Jose, CA, USA). Mitochondrial fragmentation (measured by length, circularity, and roundness) was quantified by ImageJ software (NIH, Bethesda, MD, USA). Roundness [$4 \times (\text{surface area}) / (\pi \times \text{major axis}^2)$] and circularity [$4\pi \times (\text{surface area} / \text{perimeter}^2)$] are indices of sphericity, with values of 1 indicating perfect spheroids.

Statistics

Values are given as the mean SE. Student's *t* test was performed for comparisons of 2 groups. Statistical significance was determined at $P < 0.05$. 2-way ANOVA was performed to compare various transfection groups. Tukey test was applied for *post hoc* comparisons.

RESULTS

***H. pylori* infection induces Noxa but does not degrade Mcl1 in the human GECs**

The present study aimed to assess the effect of *H. pylori* infection on Noxa expression because the Mcl1/Noxa axis plays a crucial role in regulating the life span of a cell. For this, AGS cells were infected with a *cagPAI*(+) *H. pylori* strain 26695 at an MOI of 200 for various time periods. Representative Western blot results ($n = 3$) showed that *H. pylori* time-dependently increased both Mcl1 and Noxa expression (Fig. 1A), reaching a maximal level at 5 h postinfection (p.i.). We observed that strain 26695 at an MOI of 200 and 300 equally induced Hif1 α (data not shown), but lower MOIs had no significant effect on Hif1 α expression (2). Accordingly, all future experiments were performed with the 26695 strain at an MOI of 200 for 5 h unless stated otherwise. We also performed IHC analyses on human gastric biopsy samples obtained from uninfected ($n = 5$) and infected ($n = 5$) subjects. Both Noxa and Mcl1 were significantly increased in *H. pylori*-infected samples (Fig. 1B), which corroborated our observations in cultured AGS cells. Noxa and Mcl1 are induced in various cancers (16, 17). We also observed induced expression of both Noxa and Mcl1 in surgically resected human gastric adenocarcinoma samples as compared to

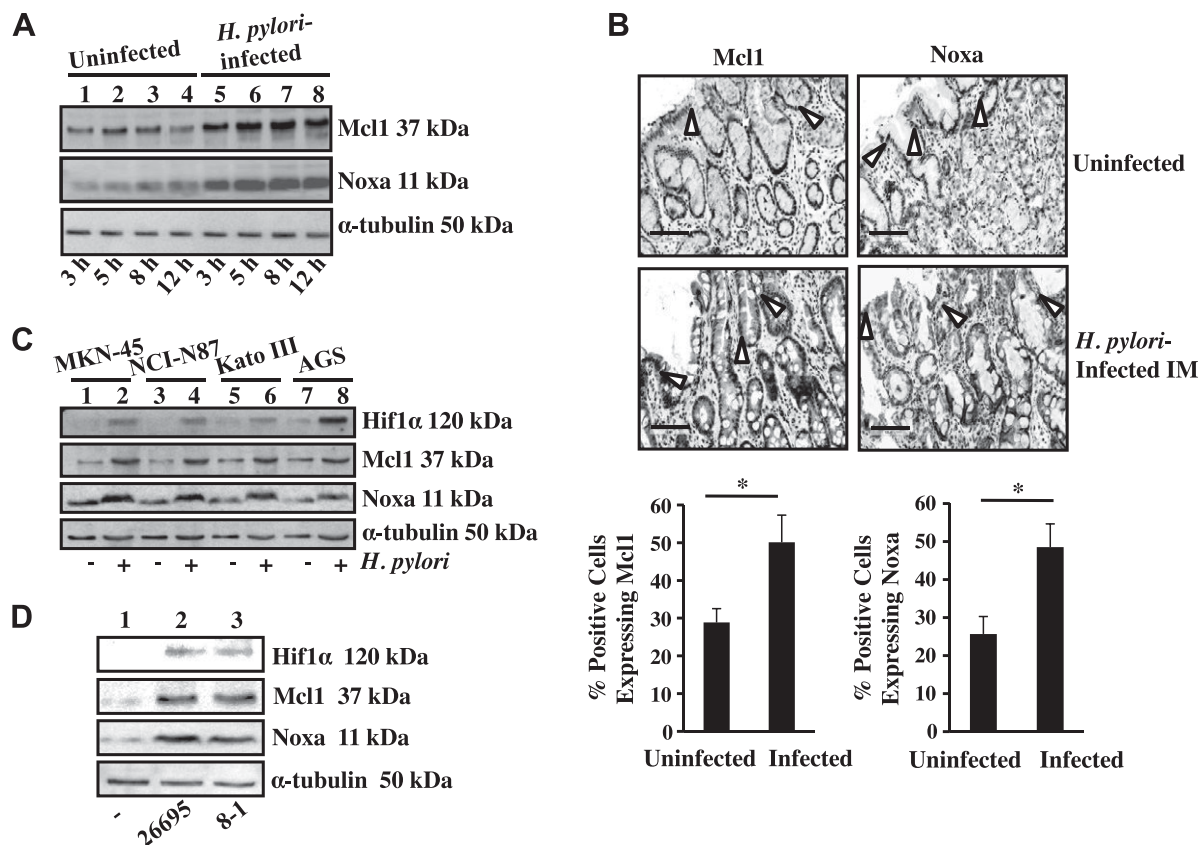


Figure 1. *H. pylori*-induced Noxa and Mcl1 expression in GECs. **A)** A representative Western blot ($n = 3$) of whole-cell lysates prepared from uninfected and infected (3, 5, 8, and 12 h with an MOI of 200) AGS cells showed time-dependent induced expression of Noxa and Mcl1. α -Tubulin was used as a loading control. **B)** Immunohistochemical staining of biopsy samples from uninfected and *H. pylori*-infected patients showing expression of Noxa as well as Mcl1 in the epithelium as well as lamina propria (open arrows indicate epithelial cell lining in the gastric mucosa). Quantification is shown of Mcl1+ and Noxa+ cells in the infected and uninfected gastric mucosa ($n = 5$). Graph shows the mean \pm SEM. $*P < 0.05$, Student's *t* test. Original magnification, $\times 50$. Scale bars, 100 μ m. **C)** Expression of Hif1 α , Mcl1, and Noxa was analyzed by immunoblotting cell lysates prepared from uninfected or *H. pylori*-infected (an MOI of 200; 5 h) MKN-45, NCI-N87, KATO III, and AGS cells. α -Tubulin was kept as a loading control. **D)** Western blot analysis of epithelial cells isolated from 3 sets of uninfected human gastric biopsy samples and separately infected with either an MOI of 200 of *cag* PAI(-) 8-1 strain or (+) 26695 strain for 5 h. IM, intestinal metaplasia.

nonneoplastic gastric tissue sections (Supplemental Fig. S1). Other gastric cancer cell lines, MKN-45, NCI-N87, and Kato III, were assessed along with AGS cells for their ability to express Mcl1 and Noxa. Western blot results revealed that expression of Noxa and Mcl1 and their transcriptional activator Hif1 α was induced in all of these GECs (Fig. 1C). Hif1 α , Noxa, and Mcl1 were equally induced by *cag* PAI(+) and *cag* PAI(-) *H. pylori* strains (26695 and 8-1, respectively) in native GECs isolated from uninfected human gastric biopsy samples (Fig. 1D).

Hif1 α and its coactivator p300 bind to the *noxa* promoter in *H. pylori*-infected GECs

Enrichment of the *noxa* promoter HRE (mean \pm SEM, $n = 3$) by ChIP assay with Hif1 α revealed Hif1 α binding to the *noxa* promoter (Fig. 2A). *In vivo* binding of Hif1 α to the *noxa* HRE was analyzed by ChIP assay using Hif1 α antibody. The PCR product of DNA in the Hif1 α immunocomplex corresponding to the human *noxa* promoter flanking the HRE sequence demonstrated specific binding of Hif1 α

that was not present in the PCR product corresponding to the 5' far upstream region (Fig. 2B). Streptavidin-covered magnetic beads were coated with *noxa* HRE-specific oligos as well as HRE-mut oligo, and nuclear extracts from uninfected and infected cells were incubated with beads. Hif1 α and p300 binding to the *noxa* HRE (Fig. 2C) was observed only in *H. pylori*-infected cells. Coincubation of AGS cells with 150 nM Echinomycin (an inhibitor of DNA-binding activity of Hif1 and a peptide antibiotic) at the time of *H. pylori* infection abrogated Noxa expression induced by *H. pylori* (Fig. 2D), further indicating the importance of Hif1 in inducing Noxa expression in *H. pylori*-infected GECs. Because the human Noxa promoter has a p53-binding site, we assessed the expression of p53 and phospho-(Ser¹⁵) p53 in *H. pylori*-infected AGS cells. Infection for 3, 6, and 10 h with an MOI of 200 of *H. pylori* had no effect on p53 and phospho-p53 expression (data not shown). Comparison of Hif1 α shRNA stably expressing cell lines with scrambled shRNA and empty vector-expressing cells after *H. pylori* infection and Western blot analysis further confirmed the importance of Hif1 α in Noxa expression in *H. pylori*-infected GECs (Fig. 2E).

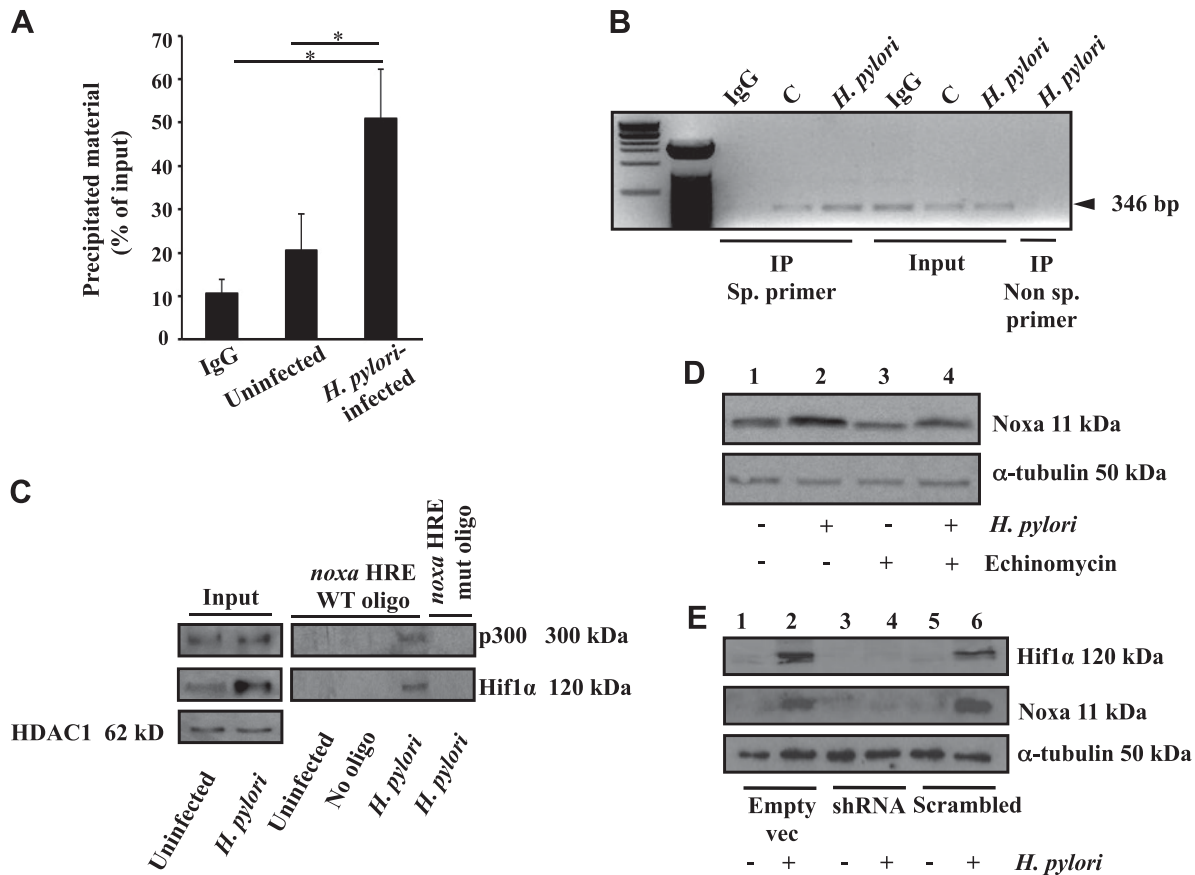


Figure 2. Hif1 α and its coactivator p300 interacted with the promoter region of *noxa* and enhanced Noxa expression after *H. pylori* infection. **A**) Enrichment of the *noxa* promoter HRE by ChIP with Hif1 α antibody relative to input DNA measured by real-time PCR (mean \pm SEM, $n = 3$). * $P < 0.05$. **B**) ChIP analysis of Hif1 α immunocomplex for the *noxa* promoter HRE. Specificity of Hif1 α binding to the *noxa* HRE was confirmed by comparing the 5' far upstream region (nonspecific [sp.] primer) with the HRE-flanking region of the *noxa* promoter. **C**) Western blotting ($n = 3$) showed binding of Hif1 α and its transcriptional coactivator p300 to the *noxa* promoter HRE (coated on streptavidin beads) after infection with an MOI of 200 of *H. pylori* for 5 h. **D**) Hif1 α -induced Noxa expression was validated by pretreating AGS cells with 150 nM Echinomycin prior to infection with an MOI of 200 of *H. pylori* for 5 h. α -Tubulin was the loading control. **E**) Western blotting ($n = 3$) showed expression of Noxa and Hif1 α in the negative control shRNA, scrambled negative control shRNA, and Hif1 α -shRNA stably expressing AGS cells. IP, immunoprecipitation; vec, vector.

Noxa is phosphorylated by JNK at Ser¹³ in *H. pylori*-infected GECs

Because the Mcl1 level was maintained in *H. pylori*-infected GECs despite sustained expression of Noxa (Fig. 1A), we wanted to assess the phosphorylation status of Noxa in infected AGS cells. Western blot ($n = 3$) analysis clearly indicated that Noxa was maximally phosphorylated at Ser residues at 5 h of *H. pylori* infection (Fig. 3A). We also found that Noxa phosphorylation by *H. pylori* was a *cag* PAI-independent event (Supplemental Fig. S2C). The *cag* PAI encodes proteins for a type IV secretion system (T4SS) that injects virulence factors into the infected host cell cytoplasm. *H. pylori* CagA protein is one such factor that is directly injected into the infected GECs, and upon phosphorylation, it enhances cell motility. To assess the *cag* PAI status of strains 26695 and 8-1, we infected AGS cells with an MOI of 200 of respective strains for 5 h. Western blotting of whole-cell lysates clearly showed CagA expression and its phosphorylation in 26695-infected cells, but not in cells infected with strain 8-1 (Supplemental Fig. S2D). GPS2.1 software (18) was used to predict potential phosphorylation sites of Noxa (Supplemental Fig. S2A) and to predict

kinases involved in its phosphorylation. Only Cdk5 and JNK appeared to have significant potential to phosphorylate at Ser¹³; p38 MAPK and ERKs phosphorylated with a much less predicted effect. However, we did not observe any expression of Cdk5 in GECs, which corroborated findings of other studies showing that the human stomach does not express Cdk5 (19, 20).

MAPKs have broad-tissue distributions except for JNK 3, which is expressed only in neurons, cardiac muscles, and testis. Phosphorylation of ERK1/ERK2, p38, and JNK occurs as early as 30 min after *H. pylori* infection and remains up-regulated until 24 h (21). We also found activation of these 3 MAPKs in infected GECs at 5 h of infection with an MOI of 200 (Fig. 3B and Supplemental Fig. S2E). MEK1 inhibitor PD98059 (25 μ M, 1 h pretreatment prior to infection) or p38 MAPK inhibitor SB203580 (25 μ M, 1 h pretreatment prior to infection) partly suppressed total Noxa and phospho-Ser-Noxa (P-S-Noxa) expression. This result corroborated findings of other studies showing that inhibition of ERK and p38 MAPK causes suppression of Noxa expression (22). In contrast, JNK inhibitor II or SP600125 (25 μ M, 1 h pretreatment) inhibited only P-S-Noxa formation in the infected GECs without suppressing

followed by infection with *H. pylori* and Western blotting of whole-cell lysates ($n = 4$). *H. pylori*-mediated induction of Mcl1 expression was significantly blocked in S13A mutant-transfected cells (Fig. 4A). These data indicated that although WT Noxa enhanced *H. pylori* infection-mediated Mcl1 expression, the nonphosphorylatable S13A mutant Noxa was unable to do so.

Reduced Mcl1 level is associated with mitochondrial apoptotic events (25). We assessed the effect of JNK inhibition on Mcl1-Noxa interaction. Mitochondrial lysates were prepared from vehicle (DMSO)-treated, 5 h *H. pylori*-infected, or JNK inhibitor II pretreated and infected AGS cells followed by immunoprecipitation with Mcl1. We observed Mcl1-Noxa interaction exclusively in JNK inhibitor-treated and -infected mitochondria, but not in infected cells without the inhibitor (Fig. 4B). Furthermore, this experiment showed that although Bax was bound with Mcl1 in *H. pylori*-infected AGS cells, JNK inhibitor II pretreatment completely abrogated Mcl1-Bax interaction.

Cytochrome *c* release is the hallmark of the intrinsic apoptotic pathway, and Noxa displaces apoptotic effectors such as Bak and Bax from Mcl1 so that these effectors can undergo oligomerization resulting in cytochrome *c* release (26). To identify the effect of Noxa phosphorylation on cytochrome *c* release in *H. pylori*-infected GECs, AGS cells

were transfected with WT Noxa, S13A Noxa, or the empty vector. Cytosolic and mitochondrial fractions were Western blotted. *H. pylori*-induced cytochrome *c* release in all transfected groups, but S13A-expressing *H. pylori*-infected cells showed substantially higher cytochrome *c* release ($n = 3$) (Fig. 4C). This result suggests that the apoptotic potential of Noxa is reduced by its phosphorylation. Because the release of cytochrome *c* into the cytosol leads to the activation of caspase-3 in apoptotic cells, we sought to understand the effect of Noxa and P-S-Noxa on caspase-3 activation in *H. pylori*-infected GECs. For this, AGS cells were transfected with the aforementioned constructs or transfected with empty vector followed by infection with *H. pylori* for 10 h or left uninfected. Western blot of cytosolic lysates ($n = 3$) showed that *H. pylori* maximally cleaved caspase-3 in S13A mutant-expressing cells compared to the infected counterparts from empty vector and WT Noxa-transfected groups (Fig. 4D).

AGS cells are very small, and their mitochondrial network is easily destroyed with mitochondrial stress (27). Confocal microscopy was performed to assess whether the cell death caused by *H. pylori* was linked with mitochondrial morphology changes. pDsRed2 stably expressing AGS cells were transiently transfected with empty vector or Noxa WT or S13A mutant followed by infection with *H. pylori* for 8 h.

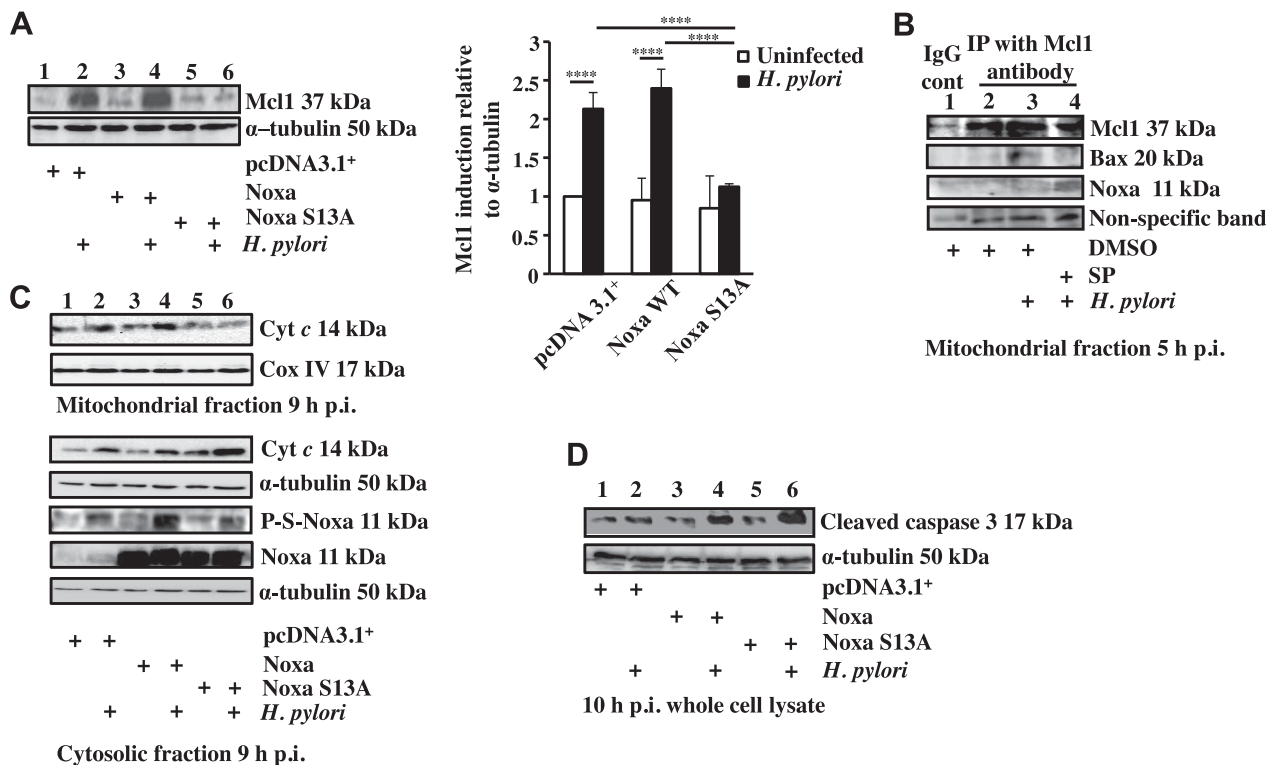


Figure 4. Mcl1 degradation, cytochrome *c* release, and cleaved caspase-3 formation were enhanced in S13A Noxa-expressing *H. pylori*-infected GECs. **A**) AGS cells were transfected with either empty vector, Noxa WT or Noxa S13A construct followed by infection for 5 h with an MOI of 200 of *H. pylori*, and Mcl1 status was analyzed by immunoblotting of whole-cell lysates. Data were analyzed by 2-way ANOVA with Tukey's *post hoc* test ($n = 4$). Error bars, SEM. **** $P < 0.0001$. **B**) Immunoprecipitation experiment assessing Mcl1-Noxa interaction and Mcl1-Bax interaction in the mitochondrial fraction of infected AGS cells. Mitochondrial extracts were immunoprecipitated with Mcl1 antibody after various treatments as indicated. A nonspecific band was used to estimate protein loading. **C**) Western blot showing phosphorylation status of Noxa and cytochrome (*Cyt c*) in the cytosol in 9 h *H. pylori*-infected AGS cells expressing either empty vector or Noxa WT or Noxa S13A. Corresponding mitochondrial fraction assessed cytochrome *c* retention status 9 h p.i. Cox IV was used as a loading control for mitochondrial fraction. **D**) Immunoblot of whole-cell lysates showing the status of cleaved caspase-3 in Noxa WT and S13A Noxa-transfected AGS cells infected with an MOI of 200 of *H. pylori* for 10 h. α-Tubulin was used as a loading control.

Mitochondrial phenotype was then assessed by confocal microscopy. The reticulotubular network of healthy mitochondria found in empty vector-transfected cells was partially disintegrated and appeared smaller in *H. pylori*-infected cells (Fig. 5A). Mitochondria lose their membrane potential and undergo fragmentation (form round and small spheroidal or punctate structures) before releasing cytochrome *c*. We found significantly greater roundness and circularity in the mitochondria from the infected S13A-expressing cells as compared to the mitochondria from pcDNA3.1⁺ and WT Noxa-expressing cells (Fig. 5B).

Noxa dephosphorylation enhances apoptosis in *H. pylori*-infected GECs

To determine the extent of cell death by *H. pylori*, AGS cells were infected with an MOI of 200 for 10 h. We stained cells with Annexin V PE to detect apoptotic cells,

and 7-AAD was used to detect necrotic population. Flow cytometric analysis revealed that *H. pylori* significantly induced apoptotic cell death (Fig. 6A and Supplemental Fig. S4A). To assess the role of Noxa WT and S13A mutations on apoptosis, AGS cells were transiently transfected with empty vector, WT Noxa, or S13A Noxa followed by infection with an MOI of 200 of *H. pylori* for 10 h. Flow cytometric analysis showed that S13A-transfected and *H. pylori*-infected cells significantly induced apoptosis compared with their counterparts from empty vector-transfected and Noxa WT-transfected groups (Fig. 6B and Supplemental Fig. S4B). Cell mortality was also calculated with trypan blue assay (data not shown).

Overall, our data confirmed that although *H. pylori*-mediated induction of Noxa-induced apoptosis, impairment of Noxa phosphorylation enhanced the apoptotic potential of Noxa in *H. pylori*-infected GECs. The effect of Noxa phosphorylation status on *H. pylori*-mediated GEC apoptosis is graphically summarized in Fig. 7.

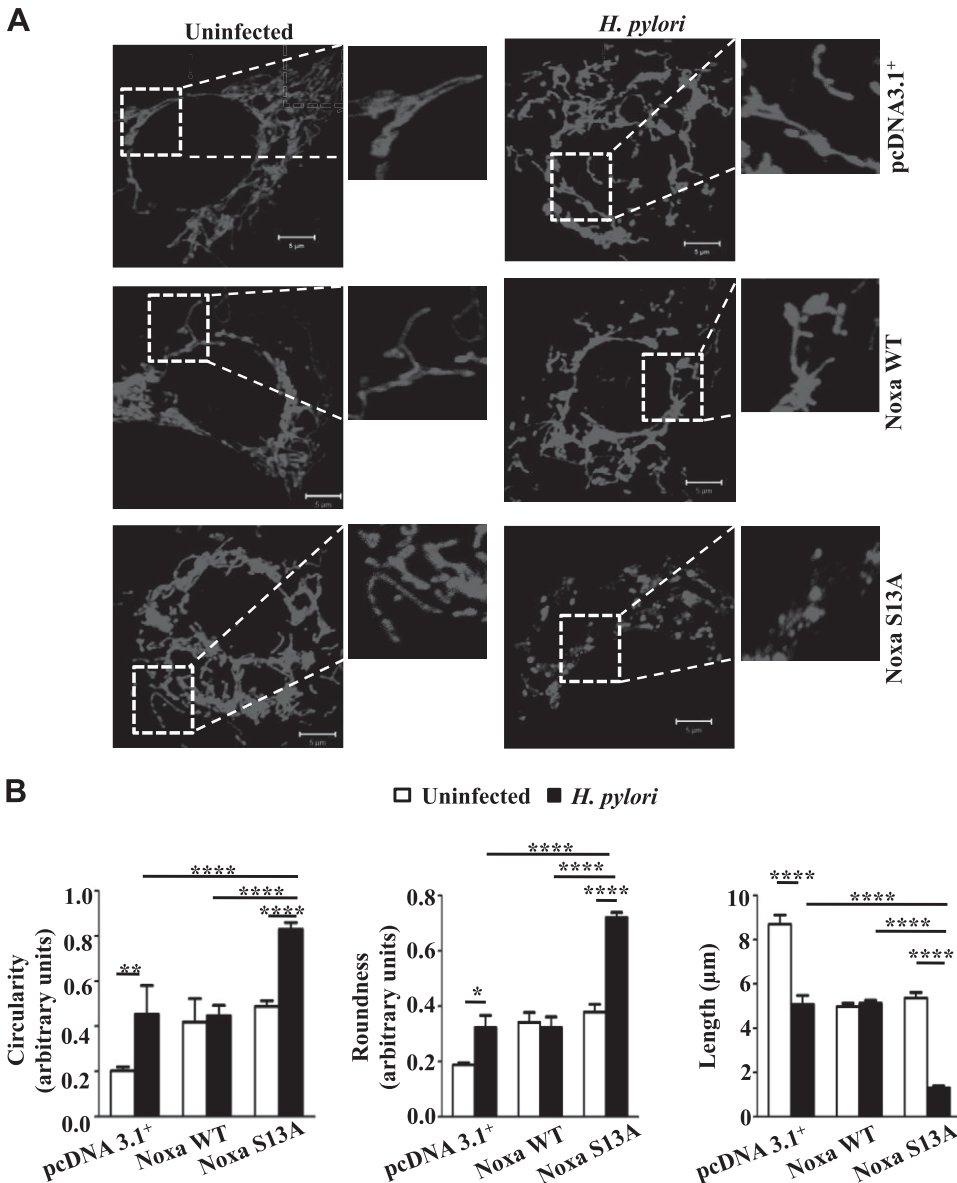


Figure 5. Non-P-Noxa increases *H. pylori*-induced mitochondrial fragmentation. A) Mitochondrial morphology was examined by confocal microscopy after transfecting empty vector (pcDNA3.1⁺), Noxa WT, and Noxa S13A constructs in pDsRed2 stably expressing AGS cells followed by infection with *H. pylori* for 8 h, with an MOI of 200. Scale bars, 5 μm. B) Mitochondrial length, roundness, and circularity information was collected from 4 cells (from 4 independent experiments), and 5 mitochondria were measured from each cell for statistical analysis. Circular mitochondrial appearance indicative of mitochondrial stress was more apparent in infected Noxa S13A-transfected cells when compared with the pcDNA3.1⁺ or Noxa WT construct-expressing infected cells. Data were analyzed by 2-way ANOVA with Tukey's *post hoc* test. Error bars, SEM. **P* < 0.05; ***P* < 0.01; *****P* < 0.0001.

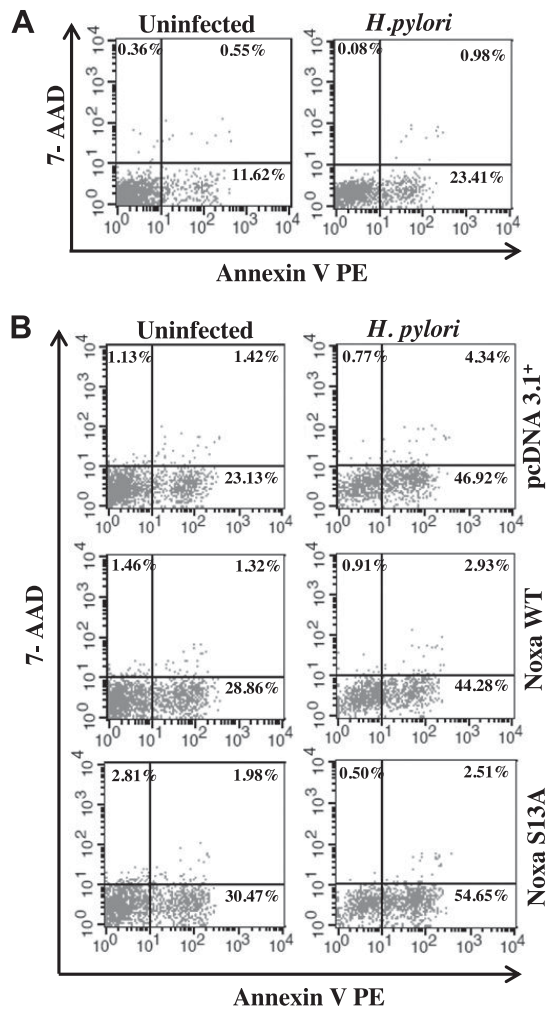


Figure 6. Non-P-Noxa enhances *H. pylori*-induced apoptosis in AGS cells. *A*) AGS cells were either infected with *H. pylori* or left uninfected. Cells were harvested and stained with Annexin V PE/7-AAD dyes. Representative flow cytometry data show that *H. pylori* induced apoptosis in infected cells ($n = 6$). Apoptotic cells are in the lower-right quadrant. *B*) AGS cells were transfected with either Noxa WT or Noxa S13A plasmid constructs or empty vector followed by infection with *H. pylori* for 10 h. A representative dot plot indicates a marked increase in *H. pylori*-induced apoptosis in S13A Noxa construct-transfected cells as compared to WT and empty vector-transfected cells ($n = 6$).

DISCUSSION

The chronic imbalance between host epithelial cell death and proliferation is a major mechanism that contributes to *H. pylori*-mediated gastric cancer because it allows accumulation of mutations in host cells (28). The BH3-only apoptotic protein Noxa binds mainly with the antiapoptotic protein Mcl1, a complex that is targeted for proteasomal degradation. Thus, Noxa functions as a critical regulator of apoptosis in Mcl1-expressing cells (29). Here, we report that although Noxa is up-regulated in *H. pylori*-infected GECs, its apoptotic function is regulated by phosphorylation. The stress-induced kinase JNK, which mediates apoptosis in the

H. pylori-infected gastric epithelium (30, 31), is responsible for Noxa phosphorylation. This also indicates that *H. pylori* can mold host apoptotic effectors toward antiapoptosis.

H. pylori infection induces gastric epithelial ROS generation and apoptosis (32). The indirect activation model of apoptosis suggests that the interaction of BH3-only proteins with their antiapoptotic partners induces conformational changes in the multi-BH domain-containing proteins Bax and Bak. This leads to auto-oligomerization of these “apoptosis effectors” in the outer membrane of the mitochondria, resulting in the release of cytochrome *c* (33). BH3-only proteins show selectivity in binding with antiapoptotic members of the Bcl2 family. As a “sensitizer,” BH3-only protein Noxa was earlier thought to have a weak proapoptotic function. However, Lowman *et al.* (11) showed that S13A Noxa-expressing leukemia cells die from glucose stress. These investigators were unable to generate stable S13A-expressing Jurkat cells. We also failed in our attempt to generate GECs with Noxa S13A mutation, which strengthened our belief that Noxa phosphorylation by *H. pylori* has some essential protective functions against apoptosis. Previously, induction of Noxa was reported to be essential but not sufficient for apoptosis (34). Thus, we surmise that Noxa phosphorylation could be one of the explanations of these findings.

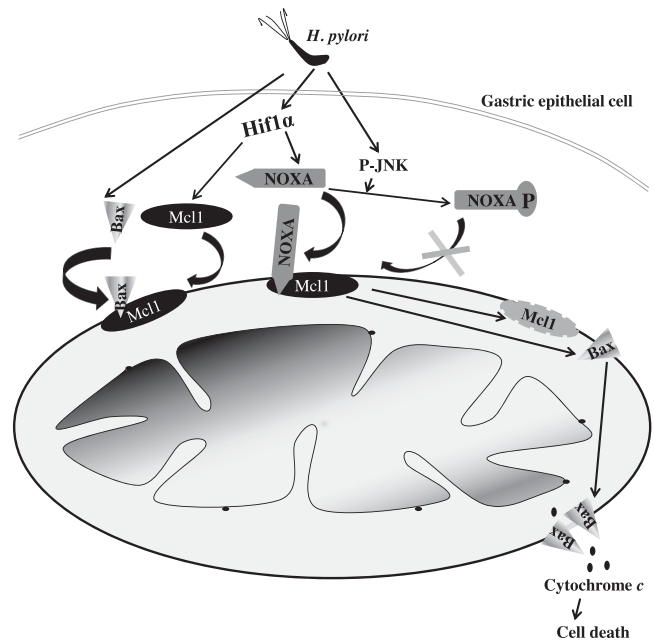


Figure 7. Regulation of apoptotic potential of Noxa in *H. pylori*-infected GECs. Hif1 α expressed in *H. pylori* infected GECs enhances Noxa expression. *H. pylori* also induces Bax translocation to mitochondria, which can bind with Mcl1 in the mitochondria. If Noxa manages to stay as non-P-Noxa, it translocates to the mitochondria, displaces Bax from Mcl1, and binds with Mcl1. As a result, Mcl1 is degraded, and free Bax is oligomerized to help in the cytochrome *c* release, resulting in apoptosis. When Noxa is phosphorylated at Ser¹³ by JNK activated in *H. pylori*-infected GECs, P-Noxa is unable to translocate to mitochondria, resulting in impairment of apoptosis. Curved arrow indicates translocation.

H. pylori induces MAPKs and regulates various cellular processes, including cell cycle, proliferation, and apoptosis (21). JNK plays a role in regulating the intrinsic apoptotic pathway because activation of JNK increases cytochrome *c* release (35). Our results reveal a new phenomenon that Noxa is phosphorylated by JNK in *H. pylori*-infected GECs and regulates the apoptotic potential of Noxa. Because JNK can induce invasiveness and motility of *H. pylori*-infected cells (36), we speculate that Noxa phosphorylation by JNK also helps in the survival of invasive gastric cancer cells. Further studies are needed to explore this hypothesis.

One of the main steps in the intrinsic apoptotic pathway is Bax translocation to mitochondria. *H. pylori* enhances Bax translocation to mitochondria followed by mitochondrial fragmentation (27). Although the Mcl1-Bak interaction is well known, a direct Mcl1-Bax interaction is not commonly observed. However, it has been shown that following Bax translocation to mitochondria, Mcl1 can inhibit Bax-induced cytochrome *c* release (37). Although the same group reports that direct interaction with Mcl1 is not required for Bax inhibition in that study, there is evidence that a Mcl1-Bax interaction exists (38). We report here that *H. pylori* induces direct interaction of Mcl1 with Bax. Our results also confirm that abrogation of JNK-mediated phosphorylation of Noxa in infected GECs results in direct Mcl1-Noxa interaction in the *H. pylori*-infected gastric epithelium. We presume that in the presence of nonphosphorylated Noxa (P-Noxa), which has a very high affinity and priority to bind with Mcl1 (39, 40), Bax is displaced from Mcl1, oligomerizes, and helps in cytochrome *c* release. p53 is crucial in regulating cell survival, apoptosis, as well as cell cycle and is a very highly mutated gene in human cancers (41). Although it is one of the main transcription factors that induce Noxa, p53-independent mechanisms of Noxa induction also exist and are targeted to treat cancers (42, 43). Almost 40% of cases of gastric cancer have p53 mutations, and *H. pylori* can cause p53 mutations as well (28, 44). A recent study suggests that p53 can even be inhibited by *H. pylori* in a mutation-independent mechanism (45). Tumor suppressor function and transcriptional activity of p53 remain inhibited in B cells of patients with MALT lymphoma (46). In our study, Hif1 α was highly induced and shown to be a major inducer of Noxa in *H. pylori*-infected GECs. Because Hif1 α (47) and *H. pylori* (48) individually can contribute to gastric cancer chemoresistance, it is likely that P-Noxa induction by *H. pylori* further increases the risk for treatment resistance in gastric cancer. We believe that the accumulation of P-Noxa resulting in antiapoptosis of the *H. pylori*-infected GECs would contribute to accumulation of mutations, leading to the increased probability of developing gastric cancer. Because Noxa and P-Noxa both are induced by *H. pylori*, it is difficult to assess a direct cause-effect relationship as the P-Noxa:Noxa ratio in gastric cancer tissue samples has not been studied yet. Further research is required to identify the prevalence of Noxa Ser¹³ mutation and P-JNK expression pattern in *H. pylori*-infected gastric biopsy samples.

Given the frequency of gastric cancer metastasis and treatment resistance, developing new targeted treatment strategies is very important. Because phosphorylation-dephosphorylation can regulate apoptotic functions of Noxa, this is a potential target molecule for future treatment approaches in *H. pylori*-induced gastric cancer. Noxa phosphorylation may also be implicated in carcinogenic events in other types of cancer. FJ

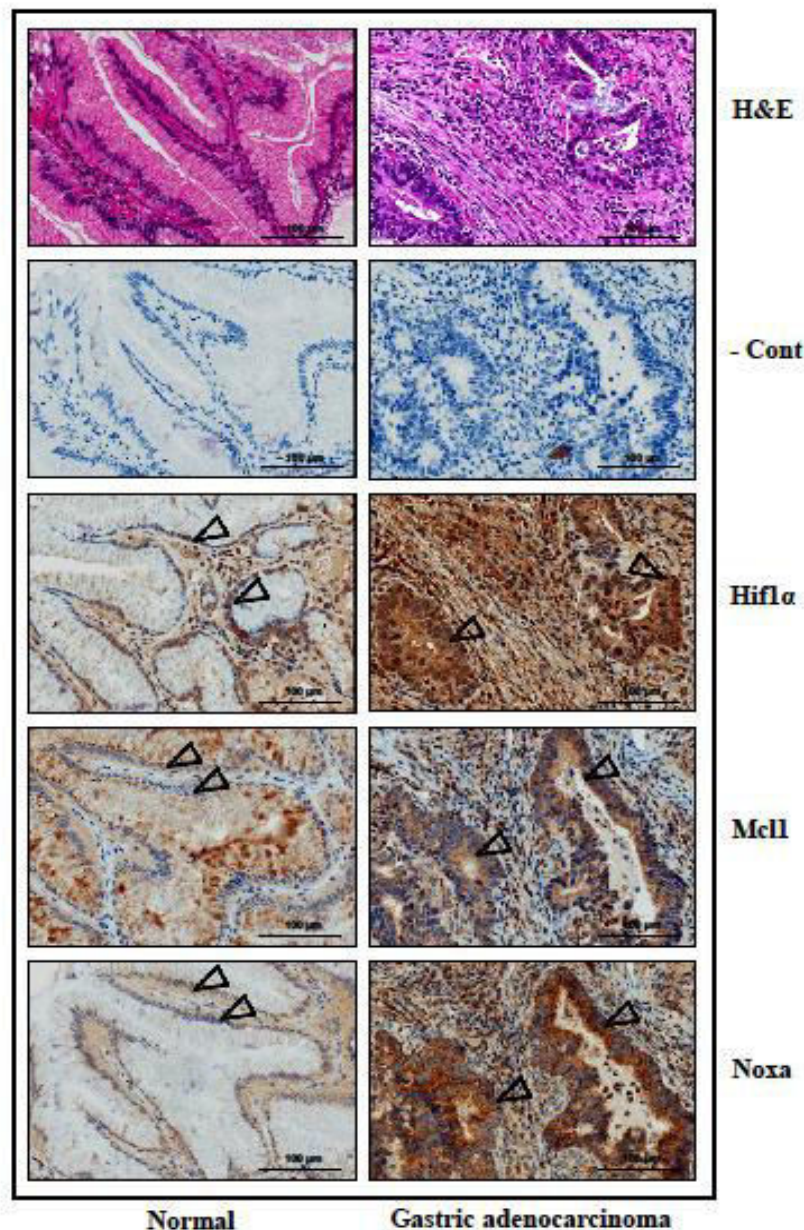
This work was supported in part by a Rapid Grant for Young Investigators (RGYI), Department of Biotechnology, India, and a Fast Track Grant, Science and Engineering Research Board, India (to A.B.); the U.S. National Institutes of Health Grant R01-DK61769 and an American Gastroenterological Association (AGA) Funderburg Research Scholar Award (to S.E.C.); an Indian Council of Medical Research (ICMR) fellowship (to S.R.); and a fellowship from Department of Atomic Energy (DAE), India (to L.D. and S.B.K.).

REFERENCES

1. Peek, Jr., R. M., and Blaser, M. J. (2002) *Helicobacter pylori* and gastrointestinal tract adenocarcinomas. *Nat. Rev. Cancer* **2**, 28–37
2. Bhattacharyya, A., Chattopadhyay, R., Hall, E. H., Mebrahtu, S. T., Ernst, P. B., and Crowe, S. E. (2010) Mechanism of hypoxia-inducible factor 1 alpha-mediated Mcl1 regulation in *Helicobacter pylori*-infected human gastric epithelium. *Am. J. Physiol. Gastrointest. Liver Physiol.* **299**, G1177–G1186
3. Park, J. H., Kim, T. Y., Jong, H. S., Kim, T. Y., Chun, Y. S., Park, J. W., Lee, C. T., Jung, H. C., Kim, N. K., and Bang, Y. J. (2003) Gastric epithelial reactive oxygen species prevent normoxic degradation of hypoxia-inducible factor-1alpha in gastric cancer cells. *Clin. Cancer Res.* **9**, 433–440
4. Wenger, R. H., Stiehl, D. P., and Camenisch, G. (2005) Integration of oxygen signaling at the consensus HRE. *Sci. STKE* **2005**, re12
5. Wang, G. L., Jiang, B. H., Rue, E. A., and Semenza, G. L. (1995) Hypoxia-inducible factor 1 is a basic-helix-loop-helix-PAS heterodimer regulated by cellular O₂ tension. *Proc. Natl. Acad. Sci. USA* **92**, 5510–5514
6. Piret, J. P., Minet, E., Cosse, J. P., Ninane, N., Debacq, C., Raes, M., and Michiels, C. (2005) Hypoxia-inducible factor-1-dependent overexpression of myeloid cell factor-1 protects hypoxic cells against tert-butyl hydroperoxide-induced apoptosis. *J. Biol. Chem.* **280**, 9336–9344
7. Kim, J. Y., Ahn, H. J., Ryu, J. H., Suk, K., and Park, J. H. (2004) BH3-only protein Noxa is a mediator of hypoxic cell death induced by hypoxia-inducible factor 1alpha. *J. Exp. Med.* **199**, 113–124
8. Wei, J., O'Brien, D., Vilgelm, A., Piazuelo, M. B., Correa, P., Washington, M. K., El-Rifai, W., Peek, R. M., and Zaika, A. (2008) Interaction of *Helicobacter pylori* with gastric epithelial cells is mediated by the p53 protein family. *Gastroenterology* **134**, 1412–1423
9. Vela, L., Gonzalo, O., Naval, J., and Marzo, I. (2013) Direct interaction of Bax and Bak proteins with Bcl-2 homology domain 3 (BH3)-only proteins in living cells revealed by fluorescence complementation. *J. Biol. Chem.* **288**, 4935–4946
10. Gomez-Bougie, P., Ménoret, E., Juin, P., Dousset, C., Pellat-Deceunynck, C., and Amiot, M. (2011) Noxa controls Mule-dependent Mcl-1 ubiquitination through the regulation of the Mcl-1/USP9X interaction. *Biochem. Biophys. Res. Commun.* **413**, 460–464
11. Lowman, X. H., McDonnell, M. A., Kosloske, A., Odumade, O. A., Jenness, C., Karim, C. B., Jemmerson, R., and Kelekar, A. (2010) The proapoptotic function of Noxa in human leukemia cells is regulated by the kinase Cdk5 and by glucose. *Mol. Cell* **40**, 823–833
12. Likui, W., Qun, L., Wanqing, Z., Haifeng, S., Fangqiu, L., and Xiaojun, L. (2009) Prognostic role of myeloid cell leukemia-1 protein (Mcl-1) expression in human gastric cancer. *J. Surg. Oncol.* **100**, 396–400

13. Bhattacharyya, A., Chattopadhyay, R., Burnette, B. R., Cross, J. V., Mitra, S., Ernst, P. B., Bhakat, K. K., and Crowe, S. E. (2009) Acetylation of apurinic/apyrimidinic endonuclease-1 regulates *Helicobacter pylori*-mediated gastric epithelial cell apoptosis. *Gastroenterology* **136**, 2258–2269
14. Dérjard, B., Hibi, M., Wu, I. H., Barrett, T., Su, B., Deng, T., Karin, M., and Davis, R. J. (1994) JNK1: a protein kinase stimulated by UV light and Ha-Ras that binds and phosphorylates the c-Jun activation domain. *Cell* **76**, 1025–1037
15. Kallunki, T., Su, B., Tsigelny, I., Sluss, H. K., Dérjard, B., Moore, G., Davis, R., and Karin, M. (1994) JNK2 contains a specificity-determining region responsible for efficient c-Jun binding and phosphorylation. *Genes Dev.* **8**, 2996–3007
16. Ploner, C., Kofler, R., and Villunger, A. (2008) Noxa: at the tip of the balance between life and death. *Oncogene* **27**(Suppl 1), S84–S92
17. Warr, M. R., and Shore, G. C. (2008) Unique biology of Mcl-1: therapeutic opportunities in cancer. *Curr. Mol. Med.* **8**, 138–147
18. Xue, Y., Ren, J., Gao, X., Jin, C., Wen, L., and Yao, X. (2008) GPS 2.0, a tool to predict kinase-specific phosphorylation sites in hierarchy. *Mol. Cell. Proteomics* **7**, 1598–1608
19. Iseki, H., Ko, T. C., Xue, X. Y., Seapan, A., Hellmich, M. R., and Townsend, Jr., C. M. (1997) Cyclin-dependent kinase inhibitors block proliferation of human gastric cancer cells. *Surgery* **122**, 187–194
20. Tsai, L. H., Takahashi, T., Caviness, Jr., V. S., and Harlow, E. (1993) Activity and expression pattern of cyclin-dependent kinase 5 in the embryonic mouse nervous system. *Development* **119**, 1029–1040
21. Ding, S. Z., Smith, Jr., M. F., and Goldberg, J. B. (2008) *Helicobacter pylori* and mitogen-activated protein kinases regulate the cell cycle, proliferation and apoptosis in gastric epithelial cells. *J. Gastroenterol. Hepatol.* **23**, e67–e78
22. Tromp, J. M., Geest, C. R., Breij, E. C., Elias, J. A., van Laar, J., Luijckx, D. M., Kater, A. P., Beaumont, T., van Oers, M. H., and Eldering, E. (2012) Tipping the Noxa/Mcl-1 balance overcomes ABT-737 resistance in chronic lymphocytic leukemia. *Clin. Cancer Res.* **18**, 487–498
23. Kodama, Y., Taura, K., Miura, K., Schnabl, B., Osawa, Y., and Brenner, D. A. (2009) Antiapoptotic effect of c-Jun N-terminal Kinase-1 through Mcl-1 stabilization in TNF-induced hepatocyte apoptosis. *Gastroenterology* **136**, 1423–1434
24. Hassan, M., Alaoui, A., Feyen, O., Mirmohammadsadegh, A., Essmann, F., Tannapfel, A., Gulbins, E., Schulze-Osthoff, K., and Hengge, U. R. (2008) The BH3-only member Noxa causes apoptosis in melanoma cells by multiple pathways. *Oncogene* **27**, 4557–4568
25. Nijhawan, D., Fang, M., Traer, E., Zhong, Q., Gao, W., Du, F., and Wang, X. (2003) Elimination of Mcl-1 is required for the initiation of apoptosis following ultraviolet irradiation. *Genes Dev.* **17**, 1475–1486
26. Willis, S. N., and Adams, J. M. (2005) Life in the balance: how BH3-only proteins induce apoptosis. *Curr. Opin. Cell Biol.* **17**, 617–625
27. Ashktorab, H., Frank, S., Khaled, A. R., Durum, S. K., Kifle, B., and Smoot, D. T. (2004) Bax translocation and mitochondrial fragmentation induced by *Helicobacter pylori*. *Gut* **53**, 805–813
28. Matsumoto, Y., Marusawa, H., Kinoshita, K., Endo, Y., Kou, T., Morisawa, T., Azuma, T., Okazaki, I. M., Honjo, T., and Chiba, T. (2007) *Helicobacter pylori* infection triggers aberrant expression of activation-induced cytidine deaminase in gastric epithelium. *Nat. Med.* **13**, 470–476
29. Alves, N. L., Derks, I. A., Berk, E., Spijker, R., van Lier, R. A., and Eldering, E. (2006) The Noxa/Mcl-1 axis regulates susceptibility to apoptosis under glucose limitation in dividing T cells. *Immunity* **24**, 703–716
30. Matsumoto, A., Isomoto, H., Nakayama, M., Hisatsune, J., Nishi, Y., Nakashima, Y., Matsushima, K., Kurazono, H., Nakao, K., Hirayama, T., and Kohno, S. (2011) *Helicobacter pylori* VacA reduces the cellular expression of STAT3 and pro-survival Bcl-2 family proteins, Bcl-2 and Bcl-XL, leading to apoptosis in gastric epithelial cells. *Dig. Dis. Sci.* **56**, 999–1006
31. Domek, M. J., Netzer, P., Prins, B., Nguyen, T., Liang, D., Wyle, F. A., and Warner, A. (2001) *Helicobacter pylori* induces apoptosis in human epithelial gastric cells by stress activated protein kinase pathway. *Helicobacter* **6**, 110–115
32. Ding, S. Z., Minohara, Y., Fan, X. J., Wang, J., Reyes, V. E., Patel, J., Dirden-Kramer, B., Boldogh, I., Ernst, P. B., and Crowe, S. E. (2007) *Helicobacter pylori* infection induces oxidative stress and programmed cell death in human gastric epithelial cells. *Infect. Immun.* **75**, 4030–4039
33. Martinou, J. C., and Youle, R. J. (2011) Mitochondria in apoptosis: Bcl-2 family members and mitochondrial dynamics. *Dev. Cell* **21**, 92–101
34. Liu, W., Swetzig, W. M., Medisetty, R., and Das, G. M. (2011) Estrogen-mediated upregulation of Noxa is associated with cell cycle progression in estrogen receptor-positive breast cancer cells. *PLoS One* **6**, e29466
35. Tournier, C., Hess, P., Yang, D. D., Xu, J., Turner, T. K., Nimnual, A., Bar-Sagi, D., Jones, S. N., Flavell, R. A., and Davis, R. J. (2000) Requirement of JNK for stress-induced activation of the cytochrome c-mediated death pathway. *Science* **288**, 870–874
36. Snider, J. L., Allison, C., Bellaire, B. H., Ferrero, R. L., and Cardelli, J. A. (2008) The beta1 integrin activates JNK independent of CagA, and JNK activation is required for *Helicobacter pylori* CagA+induced motility of gastric cancer cells. *J. Biol. Chem.* **283**, 13952–13963
37. Germain, M., Milburn, J., and Duronio, V. (2008) MCL-1 inhibits BAX in the absence of MCL-1/BAX Interaction. *J. Biol. Chem.* **283**, 6384–6392
38. Sedlak, T. W., Oltvai, Z. N., Yang, E., Wang, K., Boise, L. H., Thompson, C. B., and Korsmeyer, S. J. (1995) Multiple Bcl-2 family members demonstrate selective dimerizations with Bax. *Proc. Natl. Acad. Sci. USA* **92**, 7834–7838
39. Giam, M., Huang, D. C., and Bouillet, P. (2008) BH3-only proteins and their roles in programmed cell death. *Oncogene* **27**(Suppl 1), S128–S136
40. Zhang, L., Lopez, H., George, N. M., Liu, X., Pang, X., and Luo, X. (2011) Selective involvement of BH3-only proteins and differential targets of Noxa in diverse apoptotic pathways. *Cell Death Differ.* **18**, 864–873
41. Harris, S. L., and Levine, A. J. (2005) The p53 pathway: positive and negative feedback loops. *Oncogene* **24**, 2899–2908
42. Nikiforov, M. A., Riblett, M., Tang, W. H., Gratchouck, V., Zhuang, D., Fernandez, Y., Verhaegen, M., Varambally, S., Chinnaiyan, A. M., Jakubowiak, A. J., and Soengas, M. S. (2007) Tumor cell-selective regulation of NOXA by c-MYC in response to proteasome inhibition. *Proc. Natl. Acad. Sci. USA* **104**, 19488–19493
43. Pérez-Galán, P., Roué, G., Villamor, N., Montserrat, E., Campo, E., and Colomer, D. (2006) The proteasome inhibitor bortezomib induces apoptosis in mantle-cell lymphoma through generation of ROS and Noxa activation independent of p53 status. *Blood* **107**, 257–264
44. Wei, J., Noto, J., Zaika, E., Romero-Gallo, J., Correa, P., El-Rifai, W., Peek, R. M., and Zaika, A. (2012) Pathogenic bacterium *Helicobacter pylori* alters the expression profile of p53 protein isoforms and p53 response to cellular stresses. *Proc. Natl. Acad. Sci. USA* **109**, E2543–E2550
45. Wei, J., Nagy, T. A., Vilgelm, A., Zaika, E., Ogden, S. R., Romero-Gallo, J., Piazuolo, M. B., Correa, P., Washington, M. K., El-Rifai, W., Peek, R. M., and Zaika, A. (2010) Regulation of p53 tumor suppressor by *Helicobacter pylori* in gastric epithelial cells. *Gastroenterology* **139**, 1333–1343
46. Umehara, S., Higashi, H., Ohnishi, N., Asaka, M., and Hatakeyama, M. (2003) Effects of *Helicobacter pylori* CagA protein on the growth and survival of B lymphocytes, the origin of MALT lymphoma. *Oncogene* **22**, 8337–8342
47. Nakamura, J., Kitajima, Y., Kai, K., Mitsuno, M., Ide, T., Hashiguchi, K., Hiraki, M., and Miyazaki, K. (2009) Hypoxia-inducible factor-1alpha expression predicts the response to 5-fluorouracil-based adjuvant chemotherapy in advanced gastric cancer. *Oncol. Rep.* **22**, 693–699
48. Nardone, G., Rocco, A., Vaira, D., Staibano, S., Budillon, A., Tatangelo, F., Sciulli, M. G., Perna, F., Salvatore, G., Di Benedetto, M., De Rosa, G., and Patrignani, P. (2004) Expression of COX-2, mPGE-synthase1, MDR-1 (P-gp), and Bcl-xL: a molecular pathway of *H. pylori*-related gastric carcinogenesis. *J. Pathol.* **202**, 305–312

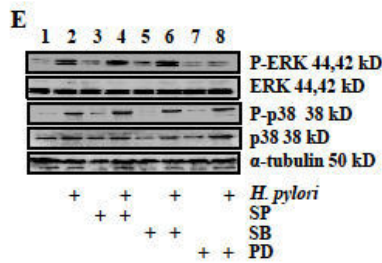
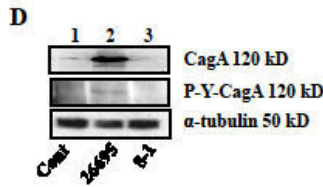
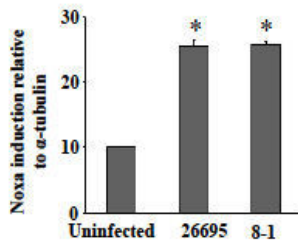
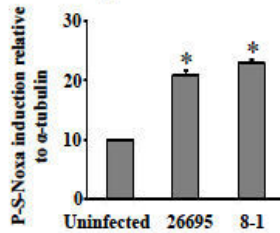
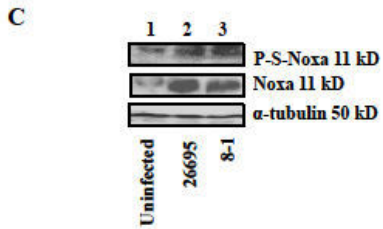
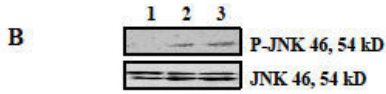
Received for publication June 14, 2014.
Accepted for publication October 8, 2014.



Supplemental Fig.S1. Expression of Hif1 α , Noxa as well as Mcl1 in human gastric surgery samples from adenocarcinoma patients as well as from nonneoplastic gastric tissues. Immunohistochemical staining of human gastric adenocarcinoma surgery samples from patients with known history of *H. pylori* infection (n=4) showing up-regulation of Hif1 α , Noxa as well as Mcl1. Negative (-ve) control (-Cont) contained no primary antibody. ▲ indicates epithelial lining and gastric mucosa. Original magnification: X20. Scale 100 μ m.

A

MPGKKARKNAQPSAPARPAELEVECATQLRRRFGDKLNFRQKLLNLSIKLFCSGT



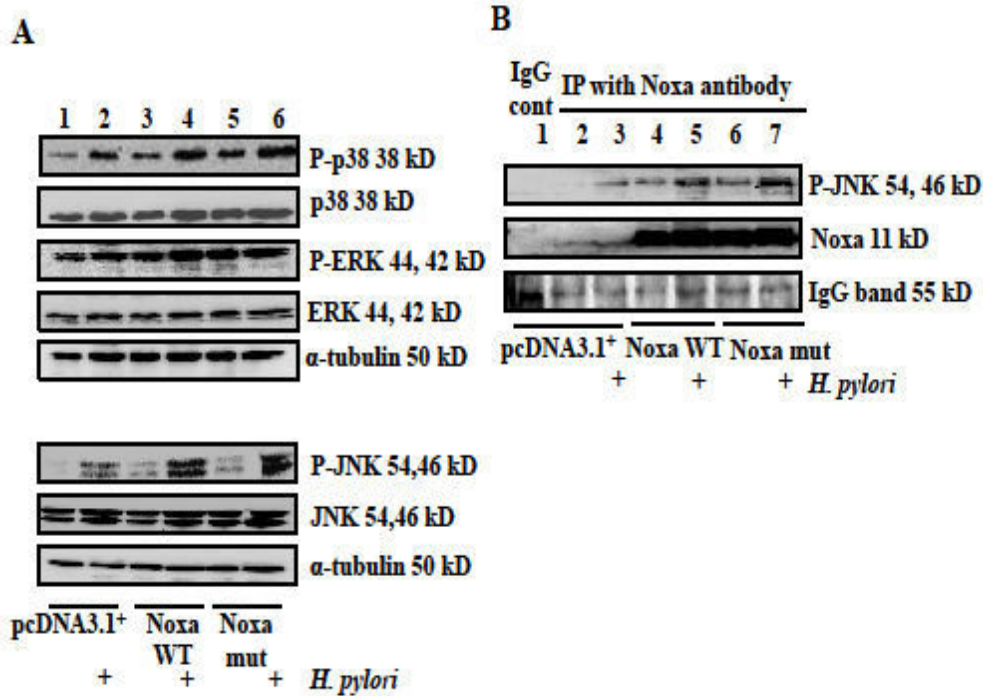
Supplemental Fig. S2A. Amino acid sequence of human Noxa. Noxa has five residues which can be phosphorylated (S and T, boldfaced and in italics). But, only S¹³ appears to be a potential kinase-target as predicted by GPS2.1 program.

Supplemental Fig. S2B. JNK and its active form P-JNK were equally induced by both 26695 and 8-1 strains. Western blot analysis of whole cell lysates prepared from AGS cells infected with 200 MOI of *H. pylori* *cag* PAI(+) strain (26695) and *cag* PAI negative strain (8-1) or left uninfected for 5h showing equal expression of JNK and P-JNK. α -tubulin was used as a loading control.

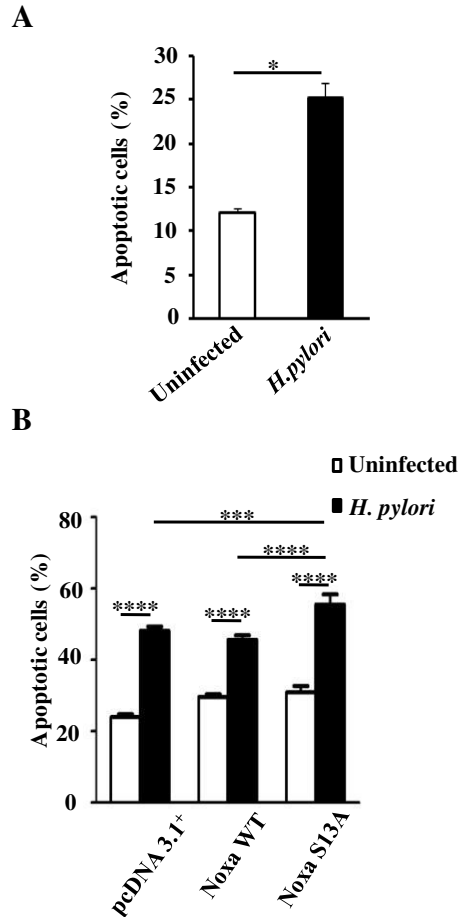
Supplemental Fig. S2C. Noxa and P-S-Noxa induction by 26695 and 8-1 strains. Western blot analysis of whole cell lysates prepared from AGS cells infected with 200 MOI of *H. pylori* *cag* PAI(+) strain (26695) and *cag* PAI negative strain (8-1) or left uninfected for 5h showing equal expression of Noxa and P-S-Noxa. α -tubulin was used as a loading control. Bars depict P-S-Noxa and Noxa expression normalized to α -tubulin (mean \pm SEM, $n = 4$), * $P < 0.05$ compared with uninfected cells.

Supplemental Fig. S2D. CagA and its phosphorylated form are only induced in *H. pylori* 26695 infected AGS cells. Western blot analysis of whole cell lysates showed CagA expression and its phosphorylation in 26695-infected cells but not in cells infected with strain 8-1.

Supplemental Fig. S2E. Expression status of P-ERK, P-p38, total ERK and p38 in AGS cells infected (5 h) with 200 MOI of *H. pylori*. Pretreatment with 25 μ M JNK inhibitor II (SP600125), 25 μ M p38 MAPK inhibitor (SB203580) and MEK 1/2 inhibitor (PD98039) were done as indicated. This data showed that JNK inhibition by SP had no effect on ERK and p38 MAPK phosphorylation. SB partially inhibited p38 MAPK phosphorylation and PD inhibited ERK phosphorylation.



Supplemental Fig. S3. Noxa induced JNK activation and enhanced interaction with P-JNK following infection with *H. pylori*. **A)** Effect of overexpression of WT and non-phosphorylatable mutant (S13A) constructs of Noxa on MAP kinases was assessed by western blot analysis in AGS cells after transfecting cells with above mentioned constructs followed by 200 MOI *H. pylori* infection for 5 h. α -tubulin was used as a loading control. **B)** Immunoprecipitation of whole cell lysates prepared from infected or uninfected empty vector or WT Noxa or S13A Noxa-transfected cells with Noxa antibody showed interaction of P-JNK with Noxa.



Supplemental Fig. S4. Nonphosphorylated Noxa enhances *H. pylori*-induced cell death in AGS cells. **A)** Analysis of the data shown in Figure. 6A by Student's t test clearly demonstrated significant increase in percentage apoptotic cell death in the *H. pylori*-infected cells (mean \pm SEM, $n=6$), $*P<0.05$. **B)** The percentage of apoptotic cell death in various transfected groups were compared with two way ANOVA with Tukey's *post hoc* test. (mean \pm SEM, $n =6$), $***P<0.001$, $****P<0.0001$.